ISSN 1019-5149 - E ISSN 2651-5032 - NLM ID 9423821

Turkish Neurosurgery

Official Journal of the Turkish Neurosurgical Society

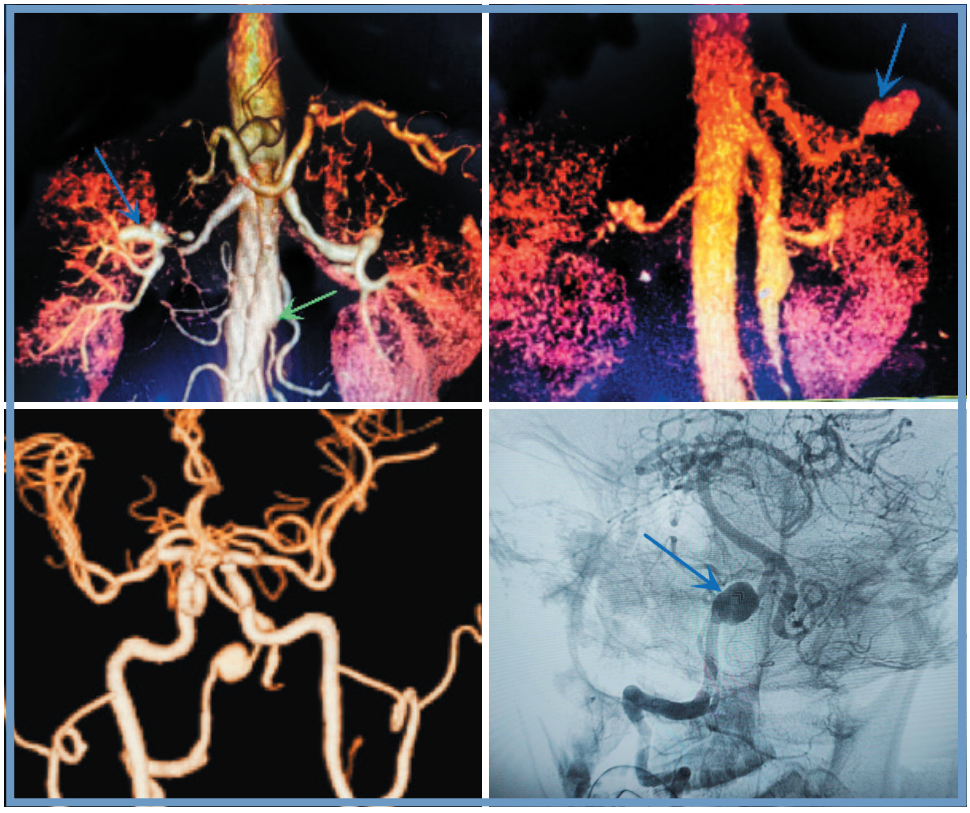

Volume 36 • Number 3 • May 2026

Turkish Neurosurgery

Official Journal of the Turkish Neurosurgical Society

ISSN: 1019-5149,
E-ISSN: 2651-5032
NLM ID: 9423821

TURKISH NEUROSURGICAL SOCIETY

Volume: 36 Number: 3 Year: 2026

www.turkishneurosurgery.org.tr

Turkish Neurosurgery has been accepted for indexing in: SCIENCE CITATION INDEX EXPANDED, INDEX MEDICUS, MEDLINE, PubMed, EBSCO, Scopus, TR Index, Islamic World Science Citation Center (ISC)

Impact Factor* : 0.8
5yr-Impact Factor* : 0.8
Journal Citation Indicator*™: 0.34

*ISI Web of Knowledge℠, Journal Citation Reports®, 2024 JCR Science Edition

Turkish
Neurosurgery

Volume: 36 Number: 3 Year: 2026

Official Journal of the Turkish Neurosurgical Society

Turkish Neurosurgery is published six times per year (bimonthly) by the Turkish Neurosurgical Society
(January, March, May, July, September, and November)

Owned and controlled by the Turkish Neurosurgical Society

Copyright owner on behalf of the Turkish Neurosurgical Society:
İlker SOLMAZ

Publishing Manager:
Hüseyin Hayri KERTMEN

Key title: Turkish Neurosurgery
Abbreviated key title: Turk Neurosurg
www.turkishneurosurgery.org.tr

ISSN: 1019-5149, **E-ISSN:** 2651-5032
NLM ID: 9423821

Turkish Neurosurgery is an open access and totally free journal.
All electronic materials can be found on internet without any charge. Please visit: http://www.turkishneurosurgery.org.tr/
2026 Subscription Rates for Printed Materials:
Within Türkiye 5000 TL (shipping costs not included); Outside Türkiye 100 € (shipping costs not included)
For further information and questions; please contact: bulus@bulustasarim.com.tr

Page layout and publishing services
BULUŞ DESIGN AND PRINTING SERVICES COMPANY
Mebusevleri Mah. Turgut Reis Cad. 11/1 Çankaya, Ankara, Türkiye
Phone: +90 312 222 44 06
E-mail: bulus@bulustasarim.com.tr

Advertisement: editor@turkishneurosurgery.org.tr

Publishing Date: 22.05.2026

Cover picture: Wang, p. 468, 469

Turkish Neurosurgical Society
Taşkent Caddesi 13/4 06500 Bahçelievler, Ankara/TÜRKİYE
Phone: +90 312 212 64 08 Fax : +90 312 215 46 26
E-mail: info@turknorosirurji.org.tr
www.turknorosirurji.org.tr www.turkishneurosurgery.org.tr

Yayın Türü: Yaygın süreli yayın
Yayın Sahibi: Türk Nöroşirürji Derneği adına İlker SOLMAZ
Sorumlu Yazı İşleri Müdürü: Hüseyin Hayri KERTMEN

5187 Sayılı Basın Yasasının 7. maddesi uyarınca dergi künyesinin Türkçesi belirtilmiştir.

Review of the articles in the journal to make sure they conform to publishing standards, typesetting, getting the journal ready for publication and finally the publishing process has been the responsibility of Buluş Design and Printing Services Company.

The paper used to print this journal conforms to ISO 9706: 1994 standard (Requirements for Permanence).
The National Library of Medicine suggests that biomedical publications be printed on acid-free paper (alkaline paper).

22
PAP

ENVIRONMENTAL INFORMATION

The company that manufactures the paper used in this journal has an ISO 14001 environmental management certificate. The company obtains all wood fiber in a sustainable manner. The forests and plantations of the company are certified. The water used in production is purified and used after recovery.

Heavy metals or film are not used for the publication of this journal. The fluids used for developing the aluminum printing templates are purified. The templates are recycled. The inks used for printing do not contain toxic heavy metals.

This journal can be recycled. Please dispose of it in recycling containers.

INSTRUCTION TO THE AUTHORS

Journal Description

Turkish Neurosurgery is a peer-reviewed, multidisciplinary, open access journal directed at an audience of neurosurgery physicians and scientists. The official language of the journal is *English*. The journal publishes original articles in the form of clinical and basic research. *Turkish Neurosurgery* will only publish studies that have institutional review board (IRB) approval and have strictly observed an acceptable follow-up period. With the exception of reference presentation, *Turkish Neurosurgery* requires that all manuscripts be prepared in accordance with the *Uniform Requirements for Manuscripts Submitted to Biomedical Journals*.

Turkish Neurosurgery periodically publishes the following papers: Research (Original Investigation, Clinical and Experimental Studies), Review Article, Case Report, Letter to Editor, Technical Note and Turkish Neuro-Excursion.

Our mission is providing a scientific forum relevant to neurosurgeons and health care providers.

Open Access Policy

As the Turkish Neurosurgery Journal, we believe science is a common denominator of the humanity which should be publicly available and free. Since its establishment in 1989, all our effort and workforce were based on volunteers and their efforts.

Definition of Open Access Publication[1]

An Open Access Publication [A] is one that meets the following two conditions:

1. The author(s) and copyright holder(s) grant(s) to all users a free, irrevocable, worldwide, perpetual right of access to, and a license to copy, use, distribute, transmit and display the work publicly and to make and distribute derivative works, in any digital medium for any responsible purpose, subject to proper attribution of authorship [B], as well as the right to make small numbers of printed copies for their personal use.

2. Complete version of the work and all supplemental materials, including a copy of the permission as stated above, in a suitable standard electronic format is deposited immediately upon initial publication in at least one online repository that is supported by an academic institution, scholarly society, government agency, or other well-established organization that seeks to enable open access, unrestricted distribution, interoperability, and long-term archiving (for the biomedical sciences, PubMed Central is such a repository).

Notes:

A. Open access is a property of individual works, not necessarily journals or publishers.

B. Community standards, rather than copyright law, will continue to provide the mechanism for enforcement of proper attribution and responsible use of the published work, as they do now.

[1] https://dash.harvard.edu/bitstream/handle/1/4725199/Suber_bethesda.htm#note1

Digital Archiving

Bulus Tasarim and the "Turkish Neurosurgery" journal provide for long-term digital preservation through Portico.

Portico is a leading digital preservation service worldwide. The content is preserved as an archival version and is not publically accessible via Portico, but is provided when required under specific conditions, such as discontinuation of the collection or catastrophic failure of the website.

Manuscript Submission

Authors are to submit their manuscripts through the web based tracking system at http://www.turkishneurosurgery.org.tr. The site contains instructions and advice on how to submit manuscripts, guidance on the creation / scanning and saving of electronic art and supporting documentation. **ORCID** identifier (ID) is required for **ALL** authors during the submission process. **ORCID ID** can be obtained free of charge at http://orcid.org. **E-mail address of all authors** should also be provided during the submission process. In addition to allowing authors to submit manuscripts on the web, the site allows authors to follow the progression of their manuscript through the peer review process. Authors who submit their manuscripts through the web-based tracking system are asked **not** to send hard copies of the manuscript to the editorial office. Please address all inquiries regarding manuscripts not yet accepted or published to the Journal's editorial office. The editorial office will acknowledge receipt of your manuscript and will send you a manuscript number for reference.

Before submission please ensure that:

One author has been designated as the correspondent with full contact details including e-mail address, postal address and phone number. In any case of editorial board could not contact with the corresponding author, Turkish Neurosurgery journal have the right to decide what is appropriate.

Submission Checklist;

1) Your title page is in .doc or .docx format, includes title of your manuscript, author names, affiliations and ORCID numbers; name and full contact information of corresponding author, running title, keywords, and authorship contribution statements-the latter can be found on the Copyright transfer and authorship contribution statement Form. Please be sure that authorship contribution statements are presented in the form as well as in the title page. Of note, authors should indicate conflicts of interest relating to their research-if any.

The Journal is not responsible for published misspelled names due to author error and the title page **must be uploaded as a separate file**. Running Head in the title page should be no more than three to five words from the title, and should NOT include the authors' names.

2) Your main document is in .doc or .docx format includes **structured abstract, key words, abbreviation list, structured main text, disclosure and conflicts of interest, references and figure legends** sections in this order. Structured main text should be organized as **Introduction, Material and Methods, Results, Discussion, and Conclusion.** Do not add any information about institution names. Also do not add figures and tables in the main document. **Be sure your main document is written in Calibri or Times New Roman, line gap set to double spaced and justified on both sides.** Journal's official language is English. Refer to drugs and therapeutic agents by their accepted generic or chemical names, and do not abbreviate them. Use code numbers only when a generic name is not yet available. In that case, supply the chemical name and a figure giving the chemical structure of the drug. Capitalize the trade names of drugs and place them in parentheses after the generic names. To comply with trademark law, include the name and location (city and country) of the manufacturer of any drug, supply, or equipment mentioned in the manuscript. Use the metric system to express the units of measure and degrees Celsius to express temperatures, and SI units rather than conventional units. Define abbreviations at first mention in text and in each table and figure. If a brand name is cited, supply the manufacturer's name and address (city and state/country).

3) All your figures are in **JPG,PNG,JPEG,WEBP** format. Color figures should have a resolution of at least **300 dpi**, black and white figures should have a resolution of at least **600 dpi**. Turkish Neurosurgery does not demand any color figure fee.

4) All your video files are in .mpeg and .mp4 format, not longer than 10 minutes, and not bigger than 40 MB. Video files should include an embedded audio narration and subtitles in English.

5) All your tables are in .doc or .docx format, created using the table creating and editing feature of the word processing software. Do not use Excel or comparable software. Upload a single text file which includes **ALL the tables in separate pages.** Cite tables consecutively in the text, and number them in that order. Key each on a separate sheet, include the table title, appropriate column heads, and explanatory legends (including definitions of any **abbreviations** used). Do not embed tables within the main text.

If your manuscript does not meet these requirements, manuscript **WILL BE RETURNED** to the corresponding author for technical revision before undergoing peer review.

Submission Steps

1. Upload signed copyright form by the corresponding author which is available at http://neurosurgery.dergisi.org/submit/Copyright_transfer_form.pdf. Choose your manuscript type and click continue.
2. Add names of institutions of all authors. If one or more author has affiliation with more institutions, specify it in the title page. Then click continue.
3. Write last name and first name of all authors. Add their institution numbers, e-mails and ORCID numbers. Standard page appears with spaces enough for 8 author names. If your paper has more authors, please fill all the first 8 authors names and affiliations then click add author. Without filling all required fields, you cannot add more authors. Do not use abbreviations in the author names. Then click continue.
4. Write the title of the manuscript. If the title contains special characters use the left below table. You can copy-paste the title from your title page. Then click continue.
5. Write the abstract of your manuscript to the field**.** Abstracts should be structured including Aim, Material and Methods, Results and Conclusion. **Abstracts should not exceed 300 words. There is no need of Turkish abstract.** Then click continue.
6. Write the keywords separated by commas. Please use keywords from https://meshb.nlm.nih.gov/search. Then click continue.
7. Click the appropriate answer stating if your manuscript has not been published and / or is not being considered for publication elsewhere or your manuscript was presented in the congress indicated below and was published in abstract form in the proceedings of the congress. Then write your cover letter to the editor to the field. Then click continue.
8. Upload your manuscript files. Be sure your files are main document (manuscript), figure(s), video(s), title page, and table(s). For every file, write the description of your file and click upload button. The names of the files you have submitted should not resemble the names or institutions of the authors. Be sure all your text files are in .doc or .docx format. When you are sure you uploaded all your files click continue.
9. When you complete all the submission process click approve for all the files you want to submit and click **Submit your Manuscript** button.

Revised Submission

Author's comments to the reviewers are required for revised submissions. Authors must address all the reviewer's concerns/suggestions and whether the change was made or not. Authors must also highlight the changes made within the text. Do not track the additions or deletions to the manuscript. If the authors do not want to revise the manuscript within a period of **two months**, the manuscript will be declined.

Ethics, patient anonymity and informed consent:

This journal adheres to the ethical standards described by the Committee on Publication Ethics (https://publicationethics.org/) and the International Committee of Medical Journal Editors (https://www.icmje.org/). Authors are expected to adhere to these standards.

It is the author's responsibility to ensure that a patient's anonymity is carefully protected and to verify that any experimental investigation with human subjects reported in the manuscript was performed with informed consent and followed all the guidelines for experimental studies with human subjects required by the institution(s) with which all the authors are affiliated. Authors should mask patients' eyes, private parts and remove patients' names from all figures. Editorial board of the Turkish Neurosurgery

have the right to demand ethical committee forms or informed consent forms **at any stage of the submission and publication.** All animal experiments should comply with the ARRIVE guidelines https://www.nc3rs.org.uk/arrive-guidelines. Also, Editorial board of the Turkish Neurosurgery have the right to withdraw any paper, even it is accepted, if there is any ethical issue.

Authorship should be limited to those who have made a significant contribution to the conception, design, execution, or interpretation of the reported study. The authors should ensure that they have written entirely original works, and if the authors have used the work and/or words of others, that this has been appropriately cited or quoted. Editorial board of the Turkish Neurosurgery have the right to withdraw any paper if there is any plagiarism. All submissions must include disclosure of all relationships that could be viewed as presenting a potential conflict of interest. All authors must disclose any financial and personal relationships with other people or organizations that could inappropriately influence (bias) their work. Examples of potential competing interests include employment, consultancies, stock ownership, honoraria, paid expert testimony, patent applications/registrations, and grants or other funding. Authors must disclose any interests in the disclosure and conflicts of interest section of the main document.

Authorship Change

Authors are expected to consider carefully the list and order of authors before submitting their manuscript and provide the definitive list of authors at the time of the original submission. Any addition, deletion or rearrangement of author names in the authorship list after submitting the paper is **inappropriate and prohibited**. Authors should **withdraw** their paper if there is a need for authorship change.

Types of Manuscripts

Turkish Neuro-Excursion: The editor will invite experts for these special types of papers which may cover a broad spectrum in various fields of medicine, science, art, history, law as well as any important theme on actuality other than core neurosurgery. The number of words, figures, tables and references are not restricted.

Research (Original Investigation, Clinical and Experimental Studies): The main text should not exceed 4500 words **excluding the** references, tables, and figure legends for original articles, including randomized controlled trials, observational (cohort, case-control or cross-sectional) studies, diagnostic accuracy studies, nonrandomized behavioral and public health intervention trials, experimental animal trials and any other retrospective or prospective clinical or experimental studies. The number of figures, tables, videos and references are not restricted. The specifications for figures and video files are given.

Review Article: All review articles should be systematic reviews and meta-analyses. A systematic review protocol describes the rationale, hypothesis, and planned methods of the review. It should be prepared before a review is started and used as a guide to carry out the review. Turkish Neurosurgery no more accept papers as "Case Report and Review of the Literature". All systematic reviews and meta-analyses SHOULD COMPLY with **PRISMA** guidelines http://www.prisma-statement.org/. Systematic reviews and meta analyses SHOULD INCLUDE a **CONSORT** Flow Diagram http://www.consort-statement.org/consort-statement/flow-diagram. Any systematic review and meta-analysis without a CONSORT Flow Diagram will be rejected.

Case Report: Turkish Neurosurgery values **demonstrative and unique case reports** with **high quality figures**. A case report should be so clear and easy to understand that the reader could replicate the case in his/her daily practice. Word count must not exceed 1500 (excluding references, tables, and figure legends). Case reports cannot have more than 15 references, and 6 figures or tables. Turkish Neurosurgery **does not accept** papers as **"Case Report and Review of the Literature"** anymore.

Technical Note: Turkish Neurosurgery values **demonstrative technical notes** with **high quality figures**. Technical notes reinforced with high-quality anatomical studies are welcome. A technical note should be so clear and easy to understand that the reader could replicate the technique in the operating room or on cadaveric specimen. The number of words must not exceed 2000, and there should not be more than 20 references. The number of figures and tables are not restricted.

Letter to the Editor: Letters should refer to the title and authors of a recent Turkish Neurosurgery article. The letter should be no longer than 300 words with no more than 3 references. Unpublished data should not be used Letters to the Editor are sent to the article authors for response. The Editor-in-Chief makes the final decision on whether letters to the editor and the responses are published.

References

The authors are responsible for the accuracy of the references. Key the references (double-spaced) at the end of the manuscript. Cite references in the text in alphabetical order within parentheses. Do not link the references to the text. Cite unpublished data, such as papers submitted but not yet accepted for publication or personal communications, in parentheses in the text (please be sure that such have a DOI number to be presented). **Do not use "et al." in the references.** List all the authors of the reference. Refer to the List of Journals Indexed in Index Medicus for abbreviations of journal names, or access the list at "http://www.nlm.nih.gov/tsd/serials/lji.html. The DOI numbers are mandatory in accordance with the library indexes; please be sure to present the DOI numbers for each reference at the end of its sentence. The reference styles for Zotero and EndNote are available on the journal's home page.

Sample references are given below:

A. Journal article

Umeoka K, Mizunari T, Murai Y, Kobayashi S, Morita A: Occlusion of the ascending pharyngeal artery during carotid artery surgery: Importance and technique. Turk Neurosurg 24: 546-548, 2014. https://doi.org/10.5137/1019-5149.JTN.9527-13.0

B. Book chapter

Martin A: Literacies for the digital age. In: Martin A, Madigan D (eds), Digital literacies for learning. Facet, 2006:3-25. DOI: https://doi.org/10.29085/9781856049870.003

C. Entire book

Smith T, Williams BM, Streefkerk R: The citation manual for students: A quick guide (2nd ed). Wiley, 2020. https://doi.org/10.1000/182

D. Example of thesis

Kanpolat Y: Experimental percutaneous access to the trigeminal ganglion and the histopathological evaluation of radiofrequency thermic lesion (Unpublished dissertation), Ankara: Ankara University, 1978:1- 52

E. Software

Epi Info [computer program]. Version 6. Atlanta: Centers for Disease Control and Prevention, 1994

F. Online journals

Friedman SA. Preeclampsia: A review of the role of prostaglandins. Obstet Gynecol [serial online]. January 1988;71:22-37. Available from: BRS Information Technologies, McLean, VA. Accessed December 15, 1990

G. Database

CANCERNET-PDQ [database online]. Bethesda, MD: National Cancer Institute, 1996. Updated March 29, 1996

H. World Wide Web

Gostin LO. Drug use and HIV/AIDS [JAMA HIV/AIDS web site]. June 1, 1996. Available at: http://www.ama-assn.org/ special/ hiv/ ethics. Accessed June 26, 1997

ARTIFICIAL INTELLIGENCE USAGE POLICY

Permitted Uses of Artificial Use (AI) Tools: Authors may use generative AI tools (e.g. ChatGPT, Bing Chat, Bard, etc.) to assist with certain aspects of manuscript preparation – for example, to improve grammar and readability, to brainstorm research questions, or to summarize background literature – provided that these tools are used responsibly and with human oversight. AI can be a helpful aid for editing and idea generation, but it must not replace the authors' own critical analysis and writing.

Authorship and Accountability: AI tools cannot be listed as an author or co-author under any circumstances. All authors listed on the paper must be human and must meet the International Committee of Medical Journal Editors (ICMJE) authorship criteria (having made substantial contributions, written or revised the text, and able to take responsibility for the work). The human authors take full responsibility for all content of the manuscript, including any portions that may have been AI-assisted. If errors, biases, or plagiarism are found in the content – even if introduced by an AI – the authors will be held accountable.

Mandatory Disclosure of AI Usage: Authors are required to disclose any use of AI in the creation of their manuscript. During submission, the corresponding author will need to answer a checkbox/question about AI use (e.g. "Did you use any generative AI or AI-assisted tools during the writing or preparation of this manuscript?"). If the answer is "Yes," the author must provide a brief description of how and where AI was used.

Location of Disclosure in Manuscript: In addition to the submission form, authors must insert an "AI Assistance Statement" in the manuscript itself. This should be placed at the end of the manuscript (just before the References) under a separate heading, for example: "Declaration of Generative AI Use."

Content of the Disclosure: The disclosure statement should identify the AI tool and version, and describe the specific purpose and section of the manuscript for which it was used. For instance: "Declaration of Generative AI Use: During the preparation of this article, the authors used ChatGPT (GPT-4, OpenAI, September 2025) to refine the English language in the Introduction and Discussion sections. The AI was not used to generate any scientific conclusions or new content, but only to improve readability. After using this tool, the authors thoroughly reviewed and edited the text to ensure accuracy and originality, and take full responsibility for the content of this manuscript."*.

This example can be adapted as needed. The key is to include which tool, for what purpose/section, and a confirmation of author oversight (i.e., that the authors reviewed and approve the AI-influenced content). Minor uses of software for spell-checking or reference formatting do not need to be declared.

Limitations on AI Use: Authors should not use AI tools to generate original scientific content or to circumvent the scholarly work. In particular:

No Generative AI for Data Analysis without Disclosure: If an AI or algorithm is part of the research (for example, analyzing images or data sets), this should be described in the Methods like any other tool.

No AI-Generated Figures or Images: Do not use AI image generators to create figures, diagrams, or any visual element of the paper, unless this is part of the study itself and is explicitly described in the Methods. Any inadvertent AI modifications to images (beyond standard brightness/contrast adjustments) are not allowed. Editors may request original image data to verify integrity.

No Undisclosed AI Text: All text must be either written by the authors or, if AI-assisted, disclosed as described. Do not submit a manuscript composed wholly by an AI – this is not acceptable and would be treated as academic misconduct (similar to plagiarism).

Confidentiality and Ethics: Do not feed sensitive or confidential information (such as unpublished data, patient details, or identifiable personal information) into any AI service unless it's in accordance with privacy laws and ethical guidelines. Many AI tools may store or reuse input data, so use them with caution regarding confidential content.

Enforcement: Submissions will be checked for compliance. Omission of a required AI disclosure or false statements about AI use will be treated seriously. It could lead to rejection of the manuscript or, if discovered later, a correction or retraction, as it violates publication ethics. Conversely, transparent disclosure of AI assistance will not negatively impact the editorial decision; it will simply be noted in the final publication to inform readers. Our journal's stance is that honesty about the use of new tools is always the best policy.

Continual Policy Updates: Finally, this is an evolving area. The journal will regularly review and update these AI usage guidelines in line with COPE recommendations and industry best practices. Any future changes will be communicated to authors via updated instructions for authors.

In summary, our neurosurgery journal will permit the limited use of AI tools in manuscript writing only with proper disclosure and human oversight. Authors must state explicitly if and how AI was used in preparing their paper, and they remain fully responsible for the integrity of their work. Under no circumstances can an AI be an author, or can AI-generated material be presented as original human work. This policy follows the lead of major journals like Nature and World Neurosurgery, which similarly require authors to report AI assistance and forbid AI authorship. By implementing these guidelines, we aim to embrace beneficial innovations while

upholding the rigor, ethics, and transparency expected in scientific publishing. Of note, The Editorial Board have the right to request revisions or withdraw any paper if there is any misuse of AI.

Biswas, SS. ChatGPT-for-Research-and-Publication-A-Step-by-Step Guide. (https://meridian.allenpress.com/jppt/article/28/6/576/496601/ChatGPT-for-Research-and-Publication-A-Step-by)(https://doi.org/10.5863/1551-6776-28.6.576)

Ramoni D, Sgura C, Liberale L, Montecucco F, Ioannidis JPA, Carbone F. Artificial intelligence in scientific medical writing: Legitimate and deceptive uses and ethical concerns. European Journal of Internal Medicine, Volume 127, 31 - 35

PEER REVIEW PROCESS

This journal uses double-blind review, which means that both the reviewer and author identities are concealed from the reviewers, and vice versa, throughout the review process.

1. Manuscript Submission

The corresponding or submitting author submits the paper to the journal through http://turkishneurosurgery.org.tr/.

2. Assessment of the Paper for Journal Requirements

The editorial office checks the paper's composition and arrangement against the journal's Author Guidelines - Instruction to the Authors (http://turkishneurosurgery.org.tr/static.php?id=7) - to make sure it includes the required sections and stylizations.

3. Evaluation by the Editor-in-Chief (EIC)

The EIC checks the paper's scientifical appropriateness for the journal, its originality and actuality. If not, the paper may be rejected without being reviewed any further.

4. EIC Assigns a Section Editor (SE)

Section Editors handle the peer review process. All manuscripts that reach this step will go through a double-blind peer-review process. In order to ensure an unbiased evaluation process, each submission will be reviewed by at least two external, independent peer reviewers who are experts in the field.

5. Invitation to Reviewers

The SE sends invitations to individuals he or she believes would be appropriate reviewers. As responses are received, further invitations are issued, if necessary, until the required number of acceptances is obtained.

6. Response to Invitations

Potential reviewers consider the invitation against their own expertise, conflicts of interest and availability. They then accept or decline.

7. Review is Conducted

The reviewer sets time aside to read the paper several times. The first read is used to form an initial impression of the work. If major problems are found at this stage, the reviewer may feel comfortable rejecting the paper without further work. Otherwise they will read the paper several more times, taking notes so as to build a detailed point-by-point review. The review is then submitted to the journal, with a recommendation to accept or reject it – or else with a request for revision (either major or minor) before it is reconsidered.

8. Journal Evaluates the Reviews

The SE considers all the returned reviews before making an overall decision. If the reviews differ widely, the editor may invite an additional reviewer so as to get an extra opinion before making a decision.

9. The Decision is Communicated

The EIC is the final authority in the decision-making process for all submissions. He or She sends a decision e-mail to the author including any relevant reviewer comments.

AFTER ACCEPTANCE

Online Proof Correction

Corresponding authors will receive an e-mail including final PDF version of their manuscript. Authors are obligated to proofreading their manuscript in 72 hours.

Turkish Neurosurgery workflow processes to get your article published quickly and accurately. Please use this proof only for checking the typesetting, editing, completeness and correctness of the text, tables and figures. Significant changes to the article as accepted for publication will only be considered at this stage with permission from the Editor. It is important to ensure that all corrections are sent back to us in one communication. Please check carefully before replying, as inclusion of any subsequent corrections cannot be guaranteed. Proofreading is solely your responsibility. **Authorship change is not accepted during proofreading and is prohibited.**

Rapid Publication Option

In accordance with the Turkish Neurosurgical Society's Board Decision on August 5, 2023, "Turkish Neurosurgery" journal is starting to publish articles with a rapid publication option (RPO). This type of publication choice will have no effect on the peer review process or acceptance of the submission since it will be requested by the authors after acceptance of the article.

What is RPO?: The RPO ensures the accepted article will be immediately prepared in electronic format (e-pdf), and it will be printed in one of the upcoming issues of the journal. This service has a publication fee that needs to be met by the authors, their institutions, or the research funders for each article that is published in a timely manner. The decision for RPO will be made by the authors, and they will only be charged upon their requests and if their paper is accepted. As there is a limited space for such option in each publishable issue, this process will be granted on a first-come, first-served basis, and the Turkish Neurosurgical Society is responsible for organizing the demands and informing the Editorial Board as well as the Publisher.

Why RPO?: There is a waiting list, and the number of articles per issue is constant and limited. It generally takes 6–14 months for a research paper to be published in a printed journal. This service allows immediate publication of the article in both electronic and printed formats. Of note, the printed article will be published in one of the upcoming issues of the journal.

Please be sure to use the RPO service and contact the society, even if you are in early need of an e-pdf manuscript.

Benefits of RPO: Here, it's important to make sure that articles are published as soon as possible, are subject to the proper quality controls, and are extensively read. By using RPO, the authors are able to publish their ideas faster, receive credit for the idea and the manuscript, get ready to strengthen their enrollment for future applications and grants, and last but not least, have increased visibility in a quick-paced setting.[1]

[1] https://www.editage.com/insights/publish-faster-progress-faster-the-basics-of-rapid-publication

RPO Price and Communication Details: The RPO charge for the journal is EUR 1000/article, including taxes.

This service is carried out by Turkish Neurosurgical Society. Please contact with: Turkish Neurosurgical Society, Taskent Caddesi 13/4 06500 Bahcelievler, Ankara/TÜRKİYE

E-mail: info@turknorosirurji.org.tr

Reprints

Reprint requests should be faxed or e-mailed with the corrected proofs by the corresponding author, if needed. Reprints are normally shipped 6 to 8 weeks after publication of the issue in which the item appears.

Contact with the Publisher: Bulus Tasarim, Mebusevleri Mah. Turgut Reis Cad. 11/1, Çankaya, Ankara, TÜRKİYE.

E-mail: bulus@bulustasarim.com.tr

The price for 2 sets of hardcopy journal*:

Within Türkiye 1500 TL (shipping costs not included);
Outside Türkiye 40 € (shipping costs not included)

**Depend on shipping cost. Please contact Bulus Tasarim.*

Manuscript Checklist (before submission. For author reference only)

1. ORCID identifier (ID) is required for all authors during the submission process. ORCID ID can be obtained free of charge at http://orcid.org	☐
2. E-mail address of all authors should be provided during the submission process.	☐
3. Title page	
Title (brief, definite, didactic)	☐
Corresponding author designated, and full mailing address included on title page	☐
E-mail address of corresponding author included on title page	☐
Running head	☐
Approval of Institutional Review Board (Decision No/Date) and/or signed patient consent forms	☐
Permission to reproduce copyrighted material	☐
Acknowledgements listed for grants, technical support, and corporate support on title page	☐
4. Structured abstract with key words (300 words)	☐
5. Manuscript text with page numbers [Microsoft Word (.doc)] (without author names and affiliations)	☐
6. Figure legends	☐
7. Tables (Word, Wordperfect)	☐
8. Figures (TIFF)	☐
9. Videos (avi, mpeg, mp4) with narration and/or subtitles	☐
10. References double-spaced and cited in alphabetical order	☐

CONTENTS

Turkish Neurosurgery

Volume: 36 Number: 3 Year: 2026

SYSTEMATIC REVIEW

ORIGINAL INVESTIGATIONS

■ Cerebrovascular-Endovascular

■ Neuro-Oncology

■ Spine and Peripheral Nerves

Turk Neurosurg 36(3):341-348, 2026
DOI: 10.5137/1019-5149.JTN.49284-25.1

Systematic Review

Received: 14.06.2025
Accepted: 04.09.2025
Published Online: 22.05.2026

Endovascular Treatment Versus Medical Management in Patients with Large Vessel Occlusion and Pre-Stroke Disability: A Systematic Review and Meta-Analysis

Tian-Yi ZHANG[1], Dian LI[1], Yi-Qiao HU[1], Heng-Zhu ZHANG[2,3]

[1]School of Life Sciences, Nanjing University, Nanjing, China
[2]Northern Jiangsu People's Hospital Affiliated to Yangzhou University, Department of Neurosurgery, Yangzhou, China
[3]Northern Jiangsu People's Hospital, Department of Neurosurgery, Yangzhou, China

Corresponding author: Heng-Zhu ZHANG ✉ zhanghengzhu@sina.com

ABSTRACT

AIM: To assess the effectiveness and safety of endovascular treatment (EVT) versus medical management (MM) in stroke patients with premorbid disabilities.

MATERIAL and METHODS: A systematic search was conducted in PubMed, Embase, and the Cochrane Library for studies on EVT in large vessel occlusion (LVO) patients with pre-stroke modified Rankin Scale (mRS) score of 2-4. The primary outcome was functional recovery, defined as returning to at least the pre-stroke mRS score within 90 days. The secondary outcomes included symptomatic intracranial hemorrhage (sICH) and 90-day mortality. The meta-analyses were conducted via random effects models.

RESULTS: Six cohort studies involving 2,106 patients were included. Compared with MM, EVT was associated with a higher likelihood of functional recovery (adjusted odds ratio [aOR], 3.26; 95% confidence interval [CI], 2.26-4.70; p<0.001) and lower risk of mortality (aOR, 0.40; 95% CI, 0.20-0.83; p=0.01). EVT was also associated with a potentially increased risk of sICH, although the difference did not reach statistical significance (aOR 2.47, 95% CI 0.81-7.52; p=0.11).

CONCLUSION: Although EVT may be associated with a higher potential risk of sICH, it improves the likelihood of functional recovery and reduces mortality in LVO patients with pre-stroke disability. Therefore, denying EVT solely on the basis of premorbid disability may be unjustified. Further high-quality randomized controlled trials are warranted to validate these findings.

KEYWORDS: Ischemic stroke, Disabled persons, Thrombectomy, Outcomes

ABBREVIATIONS: AIS: Acute ischemic stroke, **LVO:** Large vessel occlusion, **EVT:** Endovascular treatment, **BMM:** Best medical management, **mRS:** Modified rankin scale, **sICH:** Symptomatic intracranial hemorrhage, **CI:** Confidence interval, **RR:** Risk ratio, **NIHSS:** National institutes of health stroke scale

INTRODUCTION

Large vessel occlusion (LVO) leading to acute ischemic stroke (AIS) is a significant cause of disability worldwide (11). Endovascular treatment (EVT) has become the standard of care for reducing disability associated with LVO-related AIS (1). However, a significant proportion of LVO-AIS patients have pre-existing disabilities, known as pre-stroke disabilities, with nearly one-third of those undergoing EVT in clinical practice having baseline pre-stroke disabilities (4,12). Unfortunately, these patients are often excluded from randomized controlled trials (RCTs) because their prestroke modified Rankin Scale (mRS) scores (≥2) pose challenges to the traditional definition of favorable outcomes, which rely on

Tian-Yi ZHANG : 0009-0007-0426-802X
Dian LI : 0009-0007-4506-2802
Yi-Qiao HU : 0000-0002-3656-7143
Heng-Zhu ZHANG : 0000-0003-3240-5689

binary measures in clinical trials (9). Existing guidelines for treating patients with mRS scores ≥2 lack explicit strategies, and there is significant variability in EVT practices for this population, with decisions often being based on clinical judgment. This creates a therapeutic dilemma for stroke physicians managing patients with mRS scores ≥2 (5,7). Therefore, stroke physicians face a therapeutic dilemma when managing patients with mRS scores ≥2. Therefore, it is imperative to select the optimal treatment to ensure timely, successful vascular reperfusion and improve clinical outcomes for these patients.

While previous systematic reviews have provided insights, they did not include a control group receiving medical management (MM), limiting the ability to determine differences in outcomes related to the intervention. This study aims to evaluate whether EVT is superior to MM in terms of safety and effectiveness in patients with pre-stroke disabilities, providing clinicians with guidance for acute stroke treatment in this specific population.

MATERIAL and METHODS

This systematic review and meta-analysis were conducted in accordance with the Preferred Reporting Items for Systematic Reviews and Meta-Analyses (PRISMA) guidelines (1). The study protocol was prospectively registered in the international prospective register of systematic reviews (PROSPERO) with registration number CRD42023443307.

Selection Criteria

Comparative studies with English texts that met the following PICO (Patient, Intervention, Comparator, and Outcome) criteria were considered eligible for inclusion (2).

Patients: Individuals aged ≥18 years with pre-stroke disability of LVO-AIS who had pre-stroke, defined as an mRS score of 2-4.

Intervention: Receiving EVT.

Comparison: Receiving MM.

Outcomes: The primary outcome was functional recovery, which was defined as a return to at least the pre-stroke mRS score at 90 days. The secondary outcomes included symptomatic intracranial hemorrhage (sICH) and mortality at 90 days.

Search Strategy

Our search was last updated on 1 July 2023 to ensure that there were no new studies meeting the eligibility criteria. The search keywords used were as follows: (“prestroke” or “pre-stroke” or (“stroke” and (“premorbid” or “premorbid” or “pre-existing” or “preexisting” or “previous” or “baseline”))); (“morbidity” or “mobility impairment” or “disability” or “disabilities” or “dependence” or “dependent” or “dependency”); and (“reperfusion therapies” or “reperfusion treatments” or “endovascular therapy” or “endovascular treatment” or “intra-arterial therapy” or “intra-arterial treatment” or “endovascular thrombectomy” or “mechanical thrombectomy” or “intra-arterial thrombectomy” or “MT” or “EVT” or “IAT”).

Data Extraction

Two authors (T.-Y.Z. and D.L.) independently extracted information on study characteristics (first author, year of publication, study period, country, study design, number of institutions, population included, and number of patients), patient characteristics (age, sex, National Institutes of Health Stroke Scale), and clinical outcomes. When duplicate reports of the same study were found, the data were analyzed from the most complete dataset. Objections were adjudicated by the senior author (H.-Z. Z.).

Risk of Bias Assessment

The quality of the included studies was assessed via the Newcastle-Ottawa Scale (NOS) research checklist, which evaluates the selection, comparability, and outcomes of both case-control and cohort studies (3). Each study was reviewed and scored in three categories: selection of study groups (0-4 points), comparability (0-2 points), and assessment of outcomes (0-3 points), with a maximum possible score of 9 points. A score of ≥8 indicates a low risk of bias, a score of 6-7 indicates a moderate risk of bias, and a score of ≤5 indicates a high risk of bias. Potential discrepancies were resolved through discussions with the senior author (H.Z.Z.). Both reviewers (T.Y.Z. and D.L.) independently assessed the quality of all included studies, and any differences were resolved by consensus. See Table I for details.

Statistical Analysis

To derive the odds ratio (OR) from reported binary outcomes comparing EVT and BMM, we performed a meta-analysis via the Mantel-Haenszel method. The results were presented as relative risks with corresponding 95% confidence intervals (CIs). To account for variability both within and between studies, we used a random effects model for this meta-analysis. Heterogeneity among studies was assessed via Cochran’s Q statistic and the I^2 statistic. I^2 values exceeding 50% were interpreted as indicating significant heterogeneity, whereas values over 75% were considered indicative of considerable heterogeneity. A sensitivity analysis was conducted for all outcomes after adjusting for potential confounding factors. Owing to the inclusion of fewer than 10 studies in our analysis, we did not perform a publication bias assessment or meta-regression analysis. All the statistical analyses were conducted via Review Manager (RevMan) version 5.3, which was developed by the Cochrane Collaboration and is located at the Nordic Cochrane Centre in Copenhagen.

RESULTS

Overview of Included Studies

The initial search identified 1,495 records, with 357 duplicates. After reviewing the titles and abstracts, 1,120 records were excluded. A detailed examination of the remaining 18 full-text articles led to the inclusion of 6 studies in this systematic review and meta-analysis. These studies involved a total of 2,106 AIS stroke patients and compared MM with EVT (Figure 1).

Table I: Quality Assessment of the Included Studies

Article	Selection				Comparability	Outcome			Scores
	Representati-veness of the exposed cohort	Selecting of the non exposed cohort	Ascertainment of exposure	Demonstration that outcome of interest was not present at start of study	Control on the basis of the design or analysis	Asssessment of outcome	Was follow-up long enough for outcomes to occur	Adequacy of follow up of cohorts	
Kastrup et al., (6)	★	★	★	★	★	★		★	7
Sprugel et al., (11)	★	★	★	★	★★	★	★	★	9
Sykora et al., (13)	★	★	★	★	★★	★	★	★	9
Tanaka et al., (14)	★	★	★	★	★★	★	★	★	9
Siegler et al., (10)	★	★	★	★	★★	★	★	★	9
Miyake et al., (8)	★	★	★	★	★	★	★	★	8

Newcastle-Ottawa Scale for assessing the quality of studies in meta-analysis.

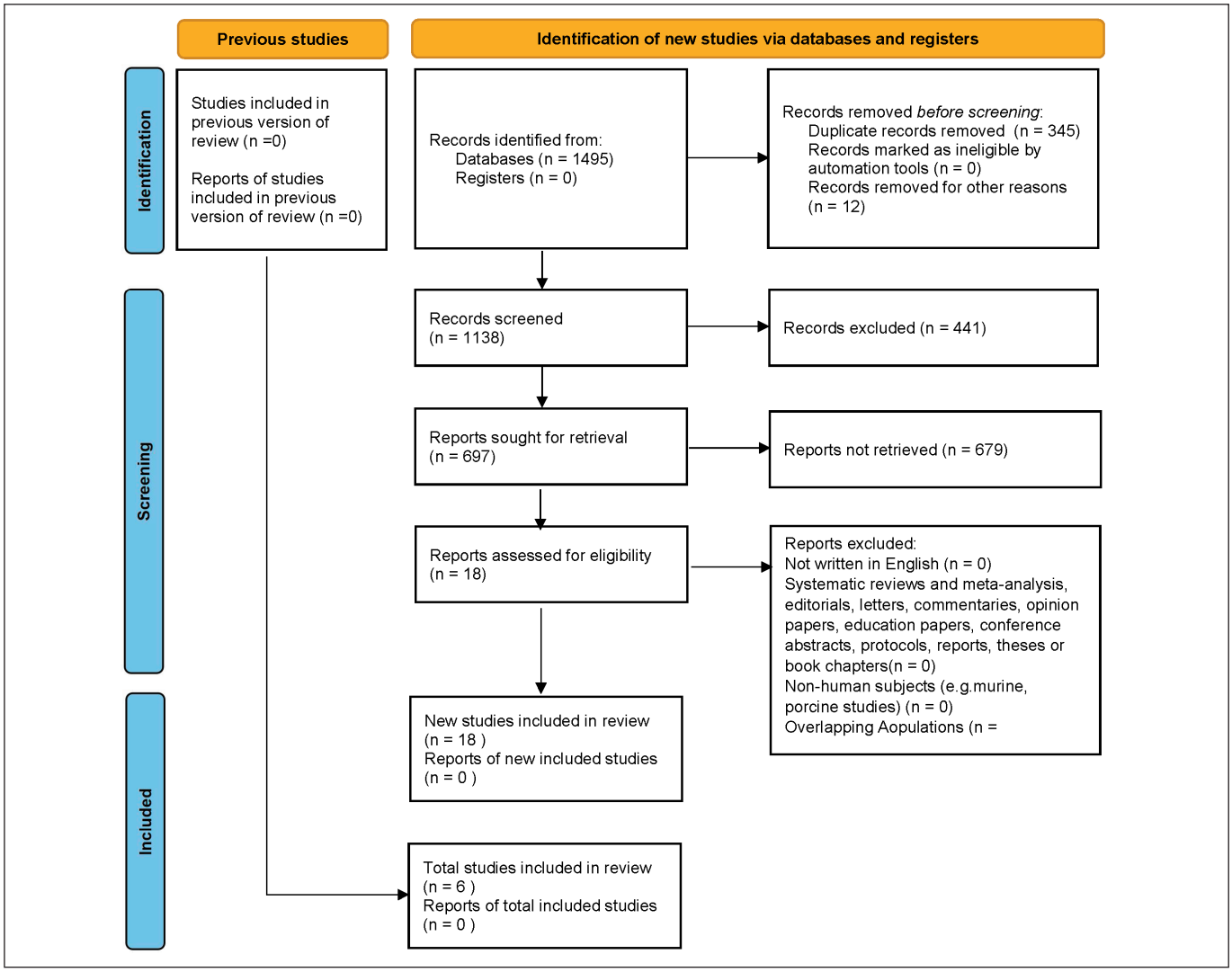

Figure 1: Study selection.

All studies included in this analysis were non-randomized, multicenter, retrospective cohort studies, with data collected from high-volume neurointerventional centers across five countries: Germany, Japan, Austria, Switzerland, and the United States. The risk of bias was evaluated via the Newcastle-Ottawa Scale (Table I), and all six studies achieved a score of 7 or higher, indicating generally good quality.

Study Characteristics and Patient Demographics

The study included 2,106 acute stroke patients aged 18 years or older, all of whom had been treated for previous proximal LAO involving the intracranial proximal internal carotid artery and/or the M1 and/or M2 segments of the middle cerebral artery, accompanied by disabling symptoms. Among these patients, 1,300 received MM, while 806 were receiving drug treatment. Table II provides a comprehensive description of the baseline characteristics of these patients. The management of each patient followed the BAO International Ischemic Stroke Management Guidelines. The control group consisted of patients who did not undergo thrombectomy during hospitalization and who received only medical treatment, whereas the intervention group included patients who underwent standard thrombectomy during their hospital stay.

The Primary Outcome was a Return to at Least the Pre-Stroke mRS Score

Among the six studies, four reported functional recovery outcomes and were included in the meta-analysis, involving 1560 pre-stroke disabled patients (with 900 receiving EVT and 660 receiving MM) (10,11,13,14). The pooled analysis for this group of AIS patients indicated that, compared with MM, EVT may be a higher likelihood of functional recovery at 90 days (OR=2.62; 95% CI, 1.53-4.49; p<0.001; Figure 2A), with a significant level of study heterogeneity and statistical significance (I^2=65%, p=0.04). The sensitivity analysis, adjusted for potential confounding factors, indicated the robustness of the

Table II: Pooled Baseline Characteristics of Included Patients

Author	Year	Definition of premorbid disability and control groups		Patients (n)	Age (median) (years)	Female, %	Return to baseline mRS, n (%)	sICH, n (%)	90-day mortality, n (%)
Tanaka et al., (14)	2021	EVT	2	70	82	65.1	49 (28.0)	6 (3.0)	31 (18.0)
			3	54					
			4	51					
		BMM	2	42	87	75.0	18 (11.0)	2 (1.0)	44 (27.0)
			3	54					
			4	68					
Sykora et al., (13)	2022	EVT	3	136	79.4±12.2	62.3	47 (27.0)	7 (4.0)	76 (43.0)
			4	33					
			5	6					
		BMM	3	185	85.2±8.8	65.2	58 (20.0)	6 (2.0)	180 (63.0)
			4	83					
			5	19					
Sprugel et al., (11)	2022	EVT	3	82	82	72.5	20 (20.0)	6 (6.0)	54 (53.0)
			4	20					
		BMM	3	80	81	72.8	8 (8.0)	1 (1.0)	76 (74.0)
			4	23					
Siegler et al., (10)	2022	EVT	2~4	448	82	66.3	118 (26.0)	31 (7.0)	170 (38.0)
		BMM	2~4	106		/	8 (8.0)	0 (0.0)	48 (45.0)
Kastrup et al., (6)	2021	EVT	3~4	142	83 ± 8	/	/	12 (8.0)	31 (22.0)
		BMM	3~4	89	86 ± 7	/	/	7 (8.0)	22 (25.0)
Miyake et al., (8)	2023	EVT	2~3	258	82.2 ± 0.7	60.1	/	/	55 (21.3)
		BMM	2~3	57	83.4 ± 1.4	68.4	/	/	9 (15.8)

EVT: *Endovascular treatment,* ***BMM:*** *Best medical management.*

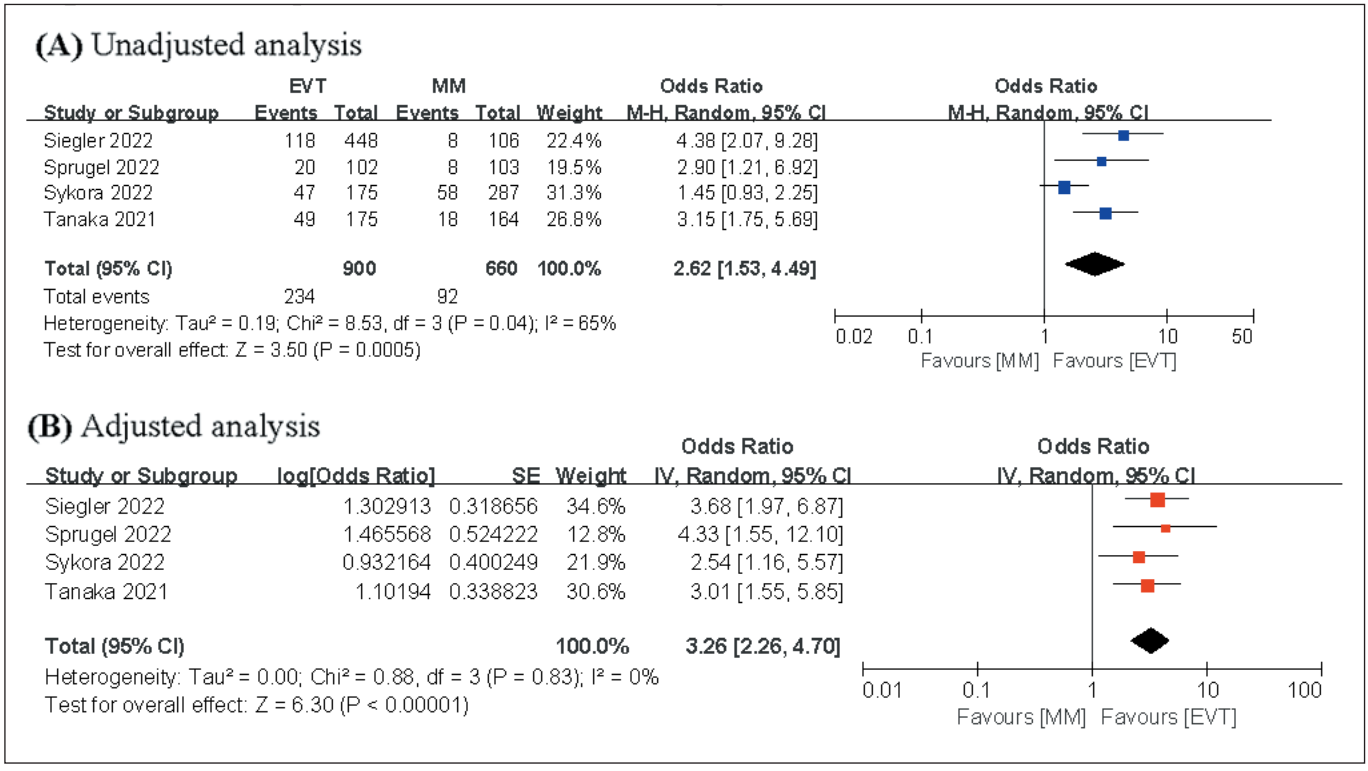

Figure 2: Forest plots for functional recovery.

outcome related to functional recovery (4 studies; adjusted OR [aOR]=3.26; 95% CI, 2.26-4.70; p<0.001; I^2 =0%; Figure 2B).

Secondary Outcomes: 90-Day Mortality and sICH Outcomes

All six studies, comprising a total of 2106 patients (1300 receiving EVT and 806 receiving MM), provided data on the 90-day mortality rate for pre-stroke disabled patients (6,8,10, 11,13,14). Specifically, the EVT group presented a lower 90-day mortality rate (OR=0.64; 95% CI, 0.47-0.88; p=0.006; Figure 3A). Notably, there was minimal heterogeneity and relatively significant statistical significance between the studies (I^2=54%, p=0.05). The sensitivity analysis indicated the robustness of the outcome related to the 90-day mortality rate (4 studies; aOR=0.40; 95% CI, 0.20-0.83; p=0.01; I^2 =62%; Figure 3B).

Among the five studies involving 1791 pre-stroke disabled patients (with 1042 receiving EVT and 749 receiving MM), data were available to assess the occurrence of sICH (6, 10,11,13,14). In terms of the rate of sICH, the EVT group demonstrated a higher risk than the MM group did (OR=2.28; 95% CI, 1.03-5.01; p=0.04), as illustrated in Figure 4A. In this case, heterogeneity was also relatively low (I^2= 29%, p=0.23). In contrast, the sensitivity analysis adjusted for confounding factors suggested a potentially higher incidence of sICH in the EVT group than in the MM group. However, the difference did not reach statistical significance (2 studies; aOR=2.47; 95% CI, 0.81-7.52; p=0.11; I^2 =4%; Figure 4B).

DISCUSSION

Our meta-analysis focused exclusively on cohort studies retrieved from databases that included patients with pre-stroke disability. The aim was to provide evidence-based treatment data specifically for this patient population. These findings suggest that, compared with MM, EVT may be associated with a higher likelihood of functional recovery and lower mortality. No significant difference was observed in the incidence of sICH after adjusting for potential confounders.

After the search, we systematically reviewed six studies involving a total of 2106 patients. The controlled studies in this review indicated that, for acute ischemic strokes caused by AIS-LVO, patients who received EVT had a better prognosis in terms of recovering baseline functionality than did those who received MM. Notably, EVT demonstrated superior efficacy in achieving a reduction in mRS scores for pre-stroke disabled patients within 90 days compared with conventional drug therapy, leading to a lower mortality rate. Additionally, the EVT group also presented a greater probability of intracranial hemorrhage within 90 days. A prior observational study by Ganesh et al. also suggested that a significant proportion of pre-stroke disabled patients may recover to their pre-stroke state after surgery, without indicating a higher incidence of treatment-related complications or supporting the routine exclusion of these patients from thrombectomy procedures (4). The study by Bala et al. yielded similar results, but in comparison with the two included studies, our study had a larger sample size, conducted a systematic review and data analysis of EVT versus MM, and provided more comprehensive data, thereby enhancing the persuasiveness of the results (1).

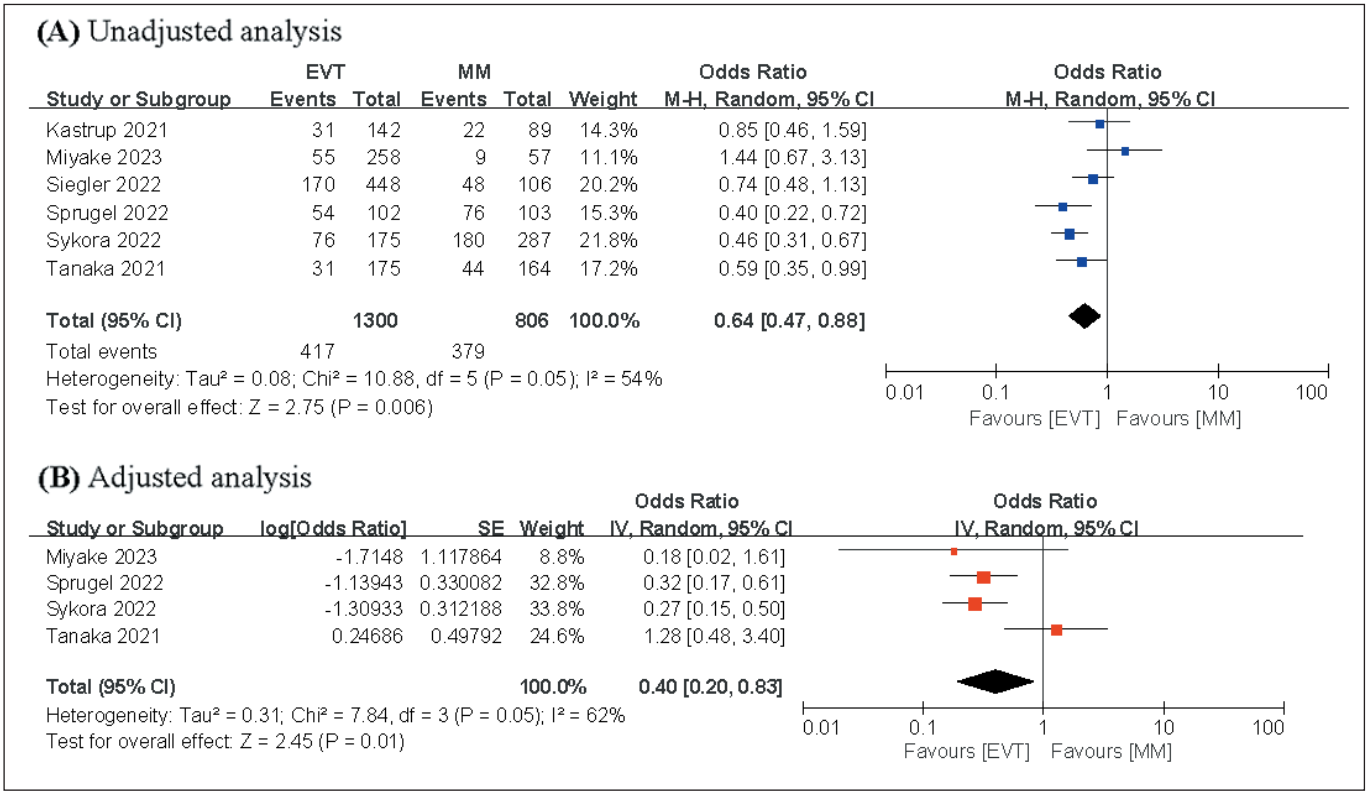

Figure 3: Forest plots for mortality.

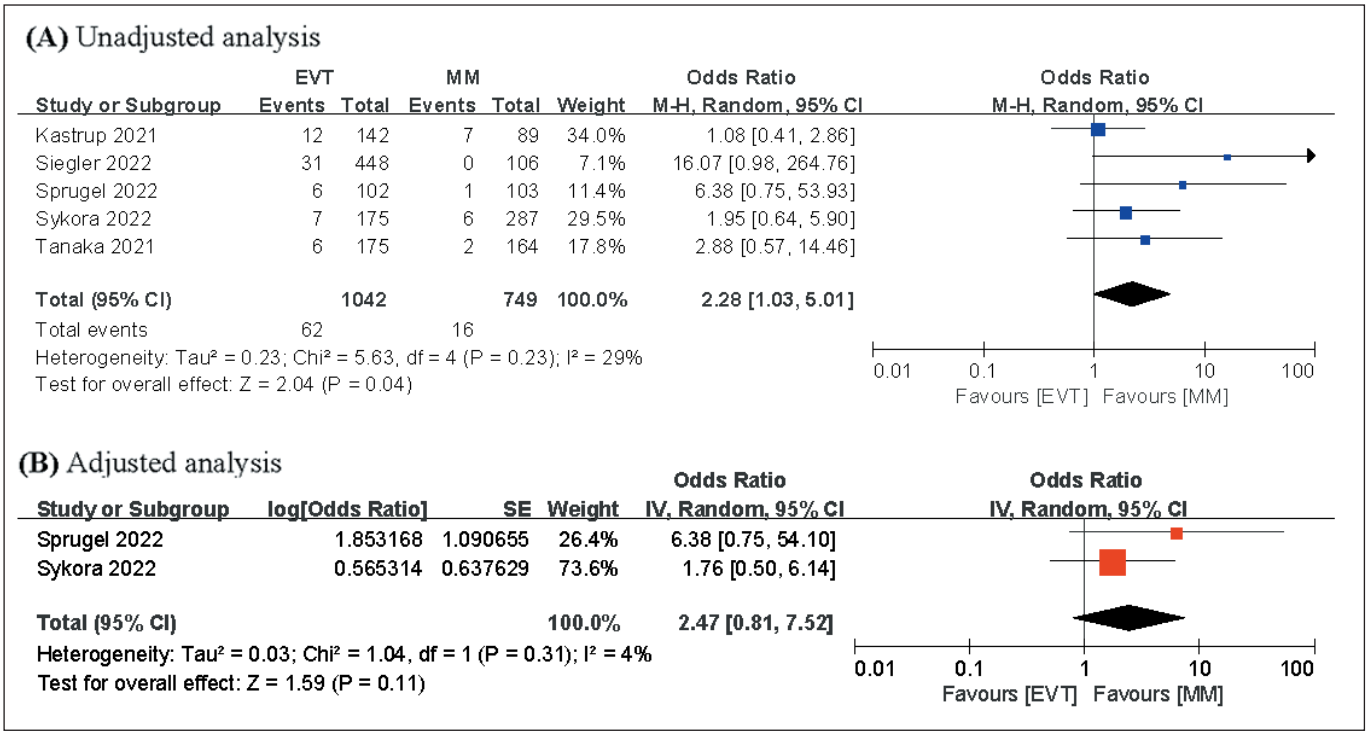

Figure 4: Forest plots for symptomatic intracranial hemorrhage.

However, the proportion of pre-stroke disabled patients within the stroke patient population is relatively small, hindering research efforts directed at this subset. Given that disability and stroke risks often increase in disabled patients, addressing this subset is crucial. With further research in this field, we anticipate a more precise assessment of the impact of endovascular treatment on pre-stroke disabled patients, facilitating the formulation of more accurate treatment strategies.

Our meta-analysis has certain inherent limitations. The included studies were essentially retrospective and observational, introducing inherent limitations. There were some differences in the baseline characteristics between groups, preventing deeper subgroup analysis and matching studies. Patients usually receive medication therapy to maintain vascular patency before undergoing EVT. Unfortunately, details regarding the type and dosage of medication remain unclear, which could influence our research results. Furthermore, after a systematic literature search, only six studies met the inclusion criteria, yielding a moderately sized overall sample. The absence of primary outcome data in one report led to slightly larger discrepancies in the results. Owing to the limited sample size, further analyses exploring confounding factors, such as meta-regression and subgroup analyses, were not feasible, potentially affecting the reliability and generalizability of the study results. On the other hand, although interdisciplinary collaboration is crucial for the rehabilitation of stroke-disabled patients, current research largely focuses on specific disciplines and lacks a comprehensive perspective and approach to interdisciplinary cooperation.

In the coming years, research on stroke treatment, whether involving endovascular treatment or drug intervention, is expected to expand. Medical institutions may increasingly emphasize stroke treatment. This study offers a new approach for researching stroke treatment in specific patient populations, ultimately leading to more personalized and detailed interventions. As healthcare professionals draw experiences from clinical guidelines and the latest research findings, treatment prospects will become more refined, thereby improving patient outcomes. We also look forward to clinicians paying more attention to such special patients. Through in-depth research and precise intervention, significant improvements in treatment outcomes for pre-stroke disabled patients are anticipated, allowing more patients to return to normal life.

CONCLUSION

This meta-analysis demonstrated that EVT may be associated with a higher likelihood of functional recovery and lower risk of mortality in AIS patients with pre-stroke disabilities, challenging the traditional hesitation to treat this population aggressively. Our findings suggest that premorbid disability alone should not preclude consideration for EVT. These results have the potential to inform more inclusive treatment guidelines. However, the conclusions are limited by the small number of eligible studies and inherent confounding biases of observational designs. Future high-quality RCTs are urgently needed to strengthen the evidence base and guide optimal therapeutic strategies in this underserved subgroup of stroke patients.

Declarations

Funding: This study was supported by grants from the national natural science foundation of china (No. 82172603), the natural science foundation of jiangsu province (No. BK20190241), the scientific research project of jiangsu provincial health commission (H2018064) and the Cross Cooperation Project of Northern Jiangsu People's Hospital (SBIC21009).

Availability of data and materials: The datasets generated and/or analyzed during the current study are available from the corresponding author by reasonable request.

Disclosure: The authors declare no competing interests.

AUTHORSHIP CONTRIBUTION

Study conception and design: TYZ, YQH, HZZ
Data collection: TYZ, DL
Analysis and interpretation of results: TYZ, YQH, HZZ
Draft manuscript preparation: TYZ, YQH, HZZ
Critical revision of the article: TYZ, DL, YQH, HZZ
Other (study supervision, fundings, materials, etc...): TYZ, HZZ
All authors (TYZ, DL, YQH, HZZ) reviewed the results and approved the final version of the manuscript.

REFERENCES

1. Bala F, Beland B, Mistry E, Almekhlafi MA, Goyal M, Ganesh A: Endovascular treatment of acute ischemic stroke in patients with pre-morbid disability: A meta-analysis. J Neurointerv Surg 15:343-349, 2023. https://doi.org/10.1136/neurintsurg-2021-018573
2. Beland B, Bala F, Ganesh A: Thrombolysis for acute ischemic stroke in patients with premorbid disability: A meta-analysis. Stroke 53:3055-3063, 2022. https://doi.org/10.1161/STROKEAHA.121.038374
3. Chen VHE, Lee GKH, Tan CH, Leow AST, Tan YK, Goh C, Gopinathan A, Yang C, Chan BPL, Sharma VK, Tan BYQ, Yeo LLL: Intra-arterial adjunctive medications for acute ischemic stroke during mechanical thrombectomy: A meta-analysis. Stroke 52:1192-1202, 2021. https://doi.org/10.1161/STROKEAHA.120.031738
4. Ganesh A, Fladt J, Singh N, Goyal M: Efficacy and safety of mechanical thrombectomy in acute stroke patients with premorbid disability. Expert Rev Med Devices 19:641-648, 2022 https://doi.org/10.1080/17434440.2022.2124109
5. Ganesh A, Luengo-Fernandez R, Pendlebury ST, Rothwell PM: Long-term consequences of worsened poststroke status in patients with premorbid disability. Stroke 49:2430-2436, 2018. https://doi.org/: 10.1161/STROKEAHA.118.022416
6. Kastrup A, Roth C, Politi M, Alexandrou M, Hildebrandt H, Schroter A, Papanagiotou P: Endovascular therapy vs. thrombolysis in pre-stroke dependent patients with large vessel occlusions within the anterior circulation. Front Neurol 12:666596, 2021. https://doi.org/: 10.3389/fneur.2021.666596
7. Milionis H, Ntaios G, Korompoki E, Vemmos K, Michel P: Statin-based therapy for primary and secondary prevention of ischemic stroke: A meta-analysis and critical overview. Int J Stroke 15:377-384, 2020 https://doi.org/: 10.1177/1747493019873594

8. Miyake S, Akimoto T, Nakai Y, Amano Y, Yamamoto R, Amari K, Yamamoto T, Takeuchi M, Morimoto M, Tsuboi Y, Kaku S, Ayabe J, Akiyama T, Yamamoto D, Ito H, Onodera H, Takaishi S, Hasegawa Y, Ueda T: Efficacy and safety of thrombectomy for acute ischaemic stroke in patients with pre-stroke mRS scores of 2-3: Real-world evaluation from an open-label, prospective, multicentre, observational study. Interv Neuroradiol 31:778-785, 2023. https://doi.org/ 10.1177/15910199231185637
9. Scuteri D, Mantovani E, Tamburin S, Sandrini G, Corasaniti MT, Bagetta G, Tonin P: Opioids in post-stroke pain: A systematic review and meta-analysis. Front Pharmacol 11:587050, 2020. https://doi.org/10.3389/fphar.2020.587050
10. Siegler JE, Qureshi MM, Nogueira RG, Tanaka K, Nagel S, Michel P, Vigilante N, Ribo M, Yamagami H, Yoshimura S, Abdalkader M, Haussen DC, Mohammaden MH, Nannoni S, Mohlenbruch MA, Henon H, Sheth SA, Ortega-Gutierrez S, Olive-Gadea M, Caparros F, Seker F, Zaidi S, Castonguay AC, Uchida K, Sakai N, Puri AS, Farooqui M, Toyoda K, Salazar-Marioni S, Takeuchi M, Farzin B, Masoud HE, Kuhn AL, Rana A, Morimoto M, Shibata M, Nonaka T, Klein P, Sathya A, Kiley NL, Cordonnier C, Strambo D, Demeestere J, Ringleb PA, Roy D, Zaidat OO, Jovin TG, Kaesmacher J, Fischer U, Raymond J, Nguyen TN: Endovascular vs medical management for late anterior large vessel occlusion with prestroke disability: Analysis of CLEAR and RESCUE-Japan. Neurology 100:e751-e763, 2023. https://doi.org/10.1212/WNL.0000000000201543
11. Sprugel MI, Sembill JA, Kremer S, Gerner ST, Knott M, Hock S, Engelhorn T, Dorfler A, Huttner HB, Schwab S: Evaluation of functional recovery following thrombectomy in patients with large vessel occlusion and prestroke disability. JAMA Netw Open 5:e2227139, 2022. https://doi.org/10.1001/jamanetworkopen.2022.27139
12. Stockley RC, Jarvis K, Boland P, Clegg AJ: Systematic review and meta-analysis of the effectiveness of mental practice for the upper limb after stroke: Imagined or real benefit? Arch Phys Med Rehabil 102:1011-1027, 2021. https://doi.org/10.1016/j.apmr.2020.09.391
13. Sykora M, Michel P, Strambo D, Krebs S, Ferrari J, Posekany A, Miksova D, Hermann K, Gattringer T, Gizewski E, Deutschmann H, Neumann C, Lang W: Mechanical thrombectomy in acute stroke patients with moderate to severe prestroke disability. J Stroke 24:396-403, 2022. https://doi.org/: 10.5853/jos.2022.00906
14. Tanaka K, Yamagami H, Yoshimoto T, Uchida K, Morimoto T, Toyoda K, Sakai N, Yoshimura S: Endovascular therapy for acute ischemic stroke in patients with prestroke disability. J Am Heart Assoc 10:e020783, 2021. https://doi.org/10.1161/JAHA.121.020783

Turk Neurosurg 36(3):349-359, 2026
DOI: 10.5137/1019-5149.JTN.47617-24.5

Systematic Review

Received: 03.10.2024
Accepted: 03.06.2025
Published Online: 22.05.2026

A Child with Three Legs or Conjoint Parasitic Twin?

Gulyara CIGDEM[1], Mehmet Emin BOLEKEN[2]

[1]Harran University, Faculty of Medicine, Department of Neurosurgery, Sanliurfa, Türkiye
[2]Harran University, Faculty of Medicine, Department of Pediatric Surgery, Sanliurfa, Türkiye

This study has been presented by Çiğdem, G. and Boleken, M.E. under the title "Dublication of the Vertebral Column and Conjoined Twins: A Rare Type of Rachipagus" at the Ninth World Congress of Spine Surgery, held between November 3–5, 2022 in Athens, Greece, and published in a special edition of World Neurosurgery (OP-31, 28;2022).

Corresponding author: Gulyara CIGDEM ✉ gulyara@hotmail.com

ABSTRACT

AIM: Rachiphagus is a rare congenital anomaly in which conjoined twins are fused at the midline of the vertebral column region. When one twin is malformed, the condition is referred to as a parasitic twin. The term "parasitic twin" also encompasses cases involving extra limbs or limb-like structures. Despite ongoing research, the underlying causes of this condition remain unknown.

MATERIAL and METHODS: This is a systematic review of the literature with a case report. A literature search was done in English language in PubMed and Semantic –Scholar from 1952 to 2023. All articles and cases with excess leg or mass which were attached at the back of the spine were reviewed and analysed.

RESULTS: A total of 65 cases with rachipagus anomaly were included in this study. Females 37 (56.9%) were affected more than males 28 (43.1%). The lower limbs were in 41 (63.1%) cases, followed by rudimental limbs and mass were in 15 (23.1%) cases, upper limbs were in 8 (12.3%) cases and rudimental upper and low limbs were in 1 (1.5%) case. In majority of cases, accessory limb or mass were attached at lumbosacral region, 27 (41.5%), followed by 12 (18.5%) cases at lumbar region, 7 (10.8%) were at thoracolumbar region, 5 (7.7%) were at sacral and other regions. More than half of the cases 34 (52%) were in Asian countries, followed by 24 (37%) cases in Africa.

CONCLUSION: Rachipagus parasitic twin is congenital abnormalities that develops during embryogenesis and exists at birth with structural deformities of the spine and additional limb or limb like mass. This article presents a novel rachipagus case and systematically reviews the relevant literature.

KEYWORDS: Conjoined twin, Parasitic twin, Polymelia, Rachipagus twin, Tripedus

ABBREVIATIONS: ASD: Atrial septal defect, **CT:** Computed tomography, **EMG:** Electromyography, **F:** Female, **HCP:** Hydrocephalus, **ICM:** Inner cell mass, **IONM:** Intraoperative neurophysiological monitoring, **LMMC:** Lipomyelomeningocele, **LL:** Lower limb, **MRI:** Magnetic resonance imaging, **M:** Male, **MMC:** Meningomyelocele, **NTD:** Neural tube defect, **SEP:** Somatosensory evoked potentials, **USG:** Ultrasonography, **UL:** Upper limb, **VSD:** Ventricular septal defect

INTRODUCTION

Rachipagus is a rare embryonic malformation characterized by a pair of conjoined or parasitic twins fused along from the midline of the vertebral column. When two twins are teratologically unequal, the larger or the normal one of these twins that supports and provides nutrients for the parasitic twin is known as the "autosite" twin. In most cases, parasitic twins manifest as an excess limb or limb-like mass protruding from the back along the vertebral column, rather than developing into a fully formed infant. The parasitic twin is attached to an autosite twin. In most cases, parasitic twins appear as an excess limb or limb like mass arising from the back of the vertebral column instead of completing himself

Gulyara CIGDEM : 0000-0002-4888-1172 Mehmet Emin BOLEKEN : 0000-0001-9006-8364

as an infant. Whether this anomaly results from an improper separation of twins or is a manifestation of aneural tube defect (NTD) is still debated. Several hypotheses have been proposed for the etiology of rachipagus. Two main theories are associated with this, one of which is neural tube defects and the other is the aberrant embryogenesis of conjoined twins, but actual cause is still unknown (30,35,37,39,55,59,69). The incidence rate is 1 in 50,000 births and up to 1 in 1-2 million live births and seems higher in females than in males with a ratio of 3:1 (37,44). The first report was in 1802 by Vincenzo Malacarne who described it as a malformation with excess limbs in a body with the term polymelia (26). Accessory limbs on the back as a rachipagus were described by Deslongchamps in 1851 and by Jones in 1889 (17,24). A PubMed search revealed 26 articles on rachipagus since 1952, two articles on tripedus since 2009 and multiple articles on parasitic twins. But only 1 case of rachipagus was reported in 1991 with three fully developed normally functioning legs (13). Notably, only one case of rachipagus with three fully developed, normally functioning legs was reported in 1991 (13).

This report presents the second documented case of a patient with three fully developed, normally functioning legs, accompanied by a comprehensive systematic review of previously published cases.

MATERIAL and METHODS

The study was approved by the local ethics committee of Harran University (No:21; Date: 31.10.2022). Written informed consent was obtained from the patient's family for publishing this clinical report.

This is a report of a case with a third additional fully formed functioning leg with a comprehensive review of the literature and meta-analyses of the previously published cases with rachipagus. The study adhered to the PRISMA 2020 guidelines for systematic reviews. A literature search was conducted using PubMed and Semantic –Scholar, spanning 1952-2023 with key-words: including rachipagus, parasitic twins, tripedus, notomelia, and polymelia. The search was restricted to articles published in English. All articles and cases were reviewed for data, type and level of the excess limbs, autosite anomalies and surgical procedures. Only conjoined twins who were fused dorsally at the midline of the spinal column were included to this study. The cases with parasitic twining from other anatomical regions of the body (heteropagus, craniopagus, omphalopagus and others) and animal studies were excluded. Finally, 64 cases with rachipagus from 47 articles were reviewed. All data of the included cases were analysed by IBM SPSS statistic version 20. Student's t-tests were used for between group comparisons and significant of p value was accepted ($p<0.05$).

Present Case

A 1-day-old, full-term female new-born, weighing 3.00 kg, was referred to the Harran University hospital, Türkiye, in July 2022, with three fully formed functioning legs. There was no relevant family history and the mother had a normal pregnancy, with regular prenatal follow-ups. The tripedus condition was diagnosed in the third trimester, and delivery was via caesarean section, but prenatal ultrasonography (USG) images were not available.

Physical examination revealed a third limb attached to the baby's back at the midline of the lumbosacral vertebral column via an iliac bone. The third leg moved in conjunction with the other two legs or spontaneously (as confirmed by review of the video material). A femoral pulse was palpable on the medial side of the thigh of the third leg. A normal female perineum was present between the normal right and left legs, and the anus was present under the third limb (Figure 1). Rudimentary external genitalia were represented by a papilla anteriorly. All three legs were normally formed with a full range of movements and responded equally to painful stimuli.

X-ray and 3D-computed tomography (CT) of the pelvis demonstrated that the additional ileum articulating with the margin of the sacrum had a partial acetabular joint with a normally sized femoral head (Figure 2A, B). Magnetic resonance imaging (MRI) revealed a hip joint, femur, and thigh muscles in the third leg, as well as a posteriorly protruding spinal cord at the S2–3 level, along with rudimentary bowel loop, uterus, and vesicle sacs (Figure 3A, B).

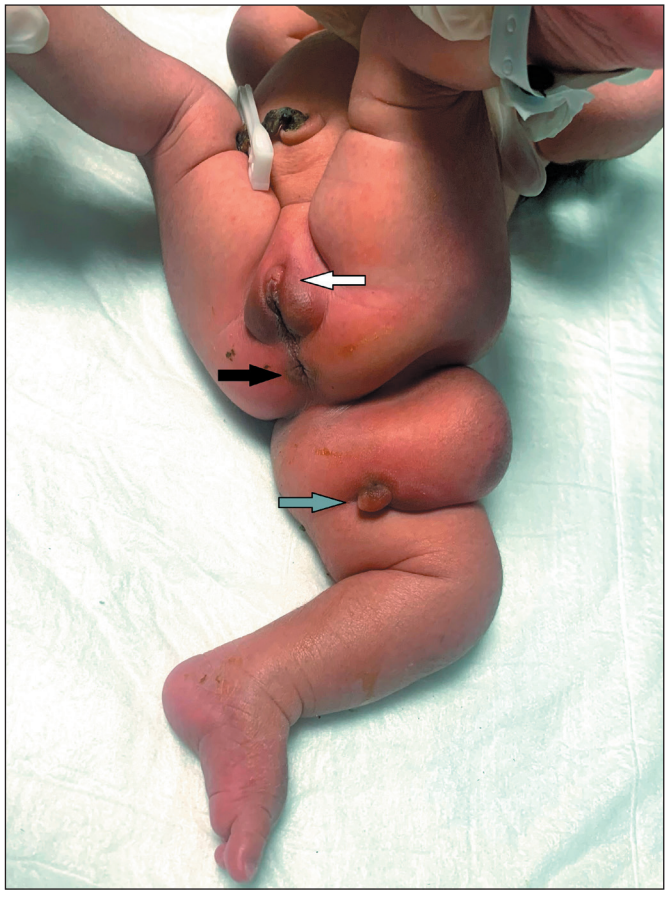

Figure 1: Lumbosacral attachment of a third leg to the back, featuring false external genitalia (black arrow). The female perineum is visible between the normal right and left legs (white arrow), and the anus is located under the third limb (grey arrow).

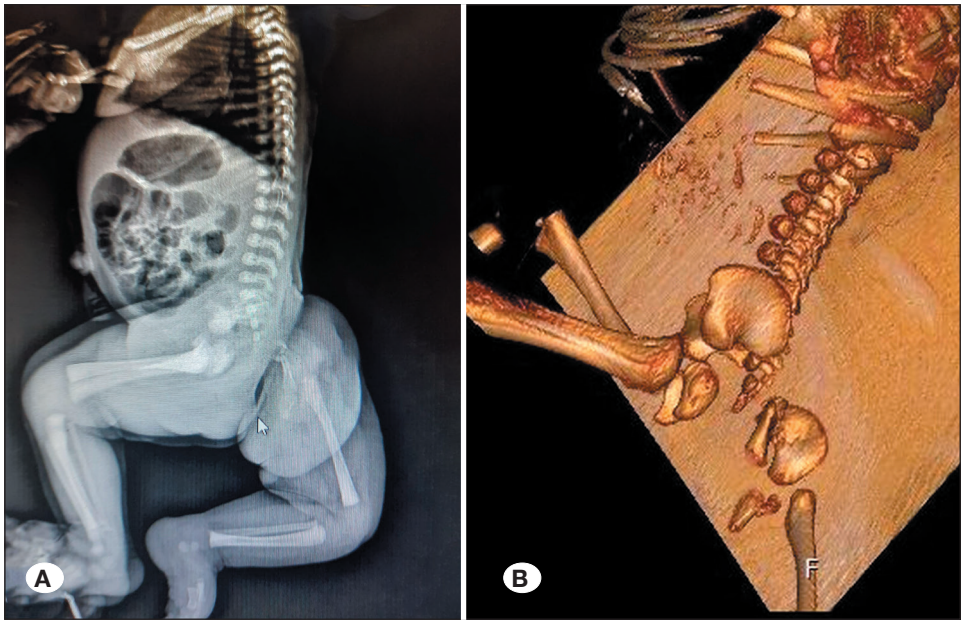

Figure 2: X-ray **(A)** and CT **(B)** lateral views of the pelvis, showing the additional ileum forming a partial acetabular joint with the head of the third femur and articulating with the sacral margin.

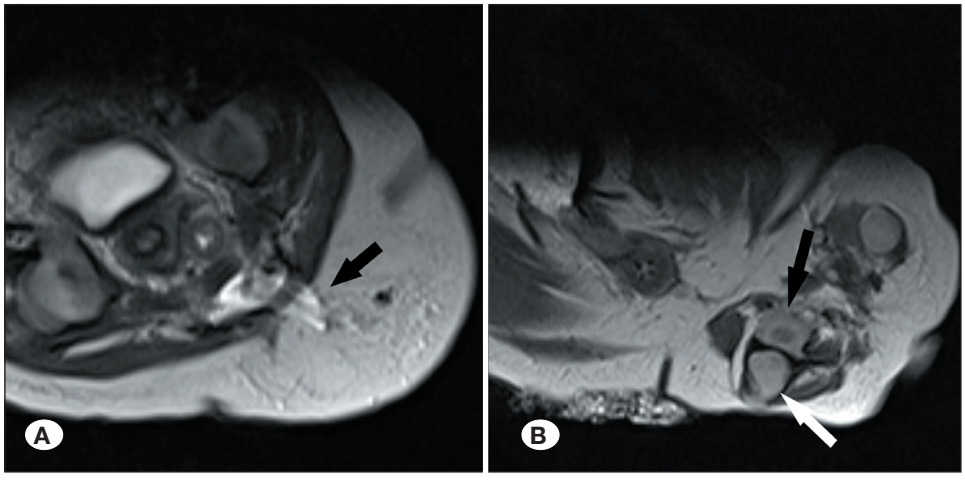

Figure 3: A) MRI-T2 weighted axial sections showing spinal cord roots protruding posteriorly at the S2–3 vertebral level (black arrow); **B)** A rudimentary bowel loop (white arrow) and uterus and vesicle sacs (black arrow) are visible.

Following a comprehensive assessment of all diagnostic tests, including CT and MRI scans, a surgical procedure was performed by a multidisciplinary team consisting of a pediatric surgeon and a neurosurgeon. The amputation was conducted under intraoperative neurophysiological monitoring (IONM) in order to precisely identify the location of neural structures and prevent any damage to the nerves of the first and the second legs. During the surgery, exploration was done while preserving an adequate flap for skin closure. The well-formed iliac bone of the parasitic leg was disarticulated from the autosite sacrum. Peripheral vascular bundles supplying the parasitic leg were ligated. The neuronal roots of the third lower limb were dissected under somatosensory evoked potential (SEP) monitoring. The SEP type of IONM was chosen because of its ease of application, ability to provide continuous monitoring during long surgeries, safety in infants, and compatibility with other monitoring techniques like electromyography (EMG) (Figure 4). The third leg was completely resected without damaging the neural structures of the sacrum, spinal cord, or both legs of the main body. The muscular cutaneous flap was well-performed, and the patient recovered smoothly, ultimately being discharged without any further complications.

RESULTS

Each case involving rachipagus was meticulously analysed to assess the data quality, excess limb characteristics, autosite anomalies, and surgical interventions (Table I).

The study found that rachipagus was more common in female infants, accounting for 56.9% (n=37), compared to male infants at 43.1% (n=28). Lower limbs were most commonly associated with rachipagus, occurring in 63.1% of cases (n=41), followed by rudimentary limbs and mases in 23.1% (n=15). Upper limbs were seen in 12.3% of cases (n=8), and a single case (1.5%) involved both rudimentary upper and lower limbs attached to the back of the spine. The findings are summarized in Table II.

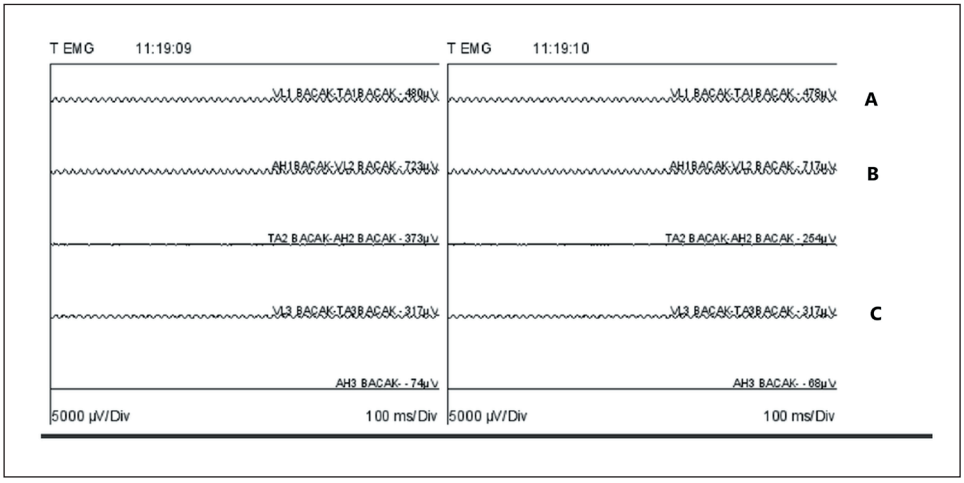

Figure 4: Intraoperative neurophysiological somatosensory evoked potentials monitoring of all three legs: **A:** right leg, **B:** left leg, **C:** additional third leg.

Table I: Summary of Cases of Rachipagus

Case	Age	Sex	Localization of appendage	Contents of parasite	Abnormalities in Autosite	Country
Copley and Derwael, 1991 (13)	8-days	M	Sacrum	Well developed LL	Spina bifida, MMC	South Africa
Ratan et al., 2004 (51)	2-days	F	Thoracolumbar	Vertebrae×2 Bowel Pelvis Bladder Fallopian tissue Limb with fused feet	Spinal dysraphism Tethered cord	India
Chadha et al., 2006 (12)	1-day	F	Lumbosacral	Anal dimple Digit like structures	Spinal dysraphism	India
Zhao et al., 2006 (72)	4-years	M	Lumbosacral	LL, pseudo navel, pseudo-penis	Hemivertebrae, Scoliosis, Lumbosacral vertebral dysplasia, Dislocation of the left hip	China
Amirjamshidi et al., 2006 (4)	6-weeks	F	Lumbar	Mass with thumb and fingers with nail beds	Spina bifida	Iran
Lende et al., 2007 (32)	2-years	F	Lower thoraco-lumbar	LL	Spina bifida MMC	Ethiopia
Snelling et al., 2008 (61)	4-months	M	Lumbar	UL like structures	High arched palate Retrognathia Posteriorly set ears Simian crease Spinal dysraphism Meningocele, hydromyelia Split, tethered cord	
Albert et al., 2008 (2)	9-months	F	Lumbosacral	Segmeted UL like structures	Spinal dysraphism Myelocystocele Teratoma	USA
Khan et al., 2009 (27)	1-day	M	Lumbosacral	LL, anal dimple, scrotum	Spina bifida	India
Sanoussi, 2010 (58)	3-months	M	Lumbar	LL	Lipoma, meningocele	Niger
	18-months	M	Thoracal	UL with two phalanges	Spina bifda	

Table I: Cont.

Case	Age	Sex	Localization of appendage	Contents of parasite	Abnormalities in Autosite	Country
Zhang et al., 2011 (71)	17-years	F	Thoracal	Breast, fallopian tube, bone	Spina bifida, Diplomyelia Scoliosis Tethered cord VSD	China
Debnath and Biswas, 2011 (15)				Well-formed limb, Intestine		India
Solak et al., 2012 (62)	2-months	F	Thoracal	A malformed UL	Lipoma	Türkiye
Ringo et al., 2012 (53)	3-days	M	Lumbosacral	LL, Phallus	MMC	Tanzania
Kota et al., 2012 (29)	5-months	M	Thoracal	Rudimentary limb	MMC	India
	3-months	M	Gluteal	Limb-like structures	MMC	
	1-day	F	Gluteal	Rudimentary limb	MMC, Anorectal anomaly, Duplication of external genitalia	
Kumar and Kumar, 2013 (31)	1-year	M	Thoracolumbar	Mass, fngers, phallus	MMC, Chiari malformation	India
Pandey et al., 2013 (45)	3-days	F	Lumbosacral	UL	MMC, Monoparesis	India
Murphy et al., 2013 (40)	7-months	M	Lumbosacral	Rudimentary LL	LMMC	USA
Oduor and Nyamal, 2014 (43)	9-days	M	Thoracolumbar	LL, UL, phallus	Spina bifida, club foot	Kenya
Bayri et al., 2014 (6)	1-day	M	Lumbosacral	LL, rudimentary pelvis	Meningocele	Türkiye
Parks and Mugamba, 2014 (47)	6-days	F	Thoracolumbar	UL, lactating breast	MMC, Kyphosis, Paraplegia, HCP, club foot	Uganda
Kim et al., 2014 (46)	1-day	F	Sacral	LL	Imperforate anus	Korea
Navaei et al., 2015 (42)	10-days	F	Lumbar	LL, hemipelvis, two toes	MMC, tethered cord	Iran
	5-days	M	Lumbar	Scrotum, primitive phallus	MMC, neurogenic bladder	
Nadeem et al., 2016 (41)	12-months	M	Lumbosacral	Limb, phallus, scrotum	Spina bifida	Pakistan
	8-months	F	Lumbosacral	Limb	Spina bifida	
	6-months	F	Lumbosacral	Limb	LMMC	
	4.5-months	F	Lumbosacral	Limb, bowel	Spina bifida, left leg weakness, urinary	
	1.5-months	F	Lumbosacral	Limb	incontinence Spina bifida	
Retnam et al., 2016 (52)	4-months	M	Lumbosacral	Rudimentary limb	MMC, Tethered cord	India
Awad et al., 2016 (5)	1-month	F	Lumbar	LL-foot, leg, knee, thigh, part of pelvis	LMMC	Egypt
Samy and Samin, 2016 (57)	28-days	F	Lumbosacral	LL, part of pelvis, phallus	Hemangioma, meningocele	Egypt
Sahlu et al., 2016 (56)	7-months	F	Lumbar	Mass, part of LL, phallus	LMMC Tethered cord Syringohydromyelia	Ethiopia
Mohammed et al., 2017 (38)	3-weeks	M	Cervicohtoracal	UL	Spina bifda	Nigeria

Table I: Cont.

Case	Age	Sex	Localization of appendage	Contents of parasite	Abnormalities in Autosite	Country
Kelani et al., 2017 (26)	5-days	M	Lumbar	LL, phallus	Meningocele Dermal sinus Umbilical herni	Niger
Raheja and Muhapatra, 2017 (50)	2-years	M	Lumbar	2 rudimentary limbs Anal dimple		India
Bodeliwala et al., 2017 (10)	1.5-year	F	Lumbar	LL, foot with syndactyled toes and nails	Club foot	India
Solomon et al., 2018 (63)		M	Lumbar	Mass, rudimentary bone	Meningocele	Ethiopia
Dejene et al., 2013 (16)	32-hours	F	Lumbosacral	LL, buttock, phallus	Cleft lip/palate, club foot	Ethiopia
2015	62-hours	M	Lumbosacral	Mass, phallus, scrotum	MMC, Cardiac (ASD, PDA)	
2018	18-hours	F	Lumbosacral	2 LL, phallus, pelvic bone, bowel	Rocker bottom feet	
Priyawansha et al., 2018 (49)	22-days	M	Thoracolumbar	LL	MMC, Umbilical hernia, Club foot	Sri Lanka
Khavanin et al., 2018 (28)	9-months	F	Cervicothoracal	Bilateral LL, pelvis, scapula	Diplomyelia, Lipoma, Thoracic kidney	USA
Adhikari et al., 2018 (1)	7-months (2-year)	M	Thoracal	LL	MMC, Diastematomyelia, Tethered cord, Hemicord	Nepal
Shrikesh et al., 2018 (60)	1-month	F	Lumbosacral	Rudimentary LL and genitalia	Large ASD	India
	3-days	F	Lumbosacral	Rudimentary LL		
Saaiq, 2020 (55)	5-months	F	Lumbosacral	LL, bowel	MMC, Tethered cord, Monoparesis	Pakistan
Zewdie, 2020 (70)	1-month	F	Lumbosacral	Mass with fngers	Meningocele	Ethiopia
	8-months	M	Lumbosacral	Mass with arm, hand Lung, lymph node	MMC, Tethered cord	
	2-months	F	Lumbosacral	Rudimentary limb, phallus	Meningocele	
	1.5-months	F	Thoracolumbar	Bilateral LL, phallus, part of pelvis,bladder	Myelocystocele, lipoma tethered cord, neurogenic bladder	
Pati et al., 2020 (48)	1-day	F	Cervical	2 accessory limbs	Cervical MMC,	India
	6-months	F	Lumbosacral	Rudimentary LL, phallus	Posterior cranial fossa, Mesocardia, ASD,VSD, Left to right shunting LMC, Tethered cord	
Mohindra et al., 2021 (39)	3-years	M	Lumbar	LL, phallus	MMC, Tethered cord	India
Bikoroti et al., 2021 (7)	1-day	F	Sacrococcygeal	Scalp, skull, cervical spine bone, and brain		Congo
Zhi, 2022 (73)	23-days	M	Thoracal	Penis and scrotum like mass		China
	6-months	F	Sacral	Hypoplastic LL with 7 toes,		
Djibrine, 2022 (18)	2-years	F	Thoracal paravertebral	Fatty clumps, cartilaginous tissue		Chad
	4-days	F	Sacral	LL		

Table I: Cont.

Case	Age	Sex	Localization of appendage	Contents of parasite	Abnormalities in Autosite	Country
Mathur et al., 2022 (35)	1-day	M	Sacrococcygeal	LL with 3 toes	Split notochord with MMC	India
	1-day	M	Sacral	Hypoplastic limb with 2 phalanges, rudimentary phallus	Ectopic right kidney, MMC	
Hailu et al., 2022 (22)	4-days	M	Lumbosacral	LL	Hemivertebra, LMMC	Africa
Present case	1-day	F	Lumbosacral	Full developed lower limb	Rudimentary loop bowel, Uterus, Vesical sacs	Türkiye
Total, n=65		M-28 F-37				

***F:** Female, **M:** male, **LL:** lower limb, **UL:** upper limb, **LMMC:** lipomyelomeningocele, **MMC:** meningomyelocele, **HCP:** hydrocephalus, **VSD:** ventricular septal defect, **ASD:** atrial septal defect.*

Table II: Distribution of the Cases in the Study

	Frequency (n)	Percent (%)
Sex		
Female	37	56.9
Male	28	43.1
Accessory Limb/Mass		
UL	8	12.3
LL	41	63.1
Rudimental limb and mass	15	23.1
UL+LL	1	1.5

***UL:** upper limb, **LL:** lower limb.*

The study showed that the lumbosacral region was the most common site of attachment of the accessory limb or limb-like mass in rachipagus cases, occurring in 41.5% of cases (n=27), followed by the lumbar region in 18.5% of cases (n=12). Other regions, such as the thoracolumbar region (10.8%) and sacral region (7.7%), had lower frequencies of attachment. The level of attachment in rachipagus cases with an accessory limb or mass is depicted in Figure 5.

Comparison of the levels of attachment of the excess limb/mass between males and females revealed no significant sex-based differences (Student's *t*-test, p>0.05).

The autosites in most cases presented congenital anomalies such as meningomyelocele, diastematomyelia, spina bifida, tethered cord, anorectal malformations, ectopic intestinal loops, neurogenic bladder, and rudimentary external genitalia.

34 (52%) cases with accessory limb or rachipagus were in Asian countries: India, Pakistan and others. 24 (37%) cases in Africa: Nigeria, Egypt, Ethiopia. 4 (6%) cases were in USA. 3 (5%) cases in Europe: all of them were in Türkiye (Figure 6).

DISCUSSION

Interest to congenital disabilities of humans or animals named as monsters appears since old ages and some of the cases are still exhibited in museums. Vallisneri in 1721 after observation of several cases of conjoined twins explained the formation of this condition as "from two germs or mature eggs, which by matching closely, over time attack and interpenetrate, so that they compose a doubled body… or with multiplied limbs, are born" (34). The progress in the number of the records with rachipagus for the last decades increased the interest in this malformation. However, its rarity limits opportunities for observation and hinders a full understanding of its embryological etiology and pathogenesis. This malformation represents a complex interplay of embryological and anatomical features. Several theories attempt to explain the mechanism for the development of an excess limb: 1) spontaneous incidence with a frequency of 10.25/1 000 000 births (25). 2) Incomplete twinning of monozygotic, monochorionic, and isosexual twins in the vertebral region associated with an additional limb or limb like mass and other organs or 3) NTDs resulting from aberrant neural fold formation during neurulation (11,26).

Kaufman, and Boer et al. suggest the first scientific fission and fusion theories of conjoined twinning. The fission theory is explained as an incomplete splitting of the embryo after fertilization on 13-15 days (11,25). The fusion theory posits the fusion of two separated embryonic disks around 13 days after fertilization. It means that two embryoblasts of monozygotic, monochorionic twins, instead of splitting away, merge together (11).

Grondahl et al. recorded the earliest embryogenesis of conjoined twins from a single zygote to an expanded blastocyst (21). Before implantation, the blastocyst contains two types of cells: the trophectoderm, which subsequently transform into extra-embryonic tissues and the inner cell mass (ICM), which is a pluripotent stem cell for embryonic tissues and transforms to all cell types of any organs of the embryo. The ICM can form two identical daughter cells through mitotic division (54,64,67). Failure of the ICM to separate in early embryogenesis may underlie the embryological theory of conjoined twinning (9).

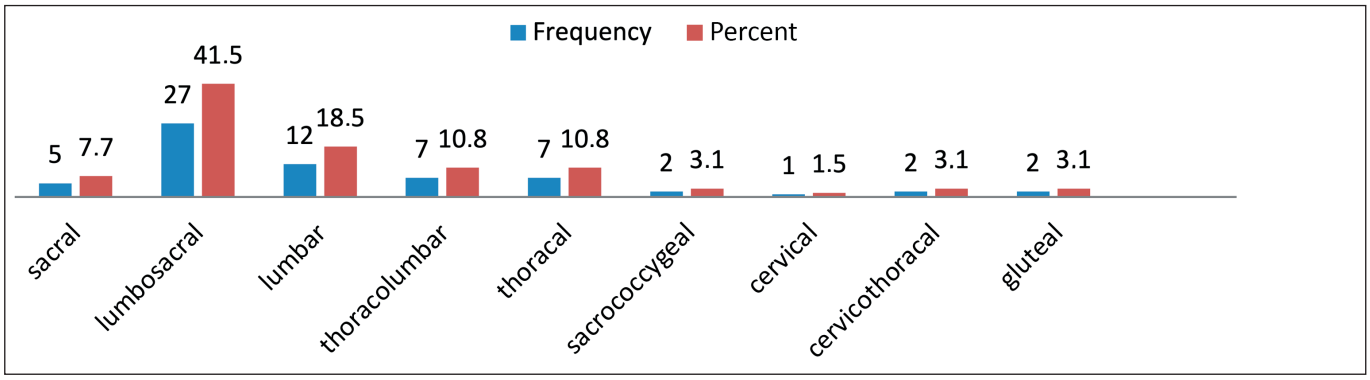

Figure 5: Level of attachment of the accessory limb/mass.

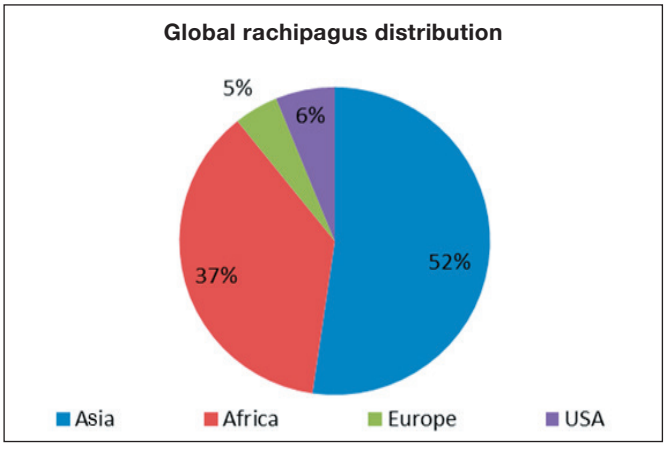

Figure 6: Global distribution of rachipagus cases.

Limbs develop between 4-5 weeks of embryonic development. Steinman collected data from pregnant women who gave birth to conjoined monozygotic twins following exposure to teratogenic factors during pregnancy. The results showed that pregnant women who used oral contraceptives and were exposed to teratogenic environmental factors had an increase in single egg duplication and conjoined twinning due to calcium depression and delayed implantation (36,65). According to Das and Mohanty-Hejmadi, vitamin A can cause polymelia by turning on or overexpressing limb-specific hox genes through unknown mechanisms (14). This implies a potential genetic cause, involving multiple genes responsible for limb development (23). Damage to the embryo during the 4–5 week stage can lead to limb developmental anomalies (68). This complex process can result in malformations, such as the parasitic twin occurring as an extra-limb or limb-like mass. Stephens et al. reported two cases of parasitic legs attached to the abdomen and suggested that ectopic legs may result from duplication of the Wolffian ridge. This duplication may more likely produce lower extremities than upper ones (66). According to our review (Table II), lower limbs are predominant, accounting for 41 cases (63.1%), often presenting as a parasitic mass.

Kelani et al. related rachipagus to NTDs as embryonic malformations characterized by an excess limb, classifying it as a dysraphic appendage (26). Most cases of rachipagus are linked to congenital NTDs, including MMC, LMMC, spina bifida, diplomyelia and tethered cord syndrome (26,31,45,71). Gardner also linked conjoined twins to neural tube closure defects, proposing that primary rupture of the neural tube can lead to secondary development of a limb-like mass or, in rare cases, a fully formed accessory limb containing skin, cartilage, bone, muscles, and nerves (20). Amirjamshidi considered congenital dorsal midline limb-like masses to be a type of hamartoma (3). According to Drews and Busch, based on his personal experience, parasitic conjoined twins can be viewed as extremely disorganized transitional forms, regardless of whether they manifest as parasites or teratomas (19). Each theory of rachipagus etiopathogenesis attempts to explain the formation of an excess limb, but every teratological, genetic, and embryological theory has its limitations.

The condition is more prevalent in females, with a female-to-male ratio of 3:1 (11). Our study highlights a significant disparity in the prevalence of additional limbs or masses between female and male infants, with females exhibiting a higher incidence. The distribution of limbs varied, with lower limbs being the most common, followed by rudimentary limbs and masses, upper limbs, and a rare occurrence of rudimentary upper and lower limbs located at the back of the spine. Globally, cases of the rachipagus are more frequently reported in Asia and Africa compared to European countries and America (11). Our study reflects this trend, with over half of the cases originating from Asian countries followed by African countries.

Conjoined twins are classified according to the site of attachment of the component of the parasitic twin: asymmetric or symmetric. The terminology describes the anatomical location, degree, and relationship of shared structures (25). These twins may share the spinal cord or have innervation from the same spinal cord, as observed in our case. Symmetric conjoined twins may be fused at ventral, dorsal, caudal, or lateral sites (11,37). Rachipagus twins are a type of symmetric conjoined twins characterized by dorsal fusion along the vertebral column above the sacrum (8). The fusion area may be at cervical, thoracal, or lumbar levels of the vertebral axis. Twins fused dorsally at the sacrum or coccyx are classified as pygopagus, distinct from rachipagus, which involves fusion higher up the vertebral column (3,8,37). Pypopagus twins often involve a parasite twin with a limb or limb-like

mass. Saaiq et al. described a morphologic classification for accessory limbs based on degree and differentiation: a) well-developed, b) moderately developed, c) mildly developed, d) poorly developed accessory lower limb (55). According to Saaiq's classification, our case is a rachipagus with a well-developed accessory lower limb with spinal dysraphism.

Modern imaging technologies like prenatal USG, MRI, or CT scans with 3D reconstruction enable early diagnosis of rachipagus anomalies (33). Surgical separation of conjoined twins poses significant challenges due to shared blood vessels, nerve roots, and vital organs, and potential cosmetic issues, necessitating meticulous pre-, intra-, and postoperative planning. Predicting the type of parasitic twinning, shared organs, neurological deficits, and associated malformations before surgery is crucial. A multidisciplinary team of neurosurgeons, pediatric surgeons, and plastic surgeons is essential for successful separation.

We have documented a rare case of rachpagus parasitic twinning with a fully developed additional low limb, exhibiting sensory and motor functions. Our case features a unique combination of anomalies, including three fully formed legs (tripedus), a protrusion and duplication of the spinal cord, with a rudimentary bowel loop, uterus, and vesicle sacs. The exact cause remains unclear, but multiple risk factors may contribute to the incidence of conjoined parasitic twinning during the early stage of fertilization.

The rarity of the rachipagus with a fully developed lower limb is a limitation of this study.

CONCLUSION

Rachipagus, conjoined or parasitic twins are a rare embryological anomaly characterized by dorsal fusion at the vertebral axis above the sacrum. The etiology of this anomaly is still unclear, but "fission or fusion" and erroneous of neural tube closure are the main theories of rachipagus. In most cases of parasitic twinning, the parasitic component typically consists of a lower limb with varying degrees of development, often attached to the lumbosacral region. A good prognosis can be achieved through early diagnosis, thorough preoperative examination, and meticulous microsurgery performed by a multidisciplinary team, incorporating spinal canal repair and cosmetic reconstructions.

Our case contributes to our understanding of rachipagus anomalies with NTDs. Further research, particularly human genetic DNA studies, is necessary to elucidate the embryogenesis of these congenital abnormalities.

Declarations

Funding: This research did not receive any specific grant from funding agencies in the public, commercial, or not-for-profit sectors.

Availability of data and materials: The datasets generated and/or analyzed during the current study are available from the corresponding author by reasonable request.

Disclosure: The authors declare no competing interests.

Informed consent: Written informed consent was obtained from the parents/legal guardians.

AUTHORSHIP CONTRIBUTION

Study conception and design: GC
Data collection: GC
Analysis and interpretation of results: GC
Draft manuscript preparation: GC
Critical revision of the article: GC, MEB
Other (study supervision, fundings, materials, etc...): GC, MEB
All authors (GC, MEB) reviewed the results and approved the final version of the manuscript.

REFERENCES

1. Adhikari R, Thapa A, Pandey C: Rudimentary third arm arising from the upper back: a rare case. Grande Med J 1:41–43, 2019. https://doi.org/10.3126/gmj.v1i1.22405
2. Albert G, Campos M, Menezes A, Vogel T, Weinstein S: Rachipagus parasite associated with myelocystocele and diastematomyelia. Pediatr Neurosurg 44(5):418-421, 2008. https://doi.org/10.1159/000149912
3. Amirjamshidi A: Dorsal midline skin covered anomalies. A hamartoma or rachipagus? Childs Nerv Syst 32: 7–8, 2016. https://doi.org/10.1007/s00381-015-2927-8
4. Amirjamshidi A, Abbassioun K, Shirani Bidabadi M: Skin-covered midline spinal anomalies: a report of four rare cases with a discussion on their genesis and milestones in surgical management. Childs Nerv Syst 22: 460–465, 2006 https://doi.org/10.1007/s00381-005-0014-2
5. Awad T, Elsayem K, Elqazaz M: Dorsolumbar parasitic rachipagus twin: case report. Egypt Spine J 19:48–54, 2016. https://doi.org/10.21608/esj.2016.4013
6. Bayri Y, Tanrıkulu B, Ekşi M, Dağçınar A: Accessory lower limb associated with spina bifida: Case report. Childs Nerv Syst 30:2123-2126, 2014. https://doi.org/10.1007/s00381-014-2475-7
7. Bikoroti JB, Jahn A, MunezaS, M. Nyundo M, Gashegu JK, Buteera AM: A rare case of sacral parasitic rachipagus. Rwanda Med J 78(4): 12-16,2021. https://doi.org/10.4314/rmj.v78i4.2
8. Bindlish A, Sawal A: A detailed description and discussion on conjoined twins. Cureus 14(9):e29526, 2022. https://doi.org/10.7759/cureus.29526
9. Bishopa L, Jonesb B, Kelleyc D, Martin D: External parasitic twins. J Pediatr Surg Case Reports 40: 62-68, 2019. https://doi.org/10.1016/j.epsc.2018.08.015
10. Bodeliwala S, Singh D, Singh H, Iqbal M, Agarwal A, Khurana P: Spinal dysraphism with tripedus: A child with three legs. Neurol India 65(1):214-216, 2017. https://doi.org/10.4103/0028-3886.198209
11. Boer LL, Schepens-Franke AN, Oostra RJ: Two is a crowd: two is a crowd: on the enigmatic etiopathogenesis of conjoined twinning. Clin Anat 32(5):722-741, 2019. https://doi.org/10.1002/ca.23387
12. Chadha R, Lal P, Singh D, Sharma A, Choudhury SR: Lumbosacral parasitic rachipagus twin. J Pediatr Surg 41(1):e 45-48, 2006. https://doi.org/10.1016/j.jpedsurg.2005.10.070

13. Copley IB, Derwael EF: Investigation and treatment of a multiple limb birth. Br J Neurosurg 5: 281-287, 1991. https://doi.org/ 10.3109/02688699109005188
14. Das P, Mohanty-Hejmadi P: Vitamin A mediated limb deformities in the common Indian toad, Bufo melanostictus (Schneider). Indian J Exp Biol 38(3): 258-64, 2000.
15. Debnath B, Biswas SK: Heteropagus twinning on back - a case report. J Indian Med Assoc 109(7):514-515, 2011.
16. Dejene B, Negash S, Mammo T, Tadesse A, Getachew H, Miliard Derbew M: Heteropagus (parasitic) twins. J Pediatr Surg Case Rep 37:44–49, 2018. https://doi.org/10.1016/j.epsc.2018.07.019
17. Deslongchamps E: Memory on a monster double monomphalien of human origin, constituting a new genre called Rachipage. CR Séances Mem Soc Biol 3: 221-235, 1851
18. Djibrine MA, Ngaringuem O, Hagré YD, Adam A, Attimer K, Ouchemi Choua O: Heteropagus conjoined twins: five cases. J Pediatr Surg Case Rep 76:102086, 2022. https://doi.org/10.1016/j.epsc.2021.102086
19. Drews U, Busch C: Sacrococcygeal teratomas (SCTs): conjoined twins or conjoined daughter? Histopathology 54, 763–779, 2009. https://doi.org/10.1111/j.1365-2559.2009.03282.x
20. Gardner JW: Hypothesis: overdistension of the neural tube may cause anomalies of non-neural organs.Teratology 22: 229–238, 1980. https://doi.org/10.1002/tera.1420220212
21. Grondahl ML, Tharin JE, Maroun LL, Jørgensen FS: Conjoined twins after single blastocyst transfer: a case report including detailed time-lapse recording of the earliest embryogenesis, from zygote to expanded blastocyst. Hum Reprod 37(4):718-724, 2022. https://doi.org/10.1093/humrep/deac004
22. Hailu SS, Solomon DZ, Gebremedhin YG, Nour AS: Dorsolumbar parasitic twin associated with lipomyelomeningocele: a case report from a tertiary teaching hospital, Ethiopia, East Africa. Radiol Case Rep 17(10):3820-3824, 2022. https://doi.org/10.1016/j.radcr.2022.07.079
23. Hassanzadeh B, Rahemi A: Polymelia with unhealed navel in an Iranian indigenous young fowl. Veterinary Research Forum 8 (1): 85 – 87, 2017. PMID: 28473903. PMCID: PMC5413317.
24. Jones R, Larkin FC: Removal of accessory limb and meningocele from the back of a child, and its anatomy. Br Med J 2(1493):310–311, 1889. https://doi.org/10.1136/bmj.2.1493.310
25. Kaufman MH: The embryology of conjoined twins. Childs Nerv Syst 20: 508–525, 2004. https://doi.org /10.1007/s00381-004-0985-4
26. Kelani AB, Moumouni H, Issa AW, Younsaa H, Fokou H, Sani R, Sanoussi S, Denholm LJ, Beever JE, Catala M: Notomelia and related neural tube defects in a baby born in Niger: case report and literature review. Childs Nerv Syst 33(3):529-534; 2017. https://doi.org/10.1007/s00381-017-3337-x
27. Khan RA, Wahab S, Ghani I: Tripedus: a form of rachipagus twinning. Congenit Anom (Kyoto) 49(4):280-281, 2009. https://doi.org/10.1111/j.1741-4520.2009.00243.x
28. Khavanin N, Ruge JR, Vicari FA, Belin EJ, Kellogg RG, Steinberg JP: Parasitic rachipagus conjoined twin: case report. J Neurosurg Pediatr 22(3):313-316, 2018. https://doi.org/10.3171/2018.3.PEDS1822
29. Kota R, Srirampur S, Kannaiyan L, Irfan GM, Sharab H, Rao S: Parasitic twinning—varied presentations. J Dr NTR Univ Health Sci 1(3):174, 2012. https://doi.org/10.4103/2277-8632.102445
30. Krishna A, Lal P: Accessory limbs associated with spina bifida - a second look. Pediatr Surg Int 15: 248-250, 1999. https://doi.org/10.1007/s003830050568
31. Kumar A, Kumar R: Accessory digit and rudimentary male external genitalia associated with spinal dysraphism: a rare case of dysraphic appendages. Indian J Neurosurg 2:101–102, 2013. https://doi.org/10.4103/2277-9167.110233
32. Lende G, Wendemu W, Mørk S, Wester K: A girl with spina bifida, an extra leg, and ectopic intestinal loops--a “foetus in foetu” or a whim of the neural crest? Acta Neurochir (Wien) 149(10):1071-1075, 2007. https://doi.org/10.1007/s00701-007-1258-2
33. Liu J, Liu Y, Xue Y, Guo Y: Prenatal ultrasound-based diagnosis of fetal OEIS complex associated with lower limb polymelia and cardiac, hepatic dysplasia: A case report. Clin Case Rep 7(11):2153-2155, 2019. https://doi.org/10.1002/ccr3.2330
34. Magno G, Boer LL, Oostra RJ, Zanatta A: The role of the University of Padua medical school in the study of conjoined twins between 18th and early 19th century. Am J Med Genet A 188(12):3423-3431, 2022. https://doi.org/10.1002/ajmg.a.62938
35. Mathur P, Sharma S, Mittal P, Yadav RK, Barolia D: Heteropagus twins: six cases with systematic review and embryological insights. Pediatr Surg Int 38(7):963-983, 2022. https://doi.org/10.1007/s00383-022-05135-w
36. Mendilcioglu I, Simsek M: Conjoined twins in a trichorionic quadruplet pregnancy after ovulation ınduction with clomiphene citrate. Fetal Diagn Ther 24 (1): 51–54, 2008. https://doi.org/10.1159/000132407
37. Mian A, Gabra NI, Sharma T, Topale N, Gielecki J, Tubbs RS, Loukas M. Conjoined twins: from conception to separation, a review. Clinic Anat 30:385–396, 2017. https://doi.org/10.1002/ca.22839
38. Mohammed D, Haruna G, Sadusi MM, Sule SA, Musa MA: Parasitic limb attached to the back: a rare case of rachipagus parasitic conjoined twinning. Int J Health Sci Res 7:410–413, 2017. Available from: https://www.ijhsr.org/IJHSR_Vol.7_Issue.5_May2017/62.pdf. Accessed June 19, 2023.
39. Mohindra S, Batish A, Patil NR, Tripathi M: Fully developed accessory lower limb with tethered cord: are these two anomalies related? Childs Nerv Syst 37:325–328, 2021. https://doi.org/10.1007/s00381-020-04616-4
40. Murphy RF, Cohen BH, Muhlbauer MS, Eubanks JS, Sawyer JR, Moisan A, Kelly DM: An accessory limb with lipomyelomeningocele in a male. Pediatr Surg Int 29:749–752, 2013. https://doi.org/10.1007/s00383-013-3269-9
41. Nadeem M, Ijaz L, Rehman L: Vestigial accessory limbs with spina bifida: Our 5 – year experience. Pak J Neurol Surg 20:187–191, 2016. https://doi.org/10.1007/s00383-022-05135-w
42. Navaei AA, Habibi Z, Moradi E, Nejat F: Parasitic rachipagus twins; report of two cases. Childs Nerv Syst 31(6):1001-1003, 2015. https://doi.org/10.1007/s00381-015-2664-z

43. Oduor P, Nyamal K: Parasitic rachipagus conjoined twins: surgical management and follow-up of a case in Kenya. Ann Afr Surg 11:54–57, 2014. https://www.ajol.info/index.php/aas/article/view/114668
44. Ozkan-Ulu H, Yilmaz Y, Sari FN, Altug N, Uras N, Dilmen U: An unusual case of heteropagus: autosite with a complex cardiac malformation. Pediatr Neonatol 52: 358-360, 2011. https://doi.org/10.1016/j.pedneo.2011.08.011
45. Pandey A, Singh S, Pandey J, Gupta V, Verma R: Lumbosacral parasitic twin associated with lipomeningomyelocele: a rare occurrence. Pediatr Neurosurg 49:110–112, 2013. https://doi.org/10.1159/000358096
46. Park KB, Kim YM, Park JY, Chung ML, Jung YJ, Nam SH: An accessory limb with an imperforate anus. Ann Surg Treat Res 87:213–216, 2014. https://doi.org/10.4174/astr.2014.87.4.213
47. Parks C, Mugamba J: Accessory limb with myelomeningocele: a rare case challenging previously held beliefs. Childs Nerv Syst 30(12):2127-2128, 2014. https://doi.org/10.1007/s00381-014-2452-1
48. Pati AB, Mahalik SK, Naik S, Das K: Heteropagus twins: a tale of two. Neurolog India, 68 (6): 1453-1455, 2020. https://doi.org/10.4103/0028-3886.304090
49. Priyawansha Y, Munasinghe K, Manike N: A rare case of heterophagus twinning. Sri Lanka J Child Health 47:279–281, 2018. https://doi.org/10.4038/sljch.v47i3.8555
50. Raheja A, Mahapatra AK: Rachipagus parasitic twin. Neurol India 65:1443–1444, 2017. https://doi.org/10.4103/0028-3886.217969
51. Ratan SK, Rattan KN, Magu S, Rohilla S, Purwar P, Mathur SK: Thoracolumbar rachipagus parasite. Pediatr Surg Int 20(4):298-300, 2004. https://doi.org/10.1007/s00383-003-1131-1
52. Retnam RK, Dhanalakshmi V, Juanita FE, GnanaMuthu JG: Polymelia associated with lipomyelomeningocele: a case report. Int J Anat Res 4(3):2813-2816, 2016. http://dx.doi.org/10.16965/ijar.2016.341
53. Ringo Y, Drake D, Sillo T, Lakhoo K: Parasitic twin within spina bifida. Afr J Paediatr Surg 9(3):240-242, 2012. https://doi.org/10.4103/0189-6725.104728
54. Rosenberg LE, Rosenberg DD: Human Genes and Genomes. Chapter 4 - Growth, fırst edition, Development and Reproduction, Elsevier 2012, 4: 27-50. ISBN: 9780123852120. eBook ISBN: 9780123852137
55. Saaiq M, Zimri FK, Zaman K: Successful treatment of well-developed accessory lower limb associated with spinal dysraphism: World J Plast Surg 9 (1): 73–81, 2020. https://doi.org/10.29252/wjps.9.1.73
56. Sahlu A, Mesfin B, Tirsit A, Debebe T, Wester K: Parasitic twin--a supernumerary limb associated with spinal malformations. A case report. Acta Neurochir 158(3):611-614, 2016. https://doi.org/10.1007/s00701-016-2710-y
57. Samy S, Amin H: Successful separation of rachipagus parasiticus neonate: case report and review of the literature. Egypt Spine J 20:51–60, 2016. https://doi.org/10.21608/esj.2016.4096
58. Sanoussi S, Rachid S, Sani CM, Mahamane B, Addo G: Rachipagus: a report of two cases - thoracic and lumbar. J Surg Tech Case Rep 2(1):27-29, 2010. https://doi.org/10.4103/2006-8808.63720
59. Sharma G, Mobin SS, Lypka M, Urata M: Heteropagus (parasitic) twins: a review J Pediatr Surg 45: 2454–2463, 2010. https://doi.org /10.1016/j.jpedsurg.2010.07.002
60. Shrikesh S, Singh US, Singh N, Sharanabasappa G, Amit N, Tanvir RK, Chetan S: Conjoined twins: a tertiary care centre experience. Sch J App Med Sci 6:1477–1480, 2018. https://doi.org /10.21276/sjams.2018.6.4.18
61. Snelling CM, Ellis PM, Smith RM, Rossiter JP: Lipomatous lumbar mass with an attached digit and associated split cord malformation. Can J Neurol Sci 35(2):250-254, 2008. https://doi.org /10.1017/s0317167100008738
62. Solak A, Ergün S, Polat I, Sahin N, Genç B: A rare form of heteropagus twinning: three-armed infant with spinal dysraphism. Case Rep Pediatr 2012: 831649, 2012. https://doi.org /10.1155/2012/831649
63. Solomon DZ, Fekadu N, Gorfu Y: Rachipagus parasitic twin in an Ethiopian neonate: a case report from the Horn of Africa. Int Res J Med Med Sci 6:56–59, 2018. https://doi.org/10.30918/IRJMMS.63.18.030
64. Spitz L: Conjoined twins. Br J Surg 83(8):1028-1030, 1996. https://doi.org/10.1002/bjs.1800830803
65. Steinman G: Mechanisms of twinning. V. Conjoined twins, stem cells and the calcium model. J Reprod Med 47(4):313-321, 2002. PMID: 12012884
66. Stephens TD, Siebert JR, Graham Jr JM, Beckwith JB: Parasitic conjoined twins, two cases, and their relation to limb morphogenesis. Teratology 26(2):115-121, 1982.https://doi.org/10.1002/tera.1420260203
67. Susana M, Lopes CS, Christine L. Mummery: Handbook Of Stem Cells 2:1-32, 2004.
68. Verma S, Khanna M, Tripathi VN, Yadav NC: Occurrence of polymelia in a female child. J Clin Imaging Sci 3:18, 2013. https://doi.org/10.4103/2156-7514.111235
69. Wilkes SL, Choi JJ, Rooks VJ: Lumbosacral lipomyelomeningocele with anomalous osseous limb in a 3-month-old female. Radiology Case Reports. Radiol Case Rep 10(1); 1051, 2015. https://doi.org/10.2484/rcr.v10i1.1051
70. Zewdie K, Negash S, Bizuneh Y, Woldemichael F, Temesgen F: Rachipagus parasitic twins: A case series and review of literature. Interdisciplinar Neurosurg 24-101049, 2021. https://doi.org/10.1016/j.inat.2020.101049
71. Zhang J, Duan H, Zhang Y, Yi Z, Bao S: Parasitic rachipagus conjoined twins with spina bifida, diplomyelia, scoliosis, tethered cord syndrome, and ventricular septal defect: case report. Neurol Med Chir 51(10):736–739, 2011. https://doi.org/10.2176/nmc.51.736
72. Zhao L, Li MQ, Sun XT, Ma ZS, Guo G, Huang YT: Congenital lumbosacral limb duplication: a case report. J Orthop Surg (Hong Kong) 14:187–191, 2006. https://doi.org/10.1177/230949900601400216
73. Zhi X, Hu B, Zhao X, Chen J, Gu C, Pu L, Fang Y, Cai C: A cohort of five cases with asymmetric conjoined twining and literature review. Pediatr Surg Int 38(1):169-181, 2022. https://doi.org/10.1007/s00383-021-05006-w

Turk Neurosurg 36(3):360-370, 2026
DOI: 10.5137/1019-5149.JTN.48860-25.2

Original Investigation
Cerebrovascular-Endovascular

Received: 24.05.2025
Accepted: 04.09.2025
Published Online: 22.05.2026

Brainstem Cavernoma: A Benign Lesion in a Malignant Location

Servet INCI, Baylar BAYLAROV

Hacettepe University, Faculty of Medicine, Department of Neurosurgery, Ankara, Türkiye

Corresponding author: Servet INCI ✉ sinci@hacettepe.edu.tr

ABSTRACT

AIM: To present our surgical experience with brainstem cavernomas and to emphasize the importance of the brainstem's internal structures.

MATERIAL and METHODS: Based on the clinical data of 25 symptomatic patients who underwent surgery for brainstem cavernomas, we reviewed their radiological findings, surgical indications, surgical timing, postoperative remnants, and outcomes. We also performed a statistical analysis of seven parameters that, based on our clinical experience, may influence outcomes in these challenging cases.

RESULTS: There were 14 male and 11 female patients, with a mean age of 36.6 years (range: 20–66 years). All patients were symptomatic and had experienced at least one episode of bleeding. Complete resection was achieved in 23 patients (92%), while two (8%) required reoperation for residual cavernoma. Postoperative mortality occurred in one patient (4%) due to malignant hyperthermia. As a result, the mean modified Rankin Scale (mRS) scores at admission, discharge, and last follow-up were 2.44, 2.14, and 1.86, respectively. Statistical analyses demonstrated that preoperative neurological status was an important parameter affecting outcome (p=0.002).

CONCLUSION: Brainstem cavernoma is a benign pathology, but it occurs in a malignant location. Therefore, advanced techniques, such as tractography, neuronavigation and neuromonitoring, should be employed in these challenging cases. However, we believe that a thorough knowledge of brainstem neuroanatomy and meticulous surgical technique are even more critical.

KEYWORDS: Brainstem, Cavernoma, Safe entry zone

ABBREVIATIONS: DSA: Digital subtraction angiography, **DTI:** Diffusion tensor imaging, **DVA:** Developmental venous anomaly, **MRI:** Magnetic resonance imaging, **mRS:** Modified rankin scale

INTRODUCTION

The first resection of a brainstem cavernoma (cavernous malformation, cavernous hemangioma) was reported almost 100 years ago by Walter Dandy (19). However, owing to its dense concentration of cranial nerve nuclei and white matter tracts within a small cross-sectional area, the brainstem has long been regarded as "terra incognita" (no man's land). Since the 1990s, brainstem surgery has been performed more safely due to advances in neurosurgical techniques, modern neuroimaging methods, and an improved understanding of the brainstem's internal structure (7,11,22).

Complications in brainstem cavernoma surgery primarily arise while entering the brainstem and/or cavernoma resection. Therefore, neurosurgeons must possess a detailed understanding of both the external and, especially, the internal structures of the brainstem. Brainstem lesions, resulting from surgical trauma, may lead to severe cranial nerve dysfunctions, motor/somatosensory deficits, cerebellar symptoms, and even death.

Servet INCI : 0009-0006-3978-1723 Baylar BAYLAROV : 0000-0002-9964-7220

We retrospectively reviewed our series of brainstem cavernoma surgeries, focusing on surgical indications, surgical timing, postoperative remnants, and factors affecting outcomes. We also aimed to highlight the importance of safe entry zones and the brainstem's intrinsic structures.

MATERIAL and METHODS

Between 1996 and 2019, 25 patients underwent surgery for symptomatic brainstem cavernoma. All surgeries were performed by the senior author (S.I.) using high magnification with a surgical microscope (Pentero, ZEISS, Oberkochen, Germany). The patients' files, surgical reports, radiological examinations, surgical videos, and follow-up data were reviewed. Ethics committee approval and informed consent were not required, as this study was conducted retrospectively.

All patients underwent preoperative brain MRI with standard sequences. Diffusion tensor imaging (DTI) with tract reconstruction was also performed in patients who underwent surgery in more recent years. Digital subtraction angiography (DSA) was performed in only two patients to rule out an arteriovenous malformation.

Throughout the series, we operated exclusively on symptomatic patients. Our surgical indications were: 1) cavernomas with repeated intralesional hemorrhages causing progressive neurological deficits; 2) symptomatic cavernomas reaching the pial surface or the fourth ventricular ependyma; and 3) cavernomas with acute hemorrhage extending beyond the lesion and causing mass effect.

All patients were started on corticosteroid therapy upon hospital admission. Preoperatively, patients and their relatives were informed about the estimated risk of rebleeding, potential surgical complications, and the high morbidity rates associated with the procedure.

Early postoperative MRI was obtained in all patients using the same sequences and planes as the preoperative scans and compared accordingly.

Patients' neurological status at admission, discharge, and last follow-up was assessed using the modified Rankin Scale (mRS) (0–6). Scores of 0–2 were considered a good outcome, while scores ≥ 3 were classified as an unfavorable (poor) outcome. These evaluations were performed by neurosurgery residents or junior neurosurgeons who had not participated in any of the surgeries included in this study.

Surgical Technique

In most cases, the appropriate surgical approach was selected using the two-point method described by Brown et al (8). In exophytic cavernomas or those adjacent to the pia mater (or ependymal surface), the lesion itself dictated the entry zone. Once the safe entry zone was reached, the pia mater was incised with microsurgical scissors, and the superficial parenchymal layer was gently dilated using the tip of bipolar forceps. After evacuating the hematoma, the cavernoma was internally decompressed, gently dissected from the surrounding neural tissue, and resected in a piecemeal manner. During resection, en bloc removal was avoided to prevent injury to the surrounding ascending/descending tracts and cranial nerve nuclei. Bipolar cauterization was not used unless obligatory. If present, the developmental venous anomaly (DVA) was preserved to prevent venous infarction. No attempt was made to remove hemosiderin-stained tissue. After meticulous hemostasis, the surgical area was carefully examined for cavernoma remnants.

Statistical Analysis

The following seven parameters, which in our experience may influence patient outcomes, were statistically analyzed: age, sex, preoperative mRS score, cavernoma location, cavernoma size, cavernoma depth, and surgical timing. All analyses were performed using SPSS version 23 (IBM Corp., Armonk, New York, USA). Data were analyzed using Fisher's Exact Test or the Pearson Chi-Square Test, as appropriate. A p-value of <0.05 was considered statistically significant.

RESULTS

A total of 14 male and 11 female patients, with a mean age of 36.6 years (range: 20–66 years), were included. The patient's demographic characteristics are summarized in Table I.

One patient had previously undergone V/P shunt placement at another hospital due to obstructive hydrocephalus. Another patient had also previously received radiotherapy at a different hospital under the suspicion of a brainstem glioma.

In this series, all patients experienced at least one bleeding episode. Thirteen patients (52%) presented with a single preoperative bleeding episode, 10 patients (40%) had two episodes, and two patients (8%) had three previous hemorrhages. In total, 39 hemorrhagic episodes were observed over 915

Table I: Characteristics of the Patients.

	Total/Average
Number of operated patients	25
Male	14
Female	11
Age at admission (years)	Mean 36.6 (20-66)
Cavernoma size (mm)	5-21
Hemorrhagic Event*	
1	13
2	10
3	2
Mean mRS score at admission	2.44
Mean mRS score at discharge	2.14
Mean mRS score at last follow-up	1.86
Mortality	1
Follow-up (months)	Mean 83.4 (2-128)

**According to past medical history of the patients and magnetic resonance imaging findings.*

patient-years. Thus, the annual hemorrhage rate was 4.2% per patient per year. The median time from the last hemorrhage to surgery was 22.4 days (range: 3–120 days). Based on measurements from TI-weighted MRI, the maximal size of the cavernomas ranged from 5 mm to 21 mm.

The most common clinical presentation was motor and sensory deficits (80.0%), followed by cranial nerve deficit(s) (72.0%), cerebellar symptoms (36.0%), headache (28.0%), and vertigo (24.0%). Interestingly, one patient with mesencephalic cavernoma presented solely with Holmes tremor (4.0%). Another patient presented with symptoms of obstructive hydrocephalus caused by a cavernoma obstructing the aqueduct of Sylvius (Figure 1).

The cavernomas were located on the mesencephalon (10 cases, 40%), the pons (11 cases, 44%), and the medulla oblongata (4 cases, 16%). Of the 25 lesions, 16 were intrinsic, eight were partially abutting the pial surface or fourth ventricular ependyma, and only one was exophytic. The surgical approaches used throughout this series and the corresponding safe entry zones are presented in Table II.

DVA was observed intraoperatively in 10 cases (40%) and was preserved in all. However, DVA had been identified on preoperative MRI in only six cases (24.0%). Complete resection of cavernoma was achieved in 23 patients (92%), as confirmed by early postoperative MRI. One patient with a residual cavernoma on postoperative MRI underwent reoperation on the second postoperative day, resulting in complete excision of the remnant. One patient developed a hematoma, causing hemiparesis on the second postoperative day. The hematoma was evacuated on the same day, and the residual cavernoma was also excised (see illustrative Case 11). In another patient, postoperative MRI revealed a suspicious remnant, but reoperation was not performed. This patient underwent MRI surveillance for 4 years.

In all patients, the diagnosis of cavernoma was confirmed by histopathological examination of the surgically resected tissue.

Complications

There were no significant intraoperative complications affecting the prognosis. Intraoperative air embolism developed in one patient operated in the sitting position, but it did not affect the course of the surgery. Postoperative pneumocephalus developed in another patient in the same position. One patient developed a supratentorial subdural effusion postoperatively

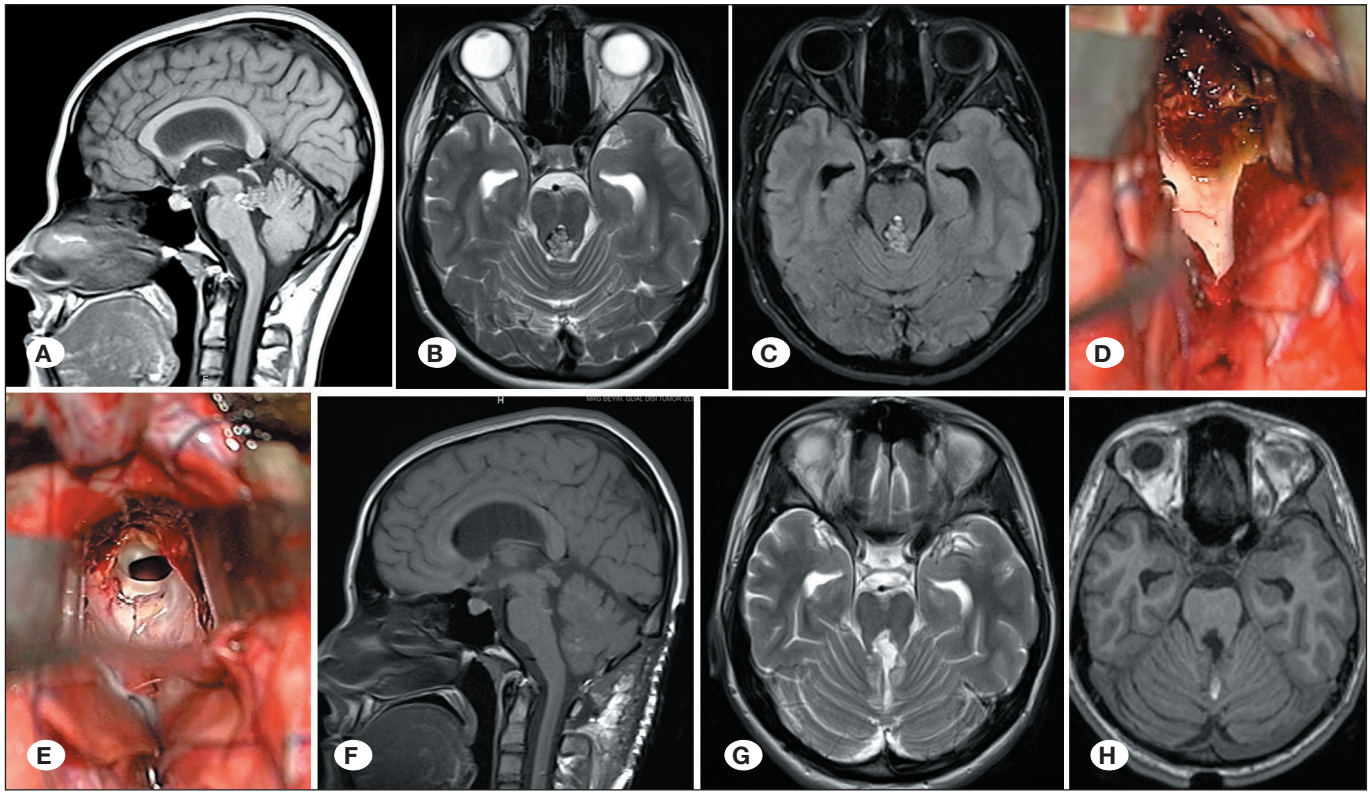

Figure 1: A 19-year-old female patient presented with a headache for several days. Magnetic resonance imaging (MRI) revealed obstructive hydrocephalus from a cavernoma within the aquaductus Sylvii (**A:** sagittal T1-weighted, **B:** axial T2-weighted, **C:** axial T1-weighted images). The patient was operated via midline suboccipital craniotomy. The vermis was partially split and the cavernoma obstructing the aqueduct was seen at the highest point of the 4th ventricle **(D)**. Gross total resection of the cavernoma was performed and the aquaductus was opened **(E)**. Post-operative MRI showed no residual lesion (**F:** sagittal T1-weighted, **G:** axial T2-weighted, **H:** axial T1-weighted images). The patient was discharged with normal neurological examination. She was still neurologically intact at her latest follow-up 36 months after surgery.

Table II: Basic Operative Approaches to Brainstem Cavernomas Used in the Study

Location	Sub-location	Approaches	Number	Used Safe Entry Zone
Mesencephalon	Ventral	Pterional/transsylvian	4	Perioculomotor
	Lateral	Subtemporal	4	Lat. Mesecephalic Sulcus
	Dorsal	Supracerebellar infratentorial	2	Infra collicular
Pons	Lateral	Retrosigmoid Subtemporal	4 2	Peritrigeminal Peritrigeminal
	Dorsal	Suboccipital transvermian Suboccipital telovelar	3 2	Suprafacial Infrafacial
Medulla Oblongata	Dorsal	Median suboccipital Median suboccipital	2 1	Post. Median fissure Post. Intermediate sulcus
	Lateral	Far lateral	1	Trans olivary

and required drainage with a burr hole. In the other patient, temporary postoperative CSF leakage occurred from the wound but did not require surgical intervention.

Outcome

Based on patients' preoperative neurological status, postoperative neurological symptoms improved in nine patients (36%), remained unchanged in 11 patients (44%), and worsened in four patients (16%). There was no surgery-related mortality. However, during the early years of this series, one patient (4%) with known myotonic dystrophy died postoperatively due to malignant hyperthermia.

Follow-up

Follow-up data were obtained for all surviving 24 patients. At followup (mean: 83.4 months; range: 2–128 months), no patient experienced clinical regression, and no rehemorrhage was observed. Two of the four patients whose postoperative status had deteriorated returned to their preoperative neurological status, while the other two remained unchanged.

As a result, the mean mRS scores at admission, discharge, and last follow-up were 2.44, 2.14, and 1.86, respectively.

Statistical Results

Seven potential parameters that may affect outcomes were evaluated using univariate analysis. The effects of six of these parameters—age, sex, location, size, depth, and timing of surgery—on the unfavorable outcomes were not statistically significant (Fisher's Exact Test). Only the preoperative mRS score was identified as a high-risk factor for unfavorable outcome (p=0.002, Pearson ChiSquare Test) (Table III).

Illustrative Cases

Case 11: A 31-year-old male patient presenting with sudden headache, left eyelid drooping, double vision, and right-sided eye weakness was referred to us. His past medical history revealed a similar but milder episode 3 months ago. MRI demonstrated a cavernoma located in the left ventral mesencephalon with an old hematoma (Figure 2A, B). DTI tractography demonstrated lateral displacement of the left corticospinal tract. Surgery was performed via left pterional craniotomy using the transsylvian approach. The left oculomotor nerve was traced to the brainstem. The left ventral surface of the mesencephalon, the exit of the oculomotor nerve, the posterior cerebral artery, and the superior cerebellar artery were visualized (Figure 2C). The surface of the mesencephalon appeared entirely normal (Figure 2D). A small incision was made just lateral to the oculomotor nerve using the tip of the bipolar forceps, reaching and draining the hematoma approximately 2 mm deep (Figure 2E). The cavernoma was then easily identified and excised in piecemeal fashion. No venous anomalies were observed. The cavity was carefully examined for any residual lesions. After achieving hemostasis, the wound was closed in the usual manner. The patient was transferred to the intensive care unit with his preoperative symptoms. On the second postoperative day, his hemiparesis worsened. MRI revealed a small hematoma and a possible residual cavernoma. The patient underwent reoperation, the hematoma was evacuated, and a small remnant located in the postero-lateral part of the cavity was excised. Postoperative MRI confirmed complete excision of the cavernoma (Figure 2F, G). In the postoperative period, his hemiparesis improved sufficiently to allow unaided walking, but oculomotor paresis remained unchanged. At his last follow-up, 8 months after surgery, he was able to walk independently. His oculomotor paresis had improved slightly but persisted.

Case 18: A 26-year-old male patient was admitted with left hemihypoesthesia that began 10 days earlier and hiccups that started 2 days prior. MRI revealed a hematoma and cavernoma on the left dorsal aspect of the medulla oblongata (Figure 3A, B). DTI-tractography demonstrated displacement of the pyramidal tract (Figure 3C). The patient was operated on via low medial suboccipital craniotomy and C1 laminectomy. Upon opening the dura, the surface of the medulla oblongata appeared completely normal (Figure 3D). Based on the multiplanar MRI findings, a small vertical myelotomy was performed along the posterior intermediate sulcus, likely overlying the hematoma. The hematoma was reached at a depth of approximately 1 mm and evacuated. The small cavernoma

Table III: Factors that May Affect Unfavorable Outcome and Results of Statistical Analysis

Factors		No. of patients	No. of unfavorable outcome (%)	p-value
Age (years)	1-40	16	8 (50)	0.677*
	>40	9	3 (33)	
Sex	Male	14	7 (50)	0.689*
	Female	11	4 (36.6)	
Preop. mRS score	0-2	12	1 (8.3)	**0.002****
	3-5	13	10 (76.9)	
Location	Mesencephalon	10	5 (50)	0.757*
	Pons	11	4 (45.4)	
	Medulla Oblongata	4	1 (25)	
Size (mm)	5-10	11	3 (27.2)	0.227*
	11-21	14	8 (57.1)	
Depth of cavernoma	Superficial	9	2 (22.2)	0.208*
	Deep	16	9 (56.2)	
Timing of surgery (weeks)	< 2	5	3 (60)	0.856*
	2-6	15	6 (40)	
	> 6	5	2 (40)	

**Fisher's Exact test, **Pearson Chi-Square test.*

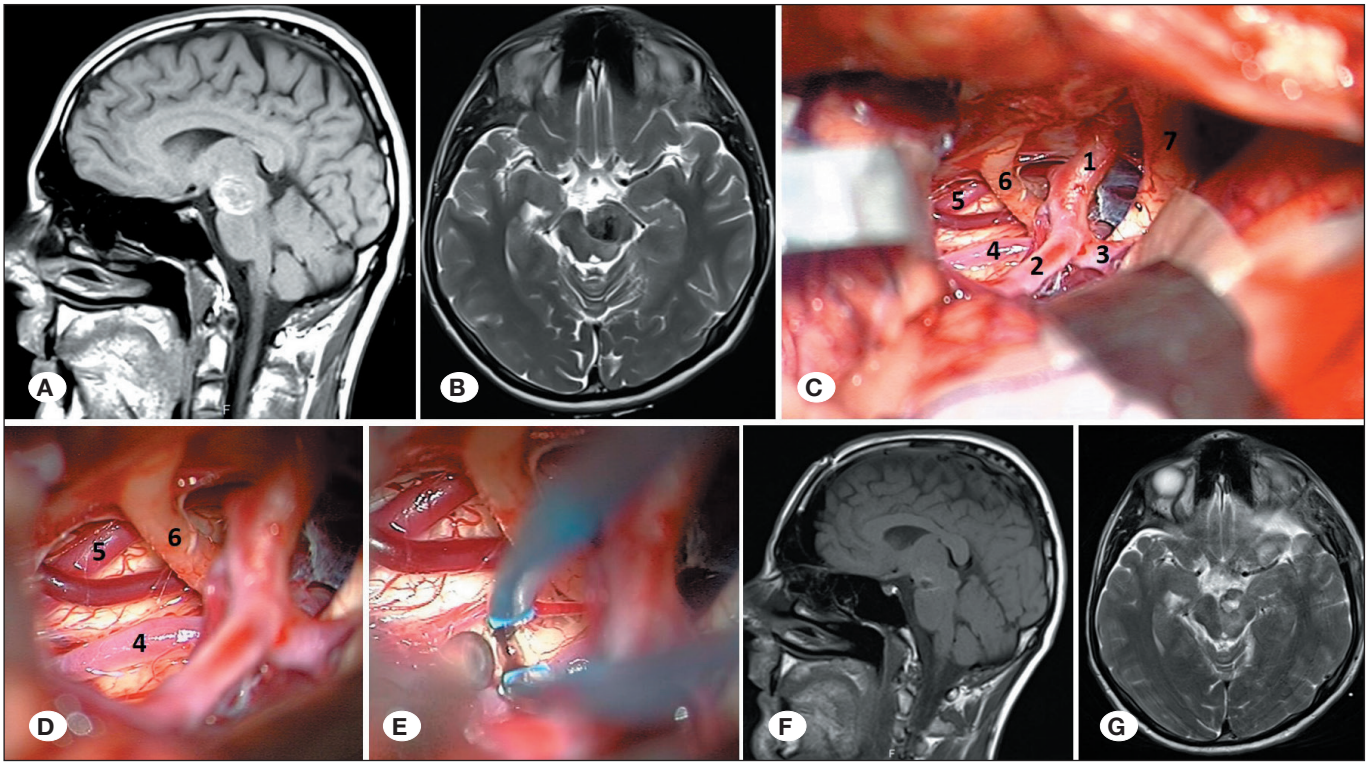

Figure 2: Case #11. **A)** T1-weighted sagittal magnetic resonance imaging (MRI) shows ventral mesencephalic cavernoma, **B)** T2-weighted axial MRI, **C)** intraoperative picture after fully splitting the left Sylvian fissure (1: ICA, 2:MCA, 3:AI, 4: Post. Cerebral Artery, 5: Sup. Cerebellar artery, 6: The oculomotor nerve, 7: The optic nerve), **D)** view of the surgical field with higher magnification, **E)** a small incision in the perioculomotor safe entry zone and drainage of the hematoma, **F)** postoperative T1-weighted sagittal image, **G)** postoperative T2-weighted axial image.

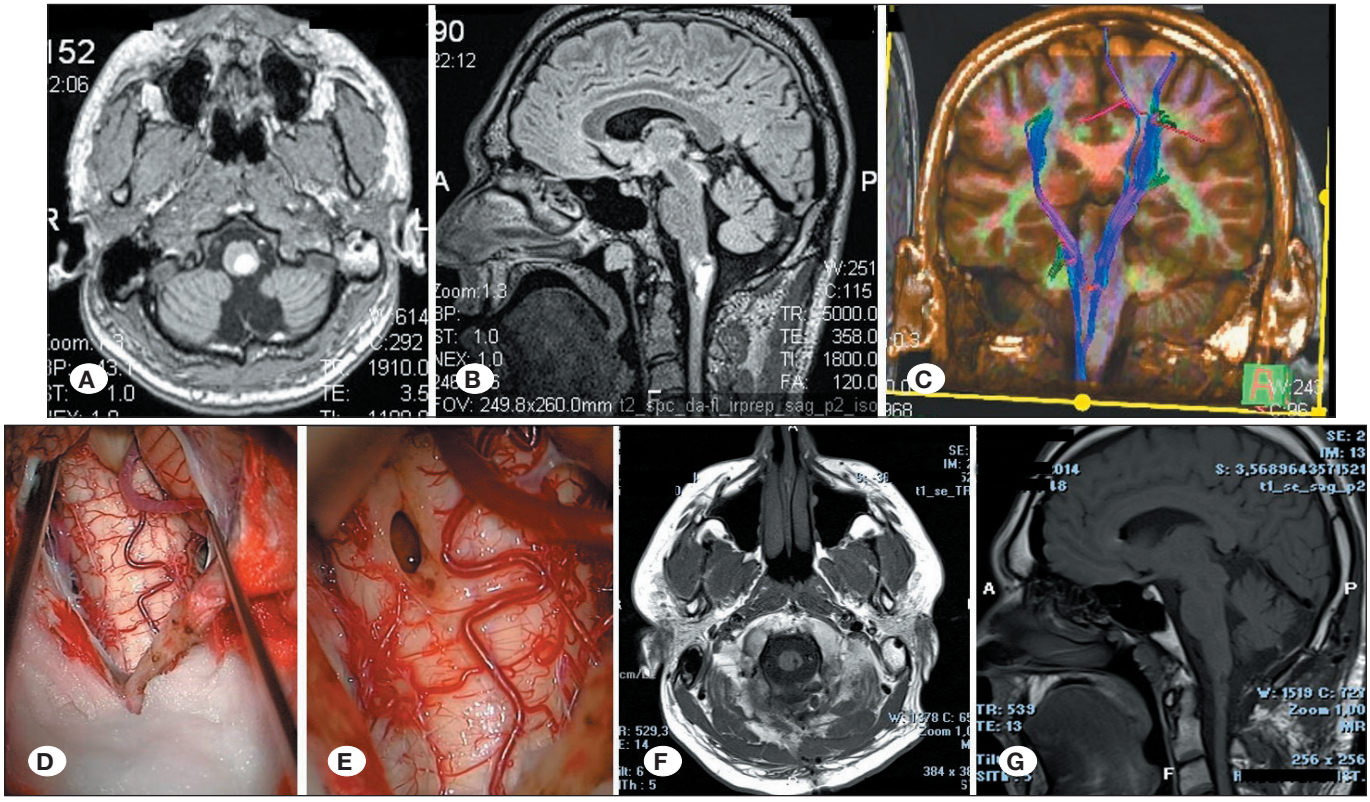

Figure 3: Case #18. **A)** T1-weighted axial magnetic resonance imaging (MRI) shows a cavernoma on the left dorsal surface of the medulla oblongata, **B)** sagittal MRI, **C)** DTI-tractography shows displacement of the pyramidal tract, **D)** the dorsal surface of the medulla oblongata was entirely normal, **E)** the cavernoma was excised with a small incision but the hemosiderin ring was left intact, **F)** axial, and **G)** sagittal T1-weighted postoperative MR images showed complete resection.

was then easily resected; however, the surrounding hemosiderin-stained tissue was not removed (Figure 3E). Postoperative MRI confirmed gross total resection of the cavernoma (Figure 3F, G). His hiccups resolved completely in the early postoperative period, and the hemihypoesthesia had also resolved by the last follow-up, 17 months later.

DISCUSSION

Brainstem surgery has several important disadvantages compared to surgeries performed in other regions of the brain: 1) the surgical corridor is longer; 2) the surgical field of view is coneshaped and gradually narrows; 3) there is little or no possibility of using a static retractor during surgery; and 4) this region contains a high density of critical tracts and cranial nerves nuclei. In conclusion, a brainstem cavernoma is a benign pathology, but it is located in a surgically malignant localization. Consequently, the morbidity rate in brainstem cavernoma surgery remains high, even in experienced hands (20,39,41,51).

Neuroradiological Imaging

MRI is the most sensitive and specific method for diagnosing brainstem cavernomas. Preoperative multiplanar MRI should be carefully reviewed, with particular attention to the following aspects: I) If the MRI is more than a few days old, a new scan should be obtained preoperatively. 2) The size of the cavernoma, rather than the hematoma, should be measured. 3) The relationship of the cavernoma to the pial or ependymal surface should be carefully assessed. This relationship is best evaluated on TI-weighted images. T2-weighted images may falsely suggest pial involvement due to blooming artifacts, even when the cavernoma is actually embedded within the brainstem (9,20,26). 4) Identification of some anatomical landmarks on the brainstem surface is important for accurate localization, including the exits of the cranial nerves, the lateral mesencephalic vein, the facial colliculus, the superior and inferior colliculus, and the olive. 5) DTI with reconstruction should be performed to demonstrate displacement of surrounding white matter tracts and to minimize the risk of surgical injury to these critical structures (21,33,47). 6) The presence of any associated DVA should be noted.

The use of neuronavigation is an important advantage, especially for deeply located cavernomas. However, it was not used in most cases in this series, as it was not available in our department at that time. While neuronavigation is valuable, it cannot replace careful evaluation of the MRI or, more importantly, detailed knowledge of the intrinsic brainstem anatomy. Therefore, the neurosurgeon needs to maintain a clear understanding of the three-dimensional anatomy of both external and, especially, internal brainstem structures during surgery.

Surgical Indication

The prevailing view among neurosurgeons is that asymptomatic patients should not undergo surgery, a position we also support (4,5,10,26,41,52). Although there is strong consensus that brainstem cavernomas causing hemorrhage and neurological symptoms warrant surgical intervention, the specific criteria for surgical intervention remain controversial. In detailed literature reviews of brainstem cavernoma surgery reported by Gross et al. (27), and Kearns et al. (32), the overall rates of complete resection were 91% and 92.3%, respectively. At long-term follow-up, the rate of improved or stable clinical symptoms was also 84% and 92.3%, respectively. Despite these satisfactory results, there remains no consensus on the specific criteria for surgical indication.

In 2021, an international consensus report on the surgical treatment of brainstem cavernomas was published (17). To summarize the report: I) asymptomatic patients or those with mild symptoms and difficult access to the cavernoma should not undergo surgery; 2) patients with multiple symptomatic hemorrhages, progressive deficits, and easy access to the cavernoma should undergo surgery; 3) patients experiencing first symptomatic hemorrhage with severe progressive deficits and mass effect should also undergo surgery; and 4) other patients who do not meet these criteria may be treated either surgically or conservatively. The decision should take into account the patient's general condition and the characteristics of the cavernoma.

To our experience, the generalized recommendations in the literature should be considered when deciding on surgery for brainstem cavernomas; however, each patient must also be evaluated individually, taking into account the following factors: age, comorbidities, neurological symptoms, location/size of the lesion, and the surgeon's experience.

Timing of Surgery

The optimal surgical timing for brainstem cavernomas remains controversial, and there is no uniform consensus. Most authors recommend performing surgery in the subacute stage (2–6 weeks) for the following reasons: I) MRI can better differentiate between the hematoma and cavernoma itself; 2) during this period, the patient's neurological status becomes more stable; 3) this interval allows sufficient time for reduction of tissue edema; and 4) the hematoma liquefies within a few weeks and can be easily aspirated, making the cavernoma itself easier to identify within the cavity formed by the hematoma (10,26,28,36,40,42). However, some authors believe that surgery should be performed earlier because: 1) gliosis developing between the hematoma and neural tissue can make resection of the cavernoma more challenging; 2) neural tissue is relieved from compression in the early period; and 3) there is a risk of rebleeding during the waiting period (9,42,48).

According to a large series of 397 patients reported by Zaidi et al., patients treated within 6 weeks after hemorrhage derived the maximum benefit from surgical intervention (51). In a recently published large clinical series (49), patients who underwent surgery during the acute period (<3 weeks) or chronic period (>8 weeks) had poorer outcomes compared with those who underwent surgery during the subacute period (3–8 weeks). Similarly, a recently published international consensus report recommends that the preferred timing for resection is between 4 and 8 weeks after the last event (17). Interestingly, however, Samii et al. found no difference in outcomes between surgery performed in the subacute stage and surgery conducted more than three months after hemorrhage (39).

We prefer to perform this surgery in the subacute stage, provided the patient's condition is suitable. However, we operated on two patients with acute hematoma and associated severe neurological deficits at an early stage. In cases of life-threatening conditions, such as coma, hemi- or quadriplegia/paresis, rapidly deteriorating neurological status, or cardio/respiratory instability, emergency surgery should be considered (3,6,46). This approach can be lifesaving.

Surgical Tips and Tricks

Based on our experience and the literature, the following points should be considered in brainstem cavernoma surgery: 1) the aim of the surgery should be the complete resection of the cavernoma, while preserving all neurological structures and any associated venous anomaly. 2) The "two-point method" described by Brown et al. should be used to select the correct surgical approach (8). However, in brainstem surgery, the shortest route may not always be the safest or most effective. Therefore, the approach can be adapted to the individual anatomy of each patient. If the trajectory intersects delicate structures (venous anomaly, motor tract, or exiting cranial nerve), the entry point may be slightly modified to avoid these structures. Hence, the surgeon should choose not only the shortest but also the safest route. 3) Microsurgical resection is performed under high-power magnification. 4) When the safe entry zone is reached, the pial or ependymal incision should be smaller than the cavernoma itself, and the superficial parenchymal layer should be gently dilated using the tip of bipolar forceps. During this procedure, the bipolar forceps should be opened and closed parallel to the fibers to avoid injuring them. 5) If present, any extracapsular hematoma should be drained first using low suction power. Hematoma usually displaces or pushes white matter tracts but does not disrupt them (1,26). Therefore, if the surgeon remains inside the hematoma cavity, the probability of tract disruption decreases. 6) The cavernoma is then internally decompressed and gently dissected from the surrounding neural tissue. 7) The lesion should be removed in a piecemeal fashion. "En bloc" resection is generally not safe in this location. 8) The gliotic margins may be functional and should, therefore, not be handled aggressively. 9) Bipolar cauterization should be used in the brainstem only when necessary, due to the risk of thermal damage. Bleeding is usually low-pressure from the dilated sinusoidal spaces and can be easily controlled with gentle pressure. 10) The surrounding hemosiderin-stained tissue should not be removed (1,37,39,41). A study using DTI-MRI tractography demonstrated the presence of viable white matter tracts passing through the hemosiderin-stained tissue (12). 11) Any associated DVA should be preserved as much as possible to maintain normal venous drainage and avoid venous infarction (1,26). The rate of intraoperative identification of venous anomalies in brain-

stem cavernomas varies between 13.9% and 58.3% in the literature (24,28,34,40). We were able to detect and preserve the venous anomaly intraoperatively in only 10 cases (40.0%). However, according to the intraoperative findings from a very large series, this association rate is 100% (1). Additionally, a study conducted using a 7 Tesla MRI reported that cavernoma-associated venous malformations were observed in all cases (18). According to these results, the cause of unexpected postoperative worsening in some patients may be venous anomalies that are not visible during surgery and can, therefore, be injured. 12) Hemostatic agents may be used to control bleeding, but they should be removed after the procedure, as they can affect the appearance of the surgical site on postoperative MRI. 13) At the end of hemostasis, bleeding control should be confirmed by increasing venous pressure using the Valsalva maneuver. 14) The patient should be referred to the intensive care unit at least for 24 hours. If the lesion is close to the lower cranial nerves, extubation should be performed only after a satisfactory cough and gag reflex are observed.

Postoperative Remnants

Some cavernomas may be multilobulated (14,35). One of these lobules may not protrude into the surgical cavity and can be overlooked. In addition, if scar tissue has formed around the cavity due to old or multiple hemorrhages, it becomes difficult to fully inspect the cavity. For this reason, even in very experienced hands, the risk of remnant varies between 6.6% and 11% (1,24). In a systematic review published in 2019, which included 2,493 patients who underwent surgery (32), the rate of remnant was found to be 7.7%. In our series, the rate of remnant was 8%. Therefore, every neurosurgeon should consider this possibility, and postoperative MRI should be performed in all cases. If a hypo- or hyperintense blood-containing nodule is observed at the edge of or within the surgical cavity, a cavernoma remnant should be suspected. If a remnant is clearly identified on postoperative MRI, early reoperation should be considered, because, as in one of our cases, the risk of rebleeding from the remnant is high (1,10,20). According to the literature review by Gross et al., approximately two-thirds of patients with partially resected cavernomas experienced rebleeding (27).

However, early postoperative MRI is not very reliable for detecting small postoperative remnants. According to a detailed study on this subject (15), early postoperative MRI has a sensitivity of 66.6% for detecting cavernoma remnants, a specificity of 76.7%, a positive predictive value of 16.6%, and a negative predictive value of 97.0%. In other words, small remnants are not always visible on early postoperative MRI. This limitation has also been highlighted in large surgical series (24,43). Accumulated blood in the surgical cavity, tissue edema, or the use of hemostatic agents can contribute to this reduced imaging accuracy.

Factors Affecting Outcome

Recently, Garcia et al. developed a surgical risk grading system based on their experience with 104 operated patients (23). The system assigns points according to the following factors: lesion size (<2 cm, 0 point; > 2 cm, 1 point), crossing the axial midpoint (no, 0 point; yes, 1 point), presence of DVA (no, 0 point; yes, 1 point), age (<40 years, 0 point; > 40 years, 1 point), and hemorrhage acuity (0–3 weeks, 0 point; 3–8 weeks, 1 point; > 8 weeks, 2 points). According to this grading system, grades 0 and 1 are associated with universally favorable functional outcomes, whereas grades 6 and 7 are associated with universally unfavorable functional outcomes. We consider this grading system valuable and important. However, based on our clinical observations and statistical analyses, preoperative neurological status also emerges as a key prognostic factor influencing outcomes (p=0.002). In fact, several authors have also reported that the preoperative neurological status is a significant predictor of surgical outcome (14,29,39,45,51).

Another factor to consider is the depth of the cavernoma. Logically, surgery for deeply located brainstem cavernomas carries a higher risk, as it requires splitting of healthy brainstem parenchyma, increasing the likelihood of injury to the cranial nerve nuclei and long tracts. Many surgical series have already emphasized that surgical risk and morbidity are higher for deep-seated brainstem cavernomas compared with superficial ones (2,20,25,27). However, a few clinical series have reported contrasting findings. In the study by Bruneau et al., cavernoma location (deep, abutting the pial surface, or extrinsic) was not significantly associated with postoperative worsening (9). According to Huang et al., a deep intrinsic cavernoma location is not necessarily associated with an unfavorable outcome (30). In another study, although the terms “deep” and “moderate depth” were not clearly defined, patients with deep cavernoma were reported to have better outcomes than those with lesions of moderate depth (16).

Although the effect of cavernoma depth on unfavorable outcomes was not statistically significant in our study (p = 0.208), a notable difference was observed between patients with superficial and deep cavernoma (22.2% and 56.2%, respectively). Therefore, we believe that the impact of cavernoma depth on outcome remains controversial.

Safe Entry Zones and Related Intrinsic Structures

Recently, we published a comprehensive review on safe entry zones to the brainstem (31). To our knowledge, 21 safe entry zones have been described for accessing brainstem cavernomas, and our series utilized nine of them (50). While a detailed discussion of safe entry zones is beyond the scope of this article, we would like to briefly emphasize their importance.

In brainstem surgery, the brainstem surface is sometimes entirely normal, with no discoloration or dark-blue area indicating a bulging hematoma. In such cases, safe entry zones to the brainstem are essential. These zones represent entry points and trajectories where tracts and cranial nerve nuclei are relatively sparse (4,13,26,31,38,44). Performing brainstem surgery through these corridors minimizes the possibility of neurological deficit. Otherwise, serious cranial nerve dysfunctions, motor symptoms, cerebellar symptoms, and even death may occur. However, it should also be noted that these safe entry zones may “no longer be safe” if the normal anatomy is distorted by the cavernoma or associated hematoma.

Limitations of this study

The limitations of our study include its retrospective design and the relatively small number of patients.

CONCLUSION

Brainstem cavernoma is a benign pathology, but it occurs in a high-risk location. Therefore, advanced techniques, such as tractography, neuronavigation and neuromonitoring, should be employed in these challenging cases. Nevertheless, we believe that detailed neuroanatomical knowledge of the brainstem and meticulous surgical technique are even more crucial.

Declarations

Funding: This research did not receive any specific grant from funding agencies in the public, commercial, or not-for-profit sectors.

Availability of data and materials: The datasets generated and/or analyzed during the current study are available from the corresponding author by reasonable request.

Disclosure: The authors declare no competing interests.

Ethical approval: Ethics committee approval and informed consent were not required, as this study was conducted retrospectively.

AUTHORSHIP CONTRIBUTION

Study conception and design: SI

Data collection: SI, BB

Analysis and interpretation of results: SI, BB

Draft manuscript preparation: SI

Critical revision of the article: SI, BB

Other (study supervision, fundings, materials, etc...): n/a

All authors (SI, BB) reviewed the results and approved the final version of the manuscript.

REFERENCES

1. Abla AA, Lekovic GP, Turner JD, de Oliveira JG, Porter R, Spetzler RF: Advances in the treatment and outcome of brainstem cavernous malformation surgery: A single-center case series of 300 surgically treated patients. Neurosurgery 68:403-415, 2011. http://doi:10.1227/NEU.0b013e3181ff9cde
2. Abla AA, Turner JD, Mitha AP, Lekovic G, Spetzler RF: Surgical approaches to brainstem cavernous malformations. Neurosurg Focus 29: E8, 2010. http://doi:10.3171/2010.6.FOCUS10128
3. Antunes CM, Marques RSF, Machado MJS, Marques LTM, Filipe MAR, Fernandes JS, Alegria CMG: Emergency surgery for brainstem cavernoma haemorrhage with severe neurological presentation. Is it indicated and worthwhile? Br J Neurosurg 34:427-433, 2020. http://doi:10.1080/02688697.2020.1753170
4. Arslan A, Ozsoy KM, Olguner SK, Acik V, Istemen I, Arslan B, Gezercan Y, Okten AI: Surgical results of brainstem cavernous malformation haemorrhage. Turk Neurosurg 30:768-775, 2020. http://doi:10.5137/1019-5149.JTN.3120720.2
5. Asaad WF, Walcott BP, Nahed BV, Ogilvy CS: Operative management of brainstem cavernous malformations. Neurosurg Focus 29:E10, 2010. http://doi:10.3171/2010.6.FOCUS10134
6. Bertalanfy H, Burkhardt JK, Kockro RA, Bozinov O, Sarnthein J: Resection of cavernous malformations of brainstem. In: Rigamonti D (eds), Cavernous Malformations of the Nervous System. Cambridge University Press, 1991:143-159. https://doi.org/10.1017/CBO9781139003636.016
7. Bertalanffy H, Gilsbach JM, Eggert HR, Seeger W: Microsurgery of deep-seated cavernous angiomas: Report of 26 cases. Acta Neurochir (Wien) 108:91-99, 1991. http://doi:10.1007/BF01418515
8. Brown AP, Thompson BG, Spetzler RF: The two-point method: Evaluating brain stem lesions. BNI Q 12:20-24, 1996.
9. Bruneau M, Bijlenga P, Reverdin A, Rilliet B, Regli L, Villemure JG, Porchet F, de Tribolet N: Early surgery for brainstem cavernomas. Acta Neurochir (Wien) 148:405-414, 2006. http://doi:10.1007/s00701-005-0671-7
10. Cannizzaro D, Sabatino G, Mancarella C, Revay M, Rossi M, Pecchioli G, Cardia A, Maira G, D'Angelo V, Fornari M: Management and surgical approaches of brainstem cavernous malformations: Our experience and literature review. Asian J Neurosurg 14:131-139, 2019. http://doi:10.4103/ajns.AJNS_290_17
11. Cantore G, Missori P, Santoro A: Cavernous angiomas of the brain stem: Intra-axial anatomical pitfalls and surgical strategies. Surg Neurol 52:84-94, 1999. http://doi:10.1016/s0090-3019(99)00036-1
12. Cauley KA, Andrews T, Gonyea JV, Filippi CG: Magnetic resonance diffusion tensor imaging and tractography of intracranial cavernous malformations: Preliminary observations and characterization of the hemosiderin rim. J Neurosurg 112:814-823, 2010. http://doi:10.3171/2009.8.JNS09586
13. Cavalcanti DD, Preul MC, Kalani MYS, Spetzler RF: Microsurgical anatomy of safe entry zones to the brainstem. J Neurosurg 124:1359-1376, 2016. http://doi:10.3171/2015.4.JNS141945
14. Cenzato M, Stefini R, Ambrosi C, Giovanelli M: Post-operative remnants of brainstem cavernomas: Incidence, risk factors and management. Acta Neurochir (Wien) 150:879-887, 2008. http://doi:10.1007/s00701-008-0008-4
15. Chen B, Göricke S, Wrede K, Jabbarli R, Wälchli T, Jägersberg M, Sure U, Dammann P: Reliable? The value of early postoperative magnetic resonance imaging after cerebral cavernous malformation surgery. World Neurosurg 103:138-144, 2017. http://doi:10.1016/j.wneu.2017.03.135
16. Chen L, Zhao Y, Zhou L, Zhu W, Pan Z, Mao Y: Surgical strategies in treating brainstem cavernous malformations. Neurosurgery 68:609-621, 2011. http://doi:10.1227/NEU.0b013e3182077531
17. Dammann P, Abla AA, Al-Shahi Salman R, Andrade-Barazarte H, Benes V, Cenzato M, Connolly ES, Cornelius JF, Couldwell WT, Sola RG, Gomez-Paz S, Hauck E, Hernesniemi J, Kivelev J, Lanzino G, Macdonald RL, Morcos JJ, Ogilvy CS, Steiger HJ, Steinberg GK, Santos AN, Rauschenbach L, Darkwah Oppong M, Schmidt B, Spetzler RF, Schaller K, Lawton MT, Sure U: Surgical treatment of brainstem cavernous malformations: An international Delphi consensus. J Neurosurg 136:1220-1230, 2021. http://doi:10.3171/2021.3.JNS2156

18. Dammann P, Wrede KH, Maderwald S, El Hindy N, Mueller O, Chen B, Zhu Y, Hütter BO, Ladd ME, Schlamann M, Sandalcioglu IE, Sure U: The venous angioarchitecture of sporadic cerebral cavernous malformations: A susceptibility weighted imaging study at 7 T MRI. J Neurol Neurosurg Psychiatry 84:194-200, 2013. http://doi:10.1136/jnnp-2012-302599
19. Dandy WE: Venous abnormalities and angiomas of the brain. Arch Surg 17:715-793, 1928. http://doi:10.1001/archsurg.1928.01140110002001
20. Ferroli P, Sinisi M, Franzini A, Giombini S, Solero CL, Broggi G: Brainstem cavernomas: Long-term results of microsurgical resection in 52 patients. Neurosurgery 56:1203-1214, 2005. http://doi:10.1227/01.neu.0000159644.04757.45
21. Flores BC, Whittemore AR, Samson DS, Barnett SL: The utility of preoperative diffusion tensor imaging in the surgical management of brainstem cavernous malformations. J Neurosurg 122:653-662, 2015. http://doi:10.3171/2014.11.JNS13680
22. Fritschi JA, Reulen HJ, Spetzler RF, Zabramski JM: Cavernous malformations of the brain stem. A review of 139 cases. Acta Neurochir (Wien) 130:35-46, 1994. http://doi:10.1007/BF01405501
23. Garcia RM, Ivan ME, Lawton MT: Brainstem cavernous malformations: Surgical results in 104 patients and a proposed grading system to predict neurological outcomes. Neurosurgery 76: 265-278, 2015. http://doi:10.1227/NEU.0000000000000602
24. Garcia RM, Oh T, Cole TS, Hendricks BK, Lawton MT: Recurrent brainstem cavernous malformations following primary resection: Blind spots, fine lines, and the right-angle method. J Neurosurg 135:671-682, 2020. http://doi:10.3171/2020.6.JNS201555
25. Garrett M, Spetzler RF: Surgical treatment of brainstem cavernous malformations. Surg Neurol 72 Suppl 2:S3-10, 2009. http://doi:10.1016/j.surneu.2009.05.031
26. Giliberto G, Lanzino DJ, Diehn FE, Factor D, Flemming KD, Lanzino G: Brainstem cavernous malformations: Anatomical, clinical, and surgical considerations. Neurosurg Focus 29:E9, 2010. http://doi:10.3171/2010.6.FOCUS10133
27. Gross BA, Batjer HH, Awad IA, Bendok BR, Du R: Brainstem cavernous malformations: 1390 surgical cases from the literature. World Neurosurg 80:89-93, 2013. http://doi:10.1016/j.wneu.2012.04.002
28. Gui S, Meng G, Xiao X, Wu Z, Zhang J: Surgical management of brainstem cavernous malformation: Report of 67 patients. World Neurosurg 122:e1162-e1171, 2019. http://doi:10.1016/j.wneu.2018.11.008
29. Hauck EF, Barnett SL, White JA, Samson D: Symptomatic brainstem cavernomas. Neurosurgery 64:61-70, 2009. http://doi:10.1227/01.NEU.0000335158.11692.53
30. Huang C, Bertalanffy H, Kar S, Tsuji Y: Microsurgical management of midbrain cavernous malformations: Does lesion depth influence the outcome? Acta Neurochir (Wien) 163:2739-2754, 2021. http://doi:10.1007/s00701-021-04915-y
31. Inci S, Baylarov B: Axial section of brainstem safe entry zones and clinical importance of intrinsic structures: A review. World Neurosurg 185:171-180, 2024. https://doi.org/10.1016/j.wneu.2024.02.088
32. Kearns KN, Chen CJ, Tvrdik P, Park MS, Kalani MYS: Outcomes of surgery for brainstem cavernous malformations: A systematic review. Stroke 50:2964-2966, 2019. http://doi:10.1161/STROKEAHA.119.026120
33. Li D, Jiao YM, Wang L, Lin FX, Wu J, Tong XZ, Wang S, Cao Y: Surgical outcome of motor deficits and neurological status in brainstem cavernous malformations based on preoperative diffusion tensor imaging: A prospective randomized clinical trial. J Neurosurg 130:286-301, 2018. http://doi:10.3171/2017.8.JNS17854
34. Li D, Yang Y, Hao SY, Wang L, Tang J, Xiao XR, Zhou H, Jia GJ, Wu Z, Zhang LW, Zhang JT: Hemorrhage risk, surgical management, and functional outcome of brainstem cavernous malformations. J Neurosurg 119:996-1008, 2013. http://doi:10.3171/2013.7.JNS13462
35. Mishima K, Sasaki T, Ojima T, Mukasa A, Kirino T: Multilobular cavernous malformation: Report of two cases. Acta Neurochir (Wien) 140:20-25, 1998. http://doi:10.1007/s007010050052
36. Ohue S, Fukushima T, Kumon Y, Ohnishi T, Friedman AH: Surgical management of brainstem cavernomas: Selection of approaches and microsurgical techniques. Neurosurg Rev 33: 315-324, 2010. http://doi:10.1007/s10143-010-0256-7
37. Ramina R, Mattei TA, de Aguiar PH, Meneses MS, Ferraz VR, Aires R, Kirchhoff DF, de Carvalho Kirchhoff D: Surgical management of brainstem cavernous malformations. Neurol Sci 32:1013-1028, 2011. http://doi:10.1007/s10072-011-0477-8
38. Recalde RJ, Figueiredo EG, de Oliveira E: Microsurgical anatomy of the safe entry zones on the anterolateral brainstem related to surgical approaches to cavernous malformations. Neurosurgery 62: 9-15, 2008. http://doi:10.1227/01.neu.0000317368.69523.40
39. Samii M, Eghbal R, Carvalho GA, Matthies C: Surgical management of brainstem cavernomas. J Neurosurg 95:825-832, 2001. http://doi:10.3171/jns.2001.95.5.0825
40. Schwartz C, Grillhösl A, Schichor C, Suchorska B, Romagna A, Tonn JC, Zausinger S: Symptomatic cavernous malformations of the brainstem: Functional outcome after microsurgical resection. J Neurol 260:2815-2822, 2013. http://doi:10.1007/s00415-013-7071-3
41. Singh H, Elarjani T, da Silva HB, Shetty R, Kim L, Sekhar LN: Brain stem cavernous malformations: Operative nuances of a less-invasive resection technique. Oper Neurosurg (Hagerstown) 15:153-173, 2018. http://doi:10.1093/ons/opx231
42. Sola RG, Pulido P, Pastor J, Ochoa M, Castedo J: Surgical treatment of symptomatic cavernous malformations of the brainstem. Acta Neurochir (Wien) 149:463-470, 2007. http://doi:10.1007/s00701-007-1113-5
43. Steinberg GK, Chang SD, Gewirtz RJ, Lopez JR: Microsurgical resection of brainstem, thalamic, and basal ganglia angiographically occult vascular malformations. Neurosurgery 46:260-270; discussion 270-271, 2020. http://doi:10.1097/00006123-200002000-00003

44. Tacyildiz AE, Barut O, Ucer M, Ozgunduz Y, Tanriover N: Medial pontine area: A safe entry to the brainstem as a cut above the rest. Turk Neurosurg 34:966-972, 2024. http://doi:10.5137/1019-5149.JTN.45710-23.1
45. Tsuji Y, Kar S, Bertalanffy H: Microsurgical management of midbrain cavernous malformations: Predictors of outcome and lesion classification in 72 patients. Oper Neurosurg (Hagerstown) 17:562-572, 2019. http://doi:10.1093/ons/opz026
46. Tumturk A, Li Y, Turan Y, Cikla U, Iskandar BJ, Baskaya MK: Emergency resection of brainstem cavernous malformations. J Neurosurg 128:1289-1296, 2018. http://doi:10.3171/2017.1.JNS161693
47. Ulrich NH, Kockro RA, Bellut D, Amaxopoulou C, Bozinov O, Burkhardt JK, Sarnthein J, Kollias SS, Bertalanffy H: Brainstem cavernoma surgery with the support of pre-and postoperative diffusion tensor imaging: Initial experiences and clinical course of 23 patients. Neurosurg Rev 37:481-492, 2014. http://doi:10.1007/s10143-014-0550-x
48. Wang CC, Liu A, Zhang JT, Sun B, Zhao YL: Surgical management of brain-stem cavernous malformations: Report of 137 cases. Surg Neurol 59:444-454, 2003. http://doi:10.1016/s0090-3019(03)00187-3
49. Xie S, Xiao XR, Xiao SW, Xie MX, Zhang JT, Wu Z, Zhang LW: Surgical managements and patient outcomes after severe hemorrhagic events from brainstem cavernous malformations. Neurosurg Rev 44:423-434, 2021. http://doi:10.1007/s10143-019-01230-0
50. Yang Y, van Niftrik B, Ma X, Velz J, Wang S, Regli L, Bozinov O: Analysis of safe entry zones into the brainstem. Neurosurg Rev 42:721-729, 2019. http://doi:10.1007/s10143-019-01081-9
51. Zaidi HA, Mooney MA, Levitt MR, Dru AB, Abla AA, Spetzler RF: Impact of timing of intervention among 397 consecutively treated brainstem cavernous malformations. Neurosurgery 81:620-626, 2017. http://doi:10.1093/neuros/nyw139
52. Zhang S, Li H, Liu W, Hui X, You C: Surgical treatment of hemorrhagic brainstem cavernous malformations. Neurol India 64:1210-1219, 2016. http://doi:10.4103/0028-3886.193825

Turk Neurosurg 36(3):371-376, 2026
DOI: 10.5137/1019-5149.JTN.49747-25.3

Original Investigation
Neuro – Oncology

Received: 30.08.2025
Accepted: 21.02.2026
Published Online: 22.05.2026

Downregulation of miR-221, miR-143, and miR-22 in Meningioma: Diagnostic Performance in a Single-Center Case–Control Study

Salim TEKIR[1], Emre OZKARA[2], Ebru ERZURUMLUOGLU[3], Zuhtu OZBEK[2], Sevilhan ARTAN[3], Hulya OZEN[4], Ali ARSLANTAS[2]

[1]Serik Hospital, Department of Neurosurgery, Antalya, Türkiye
[2]Eskisehir Osmangazi University, Faculty of Medicine, Department of Neurosurgery, Eskisehir, Türkiye
[3]Eskisehir Osmangazi University, Faculty of Medicine, Department of Genetics, Eskisehir, Türkiye
[4]University of Health Sciences, Gulhane Faculty of Medicine, Department of Medical Informatics, Ankara, Türkiye

Corresponding author: Emre OZKARA ✉ dremreozkara@gmail.com

ABSTRACT

AIM: To determine case–control differences in tissue miRNA expression and to quantify their ability to distinguish meningioma from nontumor dura.

MATERIAL and METHODS: Tissue samples from 45 intracranial meningioma cases (WHO grade I, n = 22; grade II, n = 23) and 26 dura controls were analyzed. miRNA expression levels were measured by quantitative real-time PCR (qRT-PCR), normalized to U6, and relative expression levels were calculated using the $2^{-\Delta\Delta Ct}$ method. Group and grade comparisons were performed using appropriate parametric or nonparametric tests. Diagnostic performance was evaluated using receiver operating characteristic (ROC) and area under the curve (AUC) values, with optimal cut-off points determined by the Youden index. Sensitivity and specificity were reported.

RESULTS: Compared with controls, meningioma tissues showed significant downregulation of miR-221, miR-143, and miR-22 (all $p < 0.001$), whereas miR-145 showed borderline significance ($p = 0.052$). Diagnostic discrimination was highest for miR-221 (AUC, 0.912; cut-off, ≤0.19; sensitivity, 91.11%; specificity, 88.46%), followed by miR-143 (AUC, 0.810; cut-off, ≤0.24; sensitivity, 71.11%; specificity, 92.31%) and miR-22 (AUC, 0.771; cut-off, ≤0.36; sensitivity, 82.22%; specificity, 65.38%). No significant differences in expression were observed between grade I and grade II tumors for any miRNA.

CONCLUSION: Tissue miR-221, miR-143, and miR-22 are consistently downregulated in intracranial meningioma and demonstrate clinically meaningful diagnostic performance, with miR-221 showing the highest discriminatory accuracy. These findings support the potential integration of miRNA assays into tissue-based diagnostics and warrant multicenter validation to refine cut-off values and evaluate prognostic utility.

KEYWORDS: AUC, brain neoplasms, meningioma, microRNA

ABBREVIATIONS: AUC: Area under the curve, **miRNA:** MicroRNA, **qRT-PCR:** Quantitative real-time PCR, **ROC:** Receiver operating characteristic, **WHO:** World Health Organization

Salim TEKIR : 0000-0002-4057-5170
Emre OZKARA : 0000-0001-5448-6446
Ebru ERZURUMLUOGLU : 0000-0002-1275-5174
Zuhtu OZBEK : 0000-0003-0028-4181
Sevilhan ARTAN : 0000-0001-7658-6309
Hulya OZEN : 0000-0003-4144-3732
Ali ARSLANTAS : 0000-0003-4753-2779

INTRODUCTION

Meningiomas are extra-axial tumors arising from arachnoid cap cells and account for approximately 13%–26% of all intracranial tumors. They are more prevalent in females, and headache is among the most common presenting symptoms (17,21,22). Although most meningiomas are benign, a subset demonstrates aggressive behavior and recurrence that are not fully predicted by histopathological features alone (21,22).

Current diagnostic practice increasingly relies on an integrated approach. The 2021 World Health Organization (WHO) Classification of Tumors of the Central Nervous System (CNS5) incorporates molecular criteria alongside morphology. Specifically, TERT promoter mutations and homozygous deletions of CDKN2A/B now warrant a WHO grade III designation, regardless of histology, owing to their strong association with early recurrence and poor clinical outcomes (14,16).

At the genomic level, meningiomas can be broadly classified into NF2-mutant and NF2–wild-type groups. The latter are enriched for alterations in genes such as *TRAF7*, *KLF4* (K409Q), *AKT1* (E17K), *PIK3CA*, and *SMO*, often displaying location-specific patterns (e.g., skull-base predilection) and pathway activation involving PI3K/AKT/mTOR or Hedgehog signaling. These alterations may co-occur, such as *TRAF7* mutations with *KLF4* or *AKT1*, and provide insights into tumor biology and therapeutic targets (1,3,6).

Beyond individual genetic alterations, epigenetic profiling has substantially improved risk stratification. DNA methylation–based classifications outperform histologic grading in predicting recurrence and have been translated into clinically relevant molecular groups. In addition, recurrent chromosomal losses—particularly of 1p and 14q—are common in higher-grade tumors and further refine prognostic assessment (4,7,18).

Within this molecular framework, microRNAs (miRNAs) have emerged as promising biomarkers because they reflect pathway-level activity and can be reliably quantified from routine tissue samples. Although prior studies have linked miRNA dysregulation to meningioma biology and clinical behavior, actionable diagnostic thresholds remain limited (2,9). Building on this background, we investigated the expression of miR-221, miR-143, and miR-22, with miR-145 included as a comparator, in an expanded single-center cohort and assessed their diagnostic performance using ROC-derived cut-off values.

MATERIAL and METHODS

Subjects

This study was conducted in accordance with the Declaration of Helsinki and was approved by the Clinical Practice Ethics Committee of the Eskisehir Osmangazi University Medical Faculty (approval date: May 5, 2021; Decision No. 14). Written informed consent was obtained from all participants. Tissue samples were collected from 45 patients diagnosed with intracranial meningioma between June 15, 2021, and August 15, 2023, at the Faculty of Medicine, Department of Neurosurgery. Control dura samples were obtained from 26 individuals who underwent decompressive craniectomy for cerebrovascular events.

Detection of miRNA Expression

Total microRNA was extracted using the Sanprep Column MicroRNA Mini-Preps Kit (Sangon Biotech Co., Ltd., Shanghai, China) according to the manufacturer's instructions. Complementary DNA was synthesized using the TaqMan Advanced miRNA cDNA Synthesis kit (Thermo Fisher Scientific, Inc.). Quantitative real-time PCR was performed with BrightGreen miRNA qPCR MasterMix (Applied Biological Materials, Vancouver, Canada) on a CFX96 Real-Time PCR Detection System (Bio-Rad Laboratories, Inc., Hercules, California). miRNA-specific primers for miR-143 (#MI0000459), miR-145 (#MI0000461), miR-221 (#MI0000298), and miR-22 (#MI0000078) were obtained from OriGene Technologies (Beijing, China). Gene expression levels were normalized to U6 (#MP300001), and relative expression was calculated using the $2^{-\Delta\Delta Ct}$ method (13).

Statistical Analysis

Statistical analysis was performed using IBM SPSS Statistics version 25. Quantitative variables, including miRNA expression levels and age, were presented as mean ± standard deviation or median (Q1–Q3), as appropriate, whereas categorical variables were expressed as frequencies and percentages. The Shapiro–Wilk test was used to assess normality. Group comparisons were conducted using the Student *t* test or Mann–Whitney *U* test for normally and nonnormally distributed data, respectively. Gender distributions were compared using the chi-square test. Spearman correlation analysis was used to assess linear relationships between quantitative variables.

Diagnostic performance was evaluated using receiver operating characteristic (ROC) curve analysis. The area under the ROC curve (AUC) was used to quantify discriminatory ability. Optimal cut-off values were determined using the Youden index, and corresponding sensitivity and specificity values were reported. A p value < 0.05 was considered statistically significant. Because several miRNA expression variables exhibited skewed distributions, group comparisons and biological interpretations were primarily based on median values, which were considered more representative of qRT-PCR expression data.

RESULTS

Study Participants

A total of 45 meningioma samples (22 females and 23 males) and 26 non–tumor-associated dura mater samples (14 females and 12 males) were included in this study. Among the meningioma cases, 22 tumors were classified as WHO grade I and 23 as grade II. The mean age of the meningioma and control groups was 58.36 ± 11.16 and 56.28 ± 12.36 yr, respectively. There were no statistically significant differences in age or sex distribution between the case and control groups ($p > 0.05$). Detailed clinical and demographic characteristics of the study participants are summarized in Table I.

Comparison of miRNA Expression Levels between Case and Control Groups

Compared with non–tumor-associated dura controls, meningioma tissues exhibited significant downregulation of miR-221, miR-143, and miR-22 (all $p < 0.001$). In contrast, miR-145 showed only a borderline difference between the two groups ($p = 0.052$). miRNA expression levels in patients and controls are presented in Table II. Although mean expression values appeared higher for some miRNAs in the meningioma group, median values consistently indicated lower expression in tumor tissues, reflecting skewed distributions with outliers. Therefore, conclusions regarding miRNA downregulation were primarily based on median comparisons.

Comparison of miRNA Expression Levels between WHO Grade I and Grade II Meningiomas

No statistically significant differences in miRNA expression levels were observed between WHO grade I and grade II meningioma samples (all $p > 0.05$) (Table III).

ROC Curve Analysis

Receiver operating characteristic (ROC) curve analysis demonstrated that miR-143 yielded an AUC of 0.81, with a sensitivity of 71.11% and a specificity of 92.31%. The optimal cut-off value for miR-143 was ≤0.24, as determined by the Youden index. miR-22 showed an AUC of 0.771, with a sensitivity of 82.22% and a specificity of 65.38%, at an optimal cut-off value of ≤0.36. miR-221 demonstrated the highest diagnostic accuracy, with an AUC of 0.912, sensitivity of 91.11%, and specificity of 88.46%, at a cut-off value of ≤0.19. AUC values and corresponding cut-off points are summarized in Table IV. An overview of AUCs is presented in Figure 1, and sensitivities and specificities at the selected cut-off values are shown in Figure 2.

Collectively, these findings support miR-221 as a strong tissue-based diagnostic adjunct, with miR-143 providing high specificity and miR-22 contributing to sensitivity.

Table I: Clinical and Demographic Features of Patients and Controls

Variable	Control (n=26)	Case (n=45)	p-value
Female, n (%)	14 (53.8)	22 (48.9)	0.876
Male, n (%)	12 (46.2)	23 (51.1)	
Age, mean±SD	56.28±12.36	58.36±11.16	0.476
Age, median [Q1–Q3]	58 [50–62]	60 [52–66]	

Table II: Expression Levels of miRNAs in Patients and Controls

miRNA	Control Mean±SD	Control Median [Q1–Q3]	Case Mean±SD	Case Median [Q1–Q3]	p-value
miR-143	1.70±1.94	0.94 [0.35–2.64]	1.09±3.13	0.05 [0.03–0.33]	**<0.001**
miR-145	2.72±3.48	0.76 [0.30–4.50]	6.99±17.93	0.20 [0.08–1.90]	0.052
miR-22	2.69±4.44	1.22 [0.20–3.18]	3.73±13.33	0.06 [0.01–0.25]	**<0.001**
miR-221	2.46±2.65	1.31 [0.26–4.54]	0.11±0.23	0.05 [0.01–0.13]	**<0.001**

Table III: Expression Levels in Grade 1 vs Grade 2 Meningiomas

miRNA	Grade 1 Mean±SD	Grade 1 Median [Q1–Q3]	Grade 2 Mean±SD	Grade 2 Median [Q1–Q3]
miR-143	1.85±4.31	0.05 [0.03–1.47]	0.36±0.88	0.18 [0.05–0.24]
miR-145	8.16±18.48	0.36 [0.15–6.62]	5.87±17.73	0.20 [0.01–0.87]
miR-22	3.00±11.89	0.03 [0.00–0.30]	4.43±14.81	0.20 [0.02–0.25]
miR-221	0.16±0.32	0.04 [0.01–0.16]	0.06±0.07	0.05 [0.02–0.05]

Table IV: AUC and Cut-off Values for miRNAs

Test (Biomarker)	AUC	SE	p	95% CI for AUC	Cut-off / Sensitivity / Specificity
miR-143	0.810	0.051	**<0.001**	(0.709–0.910)	≤0.24 / 71.11% / 92.31%
miR-22	0.771	0.056	**<0.001**	(0.661–0.882)	≤0.36 / 82.22% / 65.38%
miR-221	0.912	0.041	**<0.001**	(0.831–0.992)	≤0.19 / 91.11% / 88.46%

AUC: Area Under the Curve, **SE:** Standard Error, **CI:** Confidence Interval

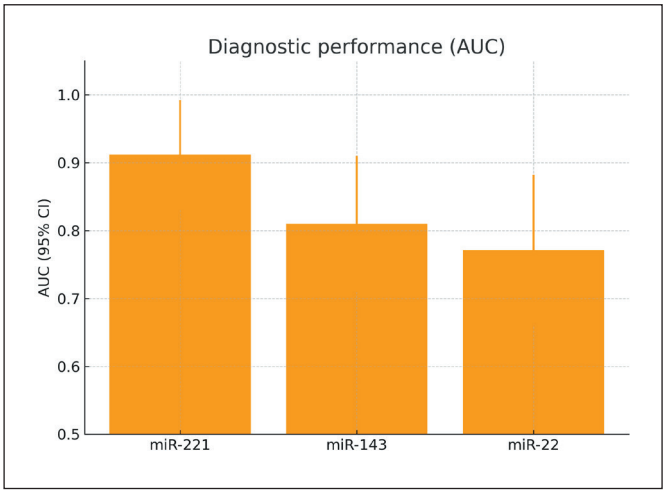

Figure 1: Diagnostic performance of miRNAs expressed as area under the curve (AUC) values. miR-221 demonstrated the highest discriminatory accuracy compared with miR-143 and miR-22.

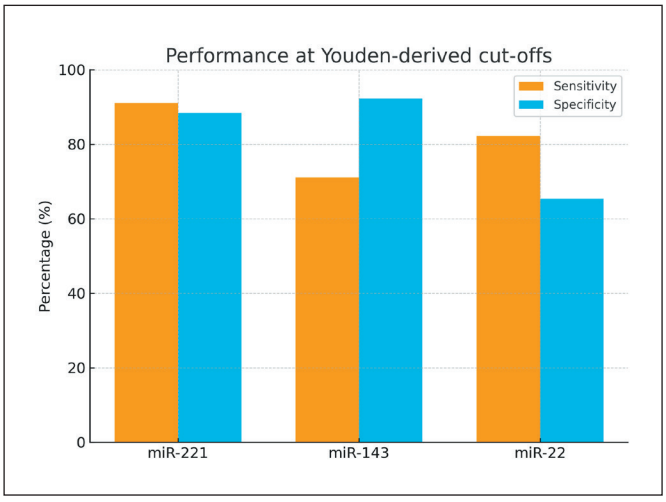

Figure 2: Sensitivity and specificity of miRNAs at Youden-derived optimal cut-off values. miR-221 showed balanced sensitivity and specificity, whereas miR-143 demonstrated higher specificity.

DISCUSSION

Meningiomas originate from arachnoid membrane cells and account for approximately 13%–26% of intracranial tumors. Although generally considered benign, meningiomas exhibit the second-highest morbidity rate after glial tumors. They typically grow slowly and are sometimes detected incidentally on radiologic imaging. The WHO Classification of Tumours of the Central Nervous System categorizes meningiomas into three histological grades and 15 subtypes to aid prognostic stratification. Approximately 90% of meningiomas are classified as WHO grade I (benign), 5%–7% as grade II (atypical), and 1%–3% as grade III (anaplastic) (21).

Meningiomas were among the earliest solid tumors investigated for genetic abnormalities, an important step toward understanding their biological behavior. Genetic insights may inform diagnosis, treatment, and preventive strategies. Familial studies indicate that first-degree relatives of patients with meningioma have an approximately twofold increased risk of developing the disease, although no consistent excess risk has been demonstrated among distant relatives at the population level (15). While this information has limited immediate diagnostic utility, it supports a heritable component that intersects with known somatic alterations and epigenetic programs in meningioma biology.

In the present cohort, tissue miR-221, miR-143, and miR-22 were significantly downregulated in meningioma samples compared with dura controls (all $p < 0.001$), whereas miR-145 showed only a borderline difference ($p = 0.052$). From a diagnostic perspective, miR-221 demonstrated the strongest discriminatory ability (AUC, 0.912; cut-off, ≤0.19; sensitivity, 91.11%; specificity, 88.46%), followed by miR-143 (AUC, 0.810; cut-off, ≤0.24; sensitivity, 71.11%; specificity, 92.31%) and miR-22 (AUC, 0.771; cut-off, ≤0.36; sensitivity, 82.22%; specificity, 65.38%). No significant differences were observed between WHO grade I and grade II tumors for any miRNA, indicating that while these markers may support diagnosis, they are insufficient for grading when used alone.

Biological Interpretation

miR-22. Although miR-22 upregulation has been reported in several malignancies and linked to metabolic reprogramming—particularly via repression of ATP-citrate lyase (ACLY) and modulation of *de novo* lipogenesis—our data demonstrate reduced miR-22 expression in meningioma tissue compared with dura controls (20,23). This discrepancy highlights the content-dependent nature of miRNA regulatory networks and underscores the importance of tissue-matched controls in biomarker development.

miR-143. Consistent with previous reports describing tumor-suppressive functions through modulation of KRAS/MAPK signaling and ERK5-dependent transcriptional programs, miR-143 expression was lower in meningioma tissues than in controls (5,19,25). The absence of grade-dependent differences suggests that miR-143 loss may represent an early or lineage-stable event rather than a driver of histologic progression.

miR-145. Prior studies in meningioma have reported downregulation of miR-145 in higher-grade tumors and inhibitory effects on cellular proliferation and migration in experimental models (11). Across multiple cancer types, miR-145 is generally regarded as a tumor suppressor (24). The borderline case–control difference observed in our study may reflect biologic heterogeneity, sample size limitations, or platform-related effects and warrants confirmation in larger cohorts.

miR-221/222 axis. Members of the miR-221/222 family are frequently upregulated and proproliferative in many epithelial cancers through repression of tumor suppressors such as $p27^{Kip1}$ and PTEN (10,12). In malignant meningioma models, inhibition of miR-221/222 enhances radiosensitivity and reduces radiation-induced invasiveness by relieving PTEN suppression (8). In contrast, the reduced miR-221 expression observed in our meningioma samples relative to dura controls

suggests lineage-specific regulation and raises the possibility that miR-221 downregulation reflects tissue identity rather than tumor aggressiveness.

Clinical Implications and Limitations

The observed downregulation of miR-221, miR-143, and miR-22, together with their ROC-derived thresholds, supports their potential use as tissue-based adjuncts to conventional histopathological diagnosis. Integration of these markers with current molecular frameworks, including DNA methylation classes and chromosomal alterations, may further enhance diagnostic and predictive accuracy (4,7,14,18). Key limitations of this study include its single-center design, lack of longitudinal outcome data, and absence of an external validation cohort. In addition, potential confounding effects of pre-analytical variables, such as ischemia time or embolization, cannot be fully excluded.

Future studies should pursue multicenter validation, evaluate associations with tumor recurrence and other prognostic outcomes, and assess multimarker panels that integrate miRNAs with genomic and epigenomic features to develop clinically actionable diagnostic and prognostic models. The use of non–tumor-associated dura mater obtained during decompressive craniectomy for cerebrovascular events represents a pragmatic and ethically feasible control strategy in neurosurgical research. Nevertheless, ischemia, inflammation, or acute pathological processes may influence miRNA expression independently of tumor biology. Such effects are expected to introduce nonspecific biological variability and would likely bias results toward underestimation rather than overestimation of tumor-specific differences. Multicenter studies incorporating alternative control tissues will be valuable for further validation.

CONCLUSION

Our findings identify miR-221, miR-143, and miR-22 as promising tissue-based diagnostic biomarkers for distinguishing intracranial meningioma from non-tumor–associated dura mater. Further multicenter validation and integration with established molecular classifiers are required before routine clinical implementation.

Declarations

Funding: Eskisehir Osmangazi University BAP TTU-2021-1721.

Availability of data and materials: The datasets used and/or analysed during the current study are available from the corresponding author on reasonable request.

Disclosure: The authors declare no conflict of interest.

AUTHORSHIP CONTRIBUTION

Study conception and design: EO, ST, EE
Data collection: ST, EO, EE
Analysis and interpretation of results: ZO, EO, HO
Draft manuscript preparation: ST, EO
Critical revision of the article: SA, AA
Other (study supervision, fundings, materials, etc...): EO, AA
All authors (ST, EO, EE, ZO, SA, HO, AA) reviewed the results and approved the final version of the manuscript.

REFERENCES

1. Abedalthagafi M, Bi WL, Aizer AA, Merrill PH, Brewster R, Agarwalla PK, Listewnik ML, Dias-Santagata D, Thorner AR, Van Hummelen P, Brastianos PK, Reardon DA, Wen PY, Al-Mefty O, Ramkissoon SH, Folkerth RD, Ligon KL, Ligon AH, Alexander BM, Dunn IF, Beroukhim R, Santagata S: Oncogenic PI3K mutations are as common as AKT1 and SMO mutations in meningioma. Neuro Oncol 18:649-655, 2016. https://doi.org/10.1093/neuonc/nov316
2. Bartel DP: Metazoan microRNAs. Cell 173:20-51, 2018. https://doi.org/10.1016/j.cell.2018.03.006
3. Brastianos PK, Horowitz PM, Santagata S, Jones RT, McKenna A, Getz G, Ligon KL, Palescandolo E, Van Hummelen P, Ducar MD, Raza A, Sunkavalli A, Macconaill LE, Stemmer-Rachamimov AO, Louis DN, Hahn WC, Dunn IF, Beroukhim R: Genomic sequencing of meningiomas identifies oncogenic SMO and AKT1 mutations. Nat Genet 45:285-289, 2013. https://doi.org/10.1038/ng.2526
4. Cai DX, Banerjee R, Scheithauer BW, Lohse CM, Kleinschmidt-Demasters BK, Perry A: Chromosome 1p and 14q FISH analysis in clinicopathologic subsets of meningioma: Diagnostic and prognostic implications. J Neuropathol Exp Neurol 60:628-636, 2001. https://doi.org/10.1093/jnen/60.6.628
5. Chen X, Guo X, Zhang H, Xiang Y, Chen J, Yin Y, Cai X, Wang K, Wang G, Ba Y, Zhu L, Wang J, Yang R, Zhang Y, Ren Z, Zen K, Zhang J, Zhang CY: Role of miR-143 targeting KRAS in colorectal tumorigenesis. Oncogene 28:1385-1392, 2009. https://doi.org/10.1038/onc.2008.474
6. Clark VE, Erson-Omay EZ, Serin A, Yin J, Cotney J, Ozduman K, Avşar T, Li J, Murray PB, Henegariu O, Yilmaz S, Günel JM, Carrión-Grant G, Yilmaz B, Grady C, Tanrikulu B, Bakircioğlu M, Kaymakçalan H, Caglayan AO, Sencar L, Ceyhun E, Atik AF, Bayri Y, Bai H, Kolb LE, Hebert RM, Omay SB, Mishra-Gorur K, Choi M, Overton JD, Holland EC, Mane S, State MW, Bilgüvar K, Baehring JM, Gutin PH, Piepmeier JM, Vortmeyer A, Brennan CW, Pamir MN, Kiliç T, Lifton RP, Noonan JP, Yasuno K, Günel M: Genomic analysis of non-NF2 meningiomas reveals mutations in TRAF7, KLF4, AKT1, and SMO. Science 339:1077-1080, 2013. https://doi.org/10.1126/science.1233009
7. Driver J, Hoffman SE, Tavakol S, Woodward E, Maury EA, Bhave V, Greenwald NF, Nassiri F, Aldape K, Zadeh G, Choudhury A, Vasudevan HN, Magill ST, Raleigh DR, Abedalthagafi M, Aizer AA, Alexander BM, Ligon KL, Reardon DA, Wen PY, Al-Mefty O, Ligon AH, Dubuc AM, Beroukhim R, Claus EB, Dunn IF, Santagata S, Bi WL: A molecularly integrated grade for meningioma. Neuro Oncol 24:796-808, 2022. https://doi.org/10.1093/neuonc/noab213
8. Garofalo M, Quintavalle C, Romano G, Croce CM, Condorelli G: miR221/222 in cancer: Their role in tumor progression and response to therapy. Curr Mol Med 12:27-33, 2012. https://doi.org/10.2174/156652412798376170
9. Garzon R, Fabbri M, Cimmino A, Calin GA, Croce CM: MicroRNA expression and function in cancer. Trends Mol Med 12: 580-587, 2006. https://doi.org/10.1016/j.molmed.2006.10.006
10. Hart M, Wach S, Nolte E, Szczyrba J, Menon R, Taubert H, Hartmann A, Stoehr R, Wieland W, Grässer FA, Wullich B: The proto-oncogene ERG is a target of microRNA miR-145 in prostate cancer. FEBS J 280:2105-2116, 2013. https://doi.org/10.1111/febs.12236

11. Kliese N, Gobrecht P, Pachow D, Andrae N, Wilisch-Neumann A, Kirches E, Riek-Burchardt M, Angenstein F, Reifenberger G, Riemenschneider MJ, Meese E, Panayotova-Dimitrova D, Gutmann DH, Mawrin C: miRNA-145 is downregulated in atypical and anaplastic meningiomas and negatively regulates motility and proliferation of meningioma cells. Oncogene 32:4712-4720, 2013. https://doi.org/10.1038/onc.2012.468
12. le Sage C, Nagel R, Egan DA, Schrier M, Mesman E, Mangiola A, Anile C, Maira G, Mercatelli N, Ciafrè SA, Farace MG, Agami R: Regulation of the p27(Kip1) tumor suppressor by miR-221 and miR-222 promotes cancer cell proliferation. EMBO J 26:3699-3708, 2007. https://doi.org/10.1038/sj.emboj.7601790
13. Livak KJ, Schmittgen TD: Analysis of relative gene expression data using real-time quantitative PCR and the 2(-Delta Delta C(T)) method. Methods 25:402-408, 2001. https://doi.org/10.1006/meth.2001.1262
14. Louis DN, Perry A, Wesseling P, Brat DJ, Cree IA, Figarella-Branger D, Hawkins C, Ng HK, Pfister SM, Reifenberger G, Soffietti R, von Deimling A, Ellison DW: The 2021 WHO classification of tumors of the central nervous system: A summary. Neuro Oncol 23:1231-1251, 2021. https://doi.org/10.1093/neuonc/noab106
15. Malmer B, Henriksson R, Grönberg H: Familial brain tumours — genetics or environment? A nationwide cohort study of cancer risk in spouses and first-degree relatives of brain tumour patients. Int J Cancer 106:260-263, 2003. https://doi.org/10.1002/ijc.11213
16. Osborn AG, Louis DN, Poussaint TY, Linscott LL, Salzman KL: The 2021 World Health Organization classification of tumors of the central nervous system: What neuroradiologists need to know. AJNR Am J Neuroradiol 43:928-937, 2022. https://doi.org/10.3174/ajnr.A7462
17. Ostrom QT, Patil N, Cioffi G, Waite K, Kruchko C, Barnholtz-Sloan JS: CBTRUS statistical report: Primary brain and other central nervous system tumors diagnosed in the United States in 2013-2017. Neuro Oncol 22:iv1-iv96, 2020. https://doi.org/10.1093/neuonc/noaa200
18. Sahm F, Schrimpf D, Stichel D, Jones DTW, Hielscher T, Schefzyk S, Okonechnikov K, Koelsche C, Reuss DE, Capper D, Sturm D, Wirsching HG, Berghoff AS, Baumgarten P, Kratz A, Huang K, Wefers AK, Hovestadt V, Sill M, Ellis HP, Kurian KM, Okuducu AF, Jungk C, Drueschler K, Schick M, Bewerunge-Hudler M, Mawrin C, Seiz-Rosenhagen M, Ketter R, Simon M, Westphal M, Lamszus K, Becker A, Koch A, Schittenhelm J, Rushing EJ, Collins VP, Brehmer S, Chavez L, Platten M, Hänggi D, Unterberg A, Paulus W, Wick W, Pfister SM, Mittelbronn M, Preusser M, Herold-Mende C, Weller M, von Deimling A: DNA methylation-based classification and grading system for meningioma: A multicentre, retrospective analysis. Lancet Oncol 18:682-694, 2017. https://doi.org/10.1016/S1470-2045(17)30155-9
19. Takaoka Y, Shimizu Y, Hasegawa H, Ouchi Y, Qiao S, Nagahara M, Ichihara M, Lee JD, Adachi K, Hamaguchi M, Iwamoto T: Forced expression of miR-143 represses ERK5/c-Myc and p68/p72 signaling in concert with miR-145 in gut tumors of Apc(Min) mice. PLoS One 7:e42137, 2012. https://doi.org/10.1371/journal.pone.0042137
20. Wang J, Li Y, Ding M, Zhang H, Xu X, Tang J: Molecular mechanisms and clinical applications of miR-22 in regulating malignant progression in human cancer (Review). Int J Oncol 50:345-355, 2017. https://doi.org/10.3892/ijo.2016.3811
21. Wen PY, Packer RJ: The 2021 WHO classification of tumors of the central nervous system: Clinical implications. Neuro Oncol 23:1215-1217, 2021. https://doi.org/10.1093/neuonc/noab120
22. Wiemels J, Wrensch M, Claus EB: Epidemiology and etiology of meningioma. J Neurooncol 99:307-314, 2010. https://doi.org/10.1007/s11060-010-0386-3
23. Xin M, Qiao Z, Li J, Liu J, Song S, Zhao X, Miao P, Tang T, Wang L, Liu W, Yang X, Dai K, Huang G: miR-22 inhibits tumor growth and metastasis by targeting ATP citrate lyase: Evidence in osteosarcoma, prostate cancer, cervical cancer and lung cancer. Oncotarget 7:44252-44265, 2016. https://doi.org/10.18632/oncotarget.10020
24. Zaman MS, Chen Y, Deng G, Shahryari V, Suh SO, Saini S, Majid S, Liu J, Khatri G, Tanaka Y, Dahiya R: The functional significance of microRNA-145 in prostate cancer. Br J Cancer 103:256-264, 2010. https://doi.org/10.1038/sj.bjc.6605742
25. Zhou LL, Dong JL, Huang G, Sun ZL, Wu J: MicroRNA-143 inhibits cell growth by targeting ERK5 and MAP3K7 in breast cancer. Braz J Med Biol Res 50:e5891, 2017. https://doi.org/10.1590/1414-431X20175891

Turk Neurosurg 36(3):377-384, 2026
DOI: 10.5137/1019-5149.JTN.49811-25.3

Original Investigation
Neuro – Oncology

Received: 08.09.2025
Accepted: 03.02.2026
Published Online: 22.05.2026

Ferulic Acid Increases Temozolomide Sensitivity in Glioblastoma Cells, Causing DNA Damage and Inhibiting Cell Proliferation

Halil ULUTABANCA[1,2], Serhat ALBAYRAK[2], Ahsen GULER[2,3], Venhar CINAR[2,4], Nursultan NURDINOV[2,5], Zuhal HAMURCU[2,4]

[1]Erciyes University, Faculty of Medicine, Department of Neurosurgery, Kayseri, Türkiye
[2]Erciyes University, Betül-Ziya Eren Genome and Stem Cell Center, Kayseri, Türkiye
[3]Fırat University, Faculty of Medicine, Department of Medical Biology, Elazığ, Türkiye
[4]Erciyes University, Faculty of Medicine, Department of Medical Biology, Kayseri, Türkiye
[5]Khoja Akhmet Yassawi International Kazakh-Turkish University, Faculty of Medicine and Dentistry, Turkestan, Kazakhstan

Corresponding author: Halil ULUTABANCA ✉ ulutabanca@gmail.com, Zuhal HAMURCU ✉ zuhal.hamurcu@gmail.com

ABSTRACT

AIM: To investigate the antitumor effects of ferulic acid (FA) on glioblastoma multiforme (GBM) cells both alone and in combination with temozolomide (TMZ), and also to determine the potential of this synergy for treatment processes.

MATERIAL and METHODS: Human glioblastoma U87-MG cells were used in this study. To evaluate the potential constructive interaction between temozolomide (TMZ) and ferulic acid (FA), a sequential treatment protocol was applied in which cells were first treated with TMZ (20, 40, and 80 μM) for 48 hours, followed by FA (1000 μM and 1500 μM) for an additional 24 hours. Cell viability was assessed using the MTS assay, clonogenic capacity was evaluated by the clonogenic assay, and nuclear morphological changes were examined by Hoechst 33258 staining. The expression levels of Cyclin D1 and PARP were also analyzed to explore the molecular mechanisms underlying the treatment effects.

RESULTS: FA treatment reduced cell viability and increased DNA damage in U87-MG cells. It suppressed the expression of Cyclin D1 and PARP. Furthermore, the combination of FA and TMZ almost completely inhibited cell proliferation and colony formation and significantly increased DNA damage.

CONCLUSION: Although FA has demonstrated antitumor activity at high concentrations, this may limit its clinical applicability. However, its ability to enhance the effects of TMZ suggests that FA could be used as a supportive treatment strategy in GBM therapy.

KEYWORDS: Glioblastoma Multiforme, Temozolomide, Ferulic Acid, DNA Damage, U87-MG

ABBREVIATIONS: GBM: Glioblastoma Multiforme, **TMZ:** Temozolomide, **FA:** Ferulic Acid, **PARP:** Poly (ADP-ribose) polymerase, **BBB:** Blood-Brain Barrier, **MGMT:** O6-Methylguanine-DNA Methyltransferase, **BER:** Base Excision Repair, **PI3K/AKT:** Phosphoinositide 3-kinase/Protein kinase B, **TG2:** Transglutaminase 2, **EMT:** Epithelial-Mesenchymal Transition, **(DMEM)/F12:** Dulbecco's Modified Eagle's Medium, **DMSO:** Dimethyl Sulfoxide, **MTS:** 3-(4,5 dimethylthiazol-2-yl) 5-(3-carboxymethoxyphenyl)-2-(4 sulphophenyl)-2H-tetrazolium), **PBS:** Phosphate Buffered Saline, **SDS:** Sodium Dodecyl Sulphate, **TBS-T:** Tris-Buffered Saline-Tween 20, **DNA:** Deoxyribonucleic Acid

Halil ULUTABANCA : 0000-0001-5912-3222
Serhat ALBAYRAK : 0000-0003-4047-6778
Ahsen GULER : 0000-0003-2873-6223
Venhar CINAR : 0000-0003-1544-8994
Nursultan NURDINOV : 0000-0001-5341-7211
Zuhal HAMURCU : 0000-0002-0711-4014

INTRODUCTION

Glioblastoma Multiforme (GBM) is the second leading cause of cancer-related deaths worldwide (8). GBM originating from glial cells is the most common and aggressive type of human brain tumor and accounts for 81% of malignant brain tumors (9,23). Surgical resection followed by chemotherapy and radiotherapy is currently the standard treatment used in the clinic for GBM (3,16). However, the therapeutic efficacy of standard treatment is low due to the invasive nature of glioblastoma, and 90% of patients experience tumor recurrence within 6-9 months after initial treatment, with a median survival time of approximately 15 months (3).

Temozolomide (TMZ), approved by the Food and Drug Administration (FDA) and widely used in the treatment of GBM, is a DNA alkylating agent that can cross the blood-brain barrier (BBB) (7,20). TMZ shows its cytotoxicity through the formation of DNA helix breaks by transferring methyl groups to the N3 region on adenines and N7, O6 regions on guanines (15,21,29), and then induces cell cycle arrest in G2/M leading to cell apoptosis (15). However, O6-methylguanine methyltransferase (MGMT) and base excision repair (BER)-based repair systems eliminate TMZ-mediated double helix breaks and methylation that reverses cell cycle arrest (10,24,28). This mechanism renders GBM resistant to TMZ and leads to decreased treatment efficacy. Therefore, finding effective therapeutic strategies and alternative compounds for the treatment of GBM is of foremost importance.

Ferulic acid (4-hydroxy-3-methoxycinnamic acid, FA) is a hydroxycinnamic acid and an abundant phenolic phytochemical with antioxidant and antitumor activities in vegetables and fruits. It has been detected in plants such as Angelica sinensis, Cimicifuga heracleifolia, and Ligusticum chuangxiong (7). It has been reported that FA can inhibit the expression and activity of many cytotoxic enzymes, including nitric oxide synthase, caspases, and cyclooxygenase (31).

FA has been reported to have a wide range of effects, including anti-inflammatory, antidiabetic, anticarcinogenic, antiapoptotic, hepatoprotective, neuroprotective, radioprotective, pulmonary protective, antiatherogenic, hypotensive, and vasodilatation effects (6). Recently, the high therapeutic potential of FA has attracted considerable interest in terms of research. The therapeutic effects of FA on various cancer types have been demonstrated in numerous studies. In osteosarcoma cells, FA stopped the cell cycle and induced apoptosis by suppressing the PI3K/Akt (Phosphoinositide 3-kinase/ Protein kinase B) pathway (27). In breast cancer cell lines, it showed cytotoxic effect by activating caspase-8 and caspase-9 (5). It was reported that nanoparticle forms of FA increased apoptosis by decreasing tissue transglutaminase 2 (TG2) expression in glioblastoma cells and inhibited proliferation by suppressing DNA synthesis in glioblastoma cells (4). In metastatic breast cancer cells, it has been shown to prevent metastasis by inhibiting epithelial-mesenchymal transition (EMT) (30).

These findings show that the anticarcinogenic effects of FA are multifaceted, and when used together with chemotherapeutic agents, they may create a potential synergistic effect. Considering the limitations in glioblastoma treatment and the prevalence of TMZ resistance, the present study focused on whether ferulic acid can improve the efficacy of TMZ and how it can stop the proliferation of glioblastoma cells. Our results showed that FA alone and in combination with TMZ suppressed cell proliferation and induced DNA damage by suppressing Cyclin D1 and PARP expression. Our data suggest that the combination of these two agents may offer a new and effective way to combat glioblastoma, making a significant contribution to current treatment strategies.

MATERIAL and METHODS

Cell Line, Culture Conditions, and Reagents

U87-MG (cat# HTB-14) cells were purchased from the American Type Culture Collection (Manassas, VA, USA). U87-MG cells were cultured in Dulbecco's Modified Eagle's Medium (DMEM)/F12 supplemented with 10% fetal bovine serum (Sigma Aldrich, St. Louis, MO). Cells were cultured at 37°C in an incubator humidified with 5% CO2 (12). Ferulic acid and temozolomide were purchased from Sigma-Aldrich (St. Louis, MO), and stock solution was prepared by dissolving them in 100% Dimethyl Sulfoxide (DMSO). They were then diluted with FBS-free medium before application to cells.

Cell Viability and Replication Experiments

Cell viability and proliferation were measured using the MTS (3-(4,5-dimethylthiazol-2-yl)-5-(3-carboxymethoxyphenyl)-2-(4-sulphophenyl)-2H-tetrazolium) assay (Promega, Madison, WI) (1,11). To observe the effects of the agents accurately, we spread the experiment protocol over a total period of 96 hours.

To start the experiment, we seeded U87-MG cells at a density of 1.20 x 10^3 cells per well in 96-well plates and designated the first 24 hours as the incubation phase to ensure that the cells adhered completely to the surface. On day 1 of the experiment, we treated the cells with increasing doses of temozolomide (10, 20, 40, and 80 μM) during a 48-hour incubation period. On the third day of the experiment, without removing the existing medium or TMZ from the medium, we proceeded to the final 24-hour incubation phase by directly adding ferulic acid (different doses ranging from 100-1500 μM) or the specified combination groups (FA 1000+TMZ 40 μM, FA 1500+TMZ 40 μM, FA 1000+TMZ 80 μM, FA 1500+TMZ 80 μM) to the final 24-hour incubation phase. After completing the 96-hour protocol, we added a marker solution containing MTS and Phenazine Methosulfate (20:1 v/v) to the cells. We incubated the cells at 37 °C for 1 hour for formazan formation. In the ultimate step, we measured absorbance at 490 nm using an ELISA reader to determine the density of viable and proliferating cells (2,12).

Colony Formation Assays

To determine the long-term effects of temozolomide and ferulic acid on the proliferation capacity and colony-forming ability of GBM cells, we selected the clonogenic assay method (2,12). For this purpose, we seeded U87-MG cells at a density of 1.5 x 10^3 cells per well in 6-well plates and left them to incubate for 48 hours to allow the cells to adhere completely to the surface.

Following this preparation step, the cells were treated with increasing doses of temozolomide (20, 40, and 80 μM), ferulic acid (1000 and 1500 μM), and their combinations (FA 1000+TMZ 40 μM, FA 1500+TMZ 40 μM). Plates were incubated at 37°C for approximately 2 weeks until colonies in the control group reached sufficient density (confluency). After the process was complete, we carefully removed the medium and washed the cells with Phosphate Buffered Saline (PBS); then, we made the colonies visible through fixation and crystal violet staining steps. During the analysis phase, we counted colonies consisting of more than 50 clearly distinguishable cells and reported our data as a percentage relative to the control group.

Western Blot Analysis

To examine changes at the molecular level, we performed Western blot analyses. We seeded the cells in T-25 flasks and incubated them for 24 hours to allow the cells to adhere. We performed our experiment using a 96-hour sequential protocol: In the first step, we treated the cells with 80 μM temozolomide for 48 hours from day 1 to day 3. On day 3 of the experiment, we added ferulic acid (1000-1500 μM) and the corresponding combination doses (FA 1000+TMZ 40 μM, FA 1500+TMZ 40 μM) to the cells and allowed the interaction to complete with a final 24-hour incubation.

At 96 hours, we harvested the cells, washed them twice with cold PBS, and lysed them in lysis buffer at 4°C. We performed precise measurements to determine protein concentrations using a commercial kit (DC kit; Bio-Rad, Hercules, CA). A 40-μg protein load from each sample was run on a 4–20% gradient SDS-polyacrylamide gel electrophoresis (SDS-PAGE) and then transferred to PVDF membranes.

To block nonspecific binding on the membranes, we incubated them for 60 minutes in a blocking buffer containing 5% nonfat milk powder (0.1% Triton X-100, TBS-T). After washing, we targeted the membranes with the following primary antibodies: PARP (Cell Signaling, cat# 9532), Cyclin D1 (Cell Signaling, cat# 9542S), and Beta Actin (Proteintech, cat# 60008-1-Ig) as a loading control. Following the washing steps, we proceeded with appropriate secondary antibodies (anti-rabbit or anti-mouse; Bio-Rad). We performed chemiluminescence detection using Clarity Western ECL Substrate (Bio-Rad) to visualize the bands; the resulting signals were visualized and analyzed using the ChemiDoc MP Imaging System (Bio-Rad) (2,12,13,14).

Apoptosis Analysis (Host Staining)

We performed Hoechst 33258 staining to observe changes in the nuclear morphology of U87-MG GBM cells and to provide morphological evidence of apoptotic cell death. Cells were seeded in 6-well plates at a density of 100,000 cells/well and allowed to adhere for 24 hours. Treatments were administered according to the 96-hour sequential protocol: cells were first treated with temozolomide (40 and 80 μM) for 48 hours, followed by the addition of ferulic acid (1000 and 1500 μM) and their combinations (FA 1000+TMZ 40 μM, FA 1500+TMZ 40 μM) for the final 24 hours. Untreated cells served as the control group. Following the 96-hour treatment, cells were fixed with 4% paraformaldehyde, washed with PBS, and stained with 200 μl Hoechst 33258 (Sigma, 0.5 mg/mL) for 15 minutes in the dark.

After staining, the solution was removed, and cells were washed three times with ice-cold PBS. Changes in nuclear morphology were assessed using a fluorescence microscope with 320-350 nm filters (Eclipse Ti, Nikon). Apoptotic cells were identified by hallmark morphological changes, such as highly condensed chromatin and fragmented nuclei (12,26).

Statistical Analysis

All experiments were performed at least in triplicate, and results were summarized as means with standard deviation. Statistical significance was determined using Student's t-test. P-values less than 0.05 were considered statistically significant. GraphPad Prism (ver. 8.0.2) software was used for data evaluation and graphing.

RESULTS

Ferulic Acid Inhibits GBM Cell Proliferation and Enhances TMZ Efficacy

To evaluate the effects of ferulic acid (FA) and temozolomide (TMZ) treatment on glioblastoma (GBM) cell proliferation and viability, MTS analysis was performed 96 hours after treatment. The results showed that U87-MG cell viability was significantly reduced in a dose-dependent manner compared to the control group (Figure 1).

TMZ (10-80 μM) treatments administered from 24 to 72 hours showed a marked decrease, particularly at the 80 μM concentration (Figure 1B). For FA application, cells were exposed to different doses (100-1500 μM) during the final 24-hour period following a 48-hour pre-incubation. FA application alone showed a potent inhibitory effect at concentrations of 700, 1000, and 1500 μM (Figure 1A).

In combination groups treated with the same sequential protocol (48 hours of TMZ followed by 24 hours of FA co-incubation), a synergistic decrease in cell viability was observed. The lower viability rate observed in the combination treatment groups compared to the control group and single FA or TMZ treatments (Figure 1C) confirms that ferulic acid enhances the cytotoxic effect of TMZ in GBM cells.

Ferulic Acid and Temozolomide Synergistically Inhibit Colony Formation

We performed clonogenic assays to observe the effects of FA and TMZ, as well as their combinations, on the clonogenic capacity of GBM cells. The results showed that when we increased the TMZ dose (20, 40, and 80 μM), the colony-forming ability of U87-MG cells decreased significantly in a dose-dependent manner compared to the control group (Figure 2A). However, the most striking results were observed with FA. We found that colony formation was completely inhibited in cells treated with FA alone (1000–1500 μM) (Figure 2B). However, the most noteworthy aspect of the study was the combination groups; when FA (1000 μM or 1500 μM) was combined with TMZ (40 μM), colony formation was eliminated (Figure 2C).

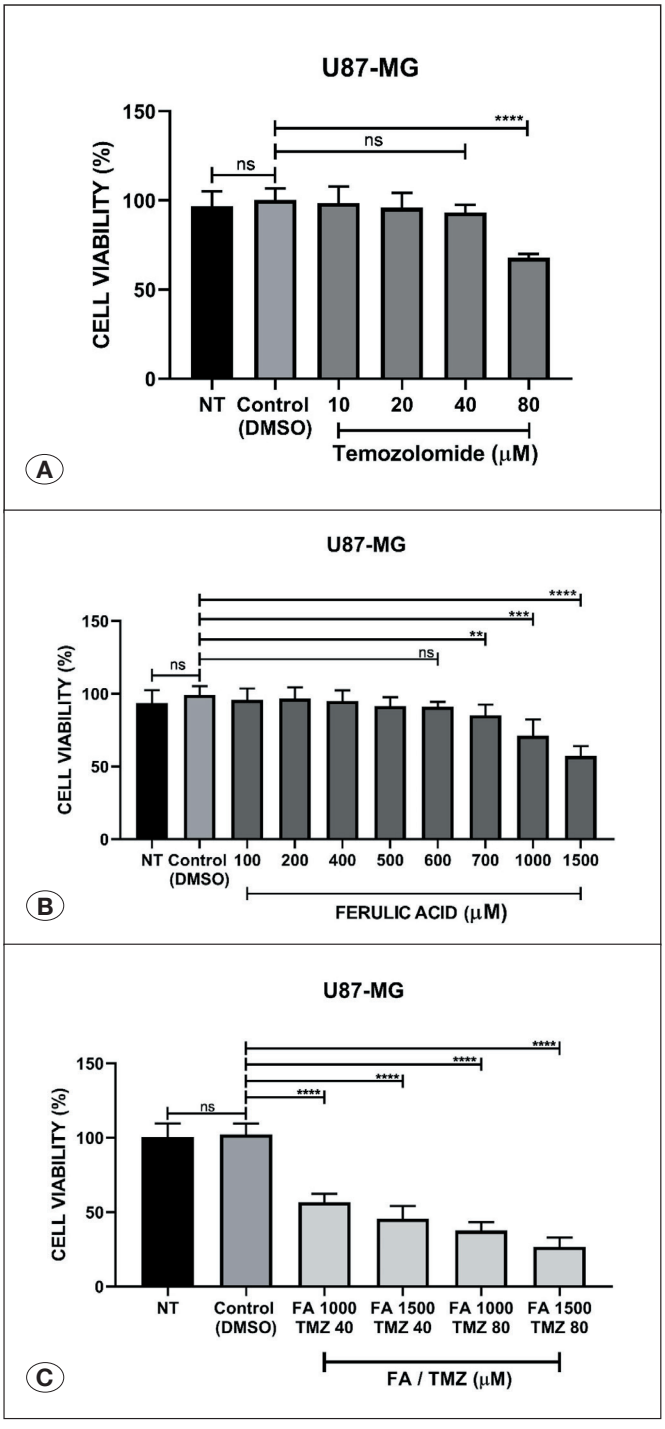

Figure 1: Effects of Ferulic Acid (FA) and Temozolomide (TMZ) on the viability of U87-MG glioblastoma cells, evaluated using the MTS assay following a 96-hour sequential treatment protocol. **A)** Cells treated with 100-1500 μM FA for the final 24 hours of the protocol showed a dose-dependent decrease in viability, with significance at 1000-1500 μM. **B)** Cells treated with 10-80 μM TMZ for a total of 72 hours exhibited a significant viability decrease at 80 μM. **C)** Sequential combination of FA (1000-1500 μM) and TMZ (40-80 μM) demonstrated a synergistic reduction in cell viability compared to the control group (ns: $p>0.05$; *$p<0.05$; **$p<0.0001$).

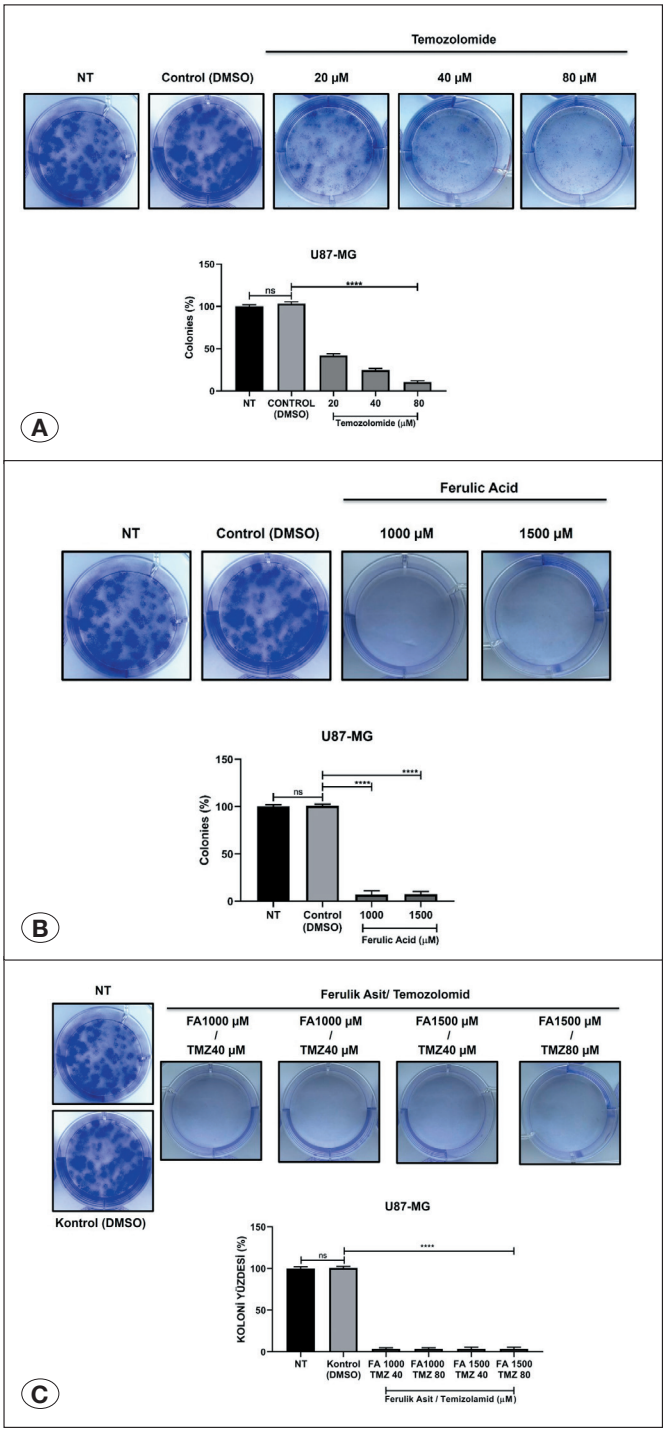

Figure 2: Impact of FA and TMZ on the clonogenic capacity of U87-MG cells. **A)** Treatment with 20, 40, and 80 μM TMZ resulted in a dose-dependent suppression of colony formation. **B)** Colony formation was completely inhibited in cells treated with 1000 and 1500 μM FA alone. **C)** The combination of FA (1000-1500 μM) and TMZ (40 μM) led to the total abolishment of colony formation, indicating a complete loss of proliferative integrity (ns: not significant; $p>0.05$; **$p<0.01$; ***$p<0.001$; ****$p<0.0001$).

These data indicate that the strategic addition of FA to TMZ treatment directly targets both the self-renewal mechanism and proliferation of U87-MG cells. This intervention results in the complete loss of the cells' clonogenic potential.

Ferulic Acid and Temozolomide Combination Suppresses Cyclin D1 and PARP Expression

To demonstrate the underlying molecular mechanisms of the anti-proliferative effect we observed, we performed Western blot analysis following a 96-hour sequential treatment protocol. At this stage, we focused on the expression levels of the PARP enzyme, which plays a key role in both DNA repair mechanisms (BER pathway) and cell death processes, and the Cyclin D1 protein, which controls the G1/S transition of the cell cycle (Figure 3A).

Our quantitative analyses revealed that the combination of FA and TMZ significantly reduced Cyclin D1 expression in U87-MG cells compared to the control group (Figure 3C). This decrease in expression directly indicates an extraordinarily strong arrest in the cell cycle. Additionally, we observed a significant decrease in PARP expression levels in the combination groups compared to the control group (Figure 3B). Given the DNA damage caused by TMZ, this decrease in PARP levels is particularly important, as it indicates that ferulic acid impairs the ability of GBM cells to repair damage and renders them much more sensitive to TMZ-induced apoptosis. In summary, the simultaneous inhibition of both proteins confirms that the combination of FA and TMZ targets glioblastoma cells for both proliferation and apoptosis simultaneously.

Ferulic Acid and Temozolomide Combination Triggers Apoptotic Changes in GBM Cells

To demonstrate changes in nuclear morphology and for apoptosis analysis, we performed Hoechst 33258 staining following a 96-hour sequential treatment regimen. Our data showed that TMZ (40 and 80 μM) administered alone for 72 hours did not cause a radical change in nuclear structure compared to the control group. However, the intense chromatin staining and structural disruptions characteristic of cells undergoing apoptosis revealed a profile markedly different from that of healthy cells (Figure 4A).

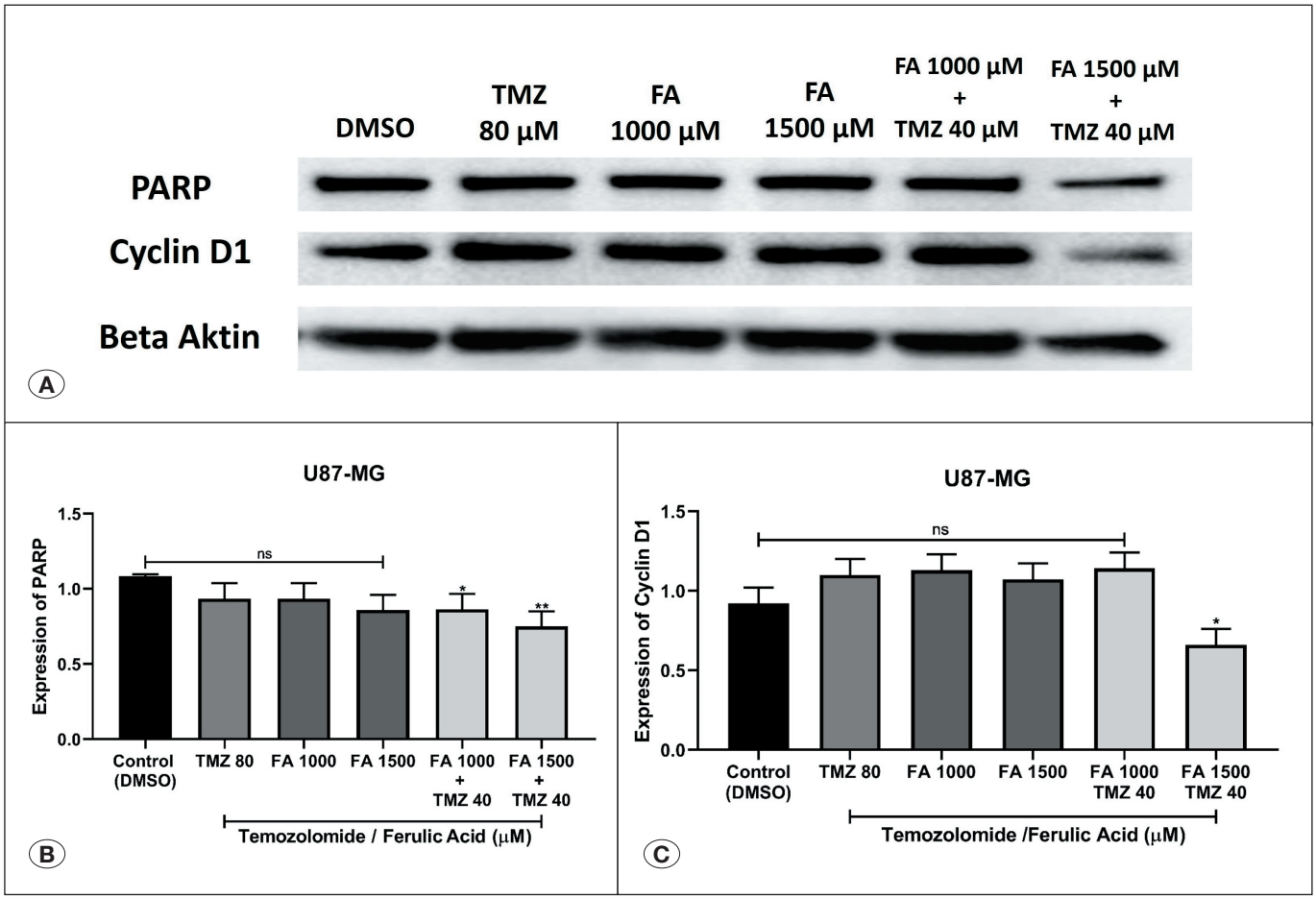

Figure 3: Molecular analysis of PARP and Cyclin D1 expression in U87-MG cells following 96-hour sequential treatment. **A)** Representative Western blot images showing the expression levels of PARP (a key BER pathway enzyme) and Cyclin D1 (a cell cycle regulator). **B)** Quantitative analysis of PARP expression, showing significant downregulation in combination groups. **C)** Quantitative analysis of Cyclin D1 expression, demonstrating a significant decrease compared to the control group. Beta-actin was used as the loading control (ns: not significant; p>0.05; **p<0.01; ***p<0.001; ****p<0.0001).

In the final 24 hours of the process, we observed that nuclear morphological changes increased in a dose-dependent manner in cells treated only with FA (1000 and 1500 µM) (Figure 4B). However, the most striking results emerged in the combination groups where TMZ and FA were administered together. A substantial proportion of cells in this group exhibited intense bright blue fluorescence, a characteristic sign of chromatin condensation and nuclear fragmentation.

The combination groups most clearly observed this transformation, where fragmented apoptotic bodies replaced the normal nuclear structure. These morphological indicators are definitive evidence of apoptosis. In conclusion, the microscopic images we obtained confirm that ferulic acid strongly supports and enhances TMZ-induced programmed cell death (apoptosis) in GBM cells.

DISCUSSION

GBM poses a significant clinical challenge due to its high malignancy, rapid progression, and resistance to current treatment approaches. Traditional treatments, including surgery, radiotherapy, and chemotherapy, can only extend the average survival time of GBM patients to a limited extent (22,25). Therefore, the development of more effective treatment strategies is crucial.

TMZ is a basic alkylating agent used in the standard treatment of GBM. Although it is known that TMZ triggers cell death through methylation on DNA (1), at least 50% of treated glioblastoma patients do not respond adequately to treatment. The most important reasons for this treatment resistance include overexpression of the O6-methylguanine-DNA methyltransferase (MGMT) gene and/or defects in DNA repair mechanisms in tumor cells. In this context, combined therapies that may increase the efficacy of TMZ in GBM treatment should be investigated (17). In our study, the effects of TMZ combination with ferulic acid (FA), a natural phenolic compound, on GBM cell line (U87-MG) were investigated, and promising results were obtained.

The researchers strategically selected the 96-hour sequential treatment protocol (48 hours of TMZ followed by 24 hours of FA) to suppress the DNA repair mechanism. This timing ensures that the phytochemical reaches cells that are in their most vulnerable state as they attempt to recover from the initial chemical attack.

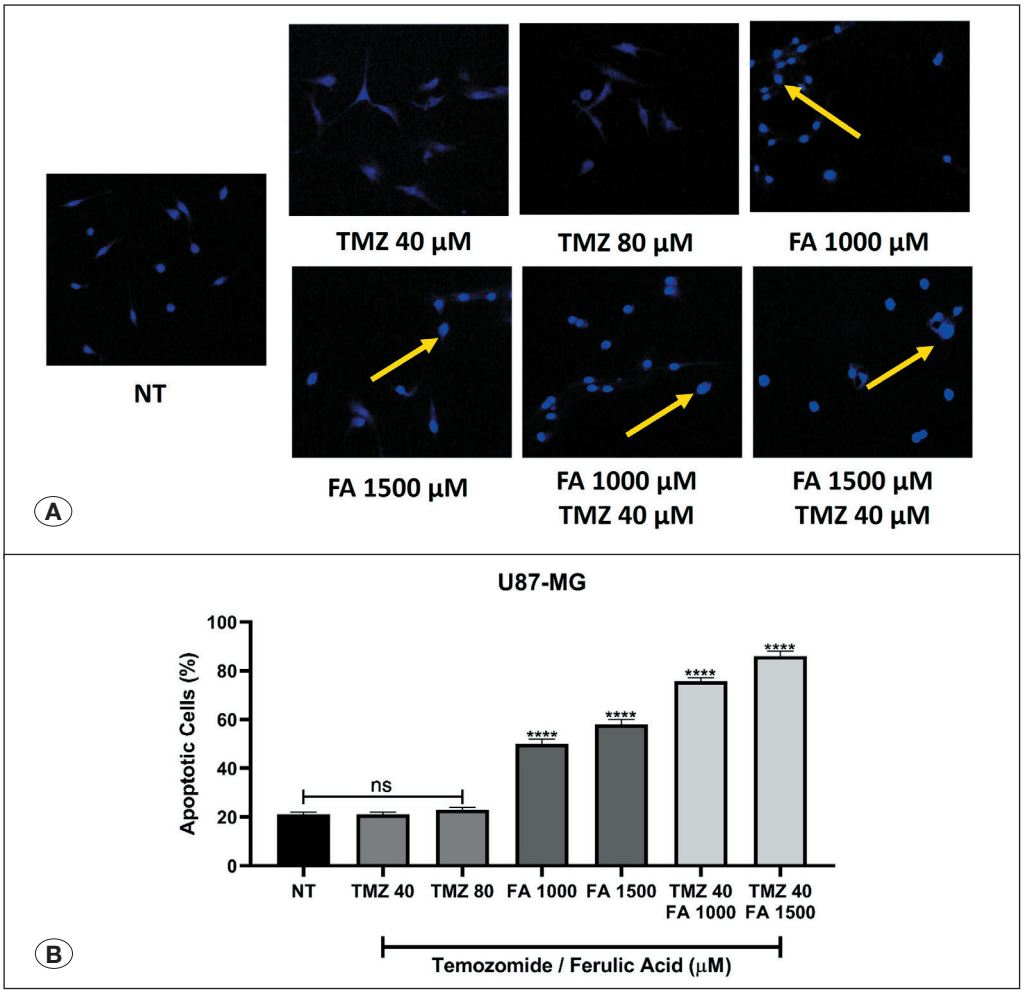

Figure 4: Morphological assessment of apoptotic cell death in U87-MG cells via Hoechst 33258 staining following sequential treatment.
A) Fluorescence microscopy images representing nuclear morphology; untreated control cells show uniform nuclei, while treated cells exhibit bright blue fluorescence. **B)** Statistical representation showing the significant increase in apoptotic cells (exhibiting nuclear fragmentation and chromatin condensation) in FA and TMZ-treated groups compared to the control (***p<0.001; ****p<0.0001).

Previous studies have reported that FA increases DNA damage in GBM cells and exhibits anticancer effects by activating apoptotic pathways (11). Similarly, Dell'Albani et al. reported that FA encapsulated in nanoparticles suppressed glioma cell proliferation four times more than free FA (4). Naumowicz et al. reported that FA and cinnamic acid compounds reduce cell viability by causing changes in the membrane surface charges of glioblastoma cells (19). Studies conducted by Morin et al. on Hs683 and LN319 cell lines indicate that FA and caffeic acid phenethyl ester compounds have therapeutic potential (18).

In this study, we demonstrated that the combination of Ferulic Acid (FA) and Temozolomide (TMZ) significantly suppressed the proliferation of U87-MG cells, and that this effect was much more pronounced compared to the use of FA alone. We determined that this effect is achieved by inhibiting the expression of Cyclin D1 and PARP, which play a critical role in DNA repair. This indicates that FA essentially disrupts the cell's DNA repair mechanism, renders the damage caused by TMZ permanent, and ultimately leads to the cell entering an irreversible death process.

DNA damage caused by TMZ is primarily repaired via Base Excision Repair (BER). The significant decrease in PARP levels observed in our analyses indicates that ferulic acid effectively suppresses this repair mechanism. Silencing PARP-1, an indispensable sensor of the BER pathway, is a known strategy in literature to enhance the effect of alkylating agents such as TMZ, but it takes on a new dimension with this combination. FA prevents the repair of DNA damage caused by TMZ, leading to the accumulation of lethal double-strand breaks in the cell and ultimately triggering apoptosis. This mechanism is clearly supported by our Hoechst 33258 staining results. The nuclear fragmentation and chromatin condensation observed in the combination groups demonstrate that this is programmed cell death, not suppression of proliferation, random tissue death (necrosis), or simple metabolic slowing.

Although our study only includes vitro experiments, ferulic acid stands out as a promising natural compound for GBM treatment. The combination of TMZ and FA could form the basis for current treatment strategies. Of course, the results shown in this study using the U87-MG cell line are not sufficient, but the genetic diversity of glioblastoma, especially factors such as TMZ resistance, is decisive for clinical success. Therefore, to generalize our findings, it is vital to validate this synergy in resistant lines such as T98G and in primary cultures obtained from patients in the next step.

CONCLUSION

In conclusion, consistent responses obtained from various analytical methods, such as MTS, colony formation, Western blot, and Hoechst staining, emphasize that FA may be a potent adjuvant in GBM treatment. However, more comprehensive in vitro and in vivo studies are needed to understand fully the clinical value of this combination. A detailed analysis of the mechanisms is required.

ACKNOWLEDGEMENTS

This study was carried out with the support of the Betül-Ziya Eren Genome and Stem Cell Center (GENKÖK). We thank the center for their valuable contributions.

We/I would like to thank the Proofreading & Editing Office of the Dean for Research at Erciyes University for copyediting and proofreading service for this manuscript.

Declarations

Funding: This study was supported by the Erciyes University Research Fund (grant number: TDK-2019-9390).

Availability of data and materials: The datasets generated and/or analyzed during the current study are available from the corresponding author on reasonable request.

Disclosure: The authors declare that they have no competing financial or non-financial interests related to this study.

Ethics Statement: This study included only in vitro cell line experiments. No human participants or animals were involved. Therefore, ethics committee approval and informed consent were not required.

AUTHORSHIP CONTRIBUTION

Study conception and design: HU, ZH

Data collection: SA, AG, VC, NN

Analysis and interpretation of results: HU, SA, AG, VC, NN, ZH

Draft manuscript preparation: HU, SA, ZH

Critical revision of the article: HU, SA, ZH

Other (study supervision, fundings, materials, etc...): HU, SA, AG, VC, NN, ZH

All authors (HU, SA, AG, VC, NN, ZH) reviewed the results and approved the final version of the manuscript.

REFERENCES

1. Belter A, Barciszewska A: Temozolomide influence on global DNA methylation in glioblastoma cell lines. Neuro-Oncology 20:279, 2018. https://doi.org/10.1093/neuonc/noy139.240
2. Cınar V, Hamurcu Z, Guler A, Nurdinov N, Ozpolat B: Serotonin 5-HT7 receptor is a biomarker poor prognostic factor and induces proliferation of triple-negative breast cancer cells through FOXM1. Breast Cancer 29:1106-1120, 2022. https://doi.org/10.1007/s12282-022-01391-9
3. Cruz Da Silva E, Mercier MC, Etienne-Selloum N, Dontenwill M, Choulier L: A systematic review of glioblastoma-targeted therapies in phases II, III, IV clinical trials. Cancers (Basel) 13:1795, 2021. https://doi.org/10.3390/cancers13081795
4. Dell'Albani P, Carbone C, Sposito G, Spatuzza M, Chiacchio MA, Grasso R, Legnani L, Santonocito D, Puglia C, Parenti R, Puglisi G, Campisi A: Effect of ferulic acid loaded in nanoparticle on tissue transglutaminase expression levels in human glioblastoma cell line. Int J Mol Sci 25:8397, 2024. https://doi.org/10.3390/ijms25158397
5. ElKhazendar M, Chalak J, El-Huneidi W, Vinod A, Abdel-Rahman WM, Abu-Gharbieh E: Antiproliferative and proapoptotic activities of ferulic acid in breast and liver cancer cell lines. Tropical Journal of Pharmaceutical Research 18:2571-2576, 2019. https://doi.org/10.4314/tjpr.v18i12.16
6. Erseçkin V, Mert H, İrak K, Yildirim S, Mert N: Nephroprotective effect of ferulic acid on gentamicin-induced nephrotoxicity in female rats. Drug Chem Toxicol 45:663–669, 2022. https://doi.org/10.1080/01480545.2020.1759620

7. Gao J, Yu H, Guo W, Kong Y, Gu L, Li Q, Yang S, Zhang Y, Wang Y: The anticancer effects of ferulic acid is associated with induction of cell cycle arrest and autophagy in cervical cancer cells. Cancer Cell Int 18:102, 2018. https://doi.org/10.1186/s12935-018-0595-y
8. Gargini R, Segura-Collar B, Herránz B, García-Escudero V, Romero-Bravo A, Núñez FJ, García-Pérez D, Gutiérrez-Guamán J, Ayuso-Sacido A, Seoane J, Pérez-Núñez A, Sepúlveda-Sánchez JM, Hernández-Laín A, Castro MG, García-Escudero R, Ávila J, Sánchez-Gómez P: The IDH-TAU-EGFR triad defines the neovascular landscape of diffuse gliomas. Sci Transl Med 12:eaax1501, 2020. https://doi.org/10.1126/scitranslmed.aax1501
9. Gargini R, Segura-Collar B, Sánchez-Gómez P: Cellular plasticity and tumor microenvironment in gliomas: The struggle to hit a moving target. Cancers 12:1622, 2020. https://doi.org/10.3390/cancers12061622
10. Gautam M, Gabrani R: Combinatorial effect of temozolomide and naringenin in human glioblastoma multiforme cell lines. Nutr Cancer 74:1071–1078, 2022. https://doi.org/10.1080/01635581.2021.1952438
11. Grasso R, Dell'Albani P, Carbone C, Spatuzza M, Bonfanti R, Sposito G, Puglisi G, Musumeci F, Scordino A, Campisi A: Synergic pro-apoptotic effects of Ferulic Acid and nanostructured lipid carrier in glioblastoma cells assessed through molecular and Delayed Luminescence studies. Sci Rep 10:4680, 2020. https://doi.org/10.1038/s41598-020-61670-3
12. Guler A, Hamurcu Z, Ulutabanca H, Cınar V, Nurdinov N, Erdem S, Ozpolat B: Flavopiridol suppresses cell proliferation and migration and induces apoptotic cell death by inhibiting oncogenic FOXM1 signaling in IDH wild-type and IDH-mutant GBM cells. Mol Neurobiol 61:1061–1079, 2024. https://doi.org/10.1007/s12035-023-03609-z
13. Hamurcu Z, Ashour A, Kahraman N, Ozpolat B: FOXM1 regulates expression of eukaryotic elongation factor 2 kinase and promotes proliferation, invasion and tumorgenesis of human triple negative breast cancer cells. Oncotarget 7:16619–16635, 2016. https://doi.org/10.18632/oncotarget.7672
14. Hamurcu Z, Delibaşı N, Nalbantoglu U, Sener E. F, Nurdinov N, Tascı B, Taheri S, Özkul Y, Donmez-Altuntas H, Canatan H, Ozpolat B: FOXM1 plays a role in autophagy by transcriptionally regulating Beclin-1 and LC3 genes in human triple-negative breast cancer cells. J Mol Med (Berl) 97:491–508, 2019. https://doi.org/10.1007/s00109-019-01750-8
15. Jiapaer S, Furuta T, Tanaka S, Kitabayashi T, Nakada M: Potential strategies overcoming the temozolomide resistance for glioblastoma. Neurol Med Chir 58:405–421, 2018. https://doi.org/10.2176/nmc.ra.2018-0141
16. Kaina B, Beltzig L, Piee-Staffa A, Haas B: Cytotoxic and senolytic effects of methadone in combination with temozolomide in glioblastoma cells. Int J Mol Sci 21:7006, 2020. https://doi.org/10.3390/ijms21197006
17. Lee SY: Temozolomide resistance in glioblastoma multiforme. Genes Dis 3:198–210, 2016. https://doi.org/10.1016/j.gendis.2016.04.007
18. Morin P, St-Coeur PD, Doiron JA, Cormier M, Poitras JJ, Surette ME, Touaibia M: Substituted caffeic and ferulic acid phenethyl esters: Synthesis, leukotrienes biosynthesis inhibition, and cytotoxic activity. Molecules 22:1124, 2017. https://doi.org/10.3390/molecules22071124
19. Naumowicz M, Kusaczuk M, Zając M, Gál M, Kotyńska J: Monitoring of the surface charge density changes of human glioblastoma cell membranes upon cinnamic and ferulic acids treatment. Int J Mol Sci 21:6972, 2020. https://doi.org/10.3390/ijms21186972
20. Nie E, Jin X, Miao F, Yu T, Zhi T, Shi Z, Wang Y, Zhang J, Xie M, You Y: TGF-β1 modulates temozolomide resistance in glioblastoma via altered microRNA processing and elevated MGMT. Neuro Oncol 23:435–446, 2021. https://doi.org/10.1093/neuonc/noaa198
21. Ortiz R, Perazzoli G, Cabeza L, Jiménez-Luna C, Luque R, Prados J, Melguizo C: Temozolomide: An updated overview of resistance mechanisms, nanotechnology advances and clinical applications. Curr Neuropharmacol 19:513–537, 2021. https://doi.org/10.2174/1570159X18666200626204005
22. Shergalis A, Bankhead A, Luesakul U, Muangsin N, Neamati N: Current challenges and opportunities in treating glioblastoma. Pharmacol Rev 70:412-445, 2018. https://doi.org/10.1124/pr.117.014944
23. Sonoda Y: Clinical impact of revisions to the WHO classification of diffuse gliomas and associated future problems. Int J Clin Oncol 25:1004–1009, 2020. https://doi.org/10.1007/s10147-020-01628-7
24. Tomar M. S, Kumar A, Srivastava C, Shrivastava A: Elucidating the mechanisms of temozolomide resistance in gliomas and the strategies to overcome the resistance. Biochim Biophys Acta Rev Cancer 1876:188616, 2021. https://doi.org/10.1016/j.bbcan.2021.188616
25. Uwishema O, Shariff S, Wojtara M, Chakik JAE, Ghosh S, Obamiro K, Enam SA: Stem cell therapies and glioma stem cells in glioblastoma: a systematic review of current challenges and research directions. Int J Emerg Med 18:144, 2025. https://doi.org/10.1186/s12245-025-00921-4
26. Ünlü Endirlik B, Bakır E, Ökçesiz A, Güler A, Hamurcu Z, Eken A, Dreij K, Gürbay A: Investigation of the toxicity of a glyphosate-based herbicide in a human liver cell line: Assessing the involvement of Nrf2 pathway and protective effects of vitamin E and α-lipoic acid. Environ Toxicol Pharmacol 96:103999, 2022. https://doi.org/10.1016/j.etap.2022.103999
27. Wang T, Gong X, Jiang R, Li H, Du W, Kuang G: Ferulic acid inhibits proliferation and promotes apoptosis via blockage of PI3K/Akt pathway in osteosarcoma cell. Am J Transl Res 8:968–980, 2016. PMID: 27158383
28. Wu S, Li X, Gao F, de Groot JF, Koul D, Yung WKA: PARP-mediated PARylation of MGMT is critical to promote repair of temozolomide-induced O6-methylguanine DNA damage in glioblastoma. Neuro Oncol 23:920-931, 2021. https://doi.org/10.1093/neuonc/noab003
29. Xia Q, Liu L, Li Y, Zhang P, Han D, Dong L: Therapeutic perspective of temozolomide resistance in glioblastoma treatment. Cancer Invest 39:627–644, 2021. https://doi.org/10.1080/07357907.2021.1952595
30. Zhang Q, Wang Z, Zhu J, Peng Z, Tang C: Ferulic acid regulates miR-17/PTEN axis to inhibit LPS-induced pulmonary microvascular endothelial cells apoptosis through activation of PI3K/Akt pathway. J Toxicol Sci 47:61–69, 2022. https://doi.org/10.2131/jts.47.61
31. Zhang X, Lin D, Jiang R, Li H, Wan J, Li H: Ferulic acid exerts antitumor activity and inhibits metastasis in breast cancer cells by regulating epithelial to mesenchymal transition. Oncol Rep 36:271-278, 2016. https://doi.org/10.3892/or.2016.4804

Turk Neurosurg 36(3):385-393, 2026
DOI: 10.5137/1019-5149.JTN.49164-25.2

Original Investigation
Spine and Peripheral Nerves

Received: 24.05.2025
Accepted: 29.08.2025
Published Online: 22.05.2026

Investigation of Age-Related Changes of the Atlas for Posterior Cervical Screw Fixation Surgery: A Morphometric Computed Tomography Study

Serkan ONER[1], Rukiye Sumeyye BAKICI[2], Halide TEMELCI[3], Seyma TOY[2], Zulal ONER[3]

[1]Izmir Bakircay University, Faculty of Medicine, Department of Radiology, İzmir, Türkiye
[2]Karabuk University, Faculty of Medicine, Department of Anatomy, Karabuk, Türkiye
[3]Izmir Bakircay University, Faculty of Medicine, Department of Anatomy, İzmir, Türkiye

This study has been presented at the 11th Anatomy Winter Days Congress between the 7 and 9 March, 2024 in Aydın, Türkiye.

Corresponding author: Zulal ONER ✉ zulal.oner@bakircay.edu.tr

ABSTRACT

AIM: To describe the morphometry of the atlas vertebrae regarding sex and age in posterior cervical surgery, provide a data source for surgery, and compare with other populations. In surgical operations, the morphology and morphometry of the atlas must be known.

MATERIAL and METHODS: Computed tomography images of 300 individuals aged 20–69 and referred to the hospital between 2020 and 2023 were used in retrospective research. The 14 parameters determined were examined in five groups formed by dividing ages into decades. The following parameters were measured: the transverse foramen area (TFA), length of the lateral mass (LLM), weight of the lateral mass (WLM), anteroposterior diameter of the left transverse foramen (ADTF), transverse diameter of the left transverse foramen (TDTF), posterior arch area (PAA), distance from the nearest point of the lateral mass on the posterior arch to the occipital condyle (OLM), posterior arch length (PAL), height of the lateral mass (HLM), and the height of the anterior tubercle of the atlas (HAT). In statistical analysis, the two-sample T-test, one-way ANOVA, and eta-squared (η^2) tests were used.

RESULTS: The HLM, WLM, PAA, PAL, OLM, HAT, TFA, ADTF, and TDTF were more considerable and statistically significant in males. It was statistically significant that the HAT and OLM were lower in the 2nd decade compared to other decades in females ($p<0.05$). In males, the LLM was smaller in the 3rd decade compared to individuals in the 2nd and 5th decades, which was statistically significant ($p<0.05$).

CONCLUSION: Based on the data presented, the present study will guide individuals in producing more appropriate screws (diameter, length) and safe surgical mediolateral angulation for the anatomical distinction between individuals' sexes and ages.

KEYWORDS: Atlas, Sex, Age, Lateral mass of atlas, Surgical technique

ABBREVIATIONS: CT: Computed tomography, **TFA:** Transverse foramen area, **LLM:** Length of lateral mass, **WLM:** Weight of lateral mass, **ADTF:** Anteroposterior diameter of left transverse foramen, **TDTF:** Transverse diameter of left transverse foramen, **NVF:** Nearest point of vertebral foramen, **FVF:** Furthest point of vertebral foramen, **PAA:** Posterior arch area, **OLM:** Distance from the nearest point of the lateral mass on the posterior arch to the occipital condyle, **PAL:** Posterior arch length, **HLM:** Height of lateral mass, **HAT:** Height of anterior tubercle of atlas, **HPT:** Height of posterior tubercle of atlas.

Serkan ONER : 0000-0002-7802-880X
Rukiye Sumeyye BAKICI : 0000-0001-8008-7174
Halide TEMELCI : 0000-0002-1314-6485
Seyma TOY : 0000-0002-6067-0087
Zulal ONER : 0000-0003-0459-1015

INTRODUCTION

The atlas (C1), categorized as an anatomically atypical vertebra with complex and variable constructions compared to other cervical vertebrae, is a crucial anatomical construction housing the bulbus and contains grooves for the C1 spinal nerve and vertebral levels (4,22). Instability or dislocation of the atlanto-occipital knuckle or C1-C2 complex may result from various sources, such as rheumatoid arthritis, broken C1-C2, ossa odontoidea, disruption of the transverse process ligaments, and tumor involvement in the surrounding area (22). Traumatization of the upper cervical spine can lead to weight-bearing instability, pain, neurological deficits, and death (28).

Posterior fixation using C1 pedicle screws and lateral mass is gaining acceptance among spine surgeons as the modality of choice for C1 instrumentation due to its preponderant biomechanical stability compared to other fixation modalities (16,22). However, proximity to important vascular and neural structures should be considered when using the fixation method. The ponticulus posticus (Kimmerle anomaly or arcuate foramen) may be confused with a wide posterior arch of the C1, while a lateral mass screw arrangement may provoke wounds to the vertebral artery (27). Additionally, a high-riding vertebral artery with a small pedicle is a substantial risk factor for a vertebral artery injury (16).

Determining the screw entry point before placing the screws is an essential detail for C1 fixation to prevent potentially fatal complications such as medulla spinalis and vertebral artery injury (28). Thus, the surgeon should have a detailed knowledge of the anatomy and morphometric features of the atlas.

Therefore, this study was designed to investigate changes in the atlas based on age for posterior cervical screw fixation surgery. Additionally, it aimed to obtain basic information about the anatomical parameters and dimensions of the atlas in developing innovative instruments.

MATERIAL and METHODS

The study was planned as a retrospective study, and approval was obtained from the Izmir Bakircay University Non-Interventional Ethics Board (Reference No: 1236 / Date:11.10.2023). Cervical computed tomography (CT) images were scanned between January 1, 2020, and October 10, 2023, in the Radiology Department of the University Hospital. Cervical CT images of 150 female and 150 male individuals aged between 20 and 69 were randomly selected in the study. Images of individuals with previous fractures in the cervical vertebrae resulting from trauma to the cranium or cervical region, a tumor, an infection, or previous surgery involving the cervical vertebrae were excluded from the study. Images with artifacts that impeded measurement were excluded from the study. During the measurements, the patients were categorized by sex and their initials were written in Excel, considering the personal data protection law.

Image Analysis

All measurements were made on the Horos (v3.3.06) workstation. The images were analyzed with two- and three-dimensional reconstructions in the standard bone screen, and the images focusing on the first cervical vertebra were positioned to the orthogonal plane in three planes (transverse, sagittal, and coronal). The images were then brought to the transverse and sagittal planes according to the parameters. Measurements were taken from the left half of the atlas only. They were performed by a radiologist (S.O.) with at least 15 years of experience, accompanied by two anatomists (PhD). Parameters were measured in the transverse and sagittal planes:

In the Transverse Plane

Transverse foramen shape (TFS): The shape of the transverse foramen was evaluated (1). It was classified as type 1 round, type 2 elliptical (anteroposterior), type 3 elliptical (transverse), type 4 kite, type 5 leaf, type 6 semicircle, or type 7 irregular.

Transverse foramen area (TFA): Transverse foramen area (Figure 1A).

Length of lateral mass (LLM): Straight length from the anterior to the posterior arch passing through the midpoint of the lateral mass of the atlas (Figure 1A).

Weight of lateral mass (WLM): Transverse width passing through the middle of the lateral mass of the atlas (Figure 1B).

Anteroposterior diameter of left transverse foramen (ADTF): The distance between the anterior and posterior points of the left transverse foramen (Figure 1C).

Transverse diameter of left transverse foramen (TDTF): The shortest distance from right to left of the left transverse foramen (Figure 1C).

Nearest point of vertebral foramen (NVF): The angle between the anterior tubercle of the atlas – the posterior tubercle of the atlas – and the transverse foramen (closest point to foramen vertebrae) (Figure 1D).

Furthest point of vertebral foramen (FVF): The angle between the anterior tubercle of the atlas – the posterior tubercle of the atlas – and the transverse foramen (farthest point to foramen vertebrae) (Figure 1E).

In the Sagittal Plane

Posterior arch area (PAA): Cross-sectional area of the posterior arch of the vertebral artery sulcus (Figure 2A).

The distance from the nearest point of the lateral mass on the posterior arch to the occipital condyle (OLM): The distance from the nearest point of the lateral mass on the posterior arch to the occipital condyle (Figure 2B).

Posterior arch length (PAL): Sagittal length of the posterior arch from the closest point to the lateral mass of the atlas (Figure 2B).

Height of lateral mass (HLM): The height of the middle of the lateral mass of the atlas (Figure 2C).

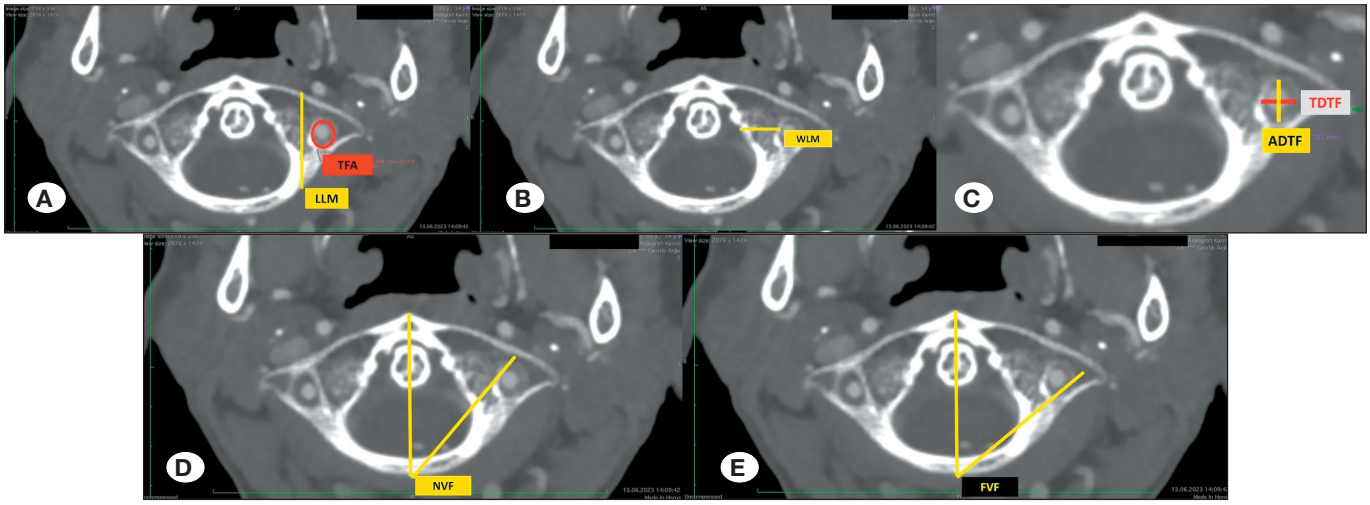

Figure 1: The horizontal plane measurements: **A) TFA:** transverse foramen area, **LLM:** length of lateral mass. **B) WLM:** weight of lateral mass. **C) ADTF:** anteroposterior diameter of left transverse foramen, **TDTF:** transverse diameter of left transverse foramen. **D) NVF:** nearest point of the vertebral foramen. **E) FVF:** furthest point of the vertebral foramen.

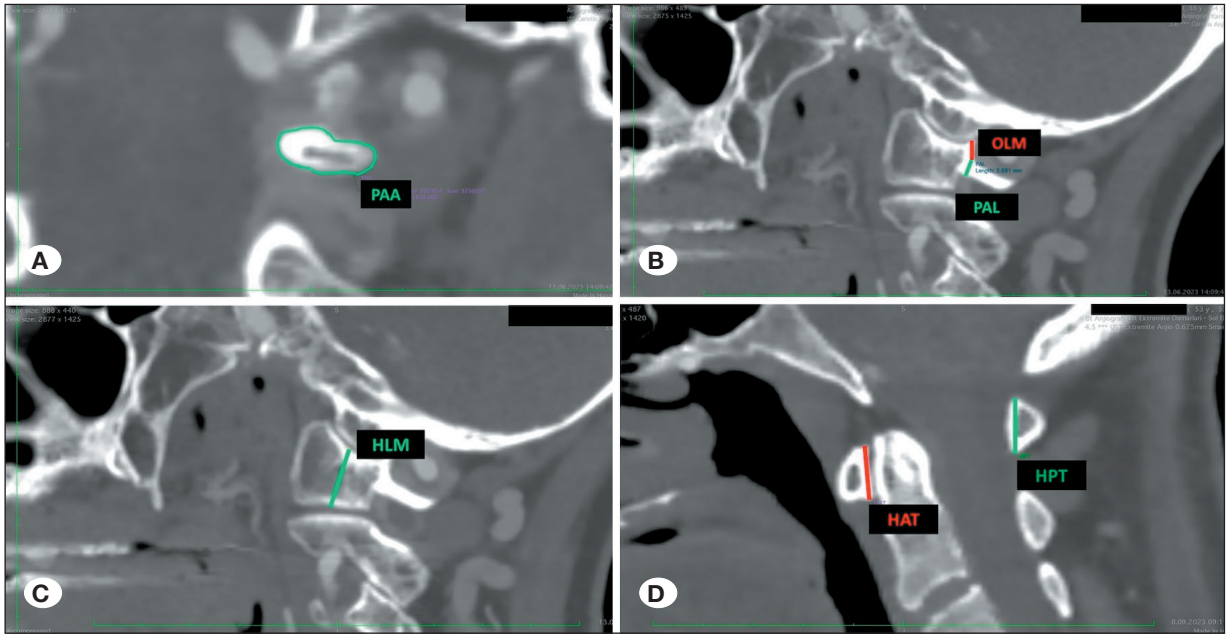

Figure 2: The sagittal plane measurements: **A) PAA:** Posterior arch area. **B) OLM:** Distance from the nearest point of the lateral mass on the posterior arch to the occipital condyle, **PAL:** Posterior arch length. **C) HLM:** Height of lateral mass. **D) HAT:** Height of anterior tubercle of atlas, **HPT:** height of posterior tubercle of atlas.

Height of anterior tubercle (HAT): The height at the midpoint of the anterior tubercle of the atlas (Figure 2C).

Height of posterior tubercle (HPT): The height of the atlas at the midpoint of the posterior tubercle (Figure 2D).

Statistical Analysis

Statistics were analyzed using IBM SPSS Statistics 22.0. Descriptive statistics (mean and standard deviation) were calculated for the parameters. The suitability of the measurement data for a normal distribution was judged with the Kolmogorov-Smirnov test. The two-sample T-test was used to determine the distribution based on sex. A one-way ANOVA test was used for the parameters suitable for a normal distribution when age was evaluated according to deciles. Post hoc, Tukey, and Tamhane's T2 tests were performed in pairwise comparisons. In parametric tests, eta-squared (η^2) calculations were performed to determine the degree of significant difference. Statistical significance was defined as a p-value below 0.05.

Power analysis: The calculated power (1-beta) based on this test is 1, considering a type I error (alpha) of 0.05, sample size of 300, effect size of 0.81, and a two-sided alternative hypothesis (H1).

Table I: Assessment of Measurements by Sex

Parameters	Male Mean±SD (CI)	Female Mean±SD (CI)	p-value[t]	η^2
TFA (mm^2)	46.6±10.0 (45.0-48.2)	41.6±8 (40.3-42.9)	**0.00***	0.69
ADTF (mm)	8.0±1.1 (7.8-8.2)	7.3±1.0 (7.1-7.5)	**0.00***	0.22
TDTF (mm)	7.5±1.1 (7.3-7.7)	6.5±0.9 (6.4-6.7)	**0.00***	0.27
WLM (mm)	15.2±1.5 (15.0-15.5)	12.9±1.3 (12.7-13.2)	**0.00***	0.47
LLM (mm)	29.3±16.3 (27.7-28.3)	27.4±2.0 (27.1-27.8)	0.16	-
PAA (mm^2)	54.7±12.5 (52.7-56.7)	40.4±10.1 (38.8-42.0)	**0.00***	0.77
HLM (mm)	13.9±1.2 (13.7-14.1)	13.3±1.3 (13.1-13.5)	**0.00***	0.35
PAL (mm)	5.3±0.8 (5.2-5.5)	4.9±6.4 (4.8-5.0)	**0.00***	0.16
OLM (mm)	5.1±1.4 (4.9-5.3)	4.2±1.0 (4.1-4.4)	**0.00***	0.24
HAT (mm)	12.1±1.7 (11.8-12.3)	10.8±1.5 (10.6-11.1)	**0.00***	0.34
HPT (mm)	11.0±1.7 (10.7-11.3)	10.2±6.7 (9.1-11.3)	0.19	-
NVF (°)	38.15±3.27 (37.6-38.6)	37.52±3.22 (37.0-38.0)	0.09	-
FVF (°)	48.33±3.42 (47.7-48.8)	47.76±3.38 (47.2-48.3)	0.15	-

p<0.001, **t: Two-sample T test, **η^2:** eta-squared, **SD:** Standard Deviation, **CI:** 95% Confidence Interval for Mean, **TFA:** Transverse foramen area, **ADTF:** Anteroposterior diameter of left transverse foramen, **TDTF:** Transverse diameter of left transverse foramen, **WLM:** Weight of lateral mass, **LLM:** Length lateral Mass, **PAA:** Posterior arch area, **HLM:** Height of lateral mass, **PAL:** Posterior arch length, **OLM:** Distance from the nearest point of the lateral mass on the posterior arch to the occipital condyle, **HAT:** Height of anterior tubercle of atlas, **HPT:** Height of posterior tubercle of atlas, **NVF:** Nearest point of vertebral foramen, **FVF:** Furthest point of vertebral foramen.*

RESULTS

A total of 300 individuals, 150 females and 150 males, were included in the study. Individuals aged between 20 and 69 were then divided into five groups, with 30 females and 30 males in every decade. The average age was 44.48 ± 14.66 for females and 44.32 ± 14.41 for males. When examining the ages of the individuals according to sex, no significant difference was detected (p>0.05).

The TFA, ADTF, TDTF, WLM, PAA, HLM, PAL, OLM, and HAT parameters were higher in males, which was statistically significant (p<0.05). The LLM, HPT, NVF, and FVF measurements were higher in males, but the gap was not statistically significant (p>0.05). Considering the size effect, it was believed that the variance observed from the morphometric measurements of the C1 vertebra was sex-dependent, with the highest rate of 77% for the PAA, followed by 69% for the TFA, and the lowest rate of 16% for the PAL (Table I). Figure 3 presents the distinction of the TFS based on sex.

No statistically significant difference was found between age groups for the TFA, ADTF, TDTF, WLM, LLM, PAA, HLM, PAL, HPT, NVF, or FVF parameters in females (p>0.05). The OLM and HAT measurements were smaller in individuals in the 2nd decade than in those in other decades. This difference was determined as statistically significant (p>0.05; Table II). Considering the effect size, it was believed that the variances observed in the decades originating from morphometric measurements of the C1 vertebra in females were age-dependent at rates of 36.7% for the HAT parameter and 41.1% for the OLM.

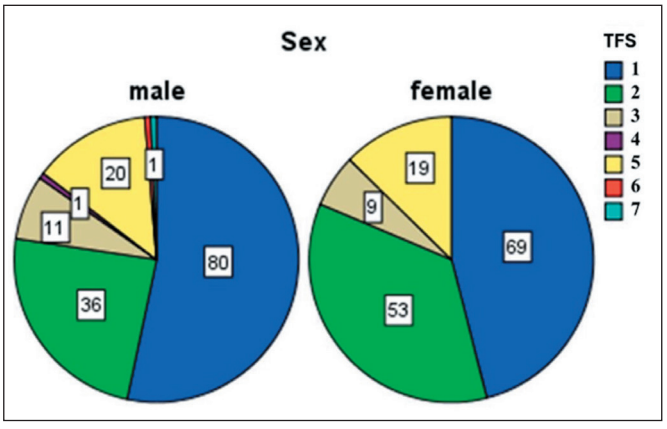

Figure 3: Distribution of transverse foramen shapes by sex.

In males, it was determined that the differences between the age groups for the TFA, ADTF, TDTF, WLM, PAA, HLM, PAL, OLM, HPT, NVF, and FVF were not statistically significant (p>0.05). The LLM measurement was smaller in individuals in the 3rd decade than in those in the 2nd and 5th decades. The HAT was smaller for individuals in the 2nd decade than those in the 4th, 5th, and 6th decades, and smaller for individuals in

the 3rd decade than those in the 6th decade (p<0.05; Table III). Considering the effect size, it was believed that the variances between decades originating from morphometric measurements of the C1 vertebra in males were age-dependent at a rate of 32.5% for the HAT and 51.5% for the OLM.

DISCUSSION

Advances in technology and experience have shown that screw fixation is preferred over cabling techniques (8). The C1 posterior arch screw technique is becoming a favored option, especially for short-segment cervical fixation and C1 rigid stable fixation (29). In cases where occipitocervical fusion is required, such as atlanto-occipital dislocation treatment (for conditions causing significant morbidity and mortality), a lateral mass screw could be used at C1 (21). Serious complications such as surgical area infection, neurological and vascular injuries, screw fracture, and bone nonunion may occur in cervical region surgery (19,20). Age-related atlas changes in adults are important because this is the first study aiming to provide a radio-anatomical basis for posterior screw fixation surgery. The results of this study will be valuable in preventing neurovascular injury and pedicle fractures due to the selection of a large screw during C1 laminar screw fixation.

In our study, the mean LLM was 27.4 ± 2.0 mm in females and 29.3 ± 16.3 mm in males, and the location of the transverse foramen was between 38° and 48° in males and 37° and 47° in females based on age group. Safe deviation angles vary significantly by sex. No previous study was found that exam-

Table II: Measurement Results for the Parameters Examined by Dividing Ages into Decades in Females

Parameters	2nd Decade Mean±SD (Min-Max)	3rd Decade Mean±SD (Min-Max)	4th Decade Mean±SD (Min-Max)	5th Decade Mean±SD (Min-Max)	6th Decade Mean±SD (Min-Max)	p-value
TFA (mm^2)	39.2±8.7 (25.4-62.6)	40.1±7.5 (25.0-58.0)	43.0±7.7 (29.0-60.2)	42.8±8.5 (30.1-56.9)	43.0±8.1 (24.5-57.2)	0.20
ADTF (mm)	7.0±1.2 (4.5-9.9)	7.3±0.8 (5.7-9.5)	7.3±0.9 (6.0-9.5)	7.4±1.0 (5.8-9.7)	7.5±0.9 (5.9-9.8)	0.28
TDTF (mm)	6.7±0.9 (5.0-9.7)	6.4±0.8 (4.3-8.2)	6.6±0.8 (4.6-8.4)	6.4±0.9 (4.9-8.8)	6.5±0.9 (4.5-8.4)	0.63
WLM (mm)	12.9±1.6 (8.7-16.3)	13.0±1.3 (9.6-15.6)	12.7±1.3 (10.8-16.4)	13.0±1.1 (10.6-15.1)	13.1±1.5 (9.5-15.5)	0.91
LLM (mm)	27.7±2.6 (20.7-31.5)	26.9±1.8 (22.9-29.4)	27.7±1.7 (23.9-31.4)	27.3±1.9 (22.6-33.0)	27.4±2.0 (20.7-31.8)	0.47
PAA (mm^2)	36.3±10.8 (22.3-65.3)	40.7±8.2 (27.8-56.1)	42.0±9.5 (22.0-58.1)	41.7±10.0 (20.1-64.2)	41.3±11.2 (20.4-63.9)	0.16
HLM (mm)	13.1±1.1 (11.4-15.7)	13.7±1.6 (11.1-18.2)	13.3±1.3 (10.8-16.5)	13.2±1.1 (11.4-15.9)	13.1±1.4 (10.5-16.8)	0.33
PAL (mm)	4.8±0.7 (3.5-6.5)	5.0±0.6 (3.7-6.3)	4.8±0.5 (3.8-5.9)	5.0±0.5 (4.0-6.1)	4.9±0.7 (3.5-6.7)	0.62
OLM (mm)	3.4±1.3 (1.2-7.5)	4.7±0.9 (2.1-6.0)	4.4±0.8 (2.4-6.1)	4.4±0.8 (2.0-5.9)	4.3±0.9 (1.8-6.2)	**0.00***
HAT (mm)	9.7±1.2 (7.1-13.3)	10.9±1.3 (8.4-14.6)	11.2±1.1 (9.1-13.0)	11.0±1.5 (8.7-15.0)	11.3±1.9 (8.9-16.3)	**0.00***
HPT (mm)	9.7±2.0 (6.4-14.0)	9.7±1.2 (8.1-12.8)	9.2±1.5 (6.9-12.0)	12.6±14.7 (6.8-90.0)	9.9±1.4 (6.7-12.9)	0.31
NVF (°)	37.94±3.39 (32.66-48.05)	37.68±2.93 (31.62-44.69)	36.38±3.47 (28.09-45.26)	38.05±2.98 (33.11-45.77)	37.56±3.21 (29.66-48.05)	0.27
FVF (°)	47.88±3.92 (41.73-59.78)	47.59±3.13 (42.24-54.51)	47.20±3.37 (38.54-55.02)	48.18±3.13 (43.85-55.38)	47.76±3.38 (38.54-59.78)	0.82

p<0.001, **SD: Standard deviation, **TFA:** Transverse foramen area, **ADTF:** Anteroposterior diameter of left transverse foramen, **TDTF:** Transverse diameter of left transverse foramen, **WLM:** Weight of lateral mass, **LLM:** Length lateral mass, **PAA:** Posterior arch area, **HLM:** Height of lateral mass, **PAL:** Posterior arch length, **OLM:** Distance from the nearest point of the lateral mass on the posterior arch to the occipital condyle, **HAT:** Height of anterior tubercle of atlas, **HPT:** Height of posterior tubercle of atlas, **NVF:** Nearest point of vertebral foramen, **FVF:** Furthest point of vertebral foramen.*

Table III: Measurement Results for the Parameters Examined by Dividing Age into Decades in Males

Parameters	2nd Decade Mean±SD (Min-Max)	3rd Decade Mean±SD (Min-Max)	4th Decade Mean±SD (Min-Max)	5th Decade Mean±SD (Min-Max)	6th Decade Mean±SD (Min-Max)	p-value
TFA (mm^2)	46.8±11.0 (31.8-76.0)	49.4±11.3 (24.8-86.9)	44.8±9.2 (27.8-65.5)	46.8±10.1 (31.1-72.0)	45.2±8.0 (30.0-62.2)	0.42
ADTF (mm)	7.6±1.1 (5.7-11.2)	8.2±1.1 (6.1-11.9)	7.9±1.0 (6.4-10.6)	8.2±1.2 (6.2-10.5)	7.9±1.0 (6.0-9.6)	0.26
TDTF (mm)	7.9±1.2 (6.3-11.0)	7.7±1.2 (5.2-9.7)	7.3±1.1 (5.3-10.0)	7.3±0.9 (6.0-10.0)	7.3±0.9 (6.0-9.8)	0.12
WLM (mm)	15.0±1.8 (11.5-18.6)	14.7±1.4 (1.7-17.0)	15.4±1.4 (11.9-18.1)	15.5±1.4 (11.9-18.1)	15.5±1.6 (11.8-20.0)	0.21
LLM (mm)	28.6±2.0 (23.3-32.3)	27.0±2.1 (22.0-30.9)	28.2±2.0 (23.5-31.4)	28.5±1.7 (23.8-32.5)	27.8±1.8 (23.3-30.4)	**0.01***
PAA (mm^2)	52.1±12.8 (31.1-94.3)	54.4±11.9 (30.9-97.1)	56.4±10.3 (40.8-92.1)	57.2±12.9 (34.9-85.9)	53.5±14.4 (27.2-92.4)	0.50
HLM (mm)	14.0±1.0 (11.5-16.2)	13.6±1.5 (10.2-16.2)	13.8±1.1 (10.3-16.0)	14.2±1.2 (11.5-16.7)	13.8±0.9 (10.9-15.2)	0.30
PAL (mm)	5.5±0.8 (3.5-7.5)	5.2±0.8 (4.0-7.4)	5.3±0.6 (3.8-6.9)	5.5±0.8 (3.1-6.9)	5.2±0.8 (4.2-7.4)	0.51
OLM (mm)	5.2±1.1 (2.5-7.7)	5.1±0.9 (3.8-7.2	5.0±1.0 (2.5-7.2)	5.0±0.7 (3.2-6.7)	5.0±1.5 (2.0-7.8)	0.98
HAT (mm)	10.8±1.1 (9.1-14.3)	11.6±1.4 (8.5-15.3)	12.5±1.7 (10.1-16.4)	12.5±1.8 (8.8-17.6)	12.9±1.5 (10.0-16.1)	**0.00***
HPT (mm)	10.9±1.8 (7.3-14.4)	10.8±1.6 (6.3-13.5)	11.2±1.4 (7.7-14.6)	11.3±2.2 (7.8-16.4)	10.7±1.7 (7.6-14.9)	0.62
NVF (°)	38.75±3.31 (32.87-46.57)	37.92±4.11 (30.01-47.56)	38.13±3.03 (31.37-43.68)	37.60±3.06 (32.54-45.24)	38.38±2.76 (31.92-44.59)	0.70
FVF (°)	48.67±3.25 (44.16-56.79)	48.47±3.89 (37.21-56.22)	48.25±3.09 (42.17-56.22)	47.85±3.69 (40.68-58.57)	48.42±3.29 (42.38-56.40)	0.91

p<0.05, **SD: Standard deviation, **TFA:** Transverse foramen area, **ADTF:** Anteroposterior diameter of left transverse foramen, **TDTF:** Transverse diameter of left transverse foramen, **WLM:** Weight of lateral mass, **LLM:** Length lateral mass, **PAA:** Posterior arch area, **HLM:** Height of lateral mass, **PAL:** posterior arch length, **OLM:** Distance from the nearest point of the lateral mass on the posterior arch to the occipital condyle, **HAT:** height of anterior tubercle of atlas, **HPT:** Height of posterior tubercle of atlas, **NVF:** Nearest point of vertebral foramen, **FVF:** Furthest point of vertebral foramen.*

ined the morphometry of the atlas in adult individuals over decades. This study is the first to provide a safe surgical area according to age in surgical interventions performed from the posterior aspect of the atlas.

A study of 135 atlases in the Egyptian population reported that FTS was observed in four different types, and the most dominant was type 1 (round) (2). In another study, the most common type of C1 was elliptical (1). In this study, FTS was observed in seven different ways in 300 CT scans. Type 1 was the most dominant in males and females. FTS was found in more diverse forms in males. We believe the differences between the studies are due to the number of individuals and population differences.

In this study, the TFA was higher in males at 46.6 mm^2; it was 41.6 mm^2 in females. Studies report that this parameter is significantly higher in males than in females (7,23).

A study explained that the ADTF was significantly higher in males than in females, and the TDTF did not differ significantly between sexes (7). Another study reported that the ADTF was 6.7 ± 1.0 mm in females and 7.1 ± 1.0 mm in males; the TDTF was 5.5 ± 0.8 mm in females and 5.9 ± 0.9 mm in males. Moreover, the differences were significant (23). This study found that the average ADTF was 7.3 ± 1.0 mm in females and 8.0 ± 1.1 mm in males; the average TDTF was 6.5 ± 0.9 mm in females and 7.5 ± 1.1 mm in males. These results were consistent with those of other studies.

In this study, the mean WLM was 12.9 ± 1.3 mm in females and 15.2 ± 1.5 mm in males. No directional difference was explained in an atlas study conducting bilateral evaluation (25). Lenz et al. reported that the was lower in females than in males, similar to our study (17).

In this study, the mean LLM was greater in males (29.3 ± 16.3 mm) than in females (27.4 ± 2.0 mm). In a study conducted on Asian individuals, the mean LLM on the left was reported as 30.07 ± 1.66 mm (25), and in Thai individuals, the ideal left screw length was stated as 28.59 ± 1.93 mm (28). The effective screw length for Asian individuals in China was defined as 21.87 mm (11), and in the Portuguese population, it was reported as 27.69 ± 2.09 mm (n=26) in males and 26.50 ± 2.09 mm (n=24) in females (19). A study conducted in the Asian population estimated the screw length as between 23.2 and 30.2 mm (16). In a study conducted in Austria, the length of the screw passing through the lateral mass was 30.1 ± 2.1 mm (n=50) on the left (15). Another study conducted in Germany reported that the LLM was higher in males (17). When examining these studies, it was observed that the screw length used in posterior cervical surgeries was between 21 and 31 mm. In posterior cervical fixation to C1, care should be taken regarding the screw used, especially in the Harms technique (9,28). The millimetric differences between studies may be due to the population differences.

This study's cross-sectional area of the PAA was 54.7 mm^2 in males and 40.4 mm^2 in females. Since this parameter differs by sex, we believe attention should be paid to the screw used in surgery. In the studies examined, this region was not evaluated by sex; only the average area (55.02 ± 18.51 mm^2) (26), height (17), and width (6) measurements were given. The HLMs in this study were greater in males (13.9 ± 1.2 mm) than in females (13.3 ± 1.3 mm). Another study found that only directions were considered and not sex (25). Therefore, PAA and HLM measurements could not be compared with other studies. The HLM should be considered for the screw diameter in surgical operations performed on type 1 and 3 Jefferson fractures. Additionally, the length of this parameter should be considered for the C1 lateral mass screws applied for the Goel-Harms technique (10) and Magerl technique (18).

In a study in Thailand, the left PAL was reported as 4.4 mm in females and 4.8 mm in males (28), and the average length in another study of pediatric individuals was 7.0 ± 1.5 mm (range 4.2–11.8 mm) (12). The height of the leanest part of the left vertebral artery groove in Japanese cadavers was determined as 4.30 ± 0.95 mm (14). Another study reported this parameter as 5.39 ± 1.58 mm on average (25). The mean PAL in this study was 4.9 ± 6.4 mm in females and 5.3 ± 0.8 mm in males. Similarly, a study conducted with Korean cadavers found that this parameter was greater in males (13). When examining studies on posterior cervical screw fixation surgery, it was observed that the screw diameter used in surgeries performed based on this parameter was 3.5 mm (4), or 3.8, 4.2, 4.5, or 5.5 mm (5, 16). The differences among studies evaluating sex may be due to population differences.

The mean OLM in our study was greater in males (5.1 ± 1.4 mm) than in females (4.2 ± 1.0 mm). Among the literature studies reviewed, none were found that evaluated this parameter. Thus, this parameter is original. The average HAT in this study was longer in males (12.1 ± 1.7 mm) than in females (10.8 ± 1.5 mm). The HPT did not differ between males (11.0 ± 1.7 mm) and females (10.2 ± 6.7 mm). Of the literature studies reviewed, none were found evaluating the HAT and HPT according to sex.

No difference was found in NVF and FVF angle measurements by sex for determining the transverse foramen localization. The transverse foramen is located between 28° and 59° in females and 30° and 58° in males. One study stated that the straight screw direction was safe for entry into C1, but a medial angulation of up to 20° could be performed (3). In another study measuring the lateralization angle, the mean value was 10.79±2.45° (28). In an atlas study, a partial radiological safety zone was defined between 19.6° medial and 11.6° lateral from an idealized entry point located 22.8 mm away (17). We believe the angle difference is due to the different reference points.

No differences were found between age groups in males and females in the TFA, ADTF, TDTF, WLM, PAA, HLM, PAL, HPT, NVF, or FVF. However, it was found that the OLM and HAT were minor in females in the 2nd decade of life compared to the other decades. Therefore, we recommend exercising more caution in surgical operations performed on females aged under 30. The LLM in males was lower in individuals in the 3rd decade than in those in the 2nd and 5th decades. Therefore, this parameter, which could be used for screw length, must be handled cautiously due to the difference in age groups in males.

In the study, males in the 2nd decade had smaller HATs than those in the 4th, 5th, and 6th decades, and those in the 3rd decade had smaller HATs than those in the 6th decade. The smallest two age groups for the HAT and HPT parameters in a pediatric study were reported as significantly smaller than the other groups (24). Children aged 4–18 in another pediatric study were divided into five groups 3 years apart. Consequently, a significant difference was found among the HPT groups except for the 7–9 and 10–12 age groups (12). Thus, we believe age groups should be considered when performing surgical operations. Although the current study is morphological, the findings may have potential clinical implications in surgical procedures involving the atlas, particularly in minimizing complications and improving surgical outcomes. Future studies could explore the relationship between morphological variations and clinical outcomes in a surgical context.

A limitation of this study is that the data were obtained from a single medical center and only reflect the characteristics of the local population. Future studies should include and examine a more diverse sample from different regions to reveal additional variations and explore their implications for cervical surgery more comprehensively.

CONCLUSION

Based on the results of this study, it was concluded that a maximum lateral angulation of 28° in females and 30° in males

(NVF-FVF) is safe in posterior cervical screw fixation surgery. The screw length (LLM) was between 20 and 33 mm in females and 22 and 32 mm in males. As the PAL is a fragile parameter, attention should be paid to the screw diameter regarding gender and age. If a 3.5 mm diameter screw is used in operations, it may be unsuitable for individuals with a PAL below 3.5 mm and may cause surgical complications. Therefore, the measurements in our study can reduce the use of intraoperative fluoroscopy by providing more appropriate screw selection in occipitocervical stabilization surgery, especially in screw surgery to the atlas. In cases where screw placement is required in the lateral mass of the atlas, this study could be taken as a guide regarding age groups. The results of this study concerning individuals without variations in the atlas may support surgeons in preoperative evaluation. However, these results should not be considered regarding ponticulus posterior, lateral ponticulus, or vertebral artery variations not located in the vertebral artery groove. Preoperative CT should be undertaken under such conditions. Additionally, this will facilitate a specific approach, as it provides information about the distances for surgery in the parameters of the transverse foramen and the vertebral artery groove through which the vertebral artery passes. We believe these detailed data will help spine surgeons achieve safe and effective screw placement.

Declarations

Funding: This research did not receive any specific grant from funding agencies in the public, commercial, or not-for-profit sectors.

Availability of data and materials: The datasets generated and/or analyzed during the current study are available from the corresponding author by reasonable request.

Disclosure: The authors declare no competing interests.

AUTHORSHIP CONTRIBUTION

Study conception and design: SO, ZO

Data collection: SO, HT

Analysis and interpretation of results: SO, RSB

Draft manuscript preparation: SO, HT, RSB

Critical revision of the article: SO, ZO, ST

Other (study supervision, fundings, materials, etc...): SO, ZO, RSB, HT, ST

All authors (SO, RSB, HT, ST, ZO) reviewed the results and approved the final version of the manuscript.

REFERENCES

1. Abdul RS, Lazarus L, Rennie C, Satyapal K: The foramen transversarium of typical and atypical cervical vertebrae: Morphology and morphometry. Int J Morphol 36:1439-1446, 2018. http://dx.doi.org/10.4067/S0717-95022018000401439.
2. Aziz J, Morgan M: Morphological study of the foramen transversarium of the atlas vertebra among Egyptian population and its clinical significance. Anatomy Physiol Biochem Int J 4:555642, 2018. http://dx.doi.org/10.19080/APBIJ.2018.04.555642
3. Blagg SE, Don AS, Robertson PA: Anatomic determination of optimal entry point and direction for C1 lateral mass screw placement. Clin Spine Surg 22:233-239, 2009. http://dx.doi.org/10.1097/BSD.0b013e31817ff95a
4. Coric D, Rossi V: Navigated, percutaneous posterior cervical minimally invasive surgery fixation: Technique and nuances. Int J Spine Surg 16:S8-S13, 2022. http://dx.doi.org/10.14444/8271
5. Coric D, Rossi VJ, Peloza J, Kim PK, Adamson TE: Percutaneous, navigated minimally invasive posterior cervical pedicle screw fixation. Int J Spine Surg 14:S14-S21, 2020. http://dx.doi.org/10.14444/7122
6. Dawes B, Perchyonok Y, Gonzalvo A: Radiological evaluation of C1 pedicle screw anatomic feasibility. J Clin Neurosci 51:18-21, 2018. https://doi.org/10.1016/j.jocn.2018.01.006
7. Golpinar M, Komut E, Salim H, Govsa F: The computed tomographic evaluation of bony bridge of C1 as bleeding risk factor at the screw placement. SRA 44:585-593, 2022. http://dx.doi.org/10.1007/s00276-022-02919-6
8. Hall GC, Kinsman MJ, Nazar RG, Hruska RT, Mansfield KJ, Boakye M, Rahme R: Atlanto-occipital dislocation. World J Orthop 6:236, 2015. http://dx.doi.org/10.5312/wjo.v6.i2.236
9. Harms J, Melcher RP: Posterior C1-C2 fusion with polyaxial screw and rod fixation. Spine (Phila Pa 1976) 26:2467-2471, 2001. http://dx.doi.org/10.1097/00007632-200111150-00014
10. Heiler U, Schray D, Pitzen T: Early intraoperative and postoperative complications of C1-C2 fixation using the Goel-Harms technique: How often? Which? Why? Unfallchirurgie (Heidelb) 125:792-800, 2022. http://dx.doi.org/10.1007/s00113-021-01080-w
11. Hu Y, Dong WX, Spiker WR, Yuan ZS, Sun XY, Zhang J, Xie H, Albert TJ: An anatomic study to determine the optimal entry point, medial angles, and effective length for safe fixation using posterior C1 lateral mass screws. Spine 40:E191-E198, 2015. http://dx.doi.org/10.1097/brs.0000000000000715
12. Ji W, Zheng M, Kong G, Qu D, Chen J, Zhu Q: Computed tomographic morphometric analysis of pediatric C1 posterior arch crossing screw fixation for atlantoaxial instability. Spine 41:91-96, 2016. http://dx.doi.org/10.1097/BRS.0000000000001156
13. Kim JH, Kwak DS, Han SH, Cho SM, You SH, Kim MK: Anatomic consideration of the C1 laminar arch for lateral mass screw fixation via C1 lateral lamina: A landmark between the lateral and posterior lamina of the C1. JKNS 54:25, 2013. https://doi.org/10.3340/jkns.2013.54.1.25
14. Kobayashi Y, Kikuchi SI, Konno SI, Sekiguchi M: Insertion of lateral mass screw of the atlas via the posterior arch: Anatomical study of screw insertion using dry bone samples of the atlas from Japanese cadavers. J Orthop Sci 13:452-455, 2008. https://doi.org/10.1007/s00776-008-1255-1
15. Krassnig R, Orlandi JA, Tackner E, Hohenberger G, Puchwein P: Computer-aided analysis for optimal screw insertion in lateral mass of C1: An anatomical study. Arch Orthop Trauma Surg 137:817-822, 2017. https://doi.org/10.1007/s00402-017-2678-y

16. Lee CK, Tan TS, Chan CYW, Kwan MK: Surgical morphometry of C1 and C2 vertebrae: A three-dimensional computed tomography analysis of 180 Chinese, Indian, and Malay patients. ASJ 11:181, 2017. http://dx.doi.org/10.4184/asj.2017.11.2.181
17. Lenz M, Harland A, Egenolf P, Perera A, Pennig L, Bredow J, Eysel P, Scheyerer MJ: Suggestion of a safe zone for C1 pedicle screws depending on anatomical peculiarities. Eur Spine J 30:3614-3619, 2021. http://dx.doi.org/10.1007/s00586-021-06993-z
18. Magerl F, Seemann PS: Stable posterior fusion of the atlas and axis by transarticular screw fixation. Cervical spine I. Strasbourg: Springer, 1987:322-327. https://doi.org/10.1007/978-3-7091-8882-8_59
19. Martins RS, Pereira CS, Lemos C, Rodrigues-Pinto R: Posterior atlantoaxial screw placement in a portuguese population: A morphometric analysis based on computed tomography scan measurements. Rev Bras Ortop (Sao Paulo) 58:48-57, 2023. http://dx.doi.org/10.1055/s-0042-1744502
20. Niu HG, Zhang JJ, Yan YZ, Zhao CK, Yang K, Zhang YS: Design of a novel lateral mass screw–plate system for the treatment of unstable atlas fractures: A finite element analysis. J Orthop Surg Res 19:120, 2024. http://dx.doi.org/10.1186/s13018-024-04582-6
21. Olguner SK, Arslan A: Occipital condyle fractures and atlanto-occipital dislocation. Turk Neurosurg 30:317-321, 2020. http://norosirurji.dergisi.org/pdf/pdf_TND_1594.pdf
22. Poodendan C, Suwannakhan A, Chawalchitiporn T, Kasai Y, Nantasenamat C, Yurasakpong L, Iamsaard S, Chaiyamoon A: Morphometric analysis of dry atlas vertebrae in a northeastern Thai population and possible correlation with sex. Surg Radiol Anat 45:175-181, 2023. http://dx.doi.org/10.1007/s00276-022-03076-6
23. Quiles-Guiñau L, Gomez-Cabrero A, Miquel-Feucht M, Blanco-Pérez E, Mata-Escolano F, Juan A, Sanchis-Gimeno J: Analysis of the cervical double transverse foramen in present Spanish population. Eur J Anat 20:337-346, 2016. https://eurjanat.com/data/pdf/eja.160178lq.pdf
24. Rao RD, Tang S, Lim C, Yoganandan N: Developmental morphology and ossification patterns of the C1 vertebra. JBJS 95:e124, 2013. http://dx.doi.org/10.2106/JBJS.L.01035
25. Tan M, Wang H, Wang Y, Zhang G, Yi P, Li Z, Wei H, Yang F: Morphometric evaluation of screw fixation in atlas via posterior arch and lateral mass. Spine 28:888-895, 2003. http://dx.doi.org/10.1097/01.BRS.0000058719.48596.CC
26. Wu C, Deng J, Wang Q, Pan J, Hu H, Li G, Tan L, Wei Q: Feasibility of atlas pedicle screw fixation perpendicular to the coronal plane-a 3D anatomic analysis. GSJ 12:1369-1374, 2022. https://doi.org/10.1177/2192568220980715
27. Young JP, Young PH, Ackermann MJ, Anderson PA, Riew KD: The ponticulus posticus: implications for screw insertion into the first cervical lateral mass. J Bone Joint Surg Am 87:2495-2498, 2005. http://dx.doi.org/10.2106/jbjs.E.00184
28. Yuwakosol P: Morphometric study for C1 pedicle screw placement in Thai patients. Asian J Neurosurg 17:429-434, 2022. http://dx.doi.org/10.1055/s-0042-1756625
29. Zhang L, Wang H: Computed tomographic morphometric analysis of lateral inclination C1 pedicle screw for atlantoaxial instability patients with a narrow C1 posterior arch. KJMS 34:700-704, 2018. http://dx.doi.org/10.1016/j.kjms.2018.08.001

Turk Neurosurg 36(3):394-405, 2026
DOI: 10.5137/1019-5149.JTN.49270-25.2

Original Investigation
Spine and Peripheral Nerves

Received: 10.06.2025
Accepted: 04.09.2025
Published Online: 22.05.2026

A Comprehensive Assessment of Clinical, Radiological, and Histopathological Parameters in Lumbar Disc Herniation Using Correlation Matrices Analysis

Cezmi Cagri TURK[1,2], Elif Sevde TOPALLI[3], Umut Ogun MUTLUCAN[2], Oktay ELTER[1,2], Gulsum AKAR[1,2], Kerem YILMAZ[1,2], Onur ELMAS[4], Dinc SUREN[3]

[1]University of Health Sciences, Hamidiye School of Medicine, Department of Neurosurgery, İstanbul, Türkiye
[2]Antalya Education and Research Hospital, Neurosurgery Clinic, Antalya, Türkiye
[3]Antalya Education and Research Hospital, Pathology Clinic, Antalya, Türkiye
[4]Suleyman Demirel University, Faculty of Medicine, Department of Physiology, Isparta, Türkiye

Corresponding author: Cezmi Cagri TURK ✉ drcezmiturk@gmail.com

ABSTRACT

AIM: To provide deeper insights into the biological mechanisms underlying disc degeneration and recurrence by studying histopathological features of excised disc tissue. Moreover, due to limited predictive role of radiological grading systems like Pfirrmann and Modic classifications in understanding postoperative outcomes and recurrence mechanisms, to perform holistic analysis on clinical, patient specific factors, radiological and histological findings on matrix correlation statistics.

MATERIAL and METHODS: We conducted a retrospective study including 87 patients who underwent lumbar discectomy between 2019 and 2024. Detailed preoperative magnetic resonance imaging (MRI) evaluations using Pfirrmann grading, along with semi-quantitative histopathological analysis, were performed. Statistical analyses included Spearman correlation and ANOVA to explore relationships between clinical, radiological, and histopathological parameters.

RESULTS: Higher Pfirrmann grades were significantly associated with radiological instability ($p<0.001$). Histopathological analysis revealed that matrix disorganization was the only parameter significantly associated with clinical recurrence: all patients with recurrent disc herniation exhibited Grade 3 matrix disorganization ($p<0.001$), while only 40.5% of non-recurrent cases showed this pattern. Spearman correlation matrices further confirmed the absence of strong linear relationships among most individual clinical, radiological, and histological variables.

CONCLUSION: Our integrated approach underscores the importance of matrix disorganization as a biomarker for recurrence risk in lumbar disc herniation. Our integrated approach underscores the importance of matrix disorganization as a histopathological hallmark and potential biomarker for recurrence risk in lumbar disc herniation. In contrast, other histological features—such as chondrocyte grouping and cellularity—did not demonstrate consistent associations with clinical or radiological parameters. Radiological instability was reliably associated with advanced disc degeneration (higher Pfirrmann grades), but did not correlate with histopathological severity. This study advocates for personalized risk stratification tools integrating multi-dimensional data.

KEYWORDS: Lumbar disc herniation, Lumbar discectomy, Predictive biomarkers, Recurrent lumbar disc herniation

Cezmi Cagri TURK : 0000-0003-1497-7827
Elif Sevde TOPALLI : 0009-0006-0336-6552
Umut Ogun MUTLUCAN : 0000-0002-5052-7244
Oktay ELTER : 0000-0002-3526-1900
Gulsum AKAR : 0000-0001-7586-5242
Kerem YILMAZ : 0000-0002-4269-5803
Onur ELMAS : 0000-0002-8380-0999
Dinc SUREN : 0000-0002-1816-7816

INTRODUCTION

Lumbar disc herniation is a leading cause of pain and disability worldwide. Although surgical intervention often provides symptomatic relief, recurrence rates remain considerable, and the underlying biological mechanisms remain unclear (12,13,16,17). Magnetic resonance imaging (MRI) has enabled the development of grading systems such as the Pfirrmann classification; however, the predictive value of radiological findings alone for postoperative outcomes is limited (1,3,8,11). Furthermore, studies report complex and often inconsistent associations between clinical risk factors and disease progression (6,17).

Histopathological changes in disc degeneration have been increasingly investigated, but most studies address only a single dimension of the disease, involve small cohorts or apply overly simplistic analyses (2,8,9,13,16). Consequently, the integration of clinical, radiological, and histopathological data to identify robust biomarkers for recurrence remains uncommon, limiting advances in surgical decision-making (10,11). There is a clear need for comprehensive studies that systematically evaluate relationships between tissue-level features and patient outcomes (12,13,14,17).

The present study addresses these gaps through a retrospective, integrative analysis of patients undergoing lumbar discectomy, we combined detailed MRI grading with semi-quantitative histopathological scoring (15), hypothesizing that multi-dimensional integration would reveal novel associations, clarify the biological determinants of recurrence, and improve prognostic accuracy in lumbar disc disease (16).

MATERIAL and METHODS

Study Design and Ethics

This retrospective observational study was approved by the Institutional Review Board (IRB: 2024-068, decision no. 6/28-09.05.2024) and conducted in accordance with the Declaration of Helsinki. Written informed consent was obtained from all patients. The study adhered to the Strengthening the Reporting of Observational Studies in Epidemiology guidelines.

Power Analysis

An a priori power analysis determined the minimum required sample size for correlation analyses. Using an alpha level of 0.05 and a statistical power of 0.90, the required sample size was calculated to be 86 patients. The final cohort included 87 participants.

Patient Population and Follow-Up

Eighty-seven consecutive adults who underwent primary lumbar discectomy for symptomatic intervertebral disc herniation between 2019 and 2024 were retrospectively reviewed. The inclusion criteria were: age > 18 years, availability of complete clinical records, preoperative lumbar MRI, and adequate excised disc material for histopathological analysis. Patients were excluded if they had a history of spinal tumor, infection, or trauma; prior lumbar instrumentation; or incomplete clinical or imaging data. The mean follow-up duration was 17 months (range, 12–60 months).

Clinical and Demographic Data

Demographic variables included age, sex, and body mass index. Smoking status, and comorbidities—hypertension, diabetes mellitus, hypothyroidism, chronic obstructive pulmonary disease, coronary artery disease, and rheumatologic diseases—were extracted from electronic medical records. Surgical details, including operated spinal levels, recurrence status (defined as symptomatic herniation at the same level requiring reoperation), and follow-up duration, were recorded. In patients with multilevel discectomy, all excised disc materials were pooled and analyzed as a single specimen per patient.

Radiological Assessment

Preoperative lumbar MRI was performed on a 1.5 T system (Achieva, Philips) using sagittal T1-weighted, sagittal T2-weighted, and axial T2-weighted sequences (slice thickness 4 mm). Two neurosurgeons, blinded to other data, independently assessed the images for Pfirrmann grade and herniation type. Discrepancies were resolved by consensus, and interobserver agreement was calculated using Cronbach's alpha. The following MRI parameters were assessed: 1) disc degeneration, graded using the Pfirrmann classification on T2-weighted images (Figure 1); 2) disc morphology, defined as protrusion (base wider than any other dimension) or extrusion (maximum diameter greater than the base), according to the criteria of Fardon et al. (4); 3) annulus–nucleus distinction, scored as clear or indistinct; 4) signal intensity, classified as homogeneous, heterogeneous, or black disc; 5) disc height, categorized as normal, decreased, or collapsed; 6) facet joint effusion, noted as absent, unilateral, or bilateral, defined as > 1 mm fluid signal within the facet joint space on axial T2-weighted images; and 7) radiological instability, defined as the presence of segmental translation > 3 mm or angulation > 10° between adjacent vertebrae on dynamic lateral flexion-extension radiographs, or the presence of a pars interarticularis defect.

Discrepancies between observers were resolved by consensus. Interobserver reliability was assessed using Cronbach's alpha.

Histopathological Analysis

Excised intervertebral disc specimens were fixed in 10% buffered formalin, paraffin-embedded, and stained with hematoxylin and eosin (H&E). Two pathologists, blinded to all clinical and radiological data, independently evaluated the specimens, resolving differences by consensus. Four histopathological parameters were assessed using a semi-quantitative system adapted from previously published criteria (2,9,14) and modified for practical applicability and internal consistency: 1) matrix organization (Grades 1–3), 2) chondrocyte grouping (Grades 1–3), 3) group cellularity (Grades 1–3), and 4) overall cellularity (excluding cartilaginous endplate areas).

Matrix organization

- Grade 1: Mild or minimal changes not meeting criteria for Grade 2 or 3

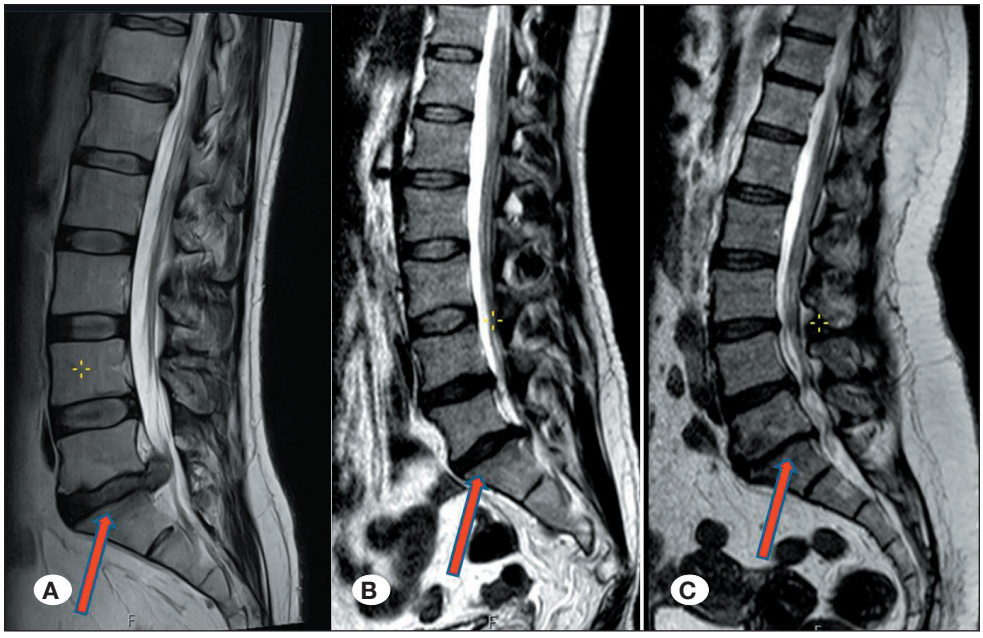

Figure 1: Representative sagittal T2-weighted magnetic resonance imaging (MRI) scans illustrating the Pfirrmann classification of lumbar disc degeneration. **A)** A Grade 2 herniated disc with mild degeneration is observed at the L5-S1 level (red arrow). Adjacent disc structures at the superior levels show minimal degeneration (Grade 1). **B)** A Grade 4 herniated disc is shown at the L5-S1 level (red arrow), with an adjacent Grade 3 disc at the L4-5 level. **C)** A severely degenerated Grade 5 herniated disc is visible at L5-S1 (red arrow), characterized by complete structural disorganization and a significant loss of signal. An adjacent Grade 3 disc is seen at the L4-5 level. The Pfirrmann grading was specifically performed on the surgically treated disc level from which the histopathological specimen was obtained.

- Grade 2: Marked myxoid changes visible at low magnification (H&E, ×40)
- Grade 3: Marked myxoid change with clear matrix separation visible at low magnification (H&E, ×40)

Chondrocyte grouping

- Grade 1: Scattered, non-grouping chondrocytes
- Grade 2: Occasional groups apparent at higher magnification (H&E, ×40)
- Grade 3: Numerous groups readily observed at low magnification (H&E, ×40)

Group cellularity

- Score 1: No grouping (as in chondrocyte grouping Grade 1)
- Score 2: Groups with ≤ 5 chondrocytes
- Score 3: Groups with > 5 chondrocytes

Overall cellularity

The total number of chondrocytes was counted in the most cellular field, excluding cartilaginous endplate areas for standardization, using a ×100 objective.

Statistical Analysis

Statistical analyses were conducted using SPSS version 27 (IBM Corp., Armonk, NY, USA). Categorical variables are presented as counts and percentages; continuous variables as mean ± standard deviation or median (interquartile range), as appropriate, normality was assessed with the Kolmogorov–Smirnov test and Q–Q plots. Categorical variables were compared using the chi-square test; continuous variables were compared using the independent-samples t-test or analysis of variance (ANOVA) for normally distributed data; Mann–Whitney U test or Kruskal–Wallis test for non-normally distributed data.

Correlations among clinical, radiological, and histopathological variables were examined using Spearman's rank correlation coefficient, and correlation matrices were generated for comprehensive visualization. Interobserver reliability was assessed with Cronbach's alpha. Statistical significance was set at $p<0.05$.

RESULTS

A total of 87 patients (mean age, 58.6 ± 11.4 years; range, 31–77 years) who underwent lumbar discectomy were included in the analysis. Females comprised 63.2% (n=55) of the cohort. The mean body weight was 78.7 ± 13.7 kg, mean height 1.64 ± 0.10 m. The mean body mass index (BMI) was 29.0 ± 4.5 kg/m². A history of smoking was reported in 23% (n=20) of patients, hypertension in 43.7% (n=38), and diabetes mellitus in 31% (n=27) of patients. The prevalence of hypothyroidism, chronic obstructive pulmonary disease, coronary artery disease, and rheumatologic disorders was 8.0%, 6.9%, 12.6%, and 4.6%, respectively (Table I).

Table I: General Characteristics and Clinical Features of the Study Cohort

Descriptives	Mean values
Age (mean±SD) (years)	58.63±11.36
Gender, Female, n (%)	55 (63.2)
Weight (mean±SD) (kg)	78.65±13.67
Height (mean±SD) (m)	1.64±0.10
BMI (mean±SD)	29.02±4.46
Smoking, n (%)	20 (23.0)
Hypertension, n (%)	38 (43.7)
Diabetes, n (%)	27 (31.0)
Hypotyroid, n (%)	7 (8.0)
COPD, n (%)	6 (6.9)
Coronary Heart Disease, n (%)	11 (12.6)
Rheumatological, n (%)	4 (4.6)
Level of discectomy, n (%)	
L5-S1	11 (12.7)
L4-5	42 (48.3)
L3-4	12 (13.8)
L2-3	2 (2.3)
L1-2	1 (1.1)
Multiple levels	19 (21.8)
Recurrence in patients, n (%)	13 (14.9)
Extrude Disk apperance on MRI (78 pt), n (%)	40 (51.3)
Radiological instability, n (%)	31 (35.6)

***BMI:** Body Mass Index, **COPD:** Chronic Obstructive Pulmonary Disease*

The most frequently operated levels were L4–L5 (48.3%) and L5–S1 (12.6%); 21.8% of patients underwent multilevel discectomy. During a mean follow-up of 17 months (range, 12–60 months), 13 patients (14.9%) experienced recurrent disc herniation requiring reoperation.

Preoperative MRI revealed an extruded disc in 51.3% of patients and a protrusion in 48.7%. Radiological instability was observed in 35.6% (n=31). The distribution of Pfirrmann grades was as follows: Grade 2 (7.6%), Grade 3 (20.3%), Grade 4 (37.9%), and Grade 5 (34.2%); no patients had Grade 1 degeneration. A "black disc" appearance on T2-weighted MRI was seen in 32.9% of patients. The annulus fibrosus–nucleus pulposus distinction was clear in only 23.1% of cases, indistinct in 50%, and unreported in the remainder. Disc height was preserved in 24.1% of patients and collapsed in 19%. Facet effusion was absent in 61.2% of cases, unilateral in 25%, and bilateral in 13.8%.

Radiological instability was significantly associated with higher mean Pfirrmann grades (4.39 ± 0.47 vs. 3.78 ± 0.75 in stable patients, p<0.001; Figure 2). No significant association was found between facet effusion and radiological instability (p>0.05). Interobserver reliability was excellent for overall MRI assessment (Cronbach's alpha = 0.784) and substantial for Pfirrmann grading (Cronbach's alpha = 0.709).

Histopathological Findings

Matrix organization was graded as follows: Grade 1 in 16.1%, Grade 2 in 34.5%, and Grade 3 in 49.4% of cases (Figure 3). Chondrocyte grouping was Grade 1 in 6.9%, Grade 2 in 23%, and Grade 3 in 70.1% of cases (Figure 4). Group cellularity was Grade 1 in 6.9%, Grade 2 in 36.8%, and Grade 3 in 56.3% of cases (Figure 5). The mean chondrocyte count (overall cellularity) was 81.2 ± 41.9 (range, 18–252).

Correlation of Radiological and Histopathological Parameters

When radiological and histopathological variables were compared using ANOVA and chi-square tests, no statistically significant associations were found between chondrocyte grouping or group cellularity and any of the following MRI parameters: disc appearance, radiological instability, Pfirrmann grade, disc structure, annulus–nucleus distinction, signal intensity, disc height, or facet effusion (all p > 0.05; Tables II-IV).

Matrix organization was significantly associated only with the annulus–nucleus distinction on MRI (p=0.034) but not with other radiological features. Patients with radiological instability exhibited higher Pfirrmann grades, but no significant differences in histopathological parameters were observed between instability groups.

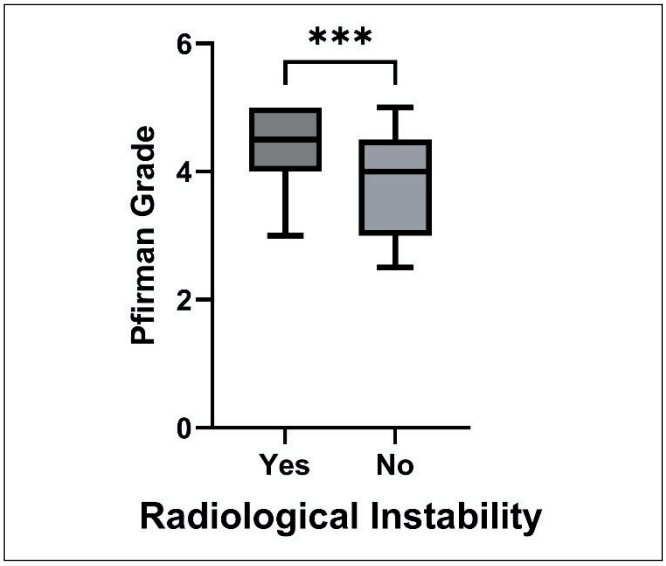

Figure 2: Box-and-whisker plot illustrating the distribution of Pfirrmann grades according to the presence or absence of radiological instability. Patients with radiological instability demonstrated significantly higher Pfirrmann grades compared to those without instability (***p<0.001). Statistical comparison was performed using the Mann–Whitney U test.

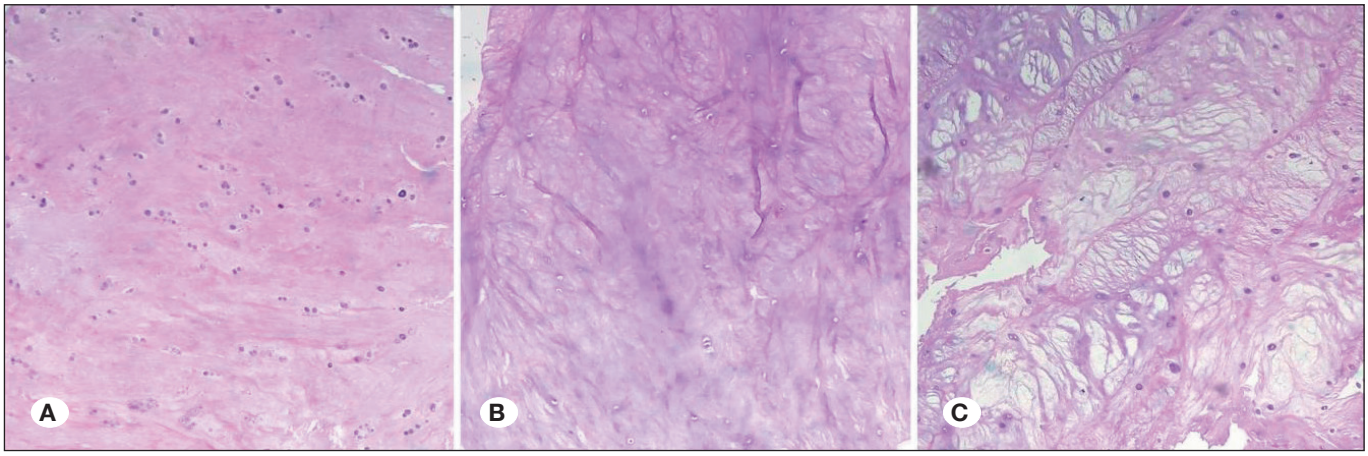

Figure 3: Representative histopathological images demonstrating the grading of matrix organization in intervertebral disc specimens. **A)** Grade 1 – Cases not meeting the criteria for grade 2 or grade 3. **B)** Grade 2 – Marked myxoid changes readily apparent at low magnification (H&E, ×40). **C)** Grade 3 – Marked myxoid change with prominent areas of matrix separation easily visible at low magnification (H&E, ×40). (H&E: hematoxylin and eosin).

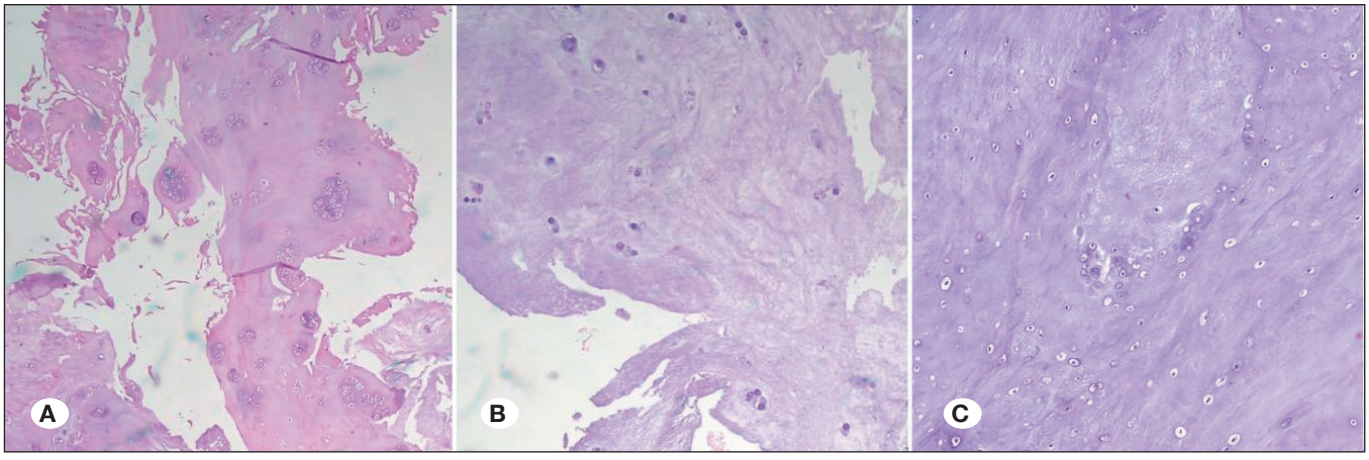

Figure 4: Representative histopathological images illustrating the grading of chondrocyte clustering in intervertebral disc specimens. **A)** Grade 1 – Isolated chondrocytes observed singly without forming clusters. **B)** Grade 2 – Occasional chondrocyte clusters detected either sporadically or on closer inspection (H&E, ×40). **C)** Grade 3 – Numerous chondrocyte clusters easily identified at low magnification (H&E, ×40). (H&E: hematoxylin and eosin).

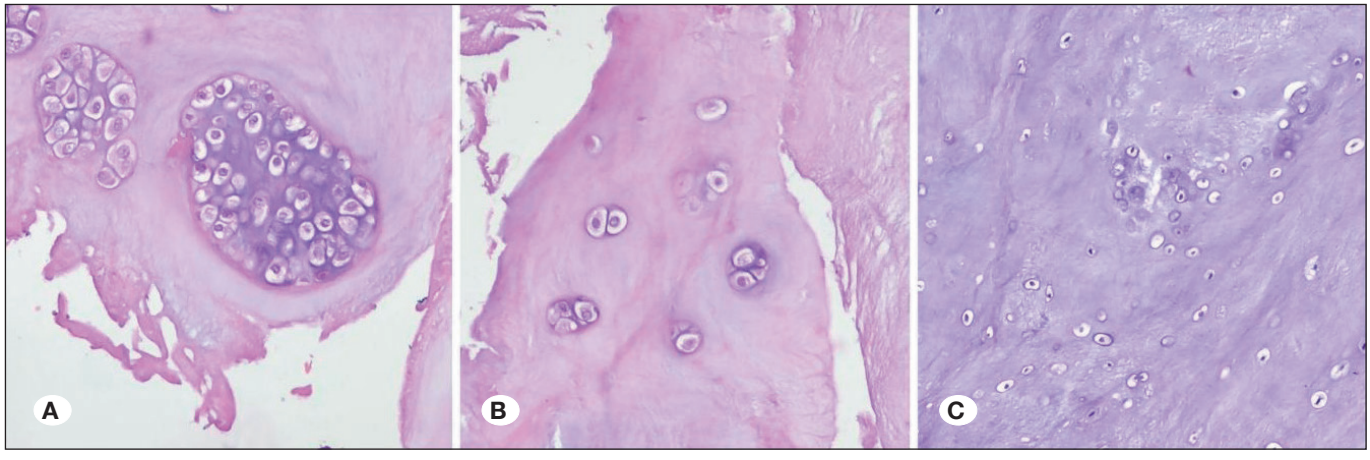

Figure 5: Representative histopathological images showing the grading of group cellularity in chondrocyte clusters within intervertebral disc specimens. **A)** Grade 2 – Chondrocyte clusters containing ≤5 cells per group. **B)** Grade 3 – Chondrocyte clusters containing >5 cells per group. **C)** Grade 1 – cases in which there is no intercellular clustering and chondrocytes are distributed individually (as single cells) (H&E, ×40). (H&E: hematoxylin and eosin).

Table II: Comparison of Histopathological Parameters Between Patients with and without Recurrent Lumbar Disc Herniation

	Recurrence (n=13)	No recurrence (n=74)	p-value
Histopathological Cellularity	99.84±57.86	77.91±37.96	0.148
Grouping Grade, n (%)			
Gr 1	1 (7.7)	5 (6.8)	0.992
Gr 2	3 (23.1)	17 (23)	
Gr 3	9 (69.2)	52 (70.2)	
Group Cellularity Grade, n (%)			
Gr 1	1 (7.7)	5 (6.8)	0.888
Gr 2	4 (30.8)	28 (37.8)	
Gr 3	8 (61.5)	41 (55.4)	
Matrix Organisation, n (%)			
Gr 1	0	14 (18.9)	**<0.001**
Gr 2	0	30 (40.5)	
Gr 3	13 (100)	30 (40.6)	

Table III: Histopathological Findings Stratified by the Presence and Laterality of Facet Joint Effusions

	Facet Effusions			
	No (n=49)	One facet (n=20)	Two facet (n=11)	p-value
Histopathological Cellularity	84.38±42.56	71.80±40.16	77.45±35.68	0.502
Grouping Grade, n (%)				
Gr 1	5 (10.2)	1 (5)	0	0.760
Gr 2	10 (20.4)	5 (25)	2 (18.2)	
Gr 3	34 (69.4)	14 (70)	9 (81.8)	
Group Cellularity Grade, n (%)				
Gr 1	5 (10.2)	1 (5)	0	0.447
Gr 2	17 (34.7)	10 (50.0)	3 (27.3)	
Gr 3	27 (55.1)	9 (45.0)	8 (72.7)	
Matrix Organisation, n (%)				
Gr 1	7 (14.3)	5 (25)	2 (18.2)	0.670
Gr 2	15 (30.6)	6 (30)	5 (45.5)	
Gr 3	27 (55.1)	9 (45)	4 (36.4)	

Recurrent Versus Non-Recurrent Cases

Mean chondrocyte cellularity was higher in recurrent cases compared with non-recurrent cases (99.8 ± 57.9 vs. 77.9 ± 38.0), although the difference did not reach statistical significance (p=0.148). The distributions of chondrocyte grouping, group cellularity, and overall cellularity grades did not differ significantly between recurrent and non-recurrent patients (all p>0.05). Notably, all recurrent cases demonstrated Grade 3 matrix organization, compared with 40.5% of non-recurrent cases (p<0.001), indicating a strong association between advanced matrix disorganization and recurrence (Table II).

Subgroup Analyses

No significant differences in histopathological cellularity, chondrocyte grouping, group cellularity, or matrix organization

Table IV: Comparison of Histopathological Features between Patients with and Without MRI-Detected Disc Extrusion

	Extrude dis apperance on MRI		
	Yes	**No**	**p-value**
Histopathological Cellularity	80.25±47.92	79.21±33.67	0.146
Grouping Grade, n (%)			
Gr 1	3 (7.5)	3 (7.9)	0.627
Gr 2	7 (17.5)	10 (26.3)	
Gr 3	30 (75)	25 (65.8)	
Group Cellularity Grade, n (%)			
Gr 1	3 (7.5)	3 (7.9)	0.908
Gr 2	14 (35.0)	15 (39.5)	
Gr 3	23 (57.5)	20 (52.6)	
Matrix Organisation, n (%)			
Gr 1	5 (12.5)	9 (23.7)	0.347
Gr 2	15 (37.5)	10 (26.3)	
Gr 3	20 (50.0)	19 (50.0)	

were observed when patients were stratified by the presence or absence of facet effusion or by disc extrusion versus protrusion on MRI (all p>0.05; Tables III-IV).

Correlation Matrix Findings

Comprehensive Spearman correlation matrices were constructed to evaluate relationships among clinical, radiological, and histopathological parameters. No strong or statistically significant correlations ($r > 0.5$, $p<0.05$) were found between individual demographic, clinical (Figure 6), or radiological variables (Figure 7) and histopathological parameters (Figure 8). The most notable correlation was between radiological instability and higher Pfirrmann grade. Heatmaps illustrated a general absence of robust linear relationships between most individual parameters.

DISCUSSION

This study provides a comprehensive evaluation of the interplay between demographic, clinical, radiological, and histopathological parameters in patients undergoing lumbar discectomy. By combining detailed MRI grading, objective assessments of radiological instability, and a semi-quantitative histopathological scoring system, we identified predictors of disc recurrence and examined the relationships between tissue-level changes and clinical–radiological findings. Notably, severe matrix disorganization on histopathology emerged as the most consistent correlate of recurrence, whereas common patient-specific factors—such as BMI, smoking, and comorbidities—did not independently predict recurrence or advanced degeneration. Additionally, higher Pfirrmann grades were strongly associated with radiological instability, underscoring the prognostic value of MRI grading in risk stratification.

Unlike most previous studies, which have examined binary relationships between either radiological and histopathological features or clinical risk factors and outcomes, our study employed an integrated, multi-modal approach. Earlier reports have primarily focused on MRI-based grading systems, such as the Pfirrmann classification (7,11) or Modic changes (3,5), in relation to gross disc pathology or symptoms, with relatively few systematically linking histopathology, imaging, and clinical data within a single cohort. Boos et al. and Rutges et al. described cellularity and matrix changes in disc degeneration, but without connecting these features to recurrence or instability in a unified framework (2,14). Our simultaneous assessment of four histopathological variables—matrix organization, chondrocyte grouping, group cellularity, and overall cellularity—alongside MRI parameters and recurrence outcomes offers new insights into the tissue-level mechanisms influencing surgical prognosis.

Consistent with earlier reports, higher Pfirrmann grades were prevalent among patients with radiological instability, with more than 70% of cases graded 4 or 5. This may reflect our institution's role as a tertiary referral center. Although advanced imaging has been proposed as a surrogate for degeneration severity (10), our study uniquely linked radiological findings with prospectively scored histopathological changes. Matrix disorganization was the only histological feature significantly associated with both radiological and clinical endpoints, being present in all recurrent cases—a relationship not previously described in detail (2,14).

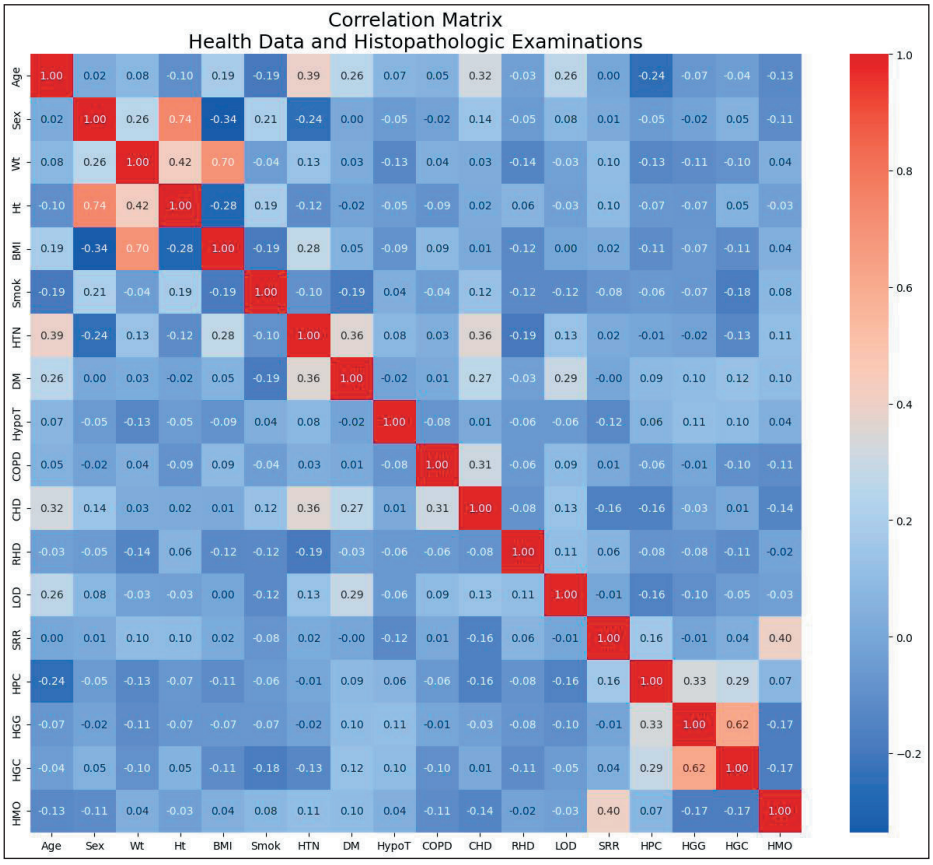

Figure 6: Correlation matrix heatmap demonstrating the relationships between clinical and demographic parameters (e.g., age, sex, BMI, smoking, comorbidities) and radiological findings in the patient cohort. The color scale indicates the strength and direction of Spearman correlation coefficients.

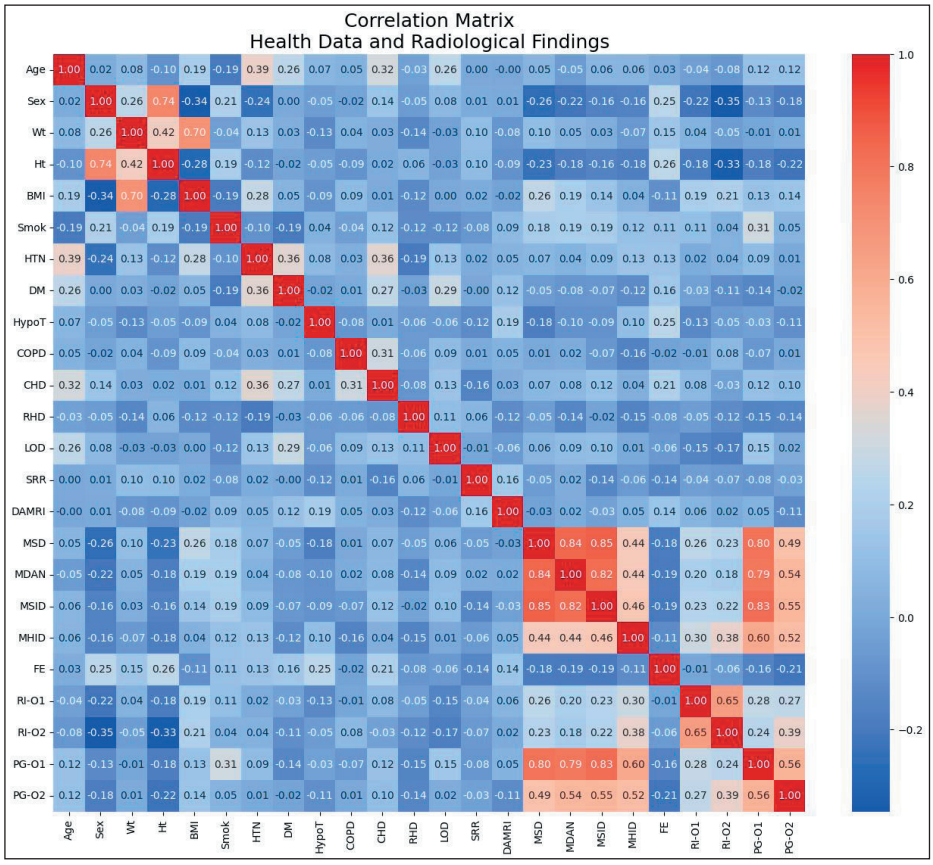

Figure 7: Correlation matrix heatmap illustrating the associations between clinical and demographic features (health data) and histopathological parameters in excised disc specimens. The color scale indicates the Spearman correlation coefficients between each pair of variables.

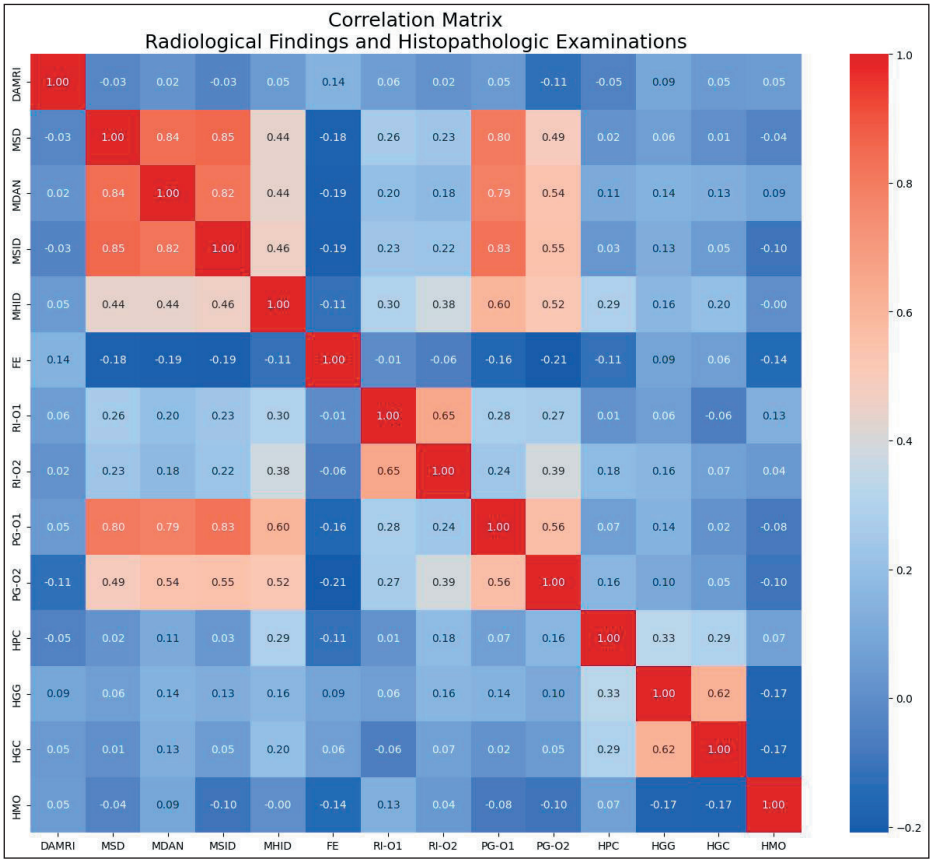

Figure 8: Correlation matrix heatmap visualizing the relationships between radiological findings and histopathological parameters in lumbar disc specimens. The color scale indicates the degree of correlation (Spearman's coefficient) between each radiological and histopathological variable.

Contrary to reports emphasizing patient-specific risk factors (6,16,17), we found no significant association between demographic variables, BMI, smoking, diabetes, or hypertension and either histopathological severity or recurrence risk. These findings suggest that the intrinsic biological state of the intervertebral disc—particularly extracellular matrix integrity—may outweigh traditional risk factors in determining prognosis. Furthermore, while MRI-based features such as facet effusion, disc extrusion, and annulus–nucleus distinction are frequently incorporated into assessment algorithms (15), they showed no consistent or statistically significant correlation with histopathological scores other than matrix organization. This discrepancy highlights the complexity of lumbar disc disease and underscores the need for integrated, multi-parameter evaluation in both research and clinical practice.

Clinically, our findings have two key implications. First, the strong association between matrix disorganization and recurrence suggests that histopathological assessment may be more prognostically relevant than many conventional risk factors, particularly in the presence of advanced radiological degeneration or instability. While MRI remains valuable for surgical planning, reliance on imaging features alone may lead to inaccurate recurrence risk estimation (7,17). Second, correlation matrix analysis across clinical, radiological, and histopathological variables—revealed a general absence of strong linear associations, except for the relationships between Pfirrmann grade and instability, and between matrix disorganization and recurrence. This multidimensionality highlights the potential utility of multi-modal, data-driven approaches—such as machine learning—for refining prognostication and enabling personalized management (18).

Strengths of our study include a large, prospectively characterized single-center cohort; standardized MRI interpretation; blinded, semi-quantitative histopathology; and systematic interobserver reliability assessment. To the best of our knowledge, few studies have conducted correlation matrix analyses across these domains. The identification of matrix disorganization as a recurrence predictor—independent of conventional clinical and radiological factors—represents a novel and clinically relevant finding.

However, several limitations should be noted. The retrospective, single-center design may limit generalizability, and although our sample size was determined by a priori power analysis, multi-center prospective validation is needed. Our histopathological scoring system, while refined for clarity and reproducibility, relied exclusively on H&E staining, limiting molecular-level insights.

Future research should validate these findings in larger, multi-institutional cohorts, extend follow-up to capture long-term outcomes such as pain and disability, and incorporate advanced techniques—including immunohistochemistry, proteomics, and gene expression profiling—to elucidate mechanisms underlying matrix disorganization. The dataset gen-

erated here could inform machine learning–based predictive models for individualized risk stratification. Prospective integration of multi-modal assessment, potentially including preoperative biopsy or non-invasive biomarkers, may bridge the current gap between imaging, tissue pathology, and clinical decision-making.

CONCLUSION

Severe matrix disorganization on histopathology emerged as the strongest tissue-level predictor of recurrence in lumbar disc herniation, underscoring the limitations of relying solely on patient demographics or conventional radiological parameters. Through the integration of standardized histopathological scoring, detailed MRI evaluation, and comprehensive statistical correlation, this study offers new insights into the multidimensional nature of lumbar disc disease. These findings support a more integrated, biologically informed approach to patient assessment and highlight the need for future research incorporating advanced analytical and molecular techniques to refine prognostication, optimize surgical decision-making, and reduce recurrence risk.

ACKNOWLEDGEMENTS

Preparation for publication of this article is partly supported by Turkish Neurosurgical Society

Declarations

Funding: This research did not receive any specific grant from funding agencies in the public, commercial, or not-for-profit sectors.

Availability of data and materials: The datasets generated and/or analyzed during the current study are available from the corresponding author by reasonable request.

Disclosure: The authors declare no competing interests.

AUTHORSHIP CONTRIBUTION

Study conception and design: CCT, DS
Data collection: EST, OE, GA, KY
Analysis and interpretation of results: UOM, OE, GA, OE
Draft manuscript preparation: CCT, EST, UOM, KY
Critical revision of the article: CCT, DS
Other (study supervision, fundings, materials, etc...): n/a
All authors (CCT, EST, UOM, OE, GA, KY, OE, DS) reviewed the results and approved the final version of the manuscript.

REFERENCES

1. Ammar A, Alwadei A, Al Hayek A, Alabbas FM, Almatrafi FR, Elshawarby M: The correlation between histopathology of herniated lumbar intervertebral disc and clinical findings. Asian J Neurosurg 15:545-553, 2020. https://doi.org/10.4103/ajns.AJNS_193_20
2. Boos N, Weissbach S, Rohrbach H, Weiler C, Spratt KF, Nerlich AG: Classification of age-related changes in lumbar intervertebral discs: 2002 Volvo Award in basic science. Spine 27:2631-44, 2002. https://doi.org/10.1097/00007632-200212010-00002.
3. Dudli S, Fields AJ, Samartzis D, Karppinen J, Lotz JC: Pathobiology of modic changes. Eur Spine J 25:3723-3734, 2016. https://doi.org/10.1007/s00586-016-4459-7.
4. Fardon DF, Williams AL, Dohring EJ, Murtagh FR, Gabriel Rothman SL, Sze GK: Lumbar disc nomenclature: Version 2.0: Recommendations of the combined task forces of the North American Spine Society, the American Society of Spine Radiology and the American Society of Neuroradiology. Spine J 14:2525-2545, 2014. https://doi.org/10.1016/j.spinee.2014.04.022.
5. Guo J, Li G, Ji X, Wu X, Zhang G, Zhou C, Ma X: Clinical and radiological risk factors of early recurrent lumbar disc herniation at six months or less: A clinical retrospective analysis in one medical center. Pain Physician 25:E1039-E1045, 2022.
6. Huang W, Han Z, Liu J, Yu L, Yu X: Risk factors for recurrent lumbar disc herniation: A systematic review and meta-analysis. Medicine (Baltimore) 95:e2378, 2016. https://doi.org/10.1097/MD.0000000000002378
7. Middendorp M, Vogl TJ, Kollias K, Kafchitsas K, Khan MF, Maataoui A: Association between intervertebral disc degeneration and the Oswestry Disability Index. J Back Musculoskelet Rehabil 30:819-823, 2017. https://doi.org/10.3233/BMR-150516
8. Munarriz PM, Paredes I, Alén JF, Castaño-Leon AM, Cepeda S, Hernandez-Lain A, Lagares A: Assessment of the correlation between histological degeneration and radiological and clinical parameters in a series of patients who underwent lumbar disc herniation surgery. Neurocirugia 29:79-85, 2018. (Spanish) https://doi.org/10.1016/j.neucir.2017.07.003.
9. Nerlich AG, Boos N, Wiest I, Aebi M: Immunolocalization of major interstitial collagen types in human lumbar intervertebral discs of various ages. Virchows Arch 432:67-76, 1998. https://doi.org/10.1007/s004280050136.
10. Ozden M, Silav ZK: Correlations of disc tissue pathological changes with pfirrmann grade in patients with disc herniation treated with microdiscectomy. Cureus 15:e37913, 2023. https://doi.org/10.7759/cureus.37913
11. Pfirrmann CW, Metzdorf A, Zanetti M, Hodler J, Boos N: Magnetic resonance classification of lumbar intervertebral disc degeneration. Spine (Phila Pa 1976) 26:1873-1878, 2001. https://doi.org/10.1097/00007632-200109010-00011
12. Ren G, Liu L, Zhang P, Xie Z, Wang P, Zhang W, Wang H, Shen M, Deng L, Tao Y, Li X, Wang J, Wang Y, Wu X: Machine learning predicts recurrent lumbar disc herniation following percutaneous endoscopic lumbar discectomy. Global Spine J 14:146-152, 2024. https://doi.org/10.1177/21925682221097650.
13. Roberts S, Evans H, Trivedi J, Menage J: Histology and pathology of the human intervertebral disc. J Bone Joint Surg Am 88 Suppl 2:10-14, 2006. https://doi.org/10.2106/JBJS.F.00019.
14. Rutges JP, Duit RA, Kummer JA, Bekkers JE, Oner FC, Castelein RM, Dhert WJ, Creemers LB: A validated new histological classification for intervertebral disc degeneration. Osteoarthritis Cartilage 21:2039-2047, 2013. https://doi.org/10.1016/j.joca.2013.10.001

15. Soydan Z, Bayramoglu E, Urut DU, Iplikcioglu AC, Sen C: Tracing the disc: The novel qualitative morphometric MRI based disc degeneration classification system. JOR Spine 7:e1321, 2024. https://doi.org/10.1002/jsp2.1321.
16. Weiler C, Lopez-Ramos M, Mayer HM, Korge A, Siepe CJ, Wuertz K, Weiler V, Boos N, Nerlich AG: Histological analysis of surgical lumbar intervertebral disc tissue provides evidence for an association between disc degeneration and increased body mass index. BMC Res Notes 4:497, 2011. https://doi.org/10.1186/1756-0500-4-497.
17. Wilson CA, Roffey DM, Chow D, Alkherayf F, Wai EK: A systematic review of preoperative predictors for postoperative clinical outcomes following lumbar discectomy. Spine J 16:1413-1422, 2016. https://doi.org/10.1016/j.spinee.2016.08.003.
18. Zehra U, Noel-Barker N, Marshall J, Adams MA, Dolan P: Associations between intervertebral disc degeneration grading schemes and measures of disc function. J Orthop Res 37:1946-1955, 2019. https://doi.org/10.1002/jor.24326.

Supplementary Table I: Comparison of Radiological Parameters according to Histopathological Chondrocyte Grouping Grades in Intervertebral Disc Specimens

Descriptive	Histopathological Grouping Grade			p-value*
	Grade 1	Grade 2	Grade 3	
Extrude Disc appearance on MRI	3 pt	7 pt	30 pt	0.637
Radiological instability	2 pt	6 pt	23 pt	0.669
Pfirrman grade 2-3	2 pt	6 pt	14 pt	0.315
Pfirrman grade 4-5	4 pt	11 pt	42 pt	0.573
MR structure of disc- Black disc	2 pt	5 pt	19 pt	0.666
MR distinction of annulus nuscleus- No	2 pt	6 pt	31 pt	0.471
MR signal intensity of disc- Hypointensity	1 pt	5 pt	21 pt	0.490
MR height of intervertebral disc- collapsed	1 pt	3 pt	11 pt	0.318
Facet effusion- no effusion	5 pt	10 pt	34 pt	0.456

**Representative subgroups (e.g., "black disc", "hypointensity") are shown as examples. The p values reflect the comparison of all categories within each radiological feature against grouping grades using Pearson's chi-square test.*

Supplementary Table II: Association Between Radiological Features and Group Cellularity Grades in Excised Disc Tissue

Descriptive	Histopathological Group Cellularity			p-value*
	Grade 1	Grade 2	Grade 3	
Extrude Disc appearance on MRI	3 pt	14 pt	23 pt	0.911
Radiological instability	2 pt	13 pt	16 pt	0.988
Pfirrman grade 2-3	2 pt	7 pt	13 pt	0.353
Pfirrman grade 4-5	4 pt	23 pt	30 pt	0.608
MR structure of disc- Black disc	2 pt	9 pt	15 pt	0.954
MR distinction of annulus nuscleus- No	2 pt	12 pt	25 pt	0.64
MR signal intensity of disc- Hypointensity	1 pt	10 pt	16 pt	0.626
MR height of intervertebral disc- collapsed	1 pt	5 pt	9 pt	0.216
Facet effusion- no effusion	5 pt	17 pt	27 pt	0.453

**Representative subgroups (e.g., "black disc", "hypointensity") are shown as examples. The p values reflect the comparison of all categories within each radiological feature against group cellularity grades using Pearson's chi-square test.*

Supplementary Table III: Radiological Features according to Matrix Organization Grades in Histopathological Analysis

Descriptive	Histopathological Matrix Organization			p-value*
	Grade 1	Grade 2	Grade 3	
Extrude Disc appearance on MRI	5 pt	15 pt	20 pt	0.356
Radiological instability	2 pt	12 pt	17 pt	0.589
Pfirrman grade 2-3	1 pt	11 pt	10 pt	0.095
Pfirrman grade 4-5	13 pt	14 pt	30 pt	0.106
MR structure of disc- Black disc	7 pt	6 pt	24 pt	0.106
MR distinction of annulus nuscleus- No	9 pt	6 pt	24 pt	**0.034**
MR signal intensity of disc- Hypointensity	7 pt	6 pt	14 pt	0.127
MR height of intervertebral disc- collapsed	4 pt	3 pt	8 pt	0.076
Facet effusion- no effusion	7 pt	15 pt	27 pt	0.473

**Representative subgroups (e.g., "black disc", "hypointensity") are shown as examples. The p values reflect the comparison of all categories within each radiological feature against matrix organization grades using Pearson's chi-square test.*

Turk Neurosurg 36(3):406-412, 2026
DOI: 10.5137/1019-5149.JTN.49227-25.2

Original Investigation
Spine and Peripheral Nerves

Received: 02.06.2025
Accepted: 19.09.2025
Published Online: 22.05.2026

Anterior Contralateral Cervical Microdiscectomy at C7-T1

Okan KAHYAOGLU[1], S. Meltem CAN[1], Halit CAVUSOGLU[1], Ismail YUCE[2], Yunus AYDIN[2]

[1]Acibadem Health Group Fulya Hospital, Clinic of Neurosurgery, Istanbul, Türkiye
[2]Acibadem Health Group Taksim Hospital, Clinic of Neurosurgery, Istanbul, Türkiye

Corresponding author: S. Meltem CAN ✉ smeltemc@yahoo.com

ABSTRACT

AIM: To retrospectively review the patients who had disc herniation at C7-T1 level and were treated using the senior author's anterior contralateral simple microdiscectomy without fusion technique.

MATERIAL and METHODS: From January 2000 to December 2021, 27 patients underwent surgery for C7-T1 disc herniation, all of which were performed by the same neurosurgeon. Clinical and radiological data were collected before surgery and at 3 and 24 months after surgery. The Short Form-36 and Neck disability questionnaire were used to assess the quality of life.

RESULTS: All patients presented with radiculopathy. There were 16 male and 11 female patients, with an average age of 40 years. The average follow-up period was 9.7 years. The postoperative Short Form-36 and Neck Disability Index scores were significantly different from the preoperative scores. Overall scores at the postoperative 24th month did not differ significantly from those obtained at the postoperative third month.

CONCLUSION: We propose that patients with symptoms of disc herniation at C7-T1 level benefit from an anterior contralateral microdiscectomy without fusion.

KEYWORDS: Anterior cervical microdiscectomy, C7-T1 disc herniation, Cervicothoracic junction, Contralateral approach

ABBREVIATIONS: AF: Annulus fibrosus, **C:** Curette, **CTJ:** Cervicothoracic junction, **HD:** Herniated disc, **LCM:** Longus colli muscle, **MCS:** Mental component score, **MRI:** Magnetic resonance imaging, **NCSS:** Number cruncher statistical system, **NDI:** Neck Disability Index, **PCS:** Physical component score, **PLL:** Posterior longitidunal ligament, **SF-36:** Short Form-36

INTRODUCTION

The C7-T1 level, known for its unique anatomical and biomechanical characteristics as well as imaging difficulties, continues to pose a challenge for surgeons due to the differences in therapeutic approach. The herniation at this level makes up 1.11% to 8% of all cervical disc herniations (1,2,4,11,14,16-18). This level marks the transition of the spine from a highly mobile cervical segment to an immobile thoracic segment. Because it is both a cervical segment level and the cervicothoracic junction segment, it is often referred to as a member of the thoracic segment.

The absence of the Luscka joint, which allows for axial rotation and flexion-extension movements, is the most important anatomical feature that distinguishes the cervicothoracic region and its important member C7-T1 level from the upper cervical levels, which are said to be biomechanically more similar to the lumbosacral junction when compared with other junction regions (12). This anatomical difference has a significant consequence; herniations almost always cause symptoms and signs of lateral-radiculopathy because they weaken the annulus laterally than centrally (9,11,13,14,16-18).

The anterior contralateral microdiscectomy for the treatment of cervical disc hernias is based on the principle of relieving the

Okan KAHYAOGLU : 0000-0002-9510-3509
S. Meltem CAN : 0000-0003-3769-5873
Halit CAVUSOGLU : 0000-0003-1877-7611
Ismail YUCE : 0000-0002-7385-9137
Yunus AYDIN : 0000-0003-4141-9556

pressure on the neural elements without causing instability by employing different approaches and instruments developed by the senior author, which differ from classical methods. Because of the anatomy of the C7-T1 level, anterior accesses present a challenge for surgeons. The technique we have described is equally applicable to the C7-T1 distance as it is to higher levels. In this study we present retrospective analyses of our unique contralateral microdiscectomy technique at the cervicothoracic junction (CTJ).

MATERIAL and METHODS

Between January 2000 and December 2021, a total of 694 patients were treated for cervical disc herniation with the contralateral simple microdiscectomy technique. Twenty-seven patients presented with such a disease at the C7-T1 level. This study included patients who met at least one of the following criteria:

1) The presence of motor weakness indicating radiculopathy, 2) correlation between clinical and magnetic resonance imaging (MRI) findings, 3) failure of conservative treatment for at least three weeks, and 4) no prior surgery for cervical pathology.

All patients underwent clinical examinations and MRI scans before surgery. A neuroradiologist interpreted MRI scans of the cervical spine taken 24 months after surgery. The Neck Disability Index (NDI) and Short Form-36 (SF-36) questionnaires, which are patient-rated instruments, were used to evaluate each patient's surgical outcome before surgery as well as 3 months and 24 months later. The NDI includes 10 items that assess the outcome of neck pain in daily life (19). SF-36 is a 36-item questionnaire that measures primarily two components made up of eight variables: physical component score (PCS) and mental component score (MCS) (21).

All procedures in studies involving human participants were carried out in accordance with the ethical standards of the Local Ethics Committee (Project No. 2024/4397) as well as the 1964 Helsinki Declaration and its subsequent amendments or comparable ethical standards. All individual participants in the study provided informed consent.

The study data were analysed statistically using the Number Cruncher Statistical System (NCSS) 2007 Statistical Software package (Utah, USA). In addition to descriptive statistics (mean and standard deviation), the Shapiro–Wilk normality test was used to examine the distribution. For time comparisons of normally distributed variables, paired one-way analysis of variance was used, and subgroup comparisons were made using the Newman–Keuls multiple comparison test. The statistical significance was set at $p<0.05$.

Surgical Technique

The operation is performed in a similar fashion to the previously described anterior simple discectomy, but it is performed on the contralateral side of the radiculopathy with some modifications. The head is held in a neutral position with a towel roll under the neck, preserving the cervical lordosis. The entire procedure is carried out using an operating microscope.

A 2-cm transverse skin incision is made just on the median of the medial border of the sternocleidomastoid muscle. After splitting the platysma muscle longitudinally, finger dissection is used to separate the areolar tissue between the carotid sheath and the tracheoesophageal bundle down to the vertebral bodies' anterior surface. Because the automatic retractors are too large to fit through a small incision, a 15-mm-wide mini-size Zenker hand retractor is used to retract the skin, trachea, and esophagus medially. A C-arm scope verifies the proper level. In contrast to the conventional technique, the longus colli muscles are not stripped. The anterior longitudinal ligament between the longus colli muscles is incised in a rectangular shape just next to the ipsilateral muscle's medial border, with a scalpel. The disc material is removed with micro-curettes and punches down to the posterior longitidinal ligament (PLL) without the use of a spreader, taking care not to remove cartilaginous endplates. However, it is not intended to remove the lateral portions of the annulus fibrosus aggressively. The lateral border of the annulus fibrosus on the intervention side and the ventrolateral part on the opposite side remain intact. If there are posterior osteophytes associated with the disc herniation, they are removed with micro-curettes and/or an air drill to decompress the spinal canal, taking care not to remove cartilaginous endplates. Following PLL excision, the epidural space, foramen, and nerve root are monitored for free sequester. The contralateral approach used in this procedure provides an additional benefit of direct microscopic visualization of the target area (Figure 1). Since 2012, 20 of all patients have undergone an interbody fat graft. The operation is complete once decompression is confirmed by direct inspection under a surgical microscope.

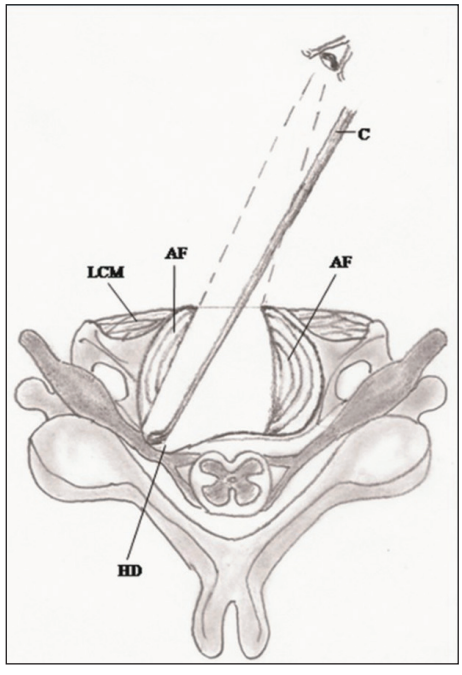

Figure 1: Illustrative drawing of anterior contralateral approach showing a wider angle of exposure to the foramen for cervical microdiscectomy. **AF:** annulus fibrosus; **C:** curette; **HD:** herniated disc; **LCM:** longus colli muscle.

RESULTS

Our cohort consisted of 16 males and 11 females with ages ranging from 29 to 52 years (mean ± standard deviation, 40.48 ± 5.76). Twenty-four of them had one level of herniation, while three had two. No patient had any signs of myelopathy. The primary complaint was the neck pain, that spread through the forearm to the fourth and fifth digits, accompanied by numbness and tingling. Twenty-two of the patients demonstrated motor weakness in their intrinsic hand muscles.

The follow-up period varied from 2 to 21 (mean=9.7) years. All 27 patients recovered immediately after the operation, with no radicular pain and a normal range of motion in their neck. No patient had hoarseness, however, six patients complained of minimal transient dysphagia immediately after the operation.

Within 4 weeks of being discharged, 17 of the 22 patients with radicular motor weakness, had returned to normal. The weakness of the involved muscles did not improve in the other five patients with neurological deficits lasting more than 6 months, necessitating the use of physical therapy.

The SF-36 and NDI scores are shown in Tables I-III. Postoperative SF-36 and NDI scores were significantly different from the preoperative values. Except for physical role functioning, there was no statistically significant difference in overall scores at the third and 24th months after surgery. Figure 2A, B shows the sagittal and axial T2-weighted MRI scans of a 51-year-old female with left C7-T1 herniation. Control MRI scans at the 24th month showed healing without fusion and good alignment (Figure 3A, B). During the follow-up period, no recurrences were observed in all patients. In the late postoperative period, no fusion was observed at the operated level in all patients.

Table I: Short Form 36 (SF-36) and The Neck Disability Index (NDI) Scores of Patients

		Preop.	3rd Month	24th Month	p-value*
SF-36 PCS	Physical Functioning	66.67±8.55	90.19±4.90	89.42±4.32	**0.0001**
	Physical role functioning	44.41±17.49	89.81±12.52	99.87±4.69	**0.0001**
	Pain	31.67±14.58	86.76±6.75	89.23±2.72	**0.0001**
	General health	49.26±11.99	67.96±8.00	66.92±9.17	**0.0001**
SF-36 MCS	Vitality	51.48±14.60	71.11±7.89	71.73±7.74	**0.0001**
	Social functioning	41.67±12.50	95.37±11.58	96.64±10.34	**0.0001**
	Emotional role	66.68±20.68	92.60±14.11	88.47±16.16	**0.0001**
	Emotional well-being	73.67±7.08	83.70±5.08	84.15±5.82	**0.0001**
NDI		28.15±8.21	8.19±2.40	7.81±2.58	**0.0001**

**One way ANOVA.*

Table II: Results of Newman Keuls Multiple Comparison Test for Subgroup Comparisons for SF-36 Physical Component Scores

	SF-36 PCS			
	Physical functioning	**Physical role functioning**	**Pain**	**General health**
Preoperative / 3rd Month	0.0001	0.0001	0.0001	0.0001
Preoperative / 24th Month	0.0001	0.0001	0.0001	0.0001
Postoperative 3rd Month / 24th Month	0.134	0.001	0.100	0.271

Table III: Results of Newman Keuls Multiple Comparison Test for Subgroup Comparisons for SF-36 Mental Component Scores and NDI

	SF-36 MSC				NDI
	Vitality	**Social functioning**	**Emotional role**	**Emotional well-being**	
Preoperative / 3rd Month	0.0001	0.0001	0.0001	0.0001	0.0001
Preoperative / 24th Month	0.0001	0.0001	0.0001	0.0001	0.0001
Postoperative 3rd Month / 24th Month	0.691	0.265	0.256	0.490	0.057

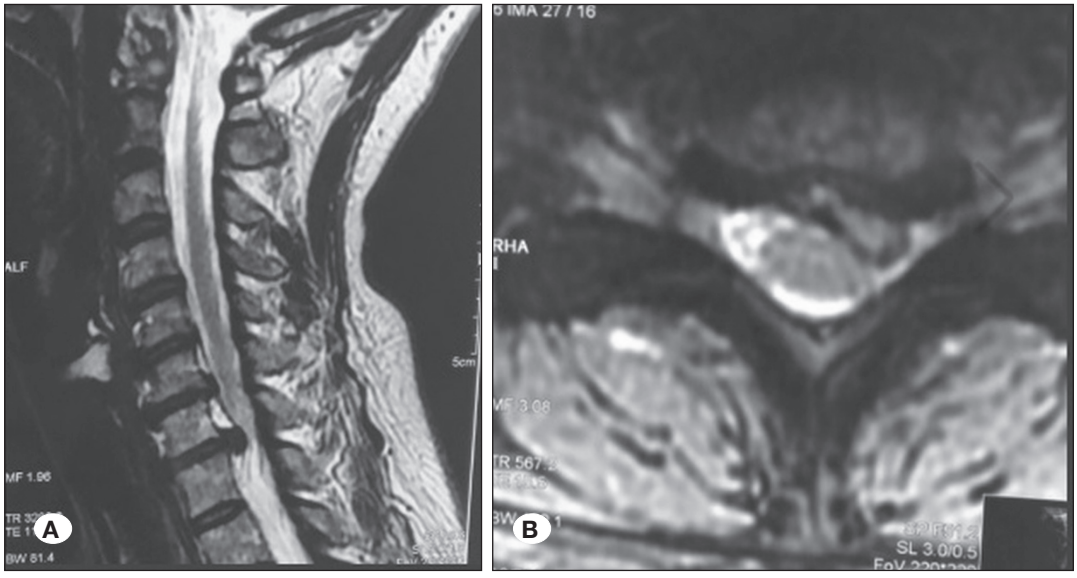

Figure 2: Preoperative sagittal **(A)** and axial **(B)** T2-weighted magnetic resonance imaging scans of a 51-year-old female with left C7-T1 herniation.

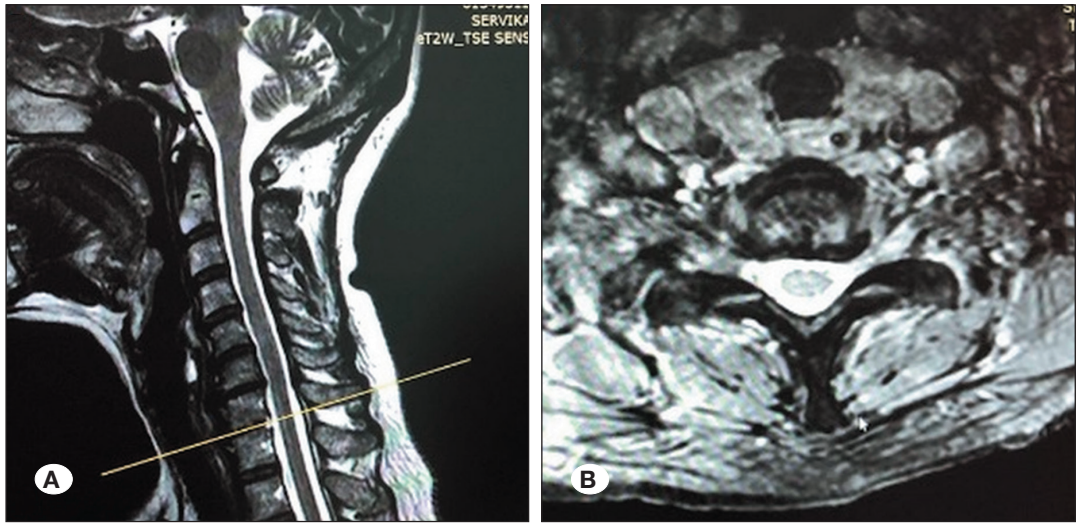

Figure 3: Sagittal **(A)** and axial **(B)** magnetic resonance imaging scans taken at postoperative 24 months, showing healing without fusion and good alignment.

DISCUSSION

We used the simple microdiscectomy, which the senior author (YA) has constantly modified since the 1990s (2,3,7). A literature search for the simple microdiscectomy technique yields numerous publications with positive results before the generalization of the instrumented fusion techniques (4-6,8). For many years, the senior author has advocated for the use simple microdiscectomy, and he has also made some modifications to overcome the limitations of the traditional technique. Except for the left-handed surgeons, the majority of medical literature recommends a right-sided approach and incision site on the neck (4,6,8). Based on the preference of left-handed surgeons in the classical literature, the senior author described the contralateral approach: The incision site is on the opposite side of the brachialgia which corresponds to the site of disc extrusion (2,3,7). Given that C7-T1 disc herniations are typically found on the lateral-foraminal, providing a contralateral view is critical. It enables resection by directly visualizing the pathology, and by directly viewing the disc piece and foramen from the opposite direction.

The most significant change is the selection of retractor system, which eliminates the bulky automated equipment. The conventional Cloward hand held retractor system, designed in the pre-microscope era, has been replaced by the Zenker hand-held retractor, which is 10–12 mm wide and available in a variety of lengths. The assistant's Zenker retractor allows for instant and intermittent retraction of the esophagus and trachea and, unlike constant retractors, does not cause blood supply issues. When the assistant becomes tired or when retraction is no longer required, the Zenker retractor is released.

The surgical incision is typically made slightly lower in the index level checked by the C-arm and close to the midline. The incision site is localized after tangential retraction of the trachea-esophageal structure to prevent lateral retraction during surgery. This is critical for the contralateral technique

due to the use of a one-sided Zenker retractor. The incision measures 15–20 mm and does not allow the surgeon to use an additional retractor. The surgeon uses a suction tube to retract the lateral part.

The intervertebral cartilage has the shape of a convex roof and faces each other as a dome. Preventing postoperative collapse involves sparing the anterior borders of the vertebrae and remaining intradiscally by avoiding end plate violation. It is not advisable to clean the lateral parts of this cupola unless there are mobile, degenerated, or floating free fragments. The lateral parts of the annulus fibrosus remain relatively stable and behave like a washer, and the dome shape of the intervertebral surface helps to maintain the physiological alignment column. After achieving all of these during the operation, postoperative vertebral collapse and alignment issues, which are common after conventional simple microdiscectomy surgery, could be avoided, making this technique extremely minimally invasive. Microforceps designed for endoscopic procedures are also useful in our technique, particularly for the removal of foraminal fragments.

Osteophytic changes are common in chronic cervical disc herniations, accompanying soft protrusions. During the decompression process, the surgeon should not only clean up the degenerated nucleus pulposus but also remove any osteophytes. Removal of osteophytes should be done behind the open cancellous bone surfaces at the upper and lower vertebral corpus edges; otherwise, it may promote bone healing and result in spontaneous fusion. The idea behind putting a fat graft into the disc space is to treat pseudoarthrosis, which preserves the motion segment by preventing fusion between the corpus edges.

The preservation of the motion segment is the most important aspect of cervical total disc replacement, also known as cervical disc prosthesis application techniques. It has gained popularity and is widely used, but in the long run, it has risks of heterotopic ossification, which reduces (15,20).

A head-down position is required to adjust the surgical microscope light array. Being parallel to the intervertebral surface is critical to avoiding end plate injury and exposing the midline of the intervertebral level. This critical procedure allows the surgeon to approach the site of protrusion directly while also gaining lateral access.

Despite difficulties in axial imaging parallel to the disc, MRI remains the gold standard for displaying the disc at the C7-T1 level. If the neurological examination findings strongly indicate this level and the MRI does not help, we will try again with thinner sections. Computed tomographic imaging at the C7–T1 level is difficult due to axial image distortion caused by the majority of the shoulders. It is also challenging to see the C7-T1 level in lateral X-rays. We do not routinely perform tomography and X-ray examinations for C7-T1 disc herniation.

In the literature, a series of interventions at this level consists of either large cervical series or only the patient series related to this level, which are presented in this article. Ryu et al. reported 36 cases of disc herniations at the cervicothoracic junction. In 21 patients, they used the Smith–Robinson technique for the anterior approach, while 15 patients had a posterior foraminotomy with discectomy. This is the largest study to date looking into the characteristics, symptom duration, clinical course, and biomechanics of cervicothoracic junction disc herniation (17). In the series of Falavigna et al., in which they evaluated the radiological diagnosis, clinical appearance, neurological outcomes and surgical planning of the anterior approach to disc herniations at the C7 – T1 level, 19 patients were operated by the anterior approach mostly from the side opposite to the herniation to optimize visualization, and they concluded that a single cage was insufficient despite the discectomy and fusion, and recommended the use of an anterior cervical plate (9). Post et al. performed anterior cervical discectomy and fusion on 10 patients, focusing on their experience with operative management, especially in terms of clinical presentation, imaging, operative exposure issues, and neurological outcomes. They encountered no difficulties during the initial intervention (16). Ozer et al. described their experience with eight patients who had C7-T2 soft foraminal disc herniations (14). In their series, they operated on patients with anterior fusion and, at one level, partial corpectomy, and they examined preoperative and postoperative neurologic charts, surgical techniques, and clinical outcomes Lee et al. investigated the clinical characteristics of 13 patients with cervicothoracic junction disc herniation. In 10 of them, anterior intervention using the standard suprasternal Smith–Robinson approach was sufficient, while two patients required manubriotomy–sternotomy, and one patient was operated on at the incorrect level (11). Mostofi et al. operated on 21 patients, with 13 undergoing posterior simple discectomy and eight undergoing anterior discectomy with fusion (13). Except for the study by Takeuchi et al. (5), which included five patients (9,11,13,14,16-18), all of the reported series involving an anterior approach for C7-T1 disc herniation used bone fusion, cage replacement, and/or anterior instrumentation. They performed an anterior keyhole foraminotomy without fusion by drilling the C7 corpus; however, only the disc fragments or osteophytes compressing the nerve root were removed.

Most series agree that the anterior approach is sufficient, but the difficulties encountered during the anterior approach are highlighted (9,11,14,16,18). Thoracic kyphosis causes the vertebral bodies at the C7-T1 level to be deeply inclined away from the surgeon. This is more of an issue for short and obese patients. The “narrowed operative space” caused by vertebral bone occlusion makes vital anatomical structures such as large blood vessels, the esophagus, the trachea, and the recurrent laryngeal nerve difficult to access. To deal with this, turn the operating table upside down in Trendelenburg position and then raise it as we do at all levels, so that the microscope is in the same plane as the distance. In our series, the technique we used posed no threat to these risky anatomical formations; no sternotomy was required in any of our patients. Except for a short-necked obese patient, we encountered no difficulties during anterior route intervention, as did Post et al. (16). In this patient, we made an incision but did not show the level. Using the C6-7 marking as a reference for the C6-7 distance, we found that we were having difficulty because it remained above the level, so we had to use a modified Zen-

ker retractor. Again, keep in mind that there may be individual differences in bone anatomy.Some authors recommend a posterior approach to the CTJ due to the difficulty of accessing it anteriorly (1). Some studies combined anterior fusion or posterior intervention with microforaminotomy (13,17), while others only performed posterior intervention (1). It was stated that posterior intervention is also appropriate because the majority of herniations are foraminal. Posterior approaches provide limited surgical workspace and the possibility of entering the wrong level (1). Excessive resection of more than 50% of the facet joint can lead to instability and hypermobility (10). There is also the view that facet joint protection is not required due to other biomechanical features of the sternum and cervicothoracic junction, which argue the opposite (13).

CONCLUSION

We believe that the contralateral approach we use at the upper cervical levels, the anterior microdiscectomy technique without fusion and the fat graft procedure are equally beneficial at the C7-T1 level and are not different from other cervical levels. Because this minimally invasive technique does not compromise stability, no interbody fusion materials or anterior instrumentation are required, which may result in complications such as manubrium, mediastinum, and other injuries as well as subsidence, displacement, or improper placement of the intervertebral material

ACKNOWLEDGEMENTS

This study was submitted as preprint in online Research Square. DOI: 10.21203/rs.3.rs-5185326/v1

Declarations

Funding: This research did not receive any specific grant from funding agencies in the public, commercial, or not-for-profit sectors.

Availability of data and materials: The datasets generated and/or analyzed during the current study are available from the corresponding author by reasonable request.

Disclosure: The authors declare no competing interests.

Informed consent: Informed consent was obtained from all individual participants included in the study.

AUTHORSHIP CONTRIBUTION

Study conception and design: OK, YA
Data collection: OK, SMC
Analysis and interpretation of results: OK, SMC, HC
Draft manuscript preparation: OK, SMC, YA
Critical revision of the article: OK, SMC, HC, IY, YA
Other (study supervision, fundings, materials, etc...): n/a
All authors (OK, SMC, HC, IY, YA) reviewed the results and approved the final version of the manuscript.

REFERENCES

1. Adamson TE: Microendoscopic posterior cervical laminoforaminotomy for unilateral radiculopathy: Results of a new technique in 100 cases. J Neurosurg 95:51-57, 2001. https://doi.org/10.3171/spi.2001.95.1.0051
2. Aydin Y, Cavusoglu H, Yuce I, Ozdilmac A, Kahyaoglu O: A prospective study of interbody fat graft application with anterior contralateral cervical microdiscectomy to preserve segmental mobility. Neurosurgery 81:627-637, 2017. https://doi. 10.1093/neuros/nyx056
3. Aydin Y, Kaya RA, Can SM, Turkmenoglu O, Cavusoglu H, Ziyal IM: Minimally invasive anterior contralateral approach for the treatment of cervical disc herniation. Surg Neurol 63:210 -218 [discussion 218-219], 2005. https://doi.org/10.1016/j.surneu.2004.07.001
4. Bertalanffy H, Eggert HR: Clinical long term–results of anterior discectomy without fusion for treatment of cervical radiculopathy and myelopathy. A follow-up of 164 cases. Acta Neurochir (Wien) 90:127-135, 1988. https://doi.org/10.1007/BF01560567
5. Bertalanffy H, Eggert HR: Complications of anterior discectomy without fusion in 450 consecutive patients. Acta Neurochir (Wien) 99:41-50, 1988. https://doi.org/ 10.1007/BF01407775
6. Bucciero A, Vizioli L, Cerillo A: Soft cervical disc herniation. An analysis of 187 cases. J Neurosurg Sci 42:125-130, 1998.
7. Cavusoglu H, Turkmenoglu O, Kaya RA, Can SM, Aydin Y: Effects of anterior contralateral cervical microdiseectomy on radiological and clinical outcome. Surg Neurol 65:446-453, 2006. https://doi.org/10.1007/s00586-007-0471-2
8. Cloward RB: The anterior approach for removal of ruptured cervical discs. J Neurosurg 15:602-614, 1958. https://doi.org/10.3171/jns.1958.15.6.0602
9. Falavigna A, Righesso O, Betemps A, Vela de los Rios PF, Guimaraes R, Ziegler M, Egger de Souza O, Guarise da Silva P, Riew DK: Surgical planning and neurological outcome after anterior approach to remove a disc herniation at the C7-T1 level in 19 patients. Spine 39:E219–E219, 2014. https://doi.org/10.1097/BRS.0000000000000109
10. Fehlings MG, Gray RJ: Posterior cervical foraminotomy for the treatment of cervical radiculopathy. J Neurosurg Spine 10: 343-346, 2009. https://doi.org/ 10.3171/2009.1.SPINE08899
11. Lee JG, Kim HS, Ju CII, Kim SW: Clinical features of herniated disc at cervicothoracic junction level treated by anterior approach. Korean J Spine 13:53-56, 2016. https://doi.org/10.14245/kjs.2016.13.2.53
12. Milne N: The role of zygapophysial joint orientation and uncinate processes in controlling motion in the cervical spine. J Anat 178:189-201, 1991.
13. Mostofi K, Peyravi M, Moghadam BG: Cervicothorasic junction disc herniation: Our experience, technical remarks, and outcome. J Craniovert Jun Spine 11:22-25, 2020. https://doi.org/10.4103/jcvjs.JCVJS_102_19
14. Ozer AF, Kaner T, Sasani M, Oktenoglu T, Cosar M: Anterior approach to disc herniation with modified anterior microforaminotomy at C7-T2: Technical note. Spine 34:1879–1883, 2009. https://doi.org/10.1097/BRS.0b013e3181aa7c62
15. Paci M, Wang MY: Cervical total disc replacement: Heterotopic ossification and complications. In: Cheng BC (ed), Handbook of Spine Technology. Springer, Cham., 2021:829-836. https://doi.org/10.1007/978-3-319-44424-6_77

16. Post NH, Cooper PR, Frempong-Boadu AK, Costa ME: Unique features of herniated discs at the cervicothoracic junction: Clinical presentation, imaging, operative management, and outcome after anterior decompressive operation in 10 Patients. Neurosurgery 58:497-501, 2006. https://doi.org/10.1227/01.NEU.0000197118.86658.A6
17. Ryu DS, Paik HK, Ahn SS, Kim KH, Chin DK, Kim KS, Cho Y, Kuh SU: Herniated discs at the cervicothoracic junction. World Neurosurg 118:E651-E658, 2018. https://doi.org/10.1016/j.wneu.2018.07.017
18. Takeuchi M, Takayasu M, Yasuda M, Kamiya M, Inukai T, Matsuo N, Osuka K: Transvertebral anterior keyhole foraminotomy without fusion for the cervicothorasic junction. Acta Neurochir 154:1797-1802, 2012. https://doi.org/10.1007/s00701-012-1484-0
19. Vernon H, Mior S: The neck disability index: A study of reliability and validity. J Manipulative Physiol Ther 14:409-415, 1991.
20. Vukic M, Marasanov SM: Cervical total disc replacement: Technique – pitfalls and pearls. In: Cheng BC (ed), Handbook of Spine Technology. Springer, Cham., 2021:808-821. https://doi.org/ 10.1007/978-3-319-44424-6_75
21. Ware J, Snow KK, Kosinski M, Gandek B: SF-36 health survey: Manual and interpretation guide. Boston (Mass): The Health Institute, New England Medical Center, 1993. https://gyansanchay.csjmu.ac.in/wp-content/uploads/2021/12/WareetalSF-36UserManual_27MB_1993_316pp-1_compressed-compressed-1-1.pdf

Turk Neurosurg 36(3):413-419, 2026
DOI: 10.5137/1019-5149.JTN.49317-25.3

Original Investigation
Spine and Peripheral Nerves

Received: 21.06.2025
Accepted: 02.10.2025
Published Online: 22.05.2026

A New Measurement Technique for Lumbosacral Transitional Vertebra and Anatomic Orientation of Sacrum (Perioperative Indicator for Lumbosacral Surgery)

Cem ATABEY[1], Ahmet GUNAYDIN[2], Ahmet EROGLU[1], Meltem Ozdemir[3], Ahmet Metin SANLI[4], Uygur ER[5]

[1]University of Health Sciences, Sultan 2. Abdulhamid Han Training and Research Hospital, Department of Neurosurgery, Istanbul, Türkiye
[2]Etlik City Hospital, Department of Neurosurgery, Ankara, Türkiye
[3]Etlik City Hospital, Department of Radiology, Ankara, Türkiye
[4]University of Health Sciences, Diskapi Yildirim Beyazit Training and Research Hospital, Department of Neurosurgery, Ankara, Türkiye
[5]Acibadem Ankara Hospital, Department of Neurosurgery, Ankara, Türkiye

This study has been presented at the EANS2019 Congress between 24 and 28 September 2019, Dublin, Ireland

Corresponding author: Cem ATABEY ✉ cematabey@gmail.com

ABSTRACT

AIM: To evaluate the orientation of the sacrum, its influence on sagittal balance, and its practical relevance in identifying a sacralized L5 or lumbarized S1 as an lumbosacral transitional vertebrae (LSTV) to help prevent complications.

MATERIAL and METHODS: Lumbosacral vertebral roentgenograms from 633 outpatients who visited our hospital between June 2018 and August 2018 were retrospectively reviewed.

RESULTS: All participants were young males with a mean age of 18.41 years (range 17-21 years). The mean ATA1 distance was 16.84 mm ± 6.28 in the 527 normal cases, 4.21 mm ± 5.32 in the 71 sacralization cases, and 21.17 mm ± 6.68 in the 35 lumbarization cases The angle distribution among the 527 patients with normal anatomy was 10.58° ± 1.3. In the 71 patients with sacralization, the angle was 8.89° ± 1.13. Among the 35 patients with lumbarization, the angle was 9.86° ± 1.76.

CONCLUSION: A new index formula, comprising the Anterior Translational Arch (ATA1) and Anterior Translational Angle (ATA2) is proposed. ATA1 as a distance measurement and ATA2 as an angular measurement were evaluated. These measurements can be easily obtained using either lumbosacral vertebral radiographs or sagittal MRI, owing to the simplicity of the calculation. This allows an easy identification of lumbarization and sacralization.

KEYWORDS: Transitional vertebra, Sacrum, Lumbosacral, Spine, Distance

ABBREVIATIONS: ATA1: Anterior translational arch (distance), **ATA2:** Anterior translational angle, **L5:** Fifth lumbar vertebra, **S1:** First sacral vertebra, **C2:** Second cervical vertebra, **S5:** Fifth sacral vertebra, **LSTV:** Lumbosacral transitional vertebrae, **ROC:** Receiver operating characteristic, **MRI:** Magnetic resonance imaging

Cem ATABEY : 0000-0002-9047-196X
Ahmet GUNAYDIN : 0000-0002-3292-5791
Ahmet EROGLU : 0000-0001-7848-1551
Meltem OZDEMIR : 0000-0002-7388-2871
Ahmet Metin SANLI : 0000-0003-4072-7522
Uygur ER : 0000-0002-6641-0075

INTRODUCTION

The configuration of the lower lumbar vertebrae and sacrum, along with pelvic orientation and lumbosacral parameters, constitutes the foundation of the vertebral column and play a crucial role in neurosurgical procedures involving this region (14).

The anatomical orientation of the L5 vertebra and the first sacral segment (S1) is primarily influenced by the intervertebral disc and facet joints (13). The structural features of the L5 vertebra and the sacral dome may also contribute to this alignment to some degree. The sacrum is anatomically complex; it is a pyramidal bone formed by the fusion of five sacral vertebrae (17), and it consists of five distinct surfaces: a midline dorsal canal, four ventral sacral foramina, and four dorsal sacral foramina (10). Longitudinally, the sacrum exhibits a curvature with a concave ventral (pelvic) surface and a convex dorsal surface.

The term "lumbosacral transitional vertebrae" (LSTV) refers to a vertebra that is either a "sacralized L5" or a "lumbarized S1." We hypothesized that lumbarization results in the sacral concave surface acquiring a convex contour and that the preoperative identification of the anatomical orientation in this region is of increased importance. This mainly radiological and anatomical study aimed to determine the orientation of the S1 vertebral body in the context of sagittal balance assessment and to explore its practical application in identifying sacralized or lumbarized S1 segments as LSTV, to prevent surgical complications.

MATERIAL and METHODS

Subjects

All participants in the study were healthy individuals undergoing medical evaluation as pilot candidates to obtain the required certification for eligibility. Lumbosacral vertebral roentgenograms from 633 outpatients who visited our hospital between June 2018 and August 2018 were retrospectively reviewed by two senior surgeons, each blinded to the other's assessments. These radiographic images were compared with sacral vertebrae classified as anatomically normal, sacralized, or lumbarized. Patients presenting with low back pain, radiculopathy, or both were excluded from the study.

Ethical approval for this study was granted by the Ethics Committee of the University of Health Sciences Türkiye, Diskapi Yildirim Beyazit Training and Research Hospital (March 08, 2021- Approval code: 106/07). Consent was not required because this study involved no human subject.

Imaging Methods

Lumbosacral vertebral roentgenograms were obtained from all subjects. The lumbosacral region was imaged in the "supine" position for both anteroposterior and neutral lateral radiographic views. The L5 and S1 vertebrae were identified by a radiologist. For lateral imaging, the patient was positioned on the table in a lateral decubitus position, with the vertebral column centered on the table. Radiolucent pillows were used, if necessary, to ensure that the vertebral column remained parallel to the table surface. In the digital X-ray system, the central portion of the detector was positioned 6 cm above the iliac crest. The patient's arms were extended forward and placed on either side of the head. Gonadal shielding was applied for male patients. The distance between the X-ray tube and the film was maintained at 100 cm.

Initially, all cases were categorized into three groups by radiologists: a normal group (control), a sacralization group (study group 1), and a lumbarization group (study group 2), based on the type of sacral transition present.

We aimed to propose a new index formula to assist in identifying sacralization or lumbarization. To achieve this, we devised a simple calculation by measuring angles and distances between lines drawn in accordance with sacral anatomy, in order to assess differences between sacralized and lumbarized vertebrae.

Measurement Methods

Anteroposterior and lateral radiographs of the entire spine were obtained from all participants using the standard techniques previously described. All radiographs were interpreted by a single radiologist with 18 years of experience in conventional radiography. Radiographic assessments and morphometric measurements were carried out using a picture archiving and communication system (Extreme PACS, Ankara, Turkey). The initial radiographic evaluation focused on vertebral identification and numbering. The total number of vertebrae was determined by summing the cervical, thoracic, and lumbar segments located above the sacrum. The first seven vertebrae were identified as cervical vertebrae, those bearing ribs directly beneath them were classified as thoracic vertebrae, and the vertebrae without ribs below those were classified as lumbar vertebrae. The first non-rib-bearing vertebra was designated as L1. A fifth lumbar vertebra that displayed characteristics of the adjacent sacral segment was classified as sacralized, whereas a first sacral vertebra showing characteristics of the adjacent lumbar segment was classified as lumbarized. The total vertebral count was documented. Using the lateral projections as the reference standard, we measured the "Anterior Translational Arch (ATA1)" as a distance and the "Anterior Translational Angle (ATA2)" as an angular value.

Measurement method for ATA1

The method for measuring the distance in millimeter (mm) referred to as ATA1 is illustrated in Figure 1. ATA1 represents the distance between the midpoint of the line connecting the anterior margins of the superior end of the first sacral vertebra and the inferior end of the last sacral vertebra (blue line) and the anterior surface of the sacral slope (yellow line) (Figure 1A).

Measurement method for ATA2

The method for measuring the angle in degree (°) (ATA2) is shown in Figure 1A. A transverse line was drawn through the superior endplate of the first sacral vertebra (S1) to identify the midpoint of its anteroposterior dimension (red line). A second line was then drawn from this midpoint to the anterior margin of the inferior end of the last sacral vertebra (green line). The ATA2 angle was defined as the angle formed between the line connecting the anterior margins of the superior end of the first

and the inferior end of the last sacral vertebrae (blue line) and the green line was termed as the ATA2 angle (Figure 1B).

Statistical Analysis

All statistical analyses were performed using SPSS version 22 (IBM Corp., Armonk, NY, USA) and Jamovi version 2.6.22. The Shapiro-Wilk test was employed to assess the normality of data distributions. Group differences were analyzed using the Kruskal-Wallis H test. In cases where the overall test was statistically significant, post hoc pairwise comparisons were conducted using the Dwass-Steel-Critchlow-Fligner method to identify specific group differences. Logistic regression analysis was used to evaluate the association between vertebral variation types (sacralization and lumbarization) and radiographic measurements (ATA1 and ATA2). Since the study cohort consisted exclusively of asymptomatic male patients aged 17-21 years, the models did not include additional covariates such as age or anthropometric variables, to avoid over-adjustment in a demographically homogeneous sample.

When compared with individuals without anatomical variations, the distance value was found to be a statistically significant risk factor in patients with lumbarization or sacralization. In individuals with sacralization, distance values significantly decreased compared to those with normal vertebral anatomy (OR = 0.74; 95% CI: 0.69-0.78), whereas in lumbarization cases, distance values significantly increased (OR = 1.13; 95% CI: 1.06-1.19). ROC analysis was used to identify the optimal cutoff value for the distance measurement based on the x-axis (1-specificity) or y-axis (sensitivity) in relation to the presence of lumbarization or sacralization. A similar ROC analysis was also performed for the "angle measurement" to determine the appropriate cutoff value.

RESULTS

All participants were young males with a mean age of 18.41 years (range 17-21 years) (Table I). None of the subjects were older than 21 years, and none reported back pain, radiculopathy, or both. A total of 527 cases were identified as anatomically normal sacra. On anteroposterior radiographs, 35 cases were confirmed as lumbarization, indicated by the presence of 6 lumbar vertebrae; on lateral lumbosacral radiographs, these cases showed a convex ventral sacral surface. Additionally, 71 cases were confirmed as sacralization, indicated by 6 sacral vertebrae on anteroposterior views and a concave ventral surface on lateral lumbosacral radiographs. These cases were classified as transitional vertebrae.

The mean ATA1 distance was 16.84 mm ± 6.28 in the 527 normal cases (Figure 2A), 4.21 mm ± 5.32 in the 71 sacralization cases (Figure 3A), and 21.17 mm ± 6.68 in the 35 lumbarization cases (Figure 4A). The differences among the three groups were statistically significant ($p < 0.05$). Pairwise comparisons also showed statistically significant differences (sacralization < normal; normal < lumbarization; sacralization < lumbarization; $p < 0.05$) (Table II).

The angle distribution among the 527 patients with normal anatomy was 10.58° ± 1.3 (Figure 2B). In the 71 patients with sacralization, the angle was 8.89° ± 1.13 (Figure 3B). Among the 35 patients with lumbarization, the angle was 9.86° ± 1.76 (Figure 4B). The difference among the three groups was statistically significant ($p < 0.05$). Pairwise comparisons also

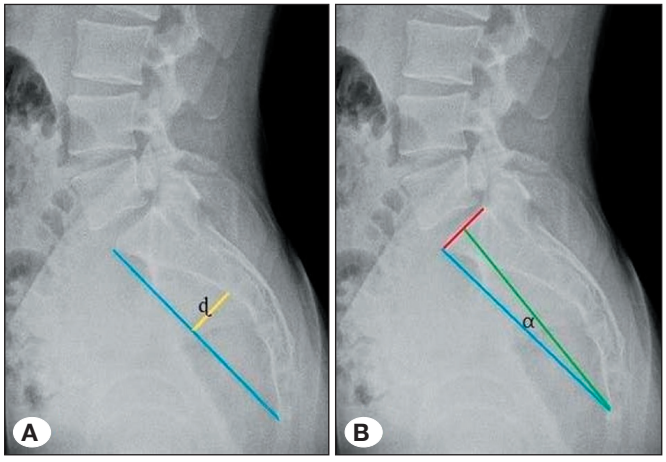

Figure 1: Lateral lumbosacral radiograph demonstrating the measurement methods of "ATA1" distance (d) in "mm" **(A)** and "ATA2" angle (α) in "degree ^{0}" **(B)**.

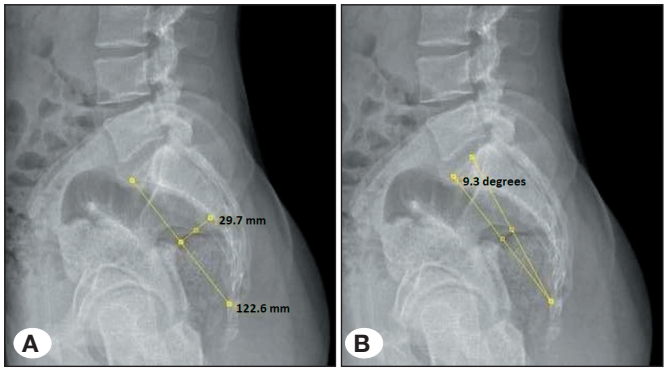

Figure 2: Lateral lumbosacral radiograph of a 20-year-old man with normal alignment of the lumbosacral segments. The measurement of the ATA1 and ATA2 are shown in **(A)** and **(B)**, respectively.

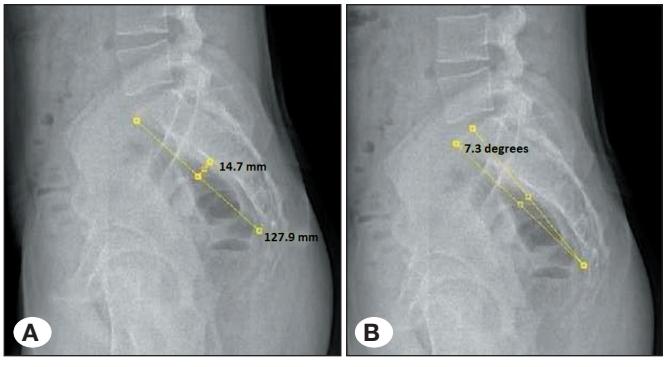

Figure 3: Lateral lumbosacral radiograph of a 20-year-old man with sacralization. The measurement of the ATA1 and ATA2 are shown in **(A)** and **(B)**, respectively.

showed statistically significant differences (sacralization < lumbarization; sacralization < normal; lumbarization < normal; $p < 0.05$) (Table III).

Angle measurements in sacralization cases were significantly lower than in the normal vertebral anatomy group (OR = 0.28; 95% CI: 0.21-0.38), corresponding to an approximately 72% reduction. In lumbarization cases, angle values were also reduced (OR = 0.64; 95% CI: 0.48-0.84), indicating a 36% decrease compared to the normal group. Distance values showed differential patterns: in sacralization, distance decreased (OR = 0.74; 95% CI: 0.69-0.78), reflecting a 26% reduction, whereas in lumbarization, distance increased (OR = 1.13; 95% CI: 1.06-1.19), corresponding to a 13% increase. These results suggest that both distance and angle values are significant predictors of anatomical variation (Table IV).

Table I: The Mean Age of the Cases was 18.41 Years

	Patients' age	
Vertebrae	**Mean (years)**	**Range (years)**
Normal (n=527)	18.46	17-21
Sacralization (n=71)	18.53	17-20
Lumbarization (n=35)	18.25	18-19

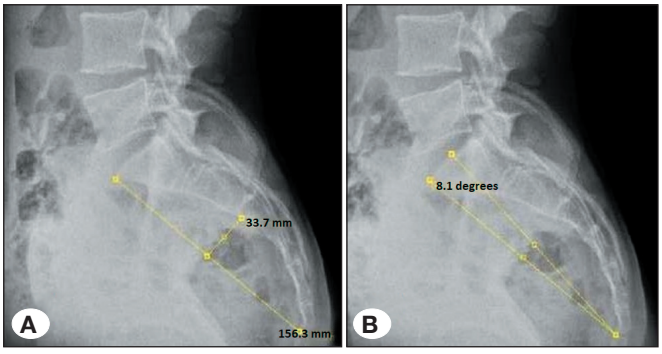

Figure 4: Lateral lumbosacral radiograph of a 19-year-old man with lumbarization. The measure-ment of the ATA1 and ATA2 are shown in **(A)** and **(B)**, respectively.

Table II: The Properties of 633 Cases of Distance Value

ATA1	Vertebrae							
	Normal [1] (n=527)		Sacralization [2] (n=71)		Lumbarization [3] (n=35)		Total (n=633)	
	Mean	**SD**	**Mean**	**SD**	**Mean**	**SD**	**Mean**	**SD**
Distance (mm)	16.84	6.28	4.21	5.32	21.17	6.68	15.66	7.48
p-value (general)	**0.0001* ($p_{1\&2}$<0.001**; $p_{1\&3}$<0.001**; $p_{2\&3}$<0.001**;**							

***ATA1:** Anterior Translational Arch, **SD:** standard deviation, *Kruskal Wallis H Test, ** Dwass-Steel-Critchlow-Fligner*

Table III: The Properties 633 Patients with Angle Values

ATA2	Vertebrae							
	Normal [1] (n=527)		Sacralization [2] (n=71)		Lumbarization [3] (n=35)		Total (n=633)	
	Mean	**SD**	**Mean**	**SD**	**Mean**	**SD**	**Mean**	**SD**
Angle (°)	10.58	1.30	8.89	1.13	9.86	1.76	10.35	1.42
p-value (general)	**0.0001* ($p_{1\&2}$<0.001**; $p_{1\&3}$<0.03**; $p_{2\&3}$<0.01**;**							

***ATA2:** Anterior Translational Angle, **SD:** standard deviation Kruskal Wallis H Test, ** Dwass-Steel-Critchlow-Fligner*

Table IV: Association of Sacralization/Lumbarization with Distance and Angle

					95% Confidence Interval	
Predictor	**Estimate**	**SE**	**p-value**	**Odds ratio**	**Lower**	**Upper**
Distance[1]	-0.30	0.029	**<0.001**	0.74	0.69	0.78
Distance[2]	0.12	0.031	**<0.001**	1.13	1.06	1.19
Angle[1]	-1.27	0.15	**<0.001**	0.28	0.21	0.38
Angle[2]	-0.45	0.15	**0.002**	0.64	0.48	0.84

***SE:** Standard Error, Estimates represent the log odds of comparison: 1 = Sacralization vs. Normal, 2 = Lumbarization vs. Normal.*

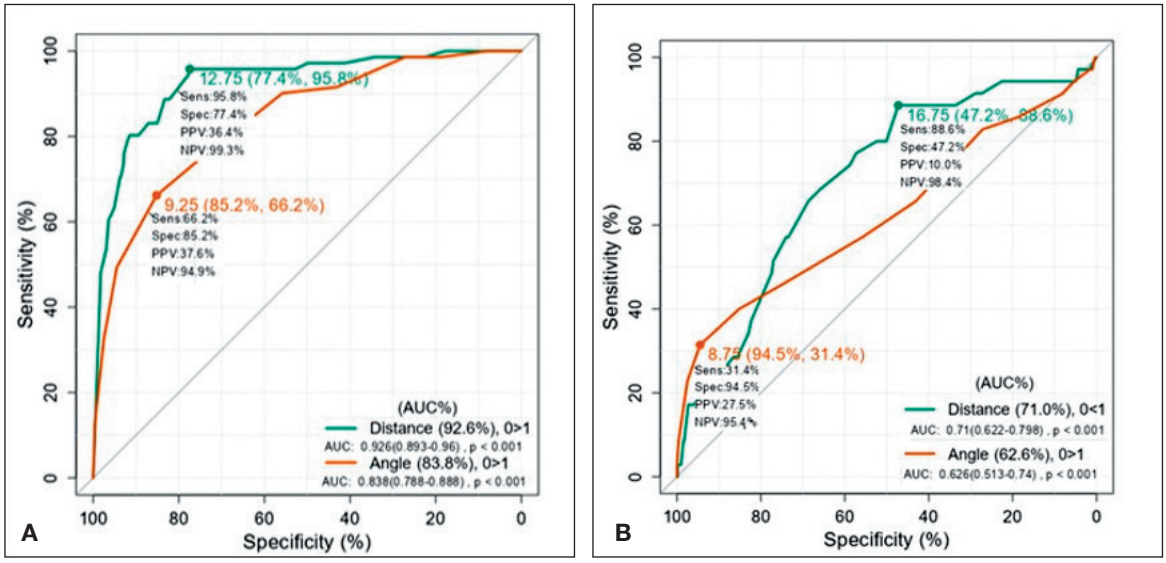

Figure 5: ROC Curves: **A)** sacralization vs. normal; **B)** lumbarization vs. normal.

ROC analysis revealed that distance values had a higher diagnostic accuracy than angle measurements for detecting sacralization (AUC = 0.926) and lumbarization (AUC = 0.710). The optimal cut-off point for distance in sacralization cases was 12.75 mm, with a sensitivity of 95.8% and specificity of 77.4%, while for lumbarization cases, the cut-off was 16.75 mm with moderate sensitivity (47.2%) and high specificity (88.5%) (Figure 5).

DISCUSSION

The sacrum is an anatomically complex and variable structure. Its ventral surface is concave in both vertical and horizontal planes and is smoother compared to the dorsal surface. The first sacral vertebral body is the largest and is most commonly utilized for dorsal or iliosacral screw fixation. A thorough understanding of sacral anatomy is essential for proper lumbosacral orientation and the management of spinal disorders. LSTV are relatively rare in the general population, though in some instances, the condition may be inherited. The relationship between low back pain and the presence of LSTV was initially described by Bertolotti in 1917, and the condition is sometimes termed "Bertolotti's syndrome" (12). This association was later questioned by Elster (4). Nevertheless, subsequent studies have reported a higher-than-expected prevalence of LSTV among patients undergoing imaging for back pain or surgery for a herniated disc (5).

The most reliable method for identifying an LSTV is through lumbosacral radiographs with vertebral counting beginning at the T12 level. However, in cases where MRI is performed without accompanying plain radiographs, careful attention must be paid to the presence of LSTV, and additional knowledge and techniques may be required for accurate identification (6). Correct spinal segmentation is crucial to avoid surgical errors, as the majority of such mistakes have been associated with patients presenting with segmental anomalies, including LSTVs (15). Accurately identifying vertebral levels is essential to localize the pathology precisely and to prevent level-related errors. Lian et al. proposed that whole-spine imaging with caudal counting from C2 represents the gold standard (8). Nonetheless, this approach is often impractical. Frequently, lumbar spine MRI is interpreted without access to plain radiographs, either because they were not performed or are unavailable. There remains no consensus on the definition of LSTV (1). Techniques such as counting from C2 downward, from S5 upward, or using anatomical landmarks like the aortic bifurcation, the right renal artery, and the iliolumbar ligament have been described. However, ATA1 and ATA2 measurements, as introduced in our study, have not been previously evaluated.

Identifying LSTV on MRI can be challenging. When LSTV is suspected, it is important to determine whether it represents a "sacralized L5" or "lumbarized S1." Incorrect identification of disc levels may lead to surgery being performed at the wrong site (9). Zhou et al. examined how variations affect the selection of the sacral endplate in LSTV cases and noted that no standardized approach exists for measuring sagittal alignment in these patients (16).

Additionally, MRI findings have demonstrated that the disc space between an LSTV and the sacrum is significantly narrower than that of a normal lumbosacral intervertebral disc space (11). To address abnormalities associated with lumbarization, it is advisable for patients suspected of having sacral anomalies to undergo an anteroposterior sacral view via conventional radiography, as was done in our study.

Castellvi et al. identified LSTV based on the morphology of the transverse processes (2), while Desmond and Buirski used the presence of disc material on T2-weighted MRI for classification (3). O'Driscoll et al. defined sacral morphology by examining whether residual disc material existed between the uppermost sacral segment (S1) and the rest of the sacrum (12). Hughes and Saifuddin recommended obtaining both

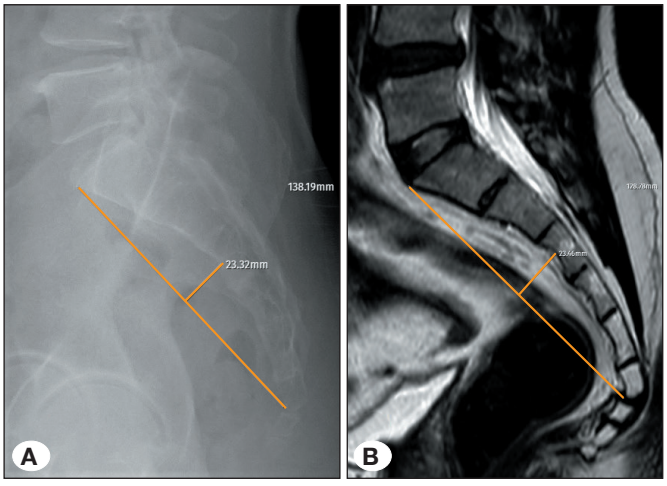

Figure 6: Lateral lumbosacral radiogram **(A)** and T2-weighted magnetic resonance mid-sagittal image of the lumbosacral vertebrae **(B)** of a patient with sacralization. The measurement of the ATA1 on radiograph and magnetic resonance image is shown in **(A)** and **(B)**, respectively.

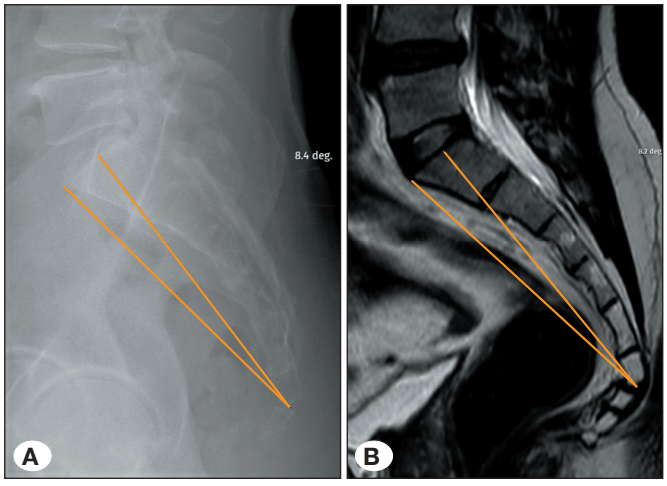

Figure 7: Lateral lumbosacral radiogram **(A)** and T2-weighted magnetic resonance mid-sagittal image of the lumbosacral vertebrae **(B)** of a patient with sacralization. The measurement of the ATA2 on radiograph and magnetic resonance image is shown in **(A)** and **(B)**, respectively.

sagittal MRI and lateral plain radiographs before surgery (7). In the present study, we relied solely on lateral plain radiographs to confirm the presence of LSTV based on observed ventral sacral convexity. While some prefer using sagittal MRI images for straightforward measurements, we believe that X-ray imaging provides clearer visualization of bone structure and definition. However, when we adapted the measurement criteria to MRI, we found that the results were similar to those obtained from plain radiographs (Figure 6,7).

The anatomical reference points used for the new measurement method in this study included the sacral endplate, the midpoint of the anteroposterior dimension of the S1 vertebra, the angle formed by the line connecting the anterior margins of the upper end of the first and the lower end of the last sacral vertebrae, and the anterior longitudinal line of the S1-S5 vertebrae. These landmarks are easily identifiable using fluoroscopy, both before and during surgery. It is proposed that the ATA1 and ATA2 indices could serve as alternatives to conventional reference lines, particularly in situations where identifying the full lateral spine from C2 to S5 is challenging. The clinical reflection of these findings is of great importance in daily practice. Because the effect of providing the general sagittal balance of the spine and restoring lumbar lordosis on surgical outcomes is now accepted by all spine surgeons. Lumbar lordosis is no longer viewed as a static parameter as it once was. Lumbar lordosis is rather a dynamic parameter that can change both the peak and the diameter of the lordosis circle, that is, the characteristic of the lordosis curve, with the number of lumbar vertebrae of the patient, in other words, the presence of lumbarization or sacralization. In addition, the orientation and dome shape of the sacrum are among the parameters that should be taken into consideration in the restoration of lordosis. This condition reveals the importance of considering ATA1 and ATA2 parameters in daily spine surgery practice.

A potential limitation of this method is that image clarity may be compromised in obese patients. The clinical implications of this anatomical and radiologic study are crucial during the preoperative evaluation phase. By design, this is an anatomo-radiologic study proposing practical indicators aimed at preoperative level identification and mitigating wrong-level surgery. Although the study is based on radiologic parameters, it provides a radiologic definition that will minimize potential complications in lumbar surgery. Although there are no direct clinical outcome data, this can be acknowledged briefly as a limitation with a suggestion for future validation studies.

CONCLUSION

The most critical complications when interpreting MRI in patients with LSTV is the possibility of surgery being performed at the wrong spinal level. Furthermore, precise identification and numbering of the thoracolumbar transition vertebrae are essential for the accurate planning of transpedicular stabilization procedures. This underscores the importance of detecting LSTV. In cases where ventral sacral convexity raises suspicion of LSTV, we emphasize the importance of obtaining lateral plain radiographs preoperatively. The ATA1 and ATA2 measurements are simple, practical, and effective tools that may support the development of a clinical consensus. We believe this contribution addresses a critical need in daily surgical practice, particularly given the lack of a widely accepted standard approach. Careful radiological assessment is especially crucial in facilities that do not use neuronavigation and continue to perform stabilization and fusion using the free-hand technique, where this method and its measurements may help avoid numerous surgical errors.

A special tribute is due to someone no longer with us: Mustafa Kemal Ataturk, the founder of the Republic of Türkiye—affec-

tionately remembered as "ATA" by the Turkish people—whose vision made it possible for Türkiye to emerge as a modern nation. If scientific endeavors continue in this country today, it is thanks to the foundation he laid.

ACKNOWLEDGEMENTS

Turkish Neurosurgical Society provided support for the grammatical editing of the manuscript by Enago native speakers.

Declarations

Funding: This research did not receive any specific grant from funding agencies in the public, commercial, or not-for-profit sectors.

Availability of data and materials: The datasets generated and/or analyzed during the current study are available from the corresponding author by reasonable request.

Disclosure: The authors declare no competing interests.

AUTHORSHIP CONTRIBUTION

Study conception and design: CA, AG
Data collection: AG, AE
Analysis and interpretation of results: MO, AMS
Draft manuscript preparation: CA
Critical revision of the article: UE
Other (study supervision, fundings, materials, etc...): n/a
All authors (CA, AG, AE, MO, AMS, UE) reviewed the results and approved the final version of the manuscript.

REFERENCES

1. Bron JL, Van Royen BJ, Wuisman PI: The clinical significance of lumbosacral transitional anomalies. Acta Orthop Belg 73: 687-695, 2007.
2. Castellvi AE, Goldstein LA, Chan DPK: Lumbosacral transitional vertebrae and their relationship with lumbar extradural defects. Spine 9: 493-495, 1984. https://doi.org/10.1097/00007632-198407000-00014.
3. Desmond RM, Buirski G: Magnetic resonance appearances of developmental disc anomalies in the lumbar spine. Australas Radiol 37: 21-29, 1993. https://doi.org/10.1111/j.1440-1673.1993.tb00002.x.
4. Elster AD: Bertolotti's syndrome revisited. Transitional vertebrae of the lumbar spine. Spine 14: 1373-1377, 1989.
5. Hahn PY, Strobel JJ, Hahn FJ: Verification of lumbosacral segments on MR images. Radiology 182: 580-581, 1992. https://doi.org/10.1148/radiology.182.2.1732988.
6. Hughes RJ, Saifuddin A: Imaging of lumbosacral transitional vertebrae. Clin Radiol 59: 984-991, 2004. https://doi.org/10.1016/j.crad.2004.02.019.
7. Hughes RJ, Saifuddin A: Numbering of lumbosacral transitional vertebrae on MRI: role of the iliolumbar ligaments. AJR Am J Roentgenol 187: 59-65, 2006. https://doi.org/10.2214/AJR.05.0415.
8. Lian J, Levine N, Cho W: A review of lumbosacral transitional vertebrae and associated vertebral numeration. European Spine Journal 27: 995-1004, 2018. https://doi.org/10.1007/s00586-018-5554-8.
9. Malanga GA, Cooke PM: Segmental anomaly leading to wrong level disc surgery in cauda equina syndrome. Pain Physician 7: 107-110, 2004.
10. Margaret A, Richard Palmer G: Computed tomography of the sacrum: 1. normal anatomy. AJR Am J Roentgenol 139: 1183-1190, 1982. https://doi.org/10.2214/ajr.139.6.1183.
11. Nicholson AA, Roberts GM: The measured height of the lumbosacral disc in patients with and without transitional vertebrae. Br J Radiol 61: 454-455, 1988. https://doi.org/10.1259/0007-1285-61-726-454.
12. O'Driscoll CM, Irwin A, Saifuddin A: Variations in morphology of the lumbosacral junction on sagittal MRI: correlation with plain radiography. Skeletal Radiol 25: 225-230, 1996. https://doi.org/10.1007/s002560050069.
13. Peleg S, Dar G, Medlej B, Steinberg N, Masharawi Y, Latimer B, Jellema L, Peled N, Arensburg B, Hershkovitz I: Orientation of the human sacrum: anthropological perspectives and methodological approaches. Am J Phys Anthropol 133: 967-977, 2007. https://doi.org/10.1002/ajpa.20599.
14. Peleg S, Dar G, Steinberg N, Masharawi Y, Been E, Abbas J, Hershkovitz I: Sacral orientation and spondylolysis. Spine 34: 906-910, 2009. https://doi.org/10.1097/BRS.0b013e3181b34b75.
15. Wigh RE: The thoracolumbar and lumbosacral transitional junctions. Spine 3: 215-222, 1980. https://doi.org/10.1097/00007632-198005000-00003.
16. Zhou PL, Moon JY, Tishelman JC, Errico TJ, Protopsaltis TS, Passias PG, Buckland AJ: Interpretation of spinal radiographic parameters in patients with transitional lumbosacral vertebrae. Spine Deformity 6: 587-592, 2018. https://doi.org/10.1016/j.jspd.2018.01.004.
17. Xu R, Ebraheim NA, Robke J, Huntoon M, Yeasting RA: Radiologic and anatomic evaluation of the anterior sacral foramens and nerve grooves. Spine 21: 407-410, 1996. https://doi.org/10.1097/00007632-199602150-00001.

Turk Neurosurg 36(3):420-432, 2026
DOI: 10.5137/1019-5149.JTN.49086-25.3

Original Investigation
Spine and Peripheral Nerves

Received: 06.05.2025
Accepted: 06.10.2025
Published Online: 22.05.2026

Lumbar Function and Muscle Preservation Following Hybrid Surgery Versus Selective Thoracic Fusion in Adolescent Idiopathic Scoliosis: A Preliminary Comparative Study

Esin Nur TASDEMIR[1,2], Murat KORKMAZ[3], Gorkem DURAK[4], Sahin KARALAR[5], Turker SAHINKAYA[1], Turgut AKGUL[3], Bulent BAYRAKTAR[1]

[1]Istanbul University, Istanbul Faculty of Medicine, Department of Sports Medicine, Istanbul, Türkiye
[2]Basaksehir Cam and Sakura City Hospital, Department of Sports Medicine, Istanbul, Türkiye
[3]Istanbul University, Istanbul Faculty of Medicine, Department of Orthopedics and Traumatology, Istanbul, Türkiye
[4]Istanbul University, Istanbul Faculty of Medicine, Department of Radiology, Istanbul, Türkiye
[5]Ceylanpinar State Hospital, Department of Orthopedics and Traumatology, Sanliurfa, Türkiye

A version of this study was previously presented as an oral presentation at the XV. International Turkish Spine Congress between 24 -27 May 2023, İzmir, Türkiye

Corresponding author: Esin Nur TASDEMIR ✉ esin.tasdemir@istanbul.edu.tr

ABSTRACT

AIM: To investigate lumbar motion and muscle change following hybrid surgery in adolescent idiopathic scoliosis (AIS).

MATERIAL and METHODS: We conducted a prospective study design including 16 patients (14 female, 2 male) who underwent either hybrid surgery or selective thoracic fusion surgery (STF) for AIS. Trunk extensor and flexor muscle strength and endurance were assessed using an isokinetic dynamometer. Range of motion (ROM) of the lumbar region was measured by a dual inclinometer. Muscle mass was calculated by evaluating the paraspinal muscles at the L2 and L5 vertebral levels in T2W axial sections of the magnetic resonance imagings. The degree of fatty degeneration was assessed by the Goutallier classification.

RESULTS: The hybrid group comprised eight female patients with a mean surgical age of 14±1.7 years and a mean follow-up time of 16.4±8.8 months. The STF group included eight patients (six females, two males) with a mean surgical age of 14.6±1.8 and a mean follow-up time of 29.5±15.4 months were included. No significant difference was observed between the lumbar ROM, trunk flexion–extension strength, and endurance ($p>0.05$) of both groups. Similarly, no significant difference was observed between the paraspinal muscle cross-sectional area and the degrees of fatty degeneration in the patient's preoperative and last follow-up. Moreover, no differences were observed in the overall Scoliosis Research Society-22 scores between the two groups ($p=0.442$).

CONCLUSION: These preliminary findings show that hybrid surgery preserves lumbar motion and does not cause iatrogenic damage to the paraspinal muscles, including the psoas major.

KEYWORDS: Vertebral body tethering, Selective thoracic fusion, Hybrid, motion-preserving surgery, Cross-sectional area

ABBREVIATIONS: VBT: Vertebral body tethering; **PSF:** Posterior spinal fusion; **AIS:** Adolescent idiopathic scoliosis; **STF:** Selective thoracic fusion surgery; **ROM:** Range of motion; **LIV:** Lowest instrumented vertebra; **MRI:** Magnetic resonance imaging; **ODI:** Oswestry Disability Index; **CSA:** Cross-sectional area; **CVMI:** Cervical vertebral maturity index; **SRS-22:** Scoliosis Research Society-22; **CI:** Confidence interval

Esin Nur TASDEMIR : 0000-0002-3814-286X
Murat KORKMAZ : 0000-0003-2809-6721
Gorkem DURAK : 0000-0002-1608-1955
Sahin KARALAR : 0000-0002-4386-9107
Turker SAHINKAYA : 0000-0003-1466-381X
Turgut AKGUL : 0000-0002-0704-3797
Bulent BAYRAKTAR : 0000-0001-8102-4896

INTRODUCTION

Fusion surgery with posterior instrumentation is the gold-standard surgical method for treating adolescent idiopathic scoliosis (AIS), demonstrating low complication rates and successful radiological results (14). Despite these advantages, long-term problems related to fusion surgery may occur (20). These negative effects are more common when the mobile lumbar region is included in the fusion area (22,31). Selective fusions reduce the fusion level, thereby preserving lumbar mobility as much as possible. In selective fusion, fusion surgery is applied to the major curves, while the other curves are left to resolve spontaneously (17). However, this technique carries the risk of estimating the residual deformity or adding to the existing deformity.

Non-fusion methods for controlling the curvature in AIS avoid fusion surgery problems. Some of these methods are growth-friendly approaches applied until bone maturation is achieved and ultimately result in fusion (9). Vertebral body tethering (VBT) allows both spine movement and keeps the curvature under control. It is described as a promising method in preadolescent patients (7,10). After the successful results obtained in studies on pigs, numerous case series regarding VBT were published. While VBT is a safe and effective treatment for thoracic and thoracolumbar idiopathic scoliosis based on approximately a decade of experience, researchers have raised concerns regarding the challenges in curve control post-VBT, including tether overcorrection and breakage, leading to elevated reoperation rates (15,33,34).

While VBT was initially described as a motion-preserving technique for skeletally immature patients with growth potential, recent reports indicated that its use gradually expanded to include skeletally mature adolescents and even selected adult cases, particularly for the lumbar curves. Consequently, hybrid systems incorporating posterior spinal fusion (PSF) for the less mobile thoracic region and VBT for the lumbar spine have recently emerged. This novel system allows for excellent three-dimensional (3D) correction in the thoracic region with PSF while preserving relative mobility in the lumbar segments with VBT (5).

The most important advantage of VBT over fusion surgery is the preservation of the arc of motion. Another advantage of VBT is its minimally invasive nature that reduces the risk of injury to the posterior paraspinal muscles (16). However, during anterior vertebral surgery (e.g., VBT), the psoas muscle, which is a large muscle located on either side of the spine in the lower back, may be affected (8). In clinical studies that evaluated the VBT results for the thoracic region, the thoracic region's mobility was preserved (28). Another study applied double-sided VBT and showed that the arc of motion was better compared to fusion surgery (29). However, no study has yet been conducted to evaluate the lumbar muscle structure and the range of motion (ROM) in patients undergoing a hybrid procedure.

The primary objective of this study is the comparison of the qualities of life, trunk muscle strengths and endurance, and ROM in the lumbar region between two groups of patients with AIS. One group underwent selective thoracic fusion surgery (STF), a known technique for preserving the lumbar ROM, while the other underwent a hybrid procedure. Our secondary objective is the investigation of the effects of the hybrid procedure on the paraspinal muscle morphology.

MATERIAL and METHODS

Study Design and Sample

This work is a case–control study. The literature provides no clear information regarding the sample size of our study; therefore, the sample size cannot be calculated. The study population comprised patients who underwent surgery at our center between 2021 and 2023. Patients who underwent hybrid surgery with a minimum follow-up of 1 year were included. Lenke 1C, 3C, 5C, and 6C patients were included in the hybrid group. The lowest instrumented vertebra (LIV) above L3 was excluded because it was intended to study the effect of VBT on the lumbar region. Patients with a history of previous spinal surgery or spondylolisthesis were excluded, considering that these conditions could affect the quality of life and functional outcomes. We compared the outcomes of the VBT group by selecting an age–gender and minimum follow-up duration-matched STF group from the cases operated in the same institution by the same surgical team. Lenke 1B and 1C patients were included in the STF group (Figure 1).

Patient Selection Criteria

The patient selection for STF in our center was based on the Moe criteria. STF was recommended in cases with a thoracic-to-lumbar (T/L) apical vertebral translation ratio greater than 1.2, thoracic apical rotation exceeding 20°, and a T/L Cobb angle ratio above 1.2 in the absence of thoracolumbar junctional kyphosis. Currently, there is no consensus in the literature regarding lumbar VBT indications. In our practice, VBT was considered as a lumbar fusion alternative when the lumbar deformity was flexible. The radiological criteria included a lumbar Cobb angle below 60° with at least 50% correction on the side-bending radiographs. The patient's preference and expectations also played a significant role in the treatment decision. Hybrid surgery was generally performed in patients who were unwilling to accept residual lumbar asymmetry following STF. All patients and families were informed about the potential complications and limitations of each technique. The treatment allocation was finalized through a shared decision-making process (Figure 1).

Surgical Technique

The intraoperative objective of the STF group was to achieve a residual main thoracic curve of ≤10–15° on coronal fluoroscopy while maintaining overall coronal and sagittal alignment. A correction was performed using a combination of rod derotation, segmental translation, and compression–distraction maneuvers, giving particular attention to preserving the lumbar curve flexibility and preventing a junctional malalignment. The instrumentation levels for VBT were selected as "Cobb-to-Cobb." In the hybrid group, lumbar VBT was performed first in the lateral decubitus position, followed by posterior thoracic fusion. The intraoperative aim was to achieve the maximum Cobb angle correction. A reduction to less than 10° was ob-

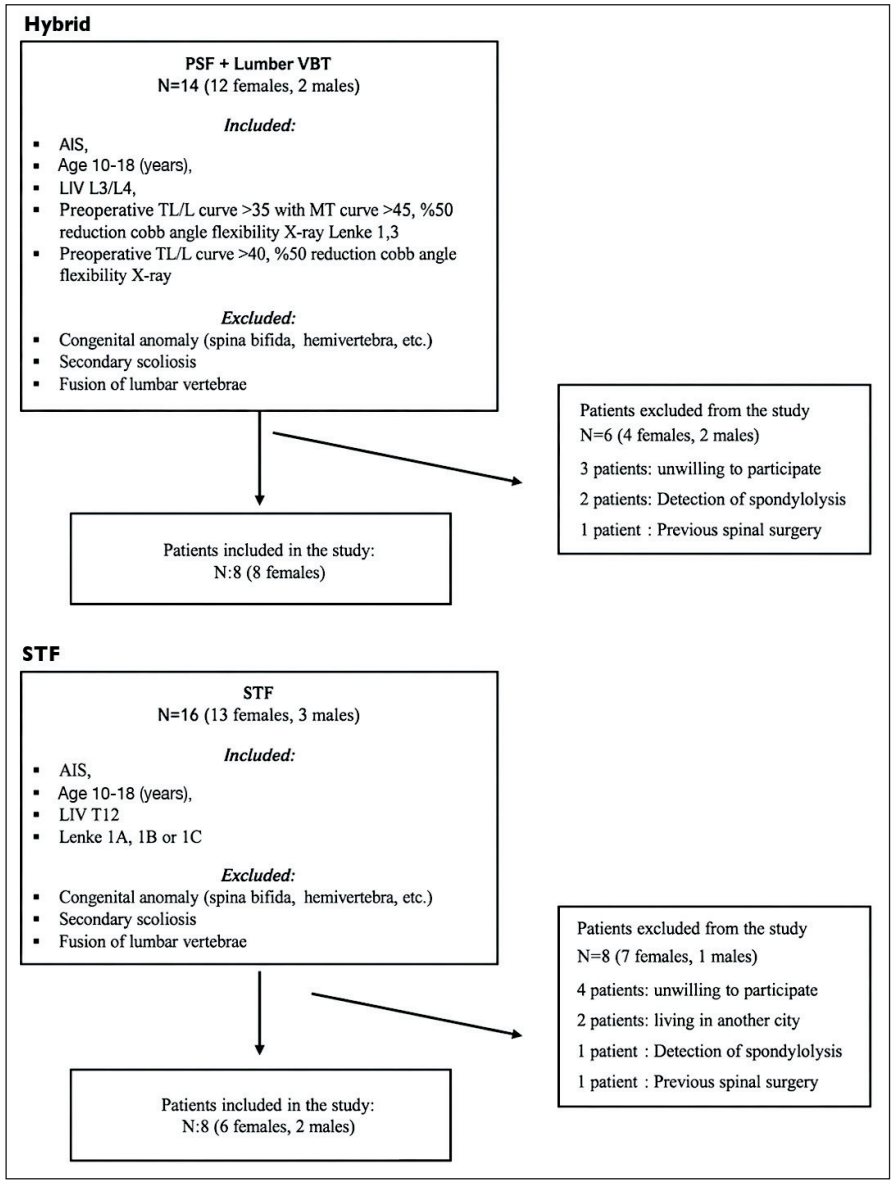

Figure 1: Study population flowchart.

PSF: posterior spinal fusion, **VBT:** vertebral body tethering, **AIS:** adolescent idiopathic scoliosis, **LIV:** lowest instrumented vertebra,**TL:** thoracolumbar, **L:** lumbar, **MT:** main thoracic, **STF:** selective thoracic fusion surgery

tained in the lateral decubitus position of all patients before proceeding to posterior instrumentation.

A single cord and one screw per vertebra were used in the first three hybrid cases. Based on the evolving literature and surgical experience, our routine technique was subsequently modified to employ a double screw–double tether configuration for each level, except for the cranial transitional vertebra. As stated, the instrumentation levels were generally selected from Cobb-to-Cobb. For STF, the LIV was chosen as the neutral and stable vertebra as defined by the central sacral vertical line. One anterior screw and two posterior pedicle screws were typically applied at the transitional vertebra.

Ethical Considerations and Data Collection

Our study was approved by the Ethics Committee of Istanbul University, Istanbul Faculty of Medicine (No: IU2022/272). All procedures were conducted in accordance with the Declaration of Helsinki. The trial was registered at ClinicalTrials.gov (NCT05347056; registration date: April 26, 2022). Following ethical approval, follow-up magnetic resonance imaging (MRI) scans were conducted during the patients' first year after surgery or at subsequent visits, contingent upon the consent of both patients and parents for their participation in this work. Written informed consent was obtained from all the participants and their parents. The data collection for the clinical outcome measures was performed prospectively as patients applied.

Outcome Measures

Clinical Evaluation

The Scoliosis Research Society-22 (SRS-22) and the Oswestry Disability Index (ODI) questionnaires were used to evaluate the clinical quality of life and the functional outcomes of the patients included in this study. The clinical measure-

ments were made by an experienced sports physician using an isokinetic dynamometer and a dual inclinometer. The "Cybex Norm" (CSMI, Stoughton, MA, USA) isokinetic dynamometer was used to evaluate the trunk extensor and flexor muscle strengths and endurance (17,24). The measurements were taken at –10° to 45° joint ROM for the trunk and at 60°/s (strength) and 120°/s angular velocities (endurance). From the results obtained, the peak torque and peak torque values per kg at 60 and 120°/s were evaluated for both flexion and extension.

The lumbar region ROM was measured using a dual inclinometer (Acumar, Lafayette Instrument, Lafayette, IN, USA). During the measurements, the main inclinometer unit was placed in the T12 spinous process. The auxiliary unit was placed in the S1 spinous process (11) (Figure 2). The patients were asked to stand upright while the flexion and the extension were measured. For the flexion measurement, the patients were asked to bend forward as far as they could without bending their knees. For the extension measurement, the patients were asked to take their trunk as far as possible from the neutral position without bending their knees. For the right–left lateral flexion measurements, the patients were asked to bend sideways without lifting their feet from the ground or leaning forward while standing upright. For the rotation measurements, the patients were asked to bend forward 90° without bending their knees. An inclinometer was placed at the previously mentioned reference points. The patients were then asked to rotate left and right.

Radiological Evaluation

The curvatures were measured by an experienced spinal surgeon who used the Cobb method and Surgimap software in all spinal anterior–posterior and lateral radiographs that were taken preoperatively, first erect and at last follow-up. The skeletal maturity in both groups was assessed through Risser staging. In addition, the cervical vertebral maturity index (CVMI) and the triradiate cartilage status were evaluated.

For the evaluation of paravertebral muscle changes, preoperative MRI and postoperative MRI with metallic artifact suppression sequence (Metal Artifact Reduction Software)

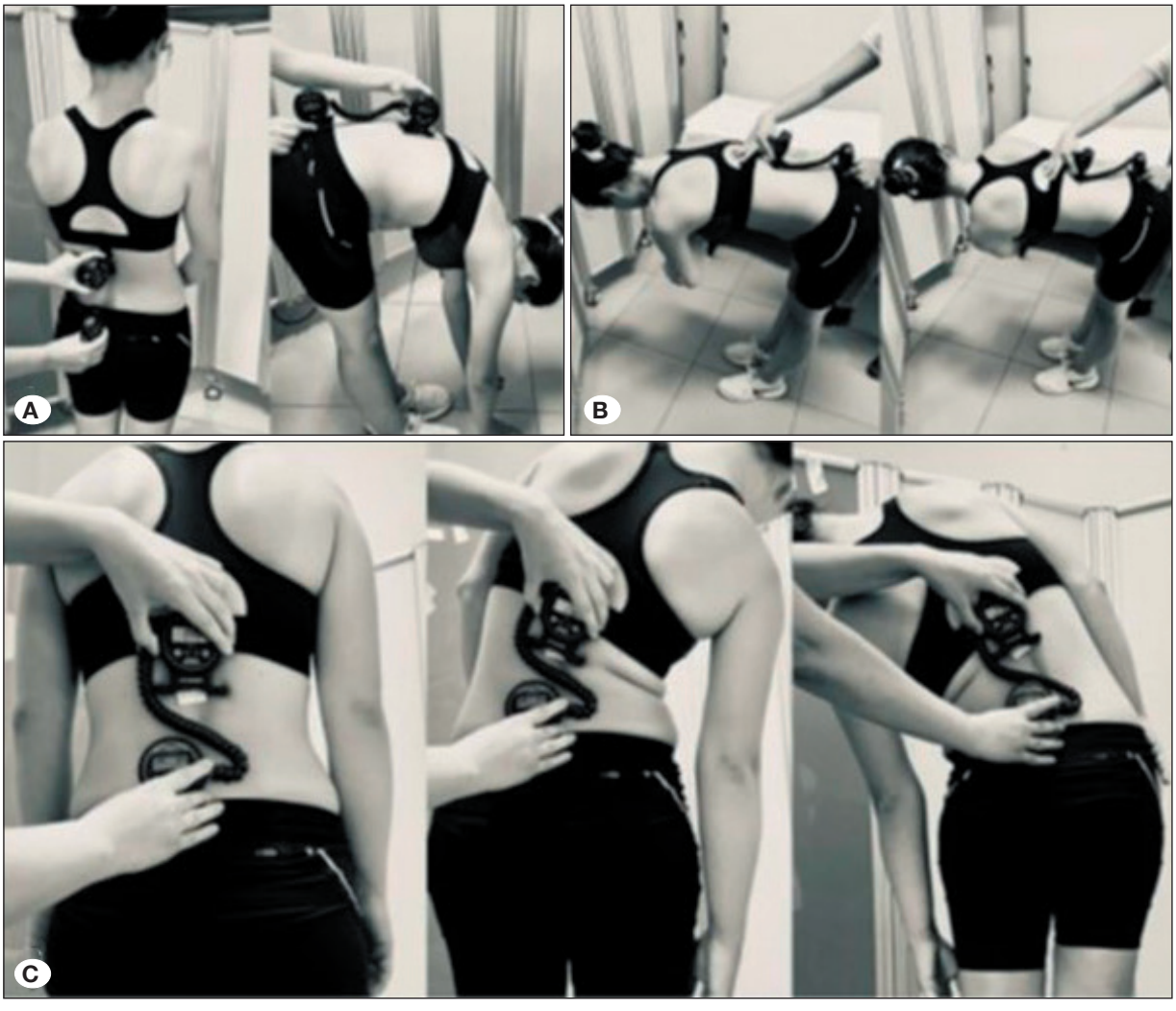

Figure 2: Lumbar spinal motion measurements using an inclinometer: **A)** flexion, **B)** rotation, and **C)** lateral flexion.

were used. The cross-sectional areas (CSAs) of the individual paraspinal muscles (i.e., multifidus, erector spinae, and psoas major) were evaluated on the T2A axial sectional images from the L2 and L5 vertebral corpus plateau superior (Figure 3). At the same time, the CSAs of the vertebral corpus were measured. We analyzed the CSA ratio to reduce the bias arising from the differences in individual body size, disk pathology, and potential patient growth during the follow-up period. This was performed by comparing the sizes of each muscle to the vertebral body (individual muscle CSA/vertebral body CSA) and expressing it as a percentage. The muscle and vertebrae corpus contours were carefully outlined. Their areas were measured independently by two musculoskeletal radiologists. The CSAs were measured in mm^2 using Extreme PACS Client (Ankara, Turkey). The Goutallier classification was employed to evaluate the degree of fatty degeneration in the lumbar region muscles (Grade 0: no fat; Grade 1: fatty streaks; Grade 2: muscle > fat; Grade 3: muscle=fat; and Grade 4: muscle < fat) (4).

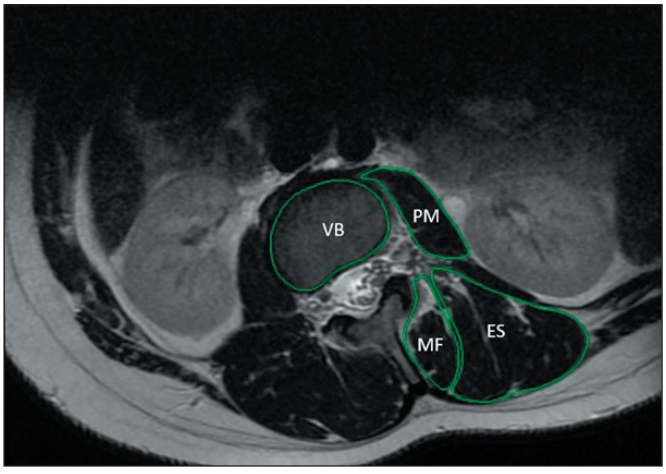

Figure 3: Measurements of the vertebrae body (VB) and the muscle cross-sectional area (CSA). CSA measurements comprised the psoas major (PM), erector spinae (ES), and multifidus (MF).

Statistical Analysis

The Shapiro–Wilk test was used to assess the normality of continuous data, confirming that the normality assumption was met. The chi-square test was performed to compare the categorical data and treatment methods. Independent sample *t*-test was used to compare the continuous data and treatment methods. The repeated measures analysis of variance was used to compare the differentiations of the presurgical post-control change between the surgical treatment methods. The McNemar chi-square test was employed to evaluate the categorical differences before the surgery post-control. The statistical significance level (α) was determined as 0.05 ($P < 0.05$). In addition to the statistical significance, 95% confidence intervals (CIs) were calculated. The clinical relevance was assessed by using the effect size analyses (Hedges' *g*) for key outcomes, including Cobb angles, lumbar ROM, and isokinetic trunk muscle strength. All statistical tests were performed using SPSS software for Windows version 12.0 (SPSS, Chicago, IL, USA).

RESULTS

Eight female patients with a mean surgical age of 14±1.7 and a mean follow-up time of 16.4±8.8 months were included in the hybrid group (Table I, Supplementary Table I). The most proximal and distal VBT instrumentation levels were T12 and L4, respectively. The hybrid group included five patients with Lenke 1C curvature and one patient with Lenke 3C, 5C, and 6 curvatures. An average of 3.7 (3–4) tethering levels was applied to the patients. All eight patients showed a left thoracolumbar/lumbar curvature. The VBT intervention was performed from the left anterolateral. The preoperative main thoracic curvature Cobb angle was 51°±6°, whereas the thoracolumbar/lumbar curvature Cobb angle was 46°±5°. The last follow-up thoracic curvature Cobb angle was 10°±6°, whereas the thoracolumbar/lumbar curvature Cobb angle was 11°±5° (Table I; Figure 4). The postoperative "first erect" radiographs were available for all patients. In the hybrid group, the mean thoracic curve changed by 4°±3°, and the lumbar curve changed by 2°±4° between the first erect and final follow-up. No complications

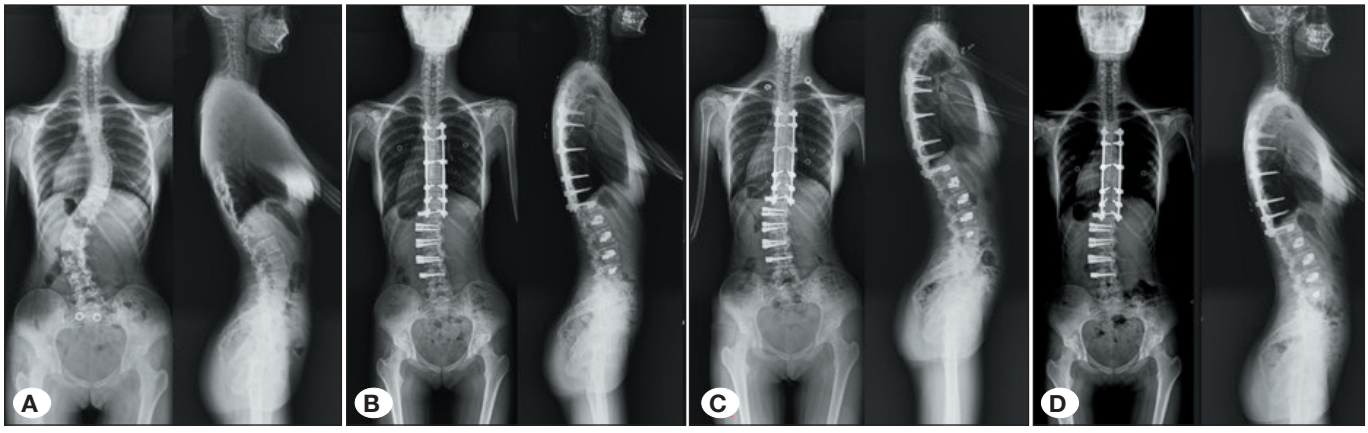

Figure 4: A) Preoperative, **B)** first erect, **C)** 6-month, and **D)** last follow-up standing anteroposterior and lateral orthoroentgenograms of an adolescent idiopathic scoliosis patient undergoing treatment for hybrid surgery.

Table I: Demographic and Radiographic Data of the Study Population

	Hybrid (n=8)	STF (n=8)	p-value	Hedges' g	95% CI
Follow-up, Mean±SD (months)	16.4±8.8	29.5±15.4	0.065		
Female Sex, n (%)	8 (100.00)	6 (75.00)			
Age, Mean±SD (years)	14 ±1.7	14.6±1.8	0.442		
Risser Score, Median (Range)	4 (0-5)	4 (2-5)			
Triradiate cartilage closed, n (%)	8 (100)	8 (100)			
CVMI Score, Median (Range)	5 (2-6)	5 (3-6)			
Lenke Classification					
1A n (%)	-	4 (50.0)			
1B n (%)	-	2 (25.0)			
1C n (%)	5 (62.5)	2 (25.0)			
3C n (%)	1 (12.5)				
5C n (%)	1 (12.5)	-			
6C n (%)	1 (12.5)	-			
Levels Tethered, Median (Range)	3.7 (3-4)	-			
Levels Fusion, Median (Range)	7.1 (6-10)	9.5 (8-10)			
LIV					
L3 n (%)	6 (75.0)	-			
L4 n (%)	2 (25.0)	-			
T12 n (%)	-	8 (100.0)			
Preoperative MT curve$^{\Phi}$ Mean±SD (Range)	51±6 (41-62)	51±10 (40-68)	0.872	0.00	[-0.98, 0.98]
First erect MT curve$^{\Phi}$ Mean±SD (Range)	8±3 (4-12)	11±4 (6-20)	0.109	–0.81	[–1.83, +0.22]
Last follow-up MT curve$^{\Phi}$ Mean±SD (Range)	10±6 (3-20)	14±7 (5-26)	0.727	-0.58	[-1.583, 0.423]
Change in MT curve$^{\Phi}$ (First erect – Last follow-up) Mean±SD (Range)	4±3	3±3	0.871	0.32	[–0.67, +1.31]
Preoperative L/TL curve$^{\Phi}$ Mean±SD (Range)	46±5 (38-51)	35±8 (29-50)	**0.027***	1.56	[0.422, 2.697]
First erect L/TL curve$^{\Phi}$ Mean±SD (Range)	9±3 (6-14)	12±8 (1-28)	0.351	–0.46	[–1.45, +0.54]
Last follow-up L/TL curve$^{\Phi}$ Mean±SD (Range)	11±5 (1-18)	13±10 (0-27)	0.952	-0.24	[-1.223, 0.745]
Change in L/TL curve$^{\Phi}$ (First erect – Last follow-up) Mean±SD (Range)	2±4	1±5	0.670	**0.21**	[–0.77, +1.19]

***n:** number, **SD:** standard deviation, **LIV:** lower instrumented vertebra, **MT:** main thoracic, **TL/L:** thoracolumbar/lumbar, **CVMI:** Cervical Vertebral Maturity Index. $^{\Phi}$degree, cobb angle magnitude, * p<0.05*

related to rod rupture or surgical access were observed. However, one patient's curve showed an overcorrection in the last 6 months after completing measurements for the study, and the tether was cut with revision surgery. All clinical, radiological, and MRI assessments were completed before the revision; therefore, the analyses of paraspinal muscle CSA and fatty degeneration for this patient reflected the pre-revision state. No post-revision measurements were included.

Eight patients (six females, two males) with a mean surgical age of 14.6±1.8 and a mean follow-up period of 29.5±15.4 months were included in the STF group (Table I, Supplementary Table I). The most proximal and distal fusion levels were T2 and T12, respectively. All patients in the STF group exhibited a Lenke 1B or 1C curvature. An average of 9.5 fusion levels (8–10) was applied to the patients. The preoperative main thoracic curvature Cobb angle was 49.8°±10°. The thoracolumbar/lumbar curvature Cobb angle was 35.5°±8°. The last follow-up thoracic curvature Cobb angle was 14.1°±7°. The thoracolumbar/lumbar curvature Cobb angle was 12.8°±10°. The corresponding changes in the STF group were 3°±3° for the thoracic curve and 1°±5° for the lumbar curve. No statistically and clinically significant differences were observed between the two groups in terms of the mean age at surgery (p=0.442), mean follow-up time (p=0.065), preoperative main thoracic curve Cobb angle (p=0.872), last control thoracic curve Cobb angle (p=0.727), last follow-up thoracolumbar/lumbar curvature Cobb angle (p=0.952), or the changes in the thoracic (p=0.871) and thoracolumbar/lumbar curves (p=0.670)

between the first erect and the last follow-up. The preoperative thoracolumbar/lumbar curvature Cobb angle was significantly higher in the hybrid group than that in the STF group (p=0.027). The effect size was large (Hedges' *g*=1.56, 95% CI: 0.42–2.69), indicating a clinically meaningful baseline difference between the groups (Table I; Figure 4).

Among the groups, no differences were found in the SRS-22 sub-scores (pain [p=0.328], self-image/view [p=0.442], function/activity [p=0.645], mental health [p=0.234], and treatment satisfaction [p=1.000]) and total scores (p=0.442) (Table II).

Table II: Last Follow-Up Scoliosis Research Society-22r Questionnaire (SRS-22r), VAS, ODI Scores, and Early Clinical Parameters

Parameter	Hybrid	STF	p-value
SRS22 Pain (Mean±SD)	4.4±0.65	4.1±0.62	0.328
SRS22 SI (Mean±SD)	3.9±0.70	3.6±0.73	0.442
SRS22 Function (Mean±SD)	4.6±0.25	4.4±0.45	0.645
SRS22 MH (Mean±SD)	3.6±0.91	3.3±0.65	0.234
SRS22 Satisfaction (Mean±SD)	4.1±1.01	4.2±0.7	1.000
SRS22 Total (Mean±SD)	4.1±0.59	3.9±0.47	0.442
VAS Mean (Min-Max)	1.3 (0-4)	1.2 (0-5)	0.959
ODI Mean (Min-Max)	6.1 (0-11.1)	7.6 (2-15.5)	0.442
Length of stay (days)	4.1±1.1	3.8±0.7	0.441
Return to school (days)	24.5±2.7	23.8±1.4	0.497

***SI:** self-image, **MH:** mental-health, **SD:** standard deviation, **VAS:** visual analogue scale, **ODI:** Oswestry disability index, **STF:** selective thoracic fusion surgery.*

Additionally, no significant differences were found between the two groups in terms of the VAS (p=0.959) and ODI scores (p=0.442) (Table II). Moreover, no significant differences were observed between the two groups regarding hospital stay duration (4.1±1.1 vs. 3.8±0.7 days; p=0.441) or return-to-school time (24.5±2.7 vs. 23.8±1.4 days; p=0.497). In other words, the addition of lumbar VBT to STF did not prolong early postoperative recovery. Six of the patients in the VBT group stated they experienced anterior thigh pain or hip flexor weakness in the postoperative period. Only one patient stated that hip flexor weakness continued at the last follow-up (Table III). All participants had an ODI score of 20 or below.

Meanwhile, the hybrid group showed a lumbar flexion of 56.1°±5.18° and an extension of 22.1°±4.31°. The right and left lateral flexions were 17.9°±1.62° and 19.7°±1.82°, respectively. The right and left rotations were 7.2°±3.15° and 6.7°±3.52°, respectively. The SFT group depicted a lumbar flexion of 55.3°±3.67° and an extension of 22.5°±3.96°. The right and left lateral flexions were 19.7°±2.42° and 19.9°±2.66°, respectively. The right and left rotations were 7.2°±3.15° and 7.1°±3.80°, respectively. No statistically and clinically significant differences were found in these values between the two groups (p>0.05) (Table IV).

Based on the isokinetic strength test findings, the effect size analyses revealed small to moderate values (Hedges' *g*=0.2–0.7) for the strength and endurance measures. In line with the non-significant p values (p>0.05), the differences between the groups were not clinically meaningful (Supplementary Table II).

No significant difference was observed between the CSA ratio and the fatty degeneration of the multifidus, erector spinae, and psoas muscles before and after surgery in both groups (Tables V–VII).

Table III: Complication Rates of the Study Groups

Complication	Hybrid (n=8) n (%)	STF (n=8) n (%)
Transient neurological symptoms (anterior thigh pain / hip flexor weakness)	6 (75.0)	0 (0)
Persistent neurological symptoms	1 (12.5)	0 (0)
Overcorrection	1 (12.5)	0 (0)
Rod breakage	0 (0)	0 (0)

Table IV: Data Regarding Lumbar Range of Motion

	Hybrid (Mean±SD)	STF (Mean±SD)	p-value	Hedges' g	95% CI
Flexion	56.1±5.18	55.3±3.67	0.328	+0.17	[–0.81, 1.15]
Extension	22.1±4.31	22.5±3.96	0.878	–0.09	[–1.07, 0.89]
Lateral Bending (right)	17.9±1.62	19.7±2.42	0.105	-0.83	[–1.85, 0.20]
Lateral Bending (left)	19.7±1.82	19.9±2.66	1.000	–0.08	[–1.06, 0.90]
Rotation (right)	7.2±3.15	7.2±1.68	0.442	0.00	[–0.98, 0.98]
Rotation (left)	7.1±3.80	7.5±1.62	0.279	-0.13	[–1.11, 0.85]

***SD:** standard deviation, **STF:** selective thoracic fusion surgery.*

Table V: Cross-Sectional Areas of the Paraspinal Muscles at Each L2 Vertebra Level

	Preoperative Hybrid Mean±SD	Last Follow Up Hybrid Mean±SD	p-value	Preoperative STF Mean±SD	Last Follow Up STF Mean±SD	p-value
L2 Multifidus CSA ratio (%)						
Right	23.3±5.4	23.3±5.4	0.202	26.6±5.1	26.6±5.1	0.696
Left	23.8±4.7	25.1±3.3	0.325	26.4±4.4	26.4±4.3	0.754
L2 Erector spina CSA ratio (%)						
Right	128.7±45.3	128.7±45.3	0.450	142.8±34.3	142.9±34.2	0.315
Left	130.4±47.5	130.5±47.5	0.743	139.8±29	142.8±33.6	0.367
L2 Psoas major CSA ratio (%)						
Right	33.7±11.3	33.7±11.3	0.144	33.4±9.1	33.3±9.1	0.403
Left	32.6±9.6	32.6±9.6	0.089	34.5±7.8	34.8±7.9	0.170

SD: *standard deviation*

Table VI: Cross-Sectional Areas of the Paraspinal Muscles at Each L5 Vertebra Level

	Preoperative Hybrid Mean±SD	Last Follow Up Hybrid Mean±SD	p-value	Preoperative STF Mean±SD	Last Follow Up STF Mean±SD	p-value
L5 Multifidus CSA ratio (%)						
Right	59.2±5.8	59.2±5.8	0.341	61.5±3.8	61.6±3.8	0.710
Left	60.5±6.4	60.6±6.4	0.142	61.4±4.3	61.5±4.2	0.707
L5 Erector spina CSA ratio (%)						
Right	68.7±17.3	69.6±17.0	0.341	84.7±13.4	84.8±13.6	0.754
Left	68.2±15.8	68.2±15.8	0.696	83.0±12.9	83.1±13.0	0.792
L5 Psoas major CSA ratio (%)						
Right	70.9±14.7	70.9±14.7	0.244	80.9±12.0	80.9±11.7	0.877
Left	70.2±4.5	70.2±4.5	0.476	85.2±19.0	85.3±18.8	0.734

SD: *standard deviation*

Table VII: Preoperative and Last Follow-Up Fatty Atrophy of The Paraspinal Muscles According to The Goutallier Classification

	Preoperative Hybrid Goutallier Grade 1* (%)	Last Follow Up Hybrid Goutallier Grade 1* (%)	Preoperative STF Goutallier Grade 1* (%)	Last Follow Up STF Goutallier Grade 1* (%)
Multifidus				
Right	25	25	37.5	37.5
Left	25	25	37.5	37.5
Erector spina				
Right	25	25	37.5	37.5
Left	25	25	37.5	37.5
Psoas major				
Right	0	0	0	0
Left	0	0	0	0

**None of the muscles had atrophy higher than Goutallier Grade 1.*

DISCUSSION

Anterior VBT is a surgical technique that has become popular in recent years because it is thought to prevent the functional complications caused by spinal fusion (30). Although VBT is recommended in patients with growth potential, its use in adult patients has also been increasing (3). With the VBT technique, contrary to the fusion technique, the biomechanics of the spinal functional unit, which is the smallest functional unit of the vertebral column, are preserved. Iatrogenic damage to the posterior paraspinal muscles is also thought to be minimized by anterolateral intervention instead of posterior surgery. Therefore, the ideal realization of movement and load distribution (shock absorption), which are the main functions of the vertebral column, can be ensured. Furthermore, the development of the adjacent segment disease can hopefully be prevented in the long term.

As the tethering technology advances, surgeons are facing the challenge of balancing the advantages of motion preservation against the potential for increased complications or the need for further surgery (5). In VBT, the primary complications include tether breakages and overcorrection. In contrast, these issues are not observed in the PSF group. The tether breakage risk is increased in cases involving larger, lumbar, and rigid curves (2). In addition to these clinical considerations, note that VBT generally requires a longer operative time, additional operating room resources, and a specialized instrumentation system that is more costly than conventional fusion implants. These factors may increase the institutional resource utilization compared with PSF and must be considered during treatment planning.

STF is a surgical method frequently used in patients with major thoracic curvature. Its long-term results are known. The quality of life of patients who underwent STF is similar to that of the normal population, even years after surgery (12). Although some residual lumbar curvature can be found in these patients, balanced and acceptable coronal curvatures do not have a negative effect on the daily life of the patients. Moreover, the preservation of the lumbar region's arc of motion (lumbar functional units) is clinically important in the long term (25).

In patients who do not meet the selective thoracic fusion criteria and require inclusion of both the lumbar and thoracic regions in the surgical field, the hybrid procedure may offer the combined benefits of rigid fixation and motion preservation while potentially reducing the likelihood of complications and the need for reoperation. Consistent with this approach, in our series, hybrid surgery was mainly applied in cases where STF was not feasible, prioritizing lumbar motion preservation and curve correction by intraoperative techniques rather than growth modulation. Furthermore, hybrid surgery was particularly recommended in patients who were unwilling to accept residual lumbar asymmetry or deformity. Patient preference played an important role in the decision-making process. In our center, costs of both STF and hybrid surgery are fully covered by the state health insurance system; therefore, financial considerations did not influence patient preference.

This study aimed to evaluate the effect of adding lumbar VBT to selective thoracic fusion on the quality of life and the lumbar region. We performed the evaluation on patients undergoing STF and who exhibited similar lumbar curves to reduce the adverse effects from residual deformities. In this manner, the negative effects of lumbar fusion or lumbar region surgeries were eliminated from the study. The positive effects were eliminated by not including the healthy control groups without a lumbar curvature or surgical treatment. The effect of VBT on the lumbar region muscles was evaluated using presurgical and postsurgical MRIs.

VBT is introduced as a dynamic system in the literature; however, only a few studies have evaluated the functional results after VBT. Pehlivanoglu et al. reported that VBT preserves spinal mobility, based on an analysis of lumbar ROM in three planes (29). This study, which used fusion patients as the control group, demonstrated that VBT preserves motion but did not show how much loss of motion it creates in individuals who were not fused. Pahys et al. separately evaluated the thoracic and lumbar region motions in VBT and in the posterior fusion groups using a 3D motion analysis system, which is the gold-standard method for the ROM evaluation. The subgrouping was performed according to the levels at which the surgery ended (≤L1, L2, L3, and L4). The statistical analysis was performed in this manner. This study identified significantly less motion loss in patients treated with VBT in the second year after the surgery compared to the posterior fusion patients (15).

The STF group that did not undergo fusion to the lumbar region and the hybrid group that underwent VBT to the lumbar region were then compared. No statistically or clinically significant differences were observed between the two groups in all the parameters tested. The lumbar movement of the patients in both groups was within the normal range (19,27). However, the patients may possibly encounter problems as the follow-up periods get longer.

In a previous study evaluating the trunk flexor-extensor endurance in a VBT group, the VBT patients were compared with those who underwent posterior fusion surgery. The trunk flexor-extensor endurance of the VBT group was significantly superior to that of the posterior fusion surgery group (29). Therefore, we evaluated both the strength (60°/s) and the endurance (120°/s) of the trunk muscles using an isokinetic dynamometer by choosing protocols and angular velocities with proven validity and reliability during the study's planning phase. No significant differences were found between the two groups in terms of the strength and endurance of the trunk muscles. In conclusion, adding lumbar VBT to STF did not have a negative effect on strength and endurance.

The paraspinal muscle morphology is believed to play a critical role in low back pain, various spinal deformity diseases, and other pain-related pathologies (13). The postoperative morphological changes in the paraspinal muscles may affect the patient outcomes and contribute to the development of adjacent segment disease in the long term. Kumaran et al. developed a finite element model and found that the reduction in the CSA after the lumbar fusion can lead to changes in the

spinal element stresses in the adjacent segments, potentially resulting in permanent postoperative low back pain (23,32). After the spinal fusion, paraspinal muscle atrophy occurs as a result of both iatrogenic damage and loss of movement in the relevant segment (18). Lu et al. suggested that the paraspinal muscle atrophy in the thoracic region and the paraspinal muscle hypertrophy in the lumbar region may develop after STF (26). In their long-term study, Kim et al. showed a significant decrease in the CSA of the paraspinal muscles in the non-fused segment, associating this change with iatrogenic damage (21). After the usage of a dynamic system (e.g., VBT), how the paraspinal muscles involved in segmental stabilization will be affected is quite important. The only literature study evaluating the multifidus fatty degeneration and atrophy in the VBT group found that mild/moderate fatty degeneration on the concave side of the preoperative curve remained unchanged after VBT (16).

In the VBT surgical technique, the lumbar vertebrae are accessed with a mini-open retroperitoneal approach by laterally opening an oblique incision. This procedure involves a retroperitoneal dissection and a posterior retraction of the psoas muscle, although it spares posterior paraspinal muscles, such as the multifidus and the erector spinae (1). Courvoisier et al. reported that paresthesia in the proximal and anteromedial parts of the thigh is common after this surgery, even if the nerve is not damaged (6). Currently, there is a lack of research or scientific studies specifically examining the effect of VBT surgery on the psoas muscle, despite its significant role in hip flexion and lumbar spine stabilization.

In this work, no significant difference was observed in the CSA ratios of multifidus, erector spinae, and psoas at both levels (i.e., L2 and L5) in the two groups. The effect size analyses were not performed for the CSA ratios because the changes were minimal and not considered clinically relevant. In some patients under both groups, the preoperative mild fatty degeneration of the multifidus and the erector spinae remained unchanged after the surgery. In our cohort, both groups were predominantly in the late pubertal stage; however, the hybrid group included skeletally immature patients. Considering their remaining growth potential, immaturity could theoretically influence the paraspinal muscle CSA, thereby representing a study limitation. For this reason, we specifically aimed to evaluate whether or not a denervation-related atrophy developed by comparing preoperative and postoperative fatty degeneration. We found no significant difference between the preoperative and postoperative fatty degeneration grades in either group, which we considered as a valuable finding. We believe that no significant difference exists in the CSA ratio of the psoas muscle on the surgical side (left side), and that the absence of fatty atrophy signs is an important finding in the hybrid group, especially at the L2 level.

Recent studies have reported positive effects of VBT on patients' quality of life (28,29). Few studies have compared clinical outcomes of thoracic VBT (34,35). Pehlivanoglu et al. compared the posterior fusion between T5–L3 and VBT surgery performed at the same levels in the study they previously published, stating that the SRS-22 scores of the VBT group were statistically significantly higher than those of the posterior fusion group (29). Pahys et al. compared the patient SRS-22 scores between the posterior fusion and VBT groups subgrouped according to the levels at which the surgery ended. In the data obtained from this work, no differences were found in terms of the SRS-22 scores in cases where the last instrumented vertebra was L3 or above (28). The present study found no statistically significant differences between the STF and hybrid groups in terms of the SRS-22 and ODI scores. Although several patients in the hybrid group reported anterior thigh pain or transient hip flexor weakness in the early postoperative period, these symptoms resolved in most cases and did not result in significant differences in overall recovery parameters, including hospital stay or return-to-school time, when compared with the STF group. However, the only last-visit scores of SRS-22, ODI, and VAS were available, limiting our ability to evaluate the longitudinal recovery trends.

To the best of our knowledge, no studies have yet evaluated the ROM, quality of life, or muscle morphology in the patient group who underwent hybrid surgery. Cherian et al., in their study publishing early radiological outcomes following hybrid surgery, indicated that the combined PSF and VBT approach could be safe and effective for idiopathic scoliosis (5). Our results indicate that, while further studies are required, the hybrid procedure can potentially serve as a technique for maintaining lumbar mobility and avoiding iatrogenic muscle injury and does not detrimentally impact the quality of life.

Limitations

This study had certain limitations. The Lenke patient classifications were different. Although radiological correction was not the primary outcome, the curve-type distribution variability may have introduced heterogeneity and can represent a potential source of bias or confounding in the interpretation of the functional outcomes. The second limitation is that skeletal maturity was assessed without Sanders staging, which is recommended in the current literature, especially for hybrid surgery. Although Sanders staging data were available for patients in the hybrid group, some preoperative evaluations in the STF group relied on retrospective data, and hand radiographs were not consistently available; therefore, Sanders staging could not be applied uniformly across the entire cohort. However, the CVMI and the triradiate cartilage status were evaluated, both of which were considered reliable methods for the maturity assessment. All patients had a closed triradiate cartilage. The majority of patients in both groups were in the late adolescent period; however, the hybrid group included relatively more skeletally immature patients, which may have influenced the results. Another important study limitation is the relatively small sample size. With only eight patients per group, the study had limited power to detect clinically meaningful differences, consequently increasing the risk of the type II error. While the effect size analyses were performed to provide additional clinical context, the small cohort restricts the generalizability of our obtained findings. In this regard, it may be beneficial to conduct studies in more homogeneous and larger patient cohorts. Another limitation is the absence of the preoperative assessments on the quality of life

(SRS-22), disability (ODI), pain (VAS), lumbar ROM, and trunk muscle strength and endurance in patients with AIS, which limits the longitudinal assessment of functional recovery and reduces the ability to evaluate changes over time.

CONCLUSION

Probably for the first time in the literature, patients who underwent a hybrid procedure were compared herein with patients who underwent STF. VBT applied to the lumbar region preserved the lumbar region movement and did not cause iatrogenic damage to the paraspinal muscles, even on the side of the surgery. Longitudinal studies are needed to observe the long-term effects of the hybrid procedure and determine the changes in the follow-up period. Studies that include larger sample groups are needed to generalize the results.

ACKNOWLEDGMENTS

The authors would like to thank Enago (www.enago.com) for the English language review.

Declarations

Funding: This research did not receive any specific grant from funding agencies in the public, commercial, or not-for-profit sectors.

Availability of data and materials: The datasets generated and/or analyzed during the current study are available from the corresponding author by reasonable request.

Disclosure: The authors declare no competing interests.

AUTHORSHIP CONTRIBUTION

Study conception and design: ENT, MK, GD, SK, TS, TA, BB
Data collection: ENT, MK, GD, SK, TS, TA
Analysis and interpretation of results: ENT, MK, GD, SK, BB
Draft manuscript preparation: ENT, TA, BB
Critical revision of the article: ENT, MK, GD, SK, TS, TA, BB
Other (study supervision, fundings, materials, etc...): ENT, TA, BB
All authors (ENT, MK, GD, SK, TS, TA, BB) reviewed the results and approved the final version of the manuscript.

REFERENCES

1. Baker C, Milbrandt T, Potter D, Larson AN: Anterior lumbar vertebral body tethering in adolescent idiopathic scoliosis: Surgical/technical tips. JPOSNA 2, 2020. https://doi.org/10.55275/JPOSNA-2020-145
2. Baroncini A, Trobisch P, Eschweiler J, Migliorini F: Analysis of the risk factors for early tether breakage following vertebral body tethering in adolescent idiopathic scoliosis. Eur Spine J 31: 2348-2354, 2022. https://doi.org/10.1007/s00586-022-07231-w
3. Baroncini A, Trobisch PD, Migliorini F: Learning curve for vertebral body tethering: Analysis on 90 consecutive patients. Spine Deform 9: 141-147, 2021. https://doi.org/10.1007/s43390-020-00191-5
4. Battaglia PJ, Maeda Y, Welk A, Hough B, Kettner N: Reliability of the goutallier classification in quantifying muscle fatty degeneration in the lumbar multifidus using magnetic resonance imaging. J Manipulative Physiol Ther 37: 190-197, 2014. https://doi.org/10.1016/j.jmpt.2013.12.010
5. Cherian D, Samdani AF, Schüpper AJ, Stein AA, Naseer Z, Pahys JM, Nice E, Hwang SW: Early outcomes in hybridfixation for idiopathic scoliosis: Posterior fusion combined with anterior vertebral body tethering. Patient series. J Neurosurg Case Lessons 6: CASE23331, 2023. https://doi.org/10.3171/case23331
6. Courvoisier A, Baroncini A, Jeandel C, Barra C, Lefevre Y, Solla F, Gouron R, Métaizeau JD, Maximin MC, Cunin V: Vertebral body tethering in AIS management-a preliminary report. Children (Basel) 10: 192, 2023. https://doi.org/10.3390/children10020192
7. Crawford III CH, Lenke LG: Growth modulation by means of anterior tethering resulting in progressive correction of juvenile idiopathic scoliosis: A case report. J Bone Joint Surg Am 92: 202-209, 2010. https://doi.org/10.2106/JBJS.H.01728
8. Cummock MD, Vanni S, Levi AD, Yu Y, Wang MY: An analysis of postoperative thigh symptoms after minimally invasive transpsoas lumbar interbody fusion. J Neurosurg Spine 15: 11-18, 2011. https://doi.org/10.3171/2011.2.SPINE10374
9. Cunin V: Early-onset scoliosis: Current treatment. Orthop Traumatol Surg Res 101: S109-118, 2015. https://doi.org/10.1016/j.otsr.2014.06.032
10. Driscoll M, Aubin C-E, Moreau A, Parent S: Biomechanical comparison of fusionless growth modulation corrective techniques in pediatric scoliosis. Med Biol Eng Comput 49: 1437-1445, 2011. https://doi.org/10.1007/s11517-011-0801-8
11. Fletcher JP, Taylor JD, Carroll CA, Richardson MB: Comparison of two handheld digital dual inclinometry techniques in the measurement of lumbar flexion active range of motion. J Sport Rehabil 30: 339-342, 2020. https://doi.org/10.1123/jsr.2019-0368
12. Hamzaoglu A, Karadereler S, Kahraman S, Akman YE, Mutlu A, Aslanturk O, Elsadig M, Sanli T, Enercan M: Clinical, radiological and HRQoL outcomes after selective thoracic fusion with minimum 15-year follow-up. Spine Deform 9: 1323-1331, 2021. https://doi.org/10.1007/s43390-021-00350-2
13. He K, Head J, Mouchtouris N, Hines K, Shea P, Schmidt R, Hoelscher C, Stricsek G, Harrop J, Sharan A: The implications of paraspinal muscle atrophy in low back pain, thoracolumbar pathology, and clinical outcomes after spine surgery: A review of the literature. Global Spine J 10: 657-666, 2020. https://doi.org/10.1177/2192568219879087.
14. Helenius L, Diarbakerli E, Grauers A, Lastikka M, Oksanen H, Pajulo O, Löyttyniemi E, Manner T, Gerdhem P, Helenius I: Back pain and quality of life after surgical treatment for adolescent idiopathic scoliosis at 5-year follow-up: Comparison with healthy controls and patients with untreated idiopathic scoliosis. J Bone Joint Surg Am 101: 1460-1466, 2019. https://doi.org/10.2106/jbjs.18.01370
15. Hoernschemeyer DG, Boeyer ME, Robertson ME, Loftis CM, Worley JR, Tweedy NM, Gupta SU, Duren DL, Holzhauser CM, Ramachandran VM: Anterior vertebral body tethering for adolescent scoliosis with growth remaining: A retrospective review of 2 to 5-year postoperative results. J Bone Joint Surg Am 102: 1169-1176, 2020. https://doi.org/10.2106/jbjs.19.00980
16. Hoernschemeyer DG, Boeyer ME, Tweedy NM, Worley JR, Crim JR: A preliminary assessment of intervertebral disc health and pathoanatomy changes observed two years following anterior vertebral body tethering. Eur Spine J 30: 3442-3449, 2021. https://doi.org/10.1007/s00586-021-06972-4

17. Ishikawa M, Nishiyama M, Kamata M: Selective thoracic fusion for King-Moe type II/Lenke 1C curve in adolescent idiopathic scoliosis: A comprehensive review of major concerns. Spine Surg Relat Res 3: 113-125, 2018. https://doi.org/10.22603/ssrr.2018-0047
18. Jiang H, Meng Y, Jin X, Zhang C, Zhao J, Wang C, Gao R, Zhou X: Volumetric and fatty infiltration imbalance of deep paravertebral muscles in adolescent idiopathic scoliosis. Med Sci Monit 23: 2089-2095, 2017. https://doi.org/10.12659/MSM.902455
19. Keeley J, Mayer TG, Cox R, Gatchel RJ, Smith J, Mooney V: Quantification of lumbar function. Part 5: Reliability of range-of-motion measures in the sagittal plane and an in vivo torso rotation measurement technique. Spine (Phila Pa 1976) ;11: 31-35, 1986.
20. Kepler CK, Meredith DS, Green DW, Widmann RF: Long-term outcomes after posterior spine fusion for adolescent idiopathic scoliosis. Curr Opin Pediatr 24: 68-75, 2012. https://doi.org/10.1097/MOP.0b013e32834ec982
21. Kim HJ, Yang JH, Chang D-G, Suk SI, Suh SW, Nam Y, Kim SI, Song KS: Long-term influence of paraspinal muscle quantity in adolescent idiopathic scoliosis following deformity correction by posterior approach. J Clin Med 10: 4790, 2021. https://doi.org/10.3390/jcm10204790
22. Kim JY, Ryu DS, Paik HK, Ahn SS, Kang MS, Kim KH, Park JY, Chin DK, Kim KS, Cho YE, Kuh SU: Paraspinal muscle, facet joint, and disc problems: Risk factors for adjacent segment degeneration after lumbar fusion. Spine J 16: 867-875, 2016. https://doi.org/10.1016/j.spinee.2016.03.010
23. Kumaran Y, Shah A, Katragadda A, Padgaonkar A, Zavatsky J, McGuire R, Serhan H, Elgafy H, Goel VK: Iatrogenic muscle damage in transforaminal lumbar interbody fusion and adjacent segment degeneration: A comparative finite element analysis of open and minimally invasive surgeries. Eur Spine J 30: 2622-2630, 2021. https://doi.org/10.1007/s00586-021-06909-x
24. Langrana NA, Lee CK: Isokinetic evaluation of trunk muscles. Spine (Phila Pa 1976) 9: 171-175, 1984. https://doi.org/10.1097/00007632-198403000-00007
25. Larson AN, Fletcher ND, Daniel C, Richards BS: Lumbar curve is stable after selective thoracic fusion for adolescent idiopathic scoliosis: A 20-year follow-up. Spine (Phila Pa 1976) 37: 833-839, 2012. https://doi.org/10.1097/BRS.0b013e318236a59f
26. Lu WW, Hu Y, Luk KD, Cheung KM, Leong JC: Paraspinal muscle activities of patients with scoliosis after spine fusion: An electromyographic study. Spine (Phila Pa 1976) 27: 1180-1185, 2002. https://doi.org/10.1097/00007632-200206010-00009
27. Magee DJ: Orthopedic physical assessment-e-book. Elsevier Health Sciences; 2014.
28. Pahys JM, Samdani AF, Hwang SW, Warshauer S, Gaughan JP, Chafetz RS: Trunk range of motion and patient outcomes after anterior vertebral body tethering versus posterior spinal fusion: Comparison using computerized 3d motion capture technology. J Bone Joint Surg Am 104: 1563-1572, 2022. https://doi.org/10.2106/jbjs.21.00992
29. Pehlivanoglu T, Oltulu I, Erdag Y, Akturk UD, Korkmaz E, Yildirim E, Sarioglu E, Ofluoglu E, Aydogan M: Comparison of clinical and functional outcomes of vertebral body tethering to posterior spinal fusion in patients with adolescent idiopathic scoliosis and evaluation of quality of life: Preliminary results. Spine Deform 9: 1175-1182, 2021. https://doi.org/10.1007/s43390-021-00323-5
30. Raitio A, Syvänen J, Helenius I: Vertebral body tethering: Indications, surgical technique, and a systematic review of published results. J Clin Med 11: 2576, 2022. https://doi.org/10.3390/jcm11092576
31. Sanchez-Raya J, Bago J, Pellise F, Cuxart A, Villanueva C: Does the lower instrumented vertebra have an effect on lumbar mobility, subjective perception of trunk flexibility, and quality of life in patients with idiopathic scoliosis treated by spinal fusion? J Spinal Disord Tech 25: 437-442, 2012. https://doi.org/10.1097/BSD.0b013e3182318622
32. Suo M, Zhang J, Sun T, Wang J, Liu X, Huang H, Li Z: The association between morphological characteristics of paraspinal muscle and spinal disorders. Ann Med 55: 2258922, 2023. https://doi.org/10.1080/07853890.2023.2258922
33. Trobisch P, Baroncini A, Berrer A, Da Paz S: Difference between radiographically suspected and intraoperatively confirmed tether breakages after vertebral body tethering for idiopathic scoliosis. Eur Spine J 31: 1045-1050, 2022. https://doi.org/10.1007/s00586-021-07107-5
34. Wong HK, Ruiz JNM, Newton PO, Gabriel Liu KP: Non-fusion surgical correction of thoracic idiopathic scoliosis using a novel, braided vertebral body tethering device: Minimum follow-up of 4 years. JB JS Open Access 4: e0026, 2019. https://doi.org/10.2106/jbjs.Oa.19.00026
35. Yucekul A, Ergene G: Outcomes of posterior spinal fusion and vertebral body tethering in patients with adolescent idiopathic scoliosis and evaluation of quality of life. ANKARA Med J 21: 441-453, 2021. https://doi.org/10.5505/amj.2021.30783

Supplementary Table I: Summary of All 16 Cases Included in the Study

No	Gender	Age	Risser Pre/Last	CMVI	Fusion Levels	VBT Levels	LIV	Lenke	T Cobb Pre/Last	TI/L Cobb Pre/Last	Complication
VBT1	F	15	4 /4	5/5	T5-11 (6)	T11-L3(4)	L3	5C	41/11	45/12	-
VBT2	F	12	0 /1	2/3	T7-11(4)	T11-L3(4)	L3	1C	58/12	48/1	Overcorrection
VBT3	F	14	1 /2	3/4	T4-12(8)	T12-L3(3)	L3	1C	49/3	38/7	-
VBT4	F	14	4 /4	5/5	T3-12(9)	T12-L3(3)	L3	1C	50/3	50/11	-
VBT5	F	17	5 /5	6/6	T5-12(7)	T12-L4(4)	L4	6C	47/13	50/14	-
VBT6	F	14	3 /4	4/5	T5-12(7)	T12-L4(4)	L4	1C	50/14	46/13	-
VBT7	F	15	4 /5	5/5	T2-12(10)	T12-L3(3)	L3	1C	62/20	39/18	-
VBT8	F	11	0 /2	2/4	T5-11(6)	T11-L3(4)	L3	3C	48/5	51/9	-
Mean							L3		51/10	46/11	
SD									6/6	5/5	
STF1	F	12	3 /4	4/5	T2-12(10)	-	T12	1A	44/5	30/6	-
STF2	M	14	4 /4	5/5	T2-12(10)	-	T12	1B	53/26	32/27	-
STF3	F	15	2 /4	3 /5	T4-12(8)	-	T12	1B	43/8	30/8	-
STF4	F	17	5 /5	6/6	T2-12(10)	-	T12	1A	40/8	30/0	-
STF5	F	15	4 /5	5/6	T2-12(10)	-	T12	1C	68/22	50/25	-
STF6	M	16	4 /5	5/6	T2-12(10)	-	T12	1C	59/17	48/17	-
STF7	F	12	4 /4	5/5	T3-12(9)	-	T12	1A	58/17	35/16	-
STF8	F	16	4 /5	5/6	T3-12(9)	-	T12	1A	41/10	29/4	-
Mean							T12		51/14	35/13	
SD									10/7	8/10	

LIV: *Lowest instrumented vertebra,* ***SD:*** *standard deviation*

Supplementary Table II: Comparison of the Lumbar Strengths and Endurance Scores of Both Groups

		Hybrid (Mean±SD)	STF (Mean±SD)	P	Hedges' g	95% CI
Flexion	Peak torque at 60 °/s (Nm)	113.75±20.37	111.87±34.41	0.645	+0.06	[–0.92, 1.04]
	Peak torque at 60°/s %BW (Nm/kg)	215.88.37±33.97	182.87±65.02	0.161	+0.60	[–0.40, 1.61]
	Peak torque at 120 °/s (Nm)	84.75±22.11	68.87±20.55	0.195	+0.70	[–0.31, 1.72]
	Peak torque at 120 °/s %BW (Nm/kg)	132.75±68.60	117.00±53.01	0.574	+0.24	[–0.74, 1.23]
Extension	Peak torque at 60 °/s (Nm)	98.88±22.09	93.37±27.75	0.721	+0.21	[–0.78, 1.19]
	Peak torque at 60°/s %BW (Nm/kg)	187.75±39.73	156.75±64.11	0.195	+0.55	[–0.45, 1.55]
	Peak torque at 120 °/s (Nm)	53.38±23.71	60.37±18.66	0.442	–0.31	[–1.30, 0.68]
	Peak torque at 120 °/s %BW (Nm/kg)	101.75±44.61	102.12±45.36	1.000	–0.01	[–0.99, 0.97]

Nm: *Newton-meter,* ***BW:*** *body weight,* ***SD:*** *standard deviation*

Turk Neurosurg 36(3):433-439, 2026
DOI: 10.5137/1019-5149.JTN.49543-25.2

Original Investigation
Spine and Peripheral Nerves

Received: 01.08.2025
Accepted: 06.10.2025
Published Online: 22.05.2026

Patterns of Pedicle Wall Violations Following Thoracolumbar Stabilization in Osteoporotic and Non-Osteoporotic Patients

Berkay AYHAN, Mehmet Emre YILDIRIM

Ankara Research and Training Hospital, Department of Neurosurgery, Ankara, Türkiye

Corresponding author: Berkay AYHAN ✉ berkayayhan@gmail.com

ABSTRACT

AIM: To investigate which pedicle level and wall were most affected by screw malposition in osteoporotic and non-osteoporotic patients undergoing thoracolumbar stabilization, and to determine whether significant differences existed between the groups.

MATERIAL and METHODS: This retrospective study analyzed pedicle screw malpositions and the specific walls involved in thoracolumbar stabilization procedures performed between 2014 and 2025 using the freehand technique with fluoroscopic guidance by the same surgical team. A total of 972 patients were included: those with a T-score ≤–2.5 (osteoporotic group) and those with a T-score > –2.5 (non-osteoporotic group). Indications for surgery included traumatic vertebral fracture, spinal stenosis, recurrent disc herniation, spinal tumor, or spondylolisthesis. All patients underwent preoperative MRI, CT, bone mineral densitometry, and X-rays, as well as postoperative CT and X-rays. Patients with acute decompression without preoperative densitometry and those treated with vertebroplasty/kyphoplasty were excluded. In cases of malposition, postoperative CT scans were used to evaluate superior, inferior, lateral, medial, and anterior cortical breaches, and comparisons were made between groups.

RESULTS: Screw malposition rates were significantly higher in osteoporotic patients across all levels, particularly in thoracic vertebrae. The medial pedicle wall was most frequently affected in this group.

CONCLUSION: In osteoporotic patients, transpedicular screw fixation using the freehand technique with fluoroscopic guidance was associated with higher malposition rates, especially involving the medial pedicle wall. These complications may be reduced through greater surgical experience and careful intraoperative technique.

KEYWORDS: Osteoporosis, spinal fusion, vertebral anatomy

INTRODUCTION

In 1948, King introduced the use of transpedicular screws for internal fixation in lumbosacral fusion (18). Intraoperative evaluation of pedicle screw placement is typically performed with fluoroscopy in posteroanterior (PA) and lateral projections, while postoperative computed tomography (CT) provides precise visualization of cortical breaches. Historically, malposition rates with freehand techniques using fluoroscopic guidance have ranged from 30% to 40% (3,8). In contrast, intraoperative CT-guided navigation systems have recently improved accuracy to more than 95.5% (24).

Postoperative CT remains the gold standard for assessing pedicle screw malposition, and several classification systems have been proposed. The Gertzbein and Robbins classification assesses the extent of pedicle breach in millimeters but accounts only for spinal canal violations and not lateral breaches (9). The Youkilis classification, although numeric, is limited to thoracic vertebrae (32). Heary's classification incorporates lateral, medial, superior, inferior, and anterior breaches but lacks quantitative measurement and is also restricted to thoracic vertebrae (12). The Wiesner classification, which was used in our study, evaluates breach distances in lumbar

Berkay AYHAN : 0000-0001-9746-1492 Mehmet Emre YILDIRIM : 0000-0001-7039-2706

vertebrae and considers all pedicle walls, defining them as minor (0-3 mm), moderate (3-6 mm), or severe (>6 mm) (31).

In this study, we aimed to determine the incidence of pedicle screw malposition and related complications in 5,552 screws placed in the thoracic and lumbosacral regions using the conventional freehand technique with fluoroscopic guidance in osteoporotic and non-osteoporotic patients. We further compared the levels of breach and the specific pedicle walls affected between the two groups.

MATERIAL and METHODS

This retrospective study was approved by the Institutional Review Board of Ankara Training and Research Hospital (protocol number E-25-619). The requirement for informed consent was waived due to the retrospective and observational design. All patient data were anonymized during collection and analysis to ensure confidentiality.

Study Design and Patient Selection

Patients who underwent transpedicular screw fixation in our spine surgery unit between 2014 and 2025 were included. Indications for surgery were spinal stenosis, spondylolisthesis, traumatic fracture, recurrent disc herniation, or spinal tumor. Only patients who underwent stabilizing procedures for spinal tumors were considered. Emergency cases without preoperative bone densitometry were excluded.

Data Collection

Demographic data, clinical diagnoses, number of screws inserted, malposition rates, and revision procedures were collected retrospectively. Osteoporosis was defined as a T-score ≤–2.5 measured by dual-energy X-ray absorptiometry (DEXA); patients with T-scores >–2.5 were classified as the non-osteoporotic group.

Imaging and Evaluation

All patients underwent preoperative magnetic resonance imaging (MRI), CT, DEXA, and radiographs, as well as postoperative CT and radiographs. Screw placement was assessed on axial and coronal CT scans. Screw length and diameter were determined according to pedicle diameter and vertebral body length. Malpositions were categorized as anterior, medial, or lateral. Medial and lateral breaches were further graded as Grade 1 (0-3 mm), Grade 2 (3-6 mm), and Grade 3 (>6 mm) (Figure 1A-D).

Surgical Technique and Evaluation Criteria

All procedures were performed using an open surgical technique with intraoperative fluoroscopy by experienced spine surgeons following consistent surgical principles. In the lumbar spine, entry points were defined at the junction of the transverse and superior articular processes, while in the thoracic spine, they were defined by the bony triangle formed by the superior articular facet, transverse process, and pars interarticularis (5,7). Patients were positioned prone, and C-arm fluoroscopy was used in PA and lateral views. Entry holes were prepared with an awl and probed before screw insertion. Titanium screws were used to minimize imaging artifacts. Data collected included patient age, sex, pre- and postoperative neurological deficits, number of screws per level, malposition sites, and revision procedures. Postoperative complications evaluated were wound infections, dural tears, cerebrospinal fluid (CSF) leaks, and delayed wound healing.

Postoperative CT scans with 1-mm slices were obtained within 12 h after surgery, or earlier if new neurological deficits occurred, and were reviewed in axial, coronal, and sagittal planes. Screw placement was assessed independently by both the operating surgeons and radiologists. Cortical breaches in medial, lateral, superior, inferior, or anterior directions were measured in millimeters and classified as mild, moderate, or severe according to Wiesner's criteria. Screws that caused neurological symptoms or mechanical instability were revised.

The study addressed the following questions:

1. Does the breach rate increase as T-score decreases?
2. Are malposition rates higher in thoracic or lumbosacral regions?
3. Which pedicle wall is most frequently violated at each level?

Statistical Analysis

Malposition and revision rates, breach patterns, and the prevalence of osteoporosis across pathologies were compared using the chi-squared (χ^2) test. Binary logistic regression was performed to identify risk factors for malposition, with the outcome variable defined as the presence of malposition (1, yes; 0, no). Predictors included osteoporosis (T-score ≤ –2.5), anatomical region (thoracic vs. lumbosacral), sex, and diagnosis. Odds ratios (OR) and 95% confidence intervals (CI) were calculated. A p-value <0.05 was considered statistically significant. All analyses and figures were generated using Python version 13.3.

RESULTS

A total of 972 patients were included, comprising 612 women (62.96%) and 360 men (37.03%). The osteoporotic group (T-score ≤ –2.5) consisted of 202 patients (20.78%) with a mean T-score of –2.9, while the non-osteoporotic group (T-score > –2.5) included 770 patients (79.22%) with a mean T-score of –1.3.

Of 475 patients with spinal stenosis, 102 (21.47%) were osteoporotic. Among 142 patients with spondylolisthesis, 45 (31.69%) were osteoporotic. Of 285 patients with fractures, 26 (9.12%) were osteoporotic. In 47 patients with recurrent disc herniation, 7 (14.89%) were osteoporotic. Among 23 patients with tumors, 2 (8.69%) were osteoporotic (Table I).

Of 4,538 screws placed in non-osteoporotic patients, 257 (5.66%) were malpositioned, of which 32 (12.45%) required revision. In osteoporotic patients, 92 of 1,014 screws (9.07%) were malpositioned, with 28 (30.43%) revised ($p < 0.001$) (Table II).

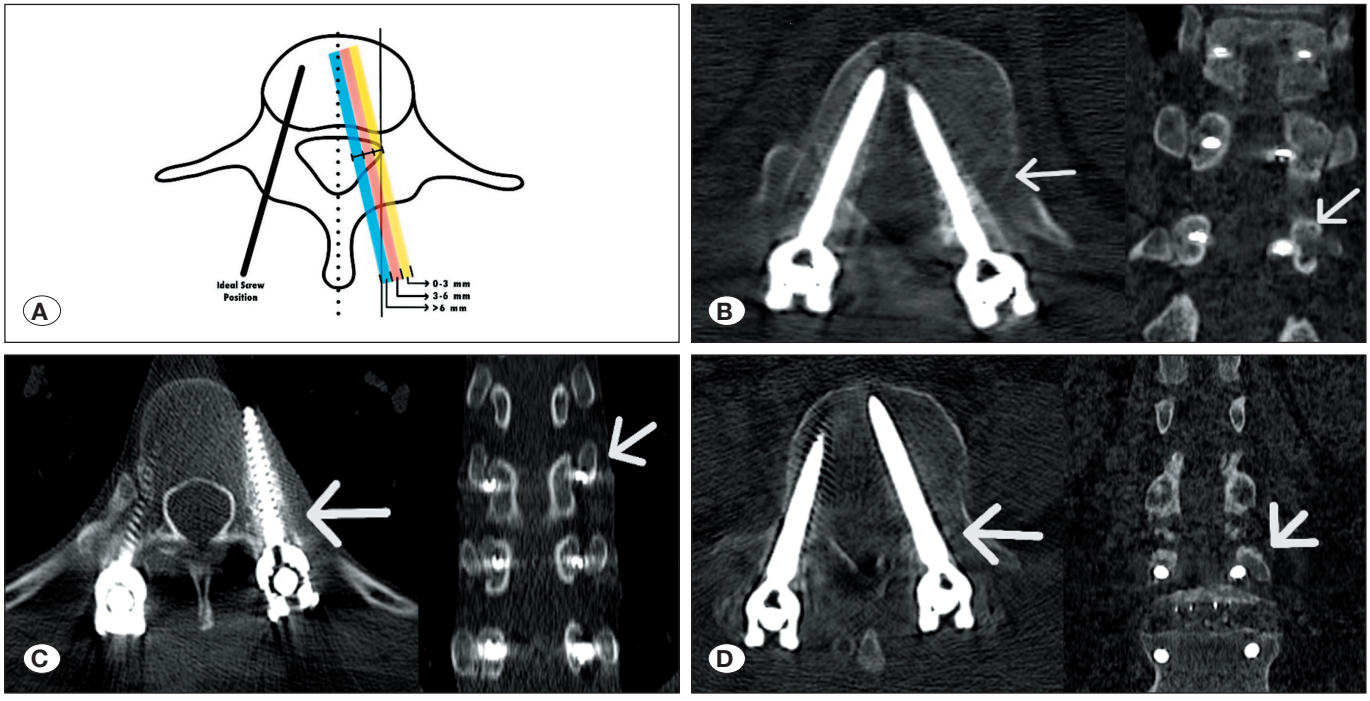

Figure 1: Examples of malpositioned pedicle screws. **A)** Schematic representation of Wiesner's classification of pedicle screw malposition: minor (0-3 mm, yellow line), moderate (3-6 mm, red line), and severe (>6 mm, blue line) (31). **B)** Computed tomography (CT) scan example of a medial malposition. **C)** Example of a lateral malposition. **D)** Example of an inferomedial malposition.

Table I: Distribution of Patients According to Diagnoses and Osteoporosis Status

Diagnosis	Patients n (%)	Non-osteoporotic Group n (%)	Osteoporotic Group n (%)	p-value
Spinal Stenosis	475 (48.8)	373 (47.2)	102 (56.0)	**0.039**
Spondylolisthesis	142 (14.6)	97 (12.2)	45 (24.7)	**<0.001**
Traumatic Fracture*	285 (29.3)	259 (31.7)	26 (14.2)	**<0.001**
Recurrent Disc Herniation	47 (4.8)	40 (5.0)	7 (3.8)	0.618
Spinal Tumour**	23 (2.3)	21 (2.6)	2 (1.0)	0.328
Total	972 (100.0)	790 (100.0)	182 (100.0)	

**A total of 94 trauma patients requiring emergency decompression who could not undergo bone mineral densitometry were excluded from the study.*
***Only patients with spinal tumours requiring stabilisation were included in the study.*

Table II. Malposition and Revision Rates in Osteoporotic and Non-Osteoporotic Patients

	Screw Counts n (%)	Malposition n (%)	Revision n (%)*
Non-osteoporotic group	4538 (81.7)	257 (5.6)	32 (12.4)
Osteoporotic group	1014 (18.3)	92 (9.0)	28 (30.4)
Total	5552 (100.0)	349 (6.2)	60 (17.1)
p-value		**<0.001**	**<0.001**

**Cases with grade 3 malposition were revised due to the potential risk of future instability. In addition, all patients with grade 1, 2, or 3 malposition who developed postoperative sciatica or neurological deficits underwent screw revision.*

Table III: Perforation Sites and Grading in Axial CT Imaging

		n (%)	Review (n=22)	n (%)	Review (n=28)	p-value
Anterior perforation*	Grade 1 (0-3 mm)	28 (10.8)	0	9 (9.7)	0	0.92
Medial perforation	Grade 1 (0-3 mm)	64 (24.9)	4	28 (30.4)	2	0.37
	Grade 2 (3-6 mm)	18 (7.0)	0	15 (16.3)	8	**0.02**
	Grade 3 (> 6 mm)	10 (3.8)	10	10 (10.8)	10	**0.03**
Lateral Perforation	Grade 1 (0-3 mm)	92 (35.7)	0	14 (15.2)	0	**<0.001**
	Grade 2 (3-6 mm)	37 (14.3)	0	8 (8.6)	0	0.22
	Grade 3 (> 6 mm)	8 (3.1)	8	8 (8.6)	8	0.06

**In 37 patients with anterior perforation, the amount of perforation ranged from 0 to 3 mm and there was no contact with any vital organs. Therefore, none of them required revisions.*

On axial CT imaging, the 257 malpositions in the non-osteoporotic group included 42 anterior (16.34%), 92 medial (35.79%), and 137 lateral (53.30%) breaches. In the osteoporotic group, the 92 malpositions included 9 anterior (9.78%), 53 medial (57.60%), and 30 lateral (32.60%) breaches. Anterior breaches (0-3 mm) did not involve critical structures and were not revised.

Grade 3 lateral breaches (8 cases) and Grade 1-3 medial breaches (26 cases) were revised due to nerve root irritation. Similar revision patterns were observed in the osteoporotic group. While lateral breaches predominated in non-osteoporotic patients, medial breaches were most common in osteoporotic patients.

At the thoracic level, 36 of 728 screws (4.94%) in non-osteoporotic patients and 24 of 164 screws (14.64%) in osteoporotic patients were malpositioned. At the lumbar level, 221 of 3,810 screws (5.80%) in non-osteoporotic patients and 68 of 850 screws (8.00%) in osteoporotic patients were malpositioned. Malposition rates were consistently higher in osteoporotic patients at both levels, particularly in the thoracic spine (Table III).

Coronal CT revealed distinct breach patterns. In non-osteoporotic patients, breaches included 78 medial, 6 medial-cranial, 8 medial-caudal, 122 lateral, 9 lateral-cranial, 6 lateral-caudal, 4 cranial, and 1 caudal. In osteoporotic patients, breaches included 43 medial, 4 medial-cranial, 6 medial-caudal, 24 lateral, 4 lateral-cranial, 2 lateral-caudal, and 1 caudal breaches (Table IV).

Postoperative complications included wound infection in nine non-osteoporotic and six osteoporotic patients, all treated successfully with antibiotics. CSF-related complications occurred in 29 and 26 patients, respectively ($p < 0.001$).

The most frequent malposition levels in non-osteoporotic patients were L5 > L4 > L3 > L2 > L1 > S1 > T12 > T11 > T10 > T9 > T7 > T8 > T6 > T5. In osteoporotic patients, the distribution was L5 > L1 > L3 > L4 > S1 > T11 > T10 > T8 > T7, with no malpositions noted at T5, T6, or T9.

Table IV: Perforation Sites and Grading in Coronal CT Imaging

	Non-osteoporıtic n=234 n (%)	Osteoporotic n=84 n (%)
Medial	78 (33.3)	43 (51.1)
Medial-cranial	6 (2.5)	4 (4.7)
Medial-caudal	8 (3.4)	6 (7.1)
Lateral	122 (52.1)	24 (28.5)
Lateral-cranial	9 (3.8)	4 (4.7)
Lateral-caudal	6 (2.5)	2 (2.3)
Cranial	4 (1.7)*	0 (0.0)
Caudal	1 (0.4)*	1 (1.1)*

**Patients with anterior perforation on axial CT*

Malposition rates in the lumbosacral region were 8% in osteoporotic versus 5.8% in non-osteoporotic patients ($p = 0.02$). Thoracic malposition rates were also significantly higher in osteoporotic patients ($p < 0.001$) (Table V).

Logistic regression analysis identified osteoporosis as a significant risk factor for screw malposition (OR, 1.6; 95% CI, 1.23-2.07; $p = 0.0004$). Thoracic region, male sex, and fracture diagnosis were not statistically significant predictors.

Overall, 257 of 4,538 screws (5.66%) in non-osteoporotic patients and 92 of 1,014 screws (9.07%) in osteoporotic patients were malpositioned. By anatomical region, malposition rates in the thoracic spine were 4.94% in non-osteoporotic versus 14.63% in osteoporotic patients, and in the lumbosacral spine were 5.80% versus 8.00%, respectively. These findings indicate that lower T-scores are associated with higher malposition risk, particularly in thoracic vertebrae.

Table V: Distribution of Malposition Ratios by Thoracic and Lumbosacral Regions and Vertebral Levels

Thoracal			Lumbosacral		
Total screws applied (n=892)	**Non-osteoporotic (n=728)**	**Osteoporosis (n=164)**	**Total screws applied (n=4660)**	**Non-osteoporotic (n=3810)**	**Osteoporosis (n=850)**
Levels	**Malposed screws**		**Levels**	**Malposed screws**	
T5	1	0	L1	12	10
T6	2	0	L2	28	15
T7	4	1	L3	44	9
T8	3	1	L4	52	7
T9	5	0	L5	76	21
T10	6	2	S1	9	6
T11	7	3	Total	221	68
T12	8	17			
Total	36	24			

DISCUSSION

Freehand transpedicular screw insertion under fluoroscopic guidance is essentially a blind technique and carries inherent risks of neurological or vascular complications (2,7,19). Reported rates of nerve root irritation reach up to 11% in cases of malposition, and revisions are frequently required (1). Anatomical factors such as canal shape may influence the direction of breaches, with round canals predisposing to medial violations and narrow canals to lateral misplacements (15).

Malposition rates as high as 40% have been reported with conventional methods (3,8). Variations in surgical technique and surgeon experience contribute substantially to these outcomes; greater experience is associated with lower malposition rates, regardless of whether conventional or navigation-assisted techniques are used (6,25).

Although intraoperative navigation systems improve screw placement accuracy (22,26), they do not appear to significantly reduce neurological complications (29). Furthermore, most existing classification systems inadequately reflect the clinical impact of breaches (9,12,31,32). For example, even a Grade 1 medial violation—considered "minor" by definition—can still cause sciatica and necessitate revision.

In this study, we applied the Wiesner classification for grading pedicle screw breaches but based revision decisions on a combination of postoperative neurological findings, mechanical instability, and sagittal balance considerations. More recently, El-Meshtawy et al. proposed a scoring system that integrates both radiological breach severity and clinical neurological deficits to better guide revision decisions (5).

Our findings align with the existing literature underscoring the clinical significance of medial wall violations, particularly given their proximity to neural structures (23,27). Medial breaches exceeding 2 mm have been shown to strongly correlate with symptomatic complications (23). Although lateral breaches are generally less likely to produce neurological symptoms, they may still warrant revision surgery due to their potential impact on patient function and pain scores, even in cases where fusion integrity is not compromised (20).

The higher revision rates observed in osteoporotic patients are likely attributable to impaired bone quality and diminished tactile feedback during screw insertion, which increase the risk of cortical wall violations and hinder intraoperative detection (11,21). Surgical experience also plays a crucial role in minimizing malpositions and subsequent revisions, as more experienced surgeons can better adjust their techniques to the challenges of osteoporotic bone (30).

Variability in revision rates across centers may reflect differences in intervention thresholds. The scoring system proposed by El-Meshtawy et al. (5), which integrates radiological breach severity with clinical symptoms, offers a more standardized and comprehensive framework for guiding revision decisions.

To our knowledge, no prior study has specifically investigated which spinal levels or pedicle walls are more susceptible to violation in osteoporotic patients. However, biomechanical evidence suggests that lateral wall violation in osteoporotic thoracic vertebrae reduces pullout strength by approximately 14.1%, with outcomes influenced by screw thread design (16).

Pedicle wall violation often results from incorrect insertion angles or intraoperative deviation, comprising screw stability. Careful preoperative planning, thorough anatomical knowledge, surgical experience, and osteoporosis management are essential to reduce the risk of malposition (13).

In osteoporotic patients, higher rates of pedicle wall violations—particularly at thoracic levels and along the medial walls—can be attributed to reduced bone mineral density and

altered microarchitecture (28), which render the pedicle cortex thinner and more fragile. These changes increase the likelihood of wall breaches during screw insertion (10). Moreover, the diminished tactile feedback encountered in osteoporotic bone makes it difficult for surgeons to detect subtle cortical violations (17). Unlike healthy bone, osteoporotic bone provides softer resistance during probing and screw placement, thereby increasing the risk of unintended breaches, especially medially (14). Because surgeons rely heavily on this "sense of touch" for guidance, surgical experience and meticulous technique remain critical. To further reduce malposition rates in this vulnerable population, the importance of comprehensive preoperative imaging, careful intraoperative technique, and—where available—the use of advanced navigation or guidance technologies should be emphasized (4,10).

CONCLUSION

The conventional freehand technique with fluoroscopy remains a practical, safe, and effective option for lumbosacral fixation. Postoperative CT imaging provides reliable assessment of screw positioning. However, in osteoporotic patients, the higher incidence of pedicle wall violations—particularly at thoracic levels and along the medial walls—underscores the need for heightened vigilance. Greater surgical experience, meticulous technique, and careful intraoperative planning are essential to minimize complications in this high-risk population.

Declarations

Funding: This research did not receive any specific grant from funding agencies in the public, commercial, or not-for-profit sectors.

Availability of data and materials: The datasets generated and/or analyzed during the current study are available from the corresponding author by reasonable request.

Disclosure: The authors declare no competing interests.

AUTHORSHIP CONTRIBUTION

Study conception and design: BA, MEY
Data collection: BA, MEY
Analysis and interpretation of results: BA, MEY
Draft manuscript preparation: BA, MEY
Critical revision of the article: BA, MEY
Other (study supervision, fundings, materials, etc...): -
All authors (BA, MEY) reviewed the results and approved the final version of the manuscript.

REFERENCES

1. Alqurashi A, Alomar SA, Bakhaidar M, Alfiky M, Baeesa SS: Accuracy of pedicle screw placement using intraoperative CT-guided navigation and conventional fluoroscopy for lumbar spondylosis. Cureus 13: e17431, 2021. https://doi.org/10.7759/cureus.17431
2. Bastian L, Knop C, Lange U, Blauth M: Transpedicular implantation of screws in the thoracolumbar spine. Results of a survey of methods, frequency and complications. Orthopade 28: 693-702, 1999. https://doi.org/10.1007/s001320050399
3. Castro WH, Halm H, Jerosch J, Malms J, Steinbeck J, Blasius S: Accuracy of pedicle screw placement in lumbar vertebrae. Spine 21: 1320-1324, 1996. https://doi.org/10.1097/00007632-199606010-00008
4. Chang HK, Chang HC, Wu JC, Huang WC, Cheng H: The effect of osteopenia and osteoporosis on screw loosening following spinal instrumentation surgery. Neurospine 21: 491-500, 2024. https://doi.org/10.14245/ns.2347284.642
5. El-Meshtawy M, Ahmed MA, Abuomira IESA, Amr AA, Ibrahim MAA: Validity of a new scoring system for assessment and decision guidance of misplaced pedicular screws. SICOT J 11: 27, 2025. https://doi.org/10.1051/sicotj/2025015
6. Fichtner J, Hofmann N, Rienmüller A, Buchmann N, Gempt J, Kirschke JS, Ringel F, Meyer B, Ryang YM: Revision rate of misplaced pedicle screws of the thoracolumbar spine—comparison of three-dimensional fluoroscopy navigation with freehand placement: a systematic analysis and review of the literature. World Neurosurg 109: e24-32, 2018. https://doi.org/10.1016/j.wneu.2017.09.091
7. Gautschi OP, Schatlo B, Schaller K, Tessitore E: Clinically relevant complications related to pedicle screw placement in thoracolumbar surgery and their management: a literature review of 35,630 pedicle screws. Neurosurg Focus 31: E8, 2011. https://doi.org/10.3171/2011.7.FOCUS11168
8. Gelalis ID, Paschos NK, Pakos EE, Politis AN, Arnaoutoglou CM, Karageorgos AC, Ploumis A, Xenakis TA: Accuracy of pedicle screw placement: a systematic review of prospective in vivo studies comparing free hand, fluoroscopy guidance and navigation techniques. Eur Spine J 21: 247-255, 2012. https://doi.org/10.1007/s00586-011-2011-3
9. Gertzbein SD, Robbins SE: Accuracy of pedicular screw placement in vivo. Spine 15: 11-14, 1990. https://doi.org/10.1097/00007632-199001000-00004
10. Götschi T, Maranta G, Bernet M, Zemp MK, Farshad M, Widmer J: Bone density-optimized pedicle screw planning enhances mechanical stability. Eur Spine J 2025. https://doi.org/10.1007/s00586-025-09170-8
11. Guo C, Wang R, Ru N, Liu Q, Zhang F, Liang J, Wu Y, Chen L: Analysis on the related factors of misplacement of freehand pedicle screws via posterior approach in degenerative scoliosis: a systematic review. BMC Musculoskelet Disord 25: 808, 2024. https://doi.org/10.1186/s12891-024-07919-8
12. Heary RF, Bono CM, Black M: Thoracic pedicle screws: postoperative computerized tomography scanning assessment. J Neurosurg 100: 325-331, 2004. https://doi.org/10.3171/spi.2004.100.4.0325
13. Isik C, Kose KC, Inanmaz ME, Tagil SM, Sarman H: The mechanisms of medial pedicle wall violation: insertion method is as important as correct cannulation of the pedicle. Adv Orthop 2014: 283783, 2014. https://doi.org/10.1155/2014/283783
14. Jiang Y, Yang X, Zhang C, Wang W, Li H, Zhao J: Bone mineral density surrounding the screw thread (thread BMD): a novel predictor for pedicle screw fixation strength. J Biomech 163: 111270, 2025. https://doi.org/10.1016/j.jbiomech.2025.111270
15. Kaya I, Bozkurt H: The Relationship Between Transpedicular Stabilization with Spinal Canal Type. Turk Neurosurg 31: 38-45, 2021. https://doi.org/10.5137/1019-5149.JTN.29214-20.2

16. Kaya O, Ozkunt O, Sungur M, Cakir MS, Baydogan M, Sariyilmaz K: Intraoperative lateral wall breach simulation in the cadaveric spine and the impact of thread designs of screws on pullout strength in the osteoporotic thoracic vertebrae: A biomechanical study in human cadavers. Acta Orthop Traumatol Turc 58: 57-61, 2024. https://doi.org/10.5152/j.aott.2024.22067
17. Keltz E, Fletcher J, Mora AJ, Yavnai N, Gueorguiev-Rüegg B, Keren Y: Orthopedic screws insertion simulation with immediate feedback enhances surgical skill. Cureus 14: e24837, 2022. https://doi.org/10.7759/cureus.24837
18. King D: Internal fixation for lumbosacral fusion. J Bone Joint Surg Am 30A: 560-565, 1948.
19. Laine T, Mäkitalo K, Schlenzka D, Tallroth K, Poussa M, Alho A: Accuracy of pedicle screw insertion: a prospective CT study in 30 low back patients. Eur Spine J 6: 402-405, 1997. https://doi.org/10.1007/BF01834068
20. LeRoy TE, Smith IC, Kim DH, Golenbock SW, Baker KC, Arnold PM, Sasso RC, Park DK, Fischgrund JS, Zaidi QH, Hwang RW: Clinical significance of lateral pedicle screw malposition in lumbar spine fusion. J Spinal Disord Tech 36: E599-E605, 2023. https://doi.org/10.1097/BSD.0000000000001440
21. Mallepally AR, Dave H, Das K: Advancement in fixation techniques for osteoporotic bone: a narrative review. Indian Spine J 8: 128-137, 2025. https://doi.org/10.4103/isj.isj_86_24
22. Mason A, Paulsen R, Babuska JM, Rajpal S, Burneikiene S, Nelson EL, Villavicencio AT: The accuracy of pedicle screw placement using intraoperative image guidance systems. J Neurosurg Spine 20: 196-203, 2014. https://doi.org/10.3171/2013.11.SPINE13413
23. Mulyadi R, Hutami WD, Suganda KD, Khalisha DF: Risk of neurologic deficit in medially breached pedicle screws assessed by computed tomography: a systematic review. Asian Spine J 18:903-912, 2024. https://doi.org/10.31616/asj.2024.0325
24. Perdomo-Pantoja A, Ishida W, Zygourakis C, Holmes C, Iyer RR, Cottrill E, Theodore N, Witham TF, Lo SL: Accuracy of Current Techniques for Placement of Pedicle Screws in the Spine: A Comprehensive Systematic Review and Meta-Analysis of 51,161 Screws. World Neurosurg 126: 664-678.e3, 2019. https://doi.org/10.1016/j.wneu.2019.02.217
25. Rivkin MA, Yocom SS: Thoracolumbar instrumentation with CT-guided navigation (O-arm) in 270 consecutive patients: accuracy rates and lessons learned. Neurosurg Focus 36: E7, 2014. https://doi.org/10.3171/2014.1.FOCUS13499
26. Tian NF, Huang QS, Zhou P, Zhou Y, Wu RK, Lou Y, Xu HZ: Pedicle screw insertion accuracy with different assisted methods: a systematic review and meta-analysis of comparative studies. Eur Spine J 20: 846-859, 2011. https://doi.org/10.1007/s00586-010-1577-5
27. Tong Y, Zhao Y, Chen B, Jiang Z: Intraoperative triggered electromyographic monitoring of pedicle screw efficiently reduces the lumbar pedicle breach and re-operative rate: a retrospective analysis based on postoperative computed tomography scan. BMC Musculoskelet Disord 24: 535, 2023. https://doi.org/10.1186/s12891-023-06658-6
28. Xu C, Ji J, Zhang Y, Huang X, Dong L: Correlation analysis of BMD in different regions of the vertebrae determined by QCT and DXA on pedicle screw loosening. Sci Rep 15: 15668, 2025. https://doi.org/10.1038/s41598-025-91816-0
29. Verma R, Krishan S, Haendlmayer K, Mohsen A: Functional outcome of computer-assisted spinal pedicle screw placement: a systematic review and meta-analysis of 23 studies including 5,992 pedicle screws. Eur Spine J 19: 370-375, 2010. https://doi.org/10.1007/s00586-009-1258-4
30. Wang Y, Kahaer A, Maimaiti A, Guo H, Rexiti P: Complication, fusion, and revision rate in the lumbar cortical bone trajectory and pedicle screw fixation techniques: a systematic review and meta-analysis. J Orthop Surg Res 18: 382, 2023. https://doi.org/10.1186/s13018-023-03820-7
31. Wiesner L, Kothe R, Rüther W: Anatomic evaluation of two different techniques for the percutaneous insertion of pedicle screws in the lumbar spine. Spine 24: 1599-1603, 1999. https://doi.org/10.1097/00007632-199908010-00015
32. Youkilis AS, Quint DJ, McGillicuddy JE, Papadopoulos SM: Stereotactic navigation for placement of pedicle screws in the thoracic spine. Neurosurgery 48: 771-778; discussion 778-779, 2001. https://doi.org/10.1097/00006123-200104000-00015

Turk Neurosurg 36(3):440-449, 2026
DOI: 10.5137/1019-5149.JTN.48548-25.4

Original Investigation
Stereotactic and Functional

Received: 31.01.2025
Accepted: 26.09.2025
Published Online: 22.05.2026

Long-Term Outcomes of Anterior Temporal Lobectomy in Adults with Temporal Lobe Epilepsy: A Comprehensive Analysis of a 20-Year, 168-Patient Cohort

Ozan HASIMOGLU[1], Tuba Ozge KARACOBAN[1], Taha HANOGLU[1], Nur Bahar GEYLAN[2], Demet KINAY[3], Gunay GUL[4], Ayten Ceyhan DIRICAN[4], Murat Mert ATMACA[5], Ozan BARUT[6], Omer Batu HERGUNSEL[7], Bekir TUGCU[1]

[1]Basaksehir Cam and Sakura City Hospital, Department of Neurosurgery, Istanbul, Türkiye
[2]Basaksehir Cam and Sakura City Hospital, Neurosurgery Nursing, Department of Neuropsychiatry, Istanbul, Türkiye
[3]University of Health Sciences Prof. Dr. Cemil Taşcıoğlu City Hospital, Department of Neurology, Istanbul, Türkiye
[4]University of Health Sciences Turkey, Bakırköy Prof. Dr. Mazhar Osman Mental Health and Neurology Training and Research Hospital, Department of Neurology, Istanbul, Türkiye
[5]Sultan 2. Abdul Hamıd Khan Educatıonal and Research Hospital, Department of Neurology, Istanbul, Türkiye
[6]Bingol State Hospital, Department of Neurosurgery, Bingol, Türkiye
[7]Sisli Hamidiye Etfal Training and Research Hospital, Department of Neurosurgery, Istanbul, Türkiye

Corresponding author: Ozan HASIMOGLU ✉ ozanhasim@hotmail.com

ABSTRACT

AIM: To evaluate the long-term clinical outcomes and histopathological classifications of anterior temporal lobectomy in adult patients with mesial temporal lobe epilepsy (TLE) associated with hippocampal sclerosis.

MATERIAL and METHODS: This was a retrospective study of 168 adult patients diagnosed with drug-resistant mesial temporal lobe epilepsy who underwent resection surgery and were histopathologically confirmed to have hippocampal sclerosis between 2006 and 2025. Preoperative evaluations included video-EEG, high-resolution brain Magnetic Resonance Imaging, neuropsychological tests, and PET-CT. Postoperative outcomes were assessed using the Engel classification. The impact of demographic characteristics, age at epilepsy onset, epilepsy duration, initial precipitating injury, family history, histopathological findings, and diagnostic evaluations on long-term seizure outcomes was evaluated using Kaplan-Meier and multivariate analyses.

RESULTS: Among the 168 patients included in the study, 95.2% achieved Engel Class I seizure freedom in the first year, with a long-term seizure freedom rate of 85.1%. The mean follow-up duration was 117.74 months. Histopathological evaluations revealed that HS-ILAE Type 1 was the most common histopathological classification, (73.8%). Longer preoperative epilepsy duration (p=0.009) and positive family history were risk factors for seizure recurrence (p=0.021). There was no significant association between histopathological classification and seizure control (p>0.05).

CONCLUSION: Anterior temporal lobectomy are effective surgical options for achieving high rates of seizure freedom in patients with mesial TLE associated with hippocampal sclerosis. Longer preoperative epilepsy duration and a positive family history were identified as negative prognostic factors for seizure recurrence. This study makes a significant contribution to the literature, with long-term outcomes of these procedures in a large cohort of adult patients with TLE.

KEYWORDS: Hippocampal sclerosis, Temporal lobe epilepsy, Anterior temporal lobectomy, Amygdalohippocampectomy, Engel classification, Histopathological classification, Outcome

Ozan HASIMOGLU : 0000-0003-1394-5188
Tuba Ozge KARACOBAN : 0009-0007-9219-3864
Taha HANOGLU : 0000-0001-5517-4735
Nur Bahar GEYLAN : 0009-0001-4548-1202
Demet KINAY : 0000-0001-6496-6080
Gunay GUL : 0000-0003-2485-1654
A. Ceyhan DIRICAN : 0000-0002-8658-1568
Murat Mert ATMACA : 0000-0003-2048-4930
Ozan BARUT : 0000-0001-6572-9589
Omer Batu HERGUNSEL : 0000-0003-3143-0575
Bekir TUGCU : 0000-0003-0385-0054

ABBREVIATIONS: EEG: Electroencephalography, **MRI:** Magnetic resonance imaging, **PET:** Positron emission tomography, **CT:** Computed tomography, **NPT:** Neuropsychological testing, **DRE:** Drug-resistant epilepsy, **TLE:** Temporal lobe epilepsy, **HS:** Hippocampal sclerosis, **ILAE:** International league against epilepsy, **FCD:** Focal cortical dysplasia, **SD:** Standard deviation, **SAH:** Subarachnoid hemorrhage, **WAIS:** Wechsler adult intelligence scale, **WMS:** Wechsler memory scale, **MRS:** Magnetic resonance spectroscopy

INTRODUCTION

Epilepsy is a common neurological disorder affecting approximately 1% of the global population, impacting millions of individuals worldwide (47). The quality of life of individuals with epilepsy is significantly compromised, not only by seizures but also by the profound social, economic, and psychological consequences of the condition. Despite being a treatable disorder, a substantial proportion of individuals with epilepsy lack access to appropriate treatment, a phenomenon referred to as the "treatment gap." This disparity is particularly pronounced in developing countries, where the treatment gap can reach as high as 75%. In the United States, approximately 1% of surgical candidates are able to access specialized epilepsy centers (35).

Approximately 20%-30% of epilepsy cases continue to experience seizures despite receiving antiepileptic treatment, including appropriate doses and durations (40). These patients are classified as having drug-resistant epilepsy (DRE), making them ideal candidates for epilepsy surgery. The management of DRE poses a significant challenge, and for this subset of patients, surgical intervention, particularly resective surgery, has emerged as an effective method for achieving seizure control.

Temporal lobe epilepsy (TLE) accounts for a substantial portion of DRE cases and is among the subgroups most responsive to surgical intervention. Notably, hippocampal sclerosis is identified as the primary histopathological cause in nearly 80% of TLE cases, often considered the hallmark of DRE (1,5,12). Characterized by neuronal loss and gliosis, predominantly in the CA1 and CA4 regions, hippocampal sclerosis remains a complex condition with pathophysiological mechanisms that are not yet fully elucidated (2,5). Various factors have been implicated in its development, including febrile convulsions, head trauma, central nervous system infections, and genetic predisposition (6,50).

Epilepsy surgery has emerged as an effective treatment modality for achieving seizure control, particularly in patients with drug-resistant TLE. Surgical procedures commonly employed in this patient population include anterior temporal lobectomy and selective amygdalohippocampectomy (16,38,39). Surgical intervention can achieve complete seizure freedom in 48% -84% of patients, depending on the duration of follow up (15,28,43,45).

The aim of this study was to evaluate the long-term clinical outcomes and histopathological classifications of anterior temporal lobectomy in adult patients with TLE caused by hippocampal sclerosis, with a follow up period spanning nearly two decades. Additionally, the study examined the impact of preoperative evaluation processes, the prognostic significance of histopathological classifications on surgical success, and the insights gained from surgical experience.

MATERIAL and METHODS

Patient Selection and Data Collection

This study was conducted with the approval of the Basaksehir Cam and Sakura City Hospital Ethics Committee under decision number 2025-67. This study includes adult patients diagnosed with drug-resistant mesial temporal lobe epilepsy who underwent resection surgery at Basaksehir Cam and Sakura City Hospital and Bakirkoy Prof. Dr. Mazhar Osman Training and Research Hospital for Psychiatry, Neurology and Neurosurgery and were histopathologically confirmed to have hippocampal sclerosis between 2006 and 2025. A total of 179 patients who underwent anterior temporal lobectomy were initially included. Eight patients were excluded due to a lack of regular follow-up, and three patients were excluded due to death from non-epilepsy-related causes. The most recent status of all patients was verified through teleconferencing.

All patients underwent a comprehensive preoperative evaluation conducted by an experienced local epilepsy surgery council, comprising epileptologists, neurosurgeons, and neuropsychologists. DRE was defined as the persistence of seizures for ≥2 years despite the use of at least two antiepileptic drugs at tolerable doses and appropriate durations. Detailed medical histories were obtained from all patients, investigating potential risk factors for hippocampal sclerosis, such as trauma, febrile convulsions, family history, central nervous system malignancies, and infections.

The comprehensive preoperative evaluation included interictal electroencephalography (EEG), video-EEG monitoring with scalp electrodes, formal neuropsychological testing, and high-resolution magnetic resonance imaging (MRI) performed under an epilepsy protocol. Additional diagnostic modalities such as Wada testing, magnetic resonance spectroscopy, and positron emission tomography (PET), were employed in selected cases. Patients exhibiting a single seizure semiology, corroborated by clinical and electrophysiological recordings from video-EEG and other noninvasive tests, were considered suitable candidates for surgery, provided that these findings converged to lateralize the hypothesized epileptogenic zone. All patients underwent with high-resolution brain MRI using 1.5- or 3-Tesla devices, adhering to epilepsy-specific imaging protocols. The diagnosis of hippocampal sclerosis was confirmed through qualitative MRI assessments performed by the epilepsy surgery team. Hippocampal volume was assessed using T1-weighted sequences, while T2 and FLAIR sequences were examined for increased signal intensity. A standardized neuropsychological test battery was administered preopera-

tively and repeated one year after surgery. This included the Wechsler Adult Intelligence Scale intelligence test, Edinburgh Handedness Inventory, digit span memory test, verbal memory processing test, Wechsler Memory Scale (WMS) story learning test, WMS visual memory subtest, and frontal function assessments including the Wisconsin Card Sorting Test, Stroop test, and verbal fluency test. Furthermore, left hemisphere functions were evaluated through language assessments and visuospatial skills testing using the Benton Facial Recognition Test and Line Orientation Test. Postoperative follow-up evaluations were conducted in the first month, third month, sixth month, first year, and annually thereafter. During these follow-ups, epileptologists were primarily responsible for adjusting or discontinuing antiepileptic medications as necessary.

Histopathological classification was performed adhering to the criteria outlined in the 2013 International League Against Epilepsy (ILAE) Commission consensus report. To ensure consistency, specimens from patients diagnosed with hippocampal sclerosis before 2013 were retrospectively re-evaluated and classified based on these criteria. Hippocampal sclerosis with widespread neuronal loss and gliosis across all regions, with predominant involvement of the CA1 and CA4 segments, was classified as HS-ILAE Type 1. Cases exhibiting predominant neuronal loss in the CA1 region were classified as HS-ILAE Type 2, whereas those with predominant CA4 involvement were classified as HS-ILAE Type 3. Patients with coexisting focal cortical dysplasia were classified as FCD-3A, and cases showing reactive gliosis without accompanying neuronal loss were categorized as no-HS. Specimens that could not be excised en bloc during surgery were classified as fragmented-HS (4).

Postoperative evaluation was conducted using the Engel classification system (17), which categorizes patients into four distinct classes based on their seizure frequency. Specifically, Engel Class I indicates complete seizure freedom or the presence of only auras; Engel Class II indicates rare seizures, occurring only a few times per year; Engel Class III indicates a significant reduction in seizure frequency, despite the persistence of seizures; and Engel Class IV indicates seizures that are unchanged or worse following surgery. Seizures occurring within the first postoperative month were excluded from the analysis, as they may be attributed to the early recovery process or intraoperative exposure to blood products. Demographic and clinical variables, preoperative findings, histopathological classifications, and early postoperative outcomes were subjected to statistical analyses to identify prognostic factors predictive of surgical success. In this study, only patients classified as Engel Class I were considered seizure-free.

Statistical Analysis

Statistical analyses were performed using SPSS version 22, while Kaplan-Meier survival analysis was conducted using Python-based statistical libraries. Continuous variables were presented as mean ± standard deviation, while categorical variables were presented as frequencies and percentages. Chi-square tests were utilized to evaluate the associations between pathological classifications (ILAE) and clinical-demographic variables. Differences between continuous variables and ILAE pathological classifications were assessed using parametric methods for independent groups. Epilepsy duration was defined as the number of years from seizure onset to the time of surgery. Patients were divided into groups based on the epilepsy duration (0–10 years, 11–20 years, 21–30 years, and >30 years) to analyze its association with ILAE pathological classifications. Similarly, epilepsy onset age was categorized into four groups: <5 years, 5–12 years, 13–18 years, and >18 years. The association between onset age and ILAE classification was evaluated using the chi-square test. The normality of continuous variables was assessed using the Shapiro-Wilk test.

Seizure control probabilities over time were calculated using Kaplan–Meier survival analysis, and between-group differences were assessed for statistical significance using the log-rank test. The distribution of patients and seizure recurrence over time intervals was analyzed using categorical classifications, with results presented as percentages.

Additionally, the frequency of postoperative complications was analyzed, and their clinical management was described in detail. Multivariate analyses were performed to identify independent prognostic factors influencing surgical outcomes. A significance threshold of $p<0.05$ was applied for all statistical evaluations.

RESULTS

A total of 168 patients (58.9% female and 41.1% male; mean age: 31.1 years) were included in the study, with a mean postoperative follow-up duration of 117.74 months. The mean age at seizure onset was 13.6 years, and the mean epilepsy duration was 17.6 years. Regarding medical history, 47.6% of patients had a history of febrile convulsions, 25.6% reported head trauma, 8.9% had a history of central nervous system infections, 0.6% had central nervous system malignancies, and 17.9% had a family history of epilepsy.

In terms of laterality, 45.8% of patients (n=77) underwent surgery on the right side and 54.2% (n=91) underwent surgery on the left side. Preoperative MRI examinations were conducted for all patients, revealing right hippocampal sclerosis in 44% (n=74), left hippocampal sclerosis in 52.4% (n=88), normal findings in 3% (n=5), and bilateral findings in 0.6% (n=1). Video-EEG monitoring was also performed on all patients, demonstrating epileptic activity in the right hemisphere in 45.2% (n=76), in the left hemisphere in 54.2% (n=91), and bilaterally in 0.6% (n=1). Neuropsychological tests (NPT) were conducted on 165 patients revealing right-sided dysfunction in 35.2% (n=58), left-sided dysfunction in 40.6% (n=67), normal findings in 6% (n=10), and bilateral dysfunction in 18.2% (n=30). Interictal PET was performed on 96 patients, revealing hypometabolism in the right mesial temporal region in 40.6%, the left mesial temporal region in 55.2%, and normal findings in 4.2%. The concordance rate between MRI and Video-EEG lateralization was 94.64% (n=159). Among these, 64.29% of patients (n=108) showed concordance between MRI, Video-EEG, and NPT lateralization, while 33.33% (n=56) exhibit-

ed concordance across MRI, Video-EEG, NPT, and PET findings (Table I). Postoperative complications occurred in 4.76% of patients. One patient required a second surgery the day after the initial operation to remove a retained surgical pad; one patient developed a subcutaneous infection that was successfully treated with wound debridement and antibiotic therapy; one patient underwent epidural hematoma drainage on the evening of surgery and recovered without sequelae. Other complications included otorrhea caused by surgical trauma to the external auditory canal, which resolved with medical treatment, and a subarachnoid hemorrhage (SAH) that healed without sequelae under clinical observation. Additionally, one patient developed foot drop of unknown etiology, which improved with physiotherapy, and another patient experienced carbamazepine-induced hyponatremia that resolved with medical treatment and medication change. Lastly, one patient underwent surgery two weeks postoperatively due to a suspected intracranial abscess caused by a cystic lesion; however, no abscess was found, and the patient was placed under follow-up.

Prognostic Variables

At the 1-year follow-up, 95.2% of patients were classified as Engel Class I, indicating complete seizure freedom or the presence of auras. Additionally, 1.8% of patients were classified as Engel Class II, 1.2% as Engel Class III, and 1.8% as Engel Class IV. In the long-term follow-up, 85.1% of patients maintained their Engel Class I status, while 10.7% were classified as Engel Class II, 3.6% as Engel Class III, and 0.6% as Engel Class IV (Figure 1). No statistically significant relation-

Table I: Clinical and Demographic Summary

Characteristic	Value
Age (Mean ± SD) (years)	31.1 ± 9.2
Gender; M, F (%)	41.1, 58.9
Epilepsy Onset Age (Mean ± SD) (years)	13.6 ± 9
Epilepsy Duration (Mean ± SD) (years)	17.6 ± 9.9
Follow-Up Duration (Mean ± SD) (months)	117.74 ± 64.99
Febrile Seizures (n)	80
Trauma (n)	43
Infection (n)	15
Malignancy (n)	1
Family History (n)	30
MTS Side [R; L (%)]	45.8; 54.2
MR Lateralization [(R; L; N; B (%)]	44.0; 52.4; 3.0; 0.6
Video EEG Lateralization [R; L; B (%)]	45.2; 54.2; 0.6
PET Lateralization [R; L; N (%)]	40.6; 55.2; 4.2
NPT Lateralization [R; L; N; B (%)]	35.2; 40.6; 6; 18.2

R: *Right,* ***L:*** *Left,* ***B:*** *Bilateral,* ***N:*** *Normal,* ***SD:*** *Standard deviation,* ***EEG:*** *Electroencephalography,* ***MRI:*** *Magnetic resonance imaging,* ***PET:*** *Positron emission tomography,* ***NPT:*** *Neuropsychological testing,* ***M:*** *male,* ***F:*** *female.*

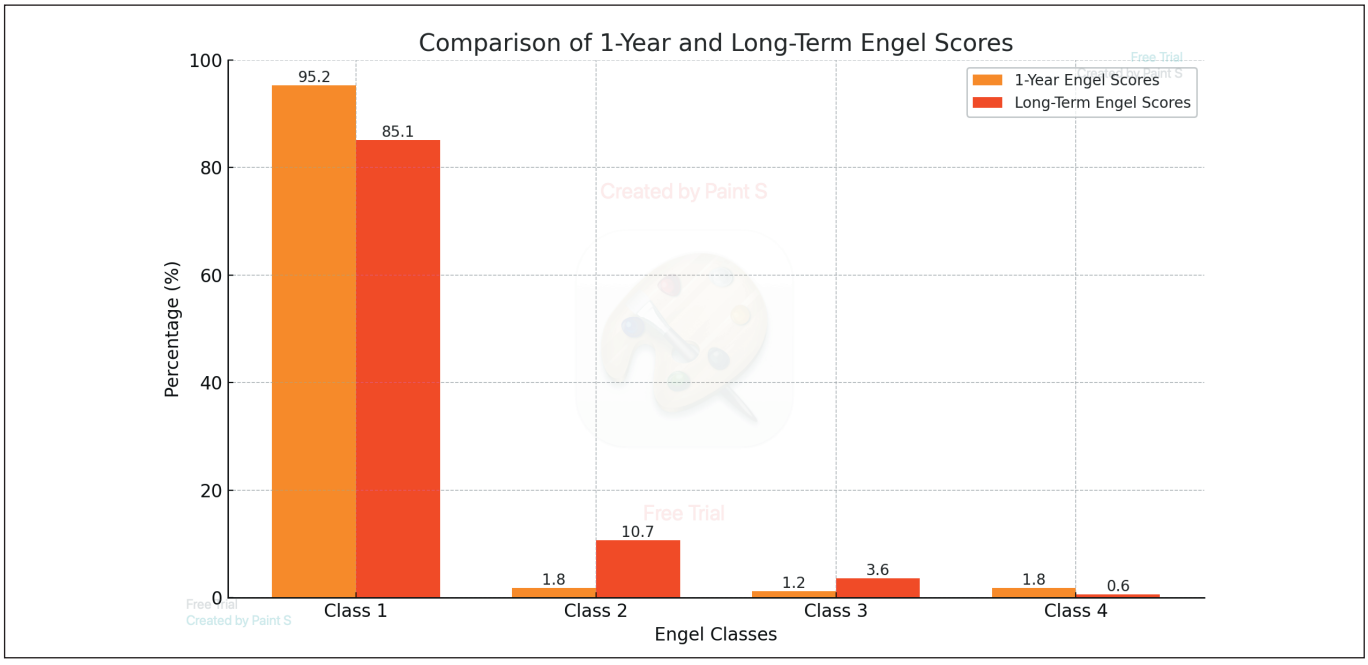

Figure 1: This figure illustrates the distribution of Engel scores at the 1-year follow-up and the long-term follow-up. The scores are categorized to evaluate seizure outcomes over time, providing a visual comparison of the immediate and sustained effects of the intervention. The chart highlights the proportion of patients achieving favorable seizure control (Engel Class I) and those with less optimal outcomes (Engel Classes II-IV) in both time frames.

ship was found between early or long-term Engel scores and any of the demographic or clinical variables analyzed.

A total of 26 patients (15.5%) experienced seizure recurrence or incomplete seizure control (Engel Classes II-IV). The average time to seizure recurrence after surgery was 27.9 months. Notably, 11.3% of patients who were seizure-free during the first year postoperatively experienced recurrence afterward (Figure 2). The relationship between age and seizure recurrence was evaluated using logistic regression analysis, which showed no statistically significant effect of age (p=0.061). Additionally, no significant association was observed between sex and seizure recurrence (p=0.221).

Analysis of the relationship between epilepsy onset age and seizure recurrence revealed no significant difference between early- and late-onset (p=0.717). However, analysis of epilepsy duration revealed a significant association between seizure recurrence and preoperative epilepsy duration (p=0.009). Patients with a longer duration of DRE before surgery had

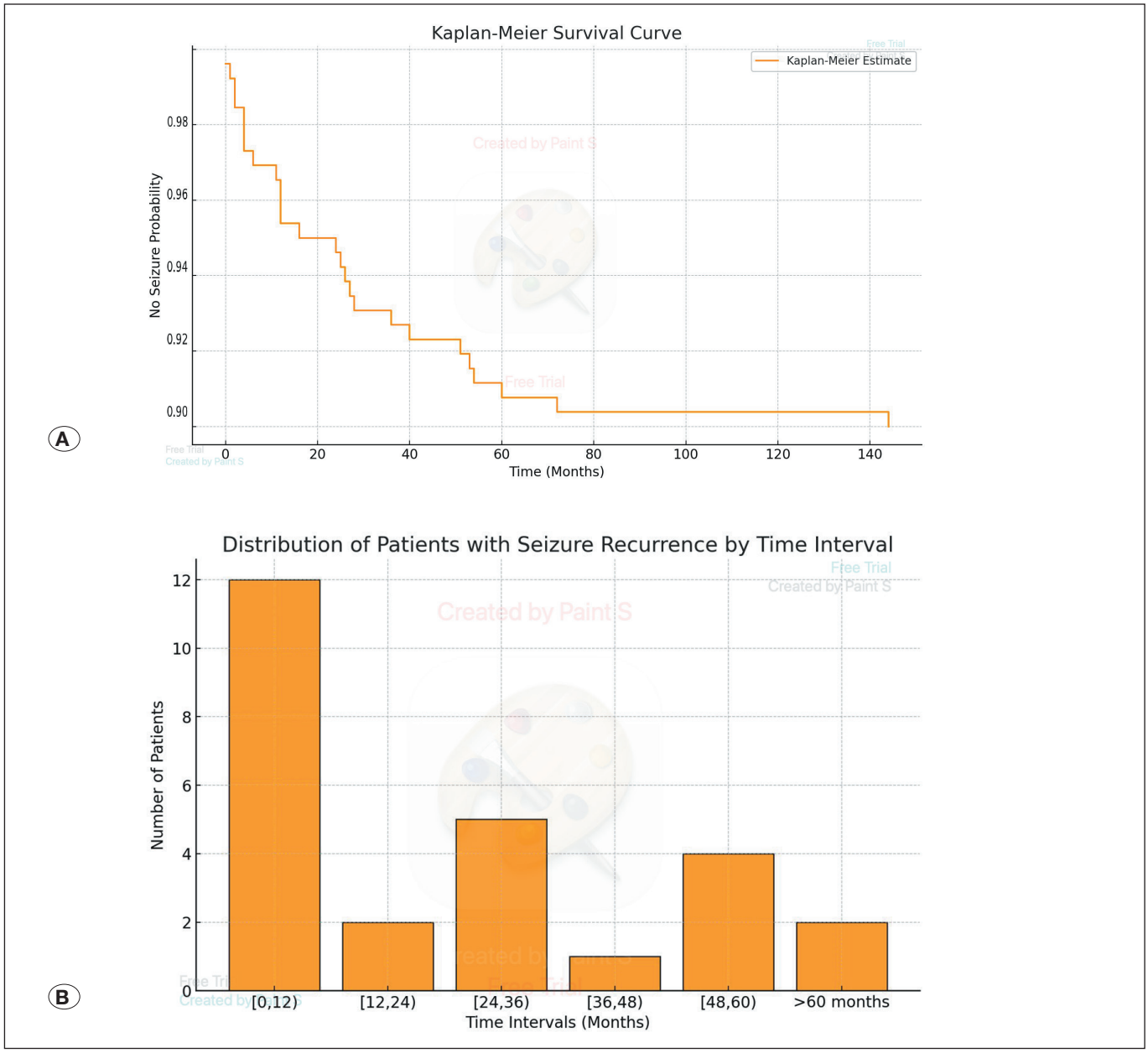

Figure 2: This composite figure combines two graphical representations related to seizure outcomes and patient follow-up. **A)** Kaplan-Meier Curve: This panel illustrates the seizure-free probability over time following surgical intervention. The x-axis represents the months since surgery, and the y-axis indicates the probability of remaining seizure-free. The stepwise declines in the curve reflect the occurrence of seizure recurrence events, providing a temporal overview of long-term seizure control among patients. **B)** Patient Distribution by Time Intervals: This panel displays the percentage distribution of patients across follow-up intervals. The x-axis categorizes patients into time intervals (in months), while the y-axis shows the proportion of the total patient population.

significantly lower postoperative seizure freedom rates. There was no significant association between a history of febrile convulsions, infections, trauma, or malignancy and seizure recurrence. However, family history was a significant risk factor for seizure recurrence (p=0.021). Concordance between MRI, video-EEG, PET, and NPT lateralization findings regarding hippocampal sclerosis showed no significant association with seizure recurrence (p=0.327). Concordance between these diagnostic modalities did not appear to influence postoperative seizure control outcomes.

Histopathological Evaluation

Histopathological classification of hippocampal sclerosis revealed that the majority of patients were categorized as HS-ILAE Type 1 (73.8%), followed by HS-ILAE Type 2 (17.3%) and Fragmented-HS (7.1%). HS-ILAE Type 3 (1.8%) was the least common classification. This classification was based on the criteria outlined in the ILAE report. Dual pathology was most frequently observed as FCD-3A, occurring in 3.57% of patients. Additionally, three patients (1.79%) were diagnosed with ganglioglioma, and one patient (0.60%) had low-grade astrocytoma in the neocortical resection specimen alongside hippocampal sclerosis. Analysis of HS-ILAE classifications by age group revealed that HS-ILAE Type 1 was the most prevalent classification across all age groups. Notably, no significant relationship was found between age groups and ILAE classifications (p=0.843). Similarly, sex showed no signification association with ILAE classifications (p=0.071). Additionally, the relationship between epilepsy onset age and ILAE classifications was not statistically significant (p=0.435). However, epilepsy duration showed a significant association with HS-ILAE classifications (p=0.044), with HS-ILAE Type 1 being more commonly observed in patients with longer epilepsy duration. An analysis of the relationship between the side of mesial temporal sclerosis (MTS) and ILAE classifications revealed a borderline significant association (p=0.054). Notably, HS-ILAE Type 1 was more frequently observed in patients with left-sided MTS, while HS-ILAE Type 2 was more common in right-sided MTS. No significant associations were identified between initial precipitating injuries (e.g., febrile seizures, trauma, infections, malignancies, or family history) and ILAE pathological classifications (p>0.05). Furthermore, ILAE pathological classifications showed no significant association with postoperative seizure freedom (p=0.166) (Table II).

DISCUSSION

This study evaluated the long-term clinical outcomes and histopathological classifications of anterior temporal lobectomy in patients with TLE caused by hippocampal sclerosis. With a follow-up period of approximately 20 years and a large cohort of 168 patients, our study provides a robust and comprehensive dataset that surpasses similar studies in the literature. All surgeries were performed by the same surgical team, ensuring a homogenous patient group. This study offers an extensive evaluation of long-term follow-up results, epilepsy-related factors, surgical nuances, and histopathological findings.

In our study, 95.1% of patients achieved Engel Class I seizure freedom (complete seizure freedom) at the 1-year follow-up, and this rate was maintained at 85.2% in the long-term follow-up. In a meta-analysis of randomized controlled trials by Lee et al., the average rate of complete seizure freedom following surgery for adult TLE was 72.4% (29). Studies conducted independently of surgical technique have reported that patients undergoing surgery for hippocampal sclerosis-associated TLE, a more homogenous subgroup, achieved seizure freedom rates of 86-90% during the first two years of follow-up (13,33,37,44,45). However, these rates decline to 62-83% in follow-ups exceeding five years (13,24,32,51). Our results exceed the rates reported in previous studies. The superior seizure control rates in our study may be attributed to several factors. A meta-analysis by McIntosh et al. revealed worse outcomes in series that included cases without radiological or histopathological lesions (33). In our cohort, all patients had histopathological confirmation of hippocampal sclerosis, and

Table II: Clinical and Demographic Characteristics by ILAE Pathology Types

	HS-ILAE Type 1	HS-ILAE Type 2	HS-ILAE Type 3	Fragmented-HS
Age (Mean, SD) (years)	31.05 (9.63)	30.93 (8.06)	34.33 (9.87)	31.92 (8.36)
Gender; F, M (%)	60.0; 40.0	69.0; 30.0	0.0; 100.0	42.0; 58.0
Epilepsy Onset Age (Mean, SD) (years)	12.76 (8.50)	17.24 (9.99)	11.67 (8.08)	13.42 (9.95)
Epilepsy Duration (Mean, SD) (years)	18.31 (9.91)	13.69 (9.52)	22.67 (17.24)	18.42 (7.45)
Febrile (%)	51.61	34.48	66.67	33.33
Trauma (%)	28.23	20.69	0.00	16.67
Infection (%)	8.06	6.90	0.00	25.00
Malignancy (%)	0.81	0.00	0.00	0.00
Family History (%)	17.74	20.69	33.33	8.33
MTS Side L; R (%)	57; 43	34; 66	100; 0	58; 42

***R:** Right, **L:** Left, **SD:** Standard Deviation, **HS-ILAE:** International League Against Epilepsy classification system for hippocampal sclerosis.*

97% had corresponding findings on MRI. Additionally, all cases in our series exhibited focal semiological and electrophysiological findings pointing to the hypothesized epileptogenic side. In the study by Siegel et al., focal epileptiform activity concordant with MRI-detected lesions was a predictor of favorable prognosis (41). Although not statistically significant, the large proportion of patients in our series with concordant radiological, electrophysiological, and neuropsychological findings suggesting the same epileptogenic focus likely contributed to the favorable outcomes. Similar concordance-related findings have been linked to good seizure control in previous studies (16,22). Lastly, increasing surgical experience appears to play a critical role in improving outcomes. In our earlier series with less experience, Engel Class I seizure freedom rates were 84% at 1 year and 68.8% at 5 years (49). Over the past 15 years, advances in patient selection and surgical expertise have likely contributed to the improved outcomes observed. Although anterior temporal lobectomy are well-established procedures, attaining consistent and safe surgical outcomes necessitates navigating an adequate learning curve (20,42). Mastery of anatomical knowledge, refined subpial dissection techniques, and precise resection boundaries significantly enhance surgical success with growing experience. Consistent with this, previous studies have demonstrated that total or extended resections can effectively achieve better seizure control, highlighting the importance of surgical precision and expertise in optimizing patient outcomes (10,18,53).

Studies have consistently shown that the majority of seizure recurrences occur within the first two years after surgery (7,27,45). For instance, Yoon et al. reported that 17% of patients who were seizure-free in the first year experienced recurrence within five years, and 30% experienced recurrence within ten years. Similarly, another study found a 14% recurrence rate within the first five years (33,52). In the present study, 15.5% of patients who achieved seizure freedom in the first year experienced seizure recurrence, with an average time to recurrence of 27.9 months. After the fifth year, the seizure recurrence rate significantly declined (Figure 2), aligning with the trends observed in the literature. Of note, all patients who experienced seizure recurrence after the first year were classified as Engel Class II or III, implying that their seizure frequency remained significantly reduced compared to the preoperative period (Figure 1).

In our series, the risk factors for seizure recurrence included a longer preoperative epilepsy duration and a family history of epilepsy. There is no clear consensus on the relationship between epilepsy duration and seizure recurrence in the literature. While some studies have reported a similar association, others have found no significant relationship (14,17,19,28). Prolonged epilepsy duration may promote the development of secondary epileptic foci, thereby increasing the risk of recurrence (26). Long-standing epilepsy has been shown to cause structural changes, such as bilateral hippocampal volume reduction and altered glucose metabolism (29). potentially triggering ipsilateral or contralateral epileptogenesis (25). However, no previous studies have established a clear link between a family history of epilepsy and seizure recurrence. This may be related to the genetic basis of familial epilepsy. Further research incorporating genetic evaluations is required to address this question. There is a consensus that age, epilepsy onset age, sex, and the side of resection do not significantly influence surgical outcomes (31,34,48,53). In our series, we observed no significant relationship between initial precipitating injuries (including febrile convulsions, central nervous system infections, malignancies, and head trauma) and surgical outcomes. This finding appears consistent with the existing literature (28). However, some studies have reported an association between prolonged febrile convulsions and favorable outcomes (33,48).

Another focus of our study was to investigate the etiological and prognostic implications of the histopathological hippocampal sclerosis classification proposed by the ILAE in 2013 (4). Given the relatively recent introduction of this classification system, long-term follow-up studies incorporating this framework are scarce in the literature. The re-evaluation and reclassification of previously collected surgical specimens according to the ILAE criteria enabled us to conduct these assessments. Consistent with existing literature, HS-ILAE Type 1 was the most common histopathological subtype identified in our cohort (21,23,46). Our study found no significant association between histopathological subtypes and factors such as age, sex, or initial precipitating injury. This finding aligns with some previous studies (9,21). However, other studies have identified associations between specific events, such as early-onset febrile seizures, and histopathological subtypes (36). In patients with a longer epilepsy duration, HS-ILAE Type 1 was more frequently observed. This finding remains controversial. Na et al. attributed this association to the vulnerability of the CA1 subfield (36). Prolonged epilepsy is expected to cause widespread neuronal loss across all Cornu Ammonis regions, a finding supported by some studies but refuted by others (8). Finally, our study found no significant association between histopathological subtypes and surgical outcomes. This topic remains contentious, with most studies failing to detect a strong correlation between subtypes and outcomes. However, some studies suggest that Type 1 may be associated with better seizure control (3,11,21,36). More robust studies with homogenous datasets are required to validate these findings.

Limitations

Some limitations of this study should be considered while interpreting the findings. First, its retrospective design inherently introduces methodological constraints in data collection and evaluation. Additionally, the relationship between seizure types, genetics, and surgical outcomes was not explored. Moreover, psychiatric and cognitive outcomes were beyond the scope of this research.

Furthermore, electrophysiological evaluations were limited to non-invasive methods, and only cases that did not require invasive electrophysiology were included, focusing on safer patients. This approach reduced the opportunity to evaluate outcomes in more complex cases. Although no patients in our series underwent invasive EEG evaluations, such cases are not uncommon among drug-resistant epilepsy populations. The lack of detailed presentation of electrophysiological findings

also restricted the ability to investigate potential correlations between surgical outcomes and electrophysiological data.

Despite these limitations, our study offers valuable insights due to its extended long-term follow-up, sizable cohort, and comprehensive evaluation processes. Future studies addressing these limitations can yield more robust findings.

CONCLUSION

This study comprehensively evaluated long-term clinical outcomes and histopathological classifications of anterior temporal lobectomy in adult patients with TLE caused by hippocampal sclerosis. With an extended follow-up period of nearly 20 years and a large, homogenous cohort of 168 patients, our study provides a significant reference in the field of epilepsy surgery. A notable strength of our research is its multifaceted approach to assessing DRE in adult patients, offering a broad perspective from preoperative evaluations to postoperative outcomes. The study also presents an in-depth analysis of the relationship between histopathological classifications and clinical outcomes. The high seizure freedom rates observed during long-term follow-up (85.1%) and the detailed analysis of prognostic factors underscore the efficacy of surgical intervention.

In conclusion, our study highlights the importance of evaluating the impact of histopathological classifications on clinical outcomes and conducting multidimensional assessments of surgical success. These findings significantly contribute to informed patient selection and the development of tailored surgical strategies in epilepsy surgery. Future studies with more homogeneous datasets are necessary to validate these findings and further refine the understanding of the complex relationships between histopathological classifications, clinical outcomes, and surgical success.

Declarations

Funding: This research did not receive any specific grant from funding agencies in the public, commercial, or not-for-profit sectors.

Availability of data and materials: The datasets generated and/or analyzed during the current study are available from the corresponding author by reasonable request.

Disclosure: The authors declare no competing interests.

AUTHORSHIP CONTRIBUTION

Study conception and design: OH, TOK, TH
Data collection: NBG, OB, MMA, TOK, TH
Analysis and interpretation of results: OH, TOK, TH, NBH, OBH
Draft manuscript preparation: DK, GG, ACD, BT
Critical revision of the article: OBH, BT
Other (study supervision, fundings, materials, etc...): BT
All authors (OH, TOK, NBG, OB, MMA, TH, OBH, DK, GG, ACD, BT) reviewed the results and approved the final version of the manuscript.

REFERENCES

1. Blair RDG: Temporal lobe epilepsy semiology. Epilepsy Res Treat 2012:751510, 2012. https://doi.org/10.1155/2012/751510
2. Blümcke I, Coras R, Miyata H, Ozkara C: Defining clinico-neuropathological subtypes of mesial temporal lobe epilepsy with hippocampal sclerosis. Brain Pathol 22:402-411, 2012. https://doi.org/10.1111/j.1750-3639.2012.00583.x
3. Blümcke I, Pauli E, Clusmann H, Schramm J, Becker A, Elger C, Merschhemke M, Meencke HJ, Lehmann T, von Deimling A, Scheiwe C, Zentner J, Volk B, Romstock J, Stefan H, Hildebrandt M: A new clinico-pathological classification system for mesial temporal sclerosis. Acta Neuropathol 113:235-244, 2007. https://doi.org/10.1007/s00401-006-0187-0
4. Blümcke I, Thom M, Aronica E, Armstrong DD, Bartolomei F, Bernasconi A, Bernasconi N, Bien CG, Cendes F, Coras R, Cross JH, Jacques TS, Kahane P, Mathern GW, Miyata H, Moshe SL, Oz B, Ozkara C, Perucca E, Sisodiya S, Wiebe S, Spreafico R: International consensus classification of hippocampal sclerosis in temporal lobe epilepsy: A Task Force report from the ILAE commission on diagnostic methods. Epilepsia 54:1315-1329, 2013. https://doi.org/10.1111/epi.12220
5. Blümcke I, Thom M, Wiestler OD: Ammon's horn sclerosis: A maldevelopmental disorder associated with temporal lobe epilepsy. Brain Pathol 12:199-211, 2002. https://doi.org/10.1111/j.1750-3639.2002.tb00436.x
6. Cendes F, Sakamoto AC, Spreafico R, Bingaman W, Becker AJ: Epilepsies associated with hippocampal sclerosis. Acta Neuropathol 128:21-37, 2014. https://doi.org/10.1007/s00401-014-1292-0
7. Chen H, Modur PN, Barot N, Van Ness PC, Agostini MA, Ding K, Gupta P, Hays R, Mickey B: Predictors of postoperative seizure recurrence: A longitudinal study of temporal and extratemporal resections. Epilepsy Res Treat 2016:7982494, 2016. https://doi.org/10.1155/2016/7982494
8. Davies KG, Hermann BP, Dohan FC Jr, Foley KT, Bush AJ, Wyler AR: Relationship of hippocampal sclerosis to duration and age of onset of epilepsy, and childhood febrile seizures in temporal lobectomy patients. Epilepsy Res 24:119-126, 1996. https://doi.org/10.1016/0920-1211(96)00008-3
9. de Lanerolle NC, Kim JH, Williamson A, Spencer SS, Zaveri HP, Eid T, Spencer DD: A retrospective analysis of hippocampal pathology in human temporal lobe epilepsy: Evidence for distinctive patient subcategories. Epilepsia 44:677-687, 2003. https://doi.org/10.1046/j.1528-1157.2003.32701.x
10. de Tisi J, Bell GS, Peacock JL, McEvoy AW, Harkness WF, Sander JW, Duncan JS: The long-term outcome of adult epilepsy surgery, patterns of seizure remission, and relapse: A cohort study. Lancet 378:1388-1395, 2011. https://doi.org/10.1016/S0140-6736(11)60890-8
11. Deleo F, Garbelli R, Milesi G, Gozzo F, Bramerio M, Villani F, Cardinale F, Tringali G, Spreafico R, Tassi L: Short- and long-term surgical outcomes of temporal lobe epilepsy associated with hippocampal sclerosis: Relationships with neuropathology. Epilepsia 57:306-315, 2016. https://doi.org/10.1111/epi.13277

12. Duarte JTC, Jardim AP, Comper SM, De Marchi LR, Gaça LB, Garcia MTFC, Sandim GB, Assunção-Leme IB, Carrete Jr H, Centeno RS: The impact of epilepsy duration in a series of patients with mesial temporal lobe epilepsy due to unilateral hippocampal sclerosis. Epilepsy Research 147:51-57, 2018. https://doi.org/10.1016/j.eplepsyres.2018.08.009
13. Dupont S, Tanguy ML, Clemenceau S, Adam C, Hazemann P, Baulac M: Long-term prognosis and psychosocial outcomes after surgery for MTLE. Epilepsia 47:2115-2124, 2006. https://doi.org/10.1111/j.1528-1167.2006.00852.x
14. Elsharkawy AE, Alabbasi AH, Pannek H, Oppel F, Schulz R, Hoppe M, Hamad AP, Nayel M, Issa A, Ebner A: Long-term outcome after temporal lobe epilepsy surgery in 434 consecutive adult patients. J Neurosurg 110:1135-1146, 2009. https://doi.org/10.3171/2008.6.JNS17613
15. Engel J Jr, McDermott MP, Wiebe S, Langfitt JT, Stern JM, Dewar S, Sperling MR, Gardiner I, Erba G, Fried I, Jacobs M, Vinters HV, Mintzer S, Kieburtz K, Early Randomized Surgical Epilepsy Trial Study G: Early surgical therapy for drug-resistant temporal lobe epilepsy: A randomized trial. JAMA 307:922-930, 2012. https://doi.org/10.1001/jama.2012.220
16. Engel J Jr, Wiebe S, French J, Sperling M, Williamson P, Spencer D, Gumnit R, Zahn C, Westbrook E, Enos B, Quality Standards Subcommittee of the American Academy of N, American Epilepsy S, American Association of Neurological S: Practice parameter: Temporal lobe and localized neocortical resections for epilepsy: Report of the quality standards subcommittee of the American Academy of Neurology, in association with the American Epilepsy Society and the American Association of Neurological Surgeons. Neurology 60:538-547, 2003. https://doi.org/10.1212/01.wnl.0000055086.35806.2d
17. Engel Jr J, Van Ness P, Rasmussen T, Ojemann L: Outcome with respect to epileptic seizures. In: Engel J Jr (ed), Surgical Treatment of the Epilepsies, 2nd ed. New York: Raven Press, 1993
18. Englot DJ, Berger MS, Barbaro NM, Chang EF: Predictors of seizure freedom after resection of supratentorial low-grade gliomas. A review. J Neurosurg 115:240-244, 2011. https://doi.org/10.3171/2011.3.JNS1153
19. Englot DJ, Breshears JD, Sun PP, Chang EF, Auguste KI: Seizure outcomes after resective surgery for extra–temporal lobe epilepsy in pediatric patients: A systematic review. J Neurosurg Pediatr 12:126-133, 2013. https://doi.org/10.3171/2013.5.PEDS1336
20. Falconer MA, Meyer A, Hill D, Mitchell W, Pond DA: Treatment of temporal-lobe epilepsy by temporal lobectomy; a survey of findings and results. Lancet 268:827-835, 1955. https://doi.org/10.1016/s0140-6736(55)90421-9
21. Gales JM, Jehi L, Nowacki A, Prayson RA: The role of histopathologic subtype in the setting of hippocampal sclerosis-associated mesial temporal lobe epilepsy. Hum Pathol 63:79-88, 2017. https://doi.org/10.1016/j.humpath.2017.02.013
22. Harkness W: Temporal lobe resections. Childs Nerv Syst 22:936-944, 2006. https://doi.org/10.1007/s00381-006-0140-5
23. Hasimoglu O, Barut O, Kapar MO, Hergunsel OB, Kinay D, Gul G, Dirican AC, Bilgic B, Tugcu B: Relation between ilae hippocampal sclerosis classification and clinical findings in temporal lobe epilepsy. Turk Neurosurg 31:404-411, 2021. https://doi.org/10.5137/1019-5149.JTN.32026-20.1
24. Hemb M, Palmini A, Paglioli E, Paglioli EB, Costa da Costa J, Azambuja N, Portuguez M, Viuniski V, Booij L, Nunes ML: An 18-year follow-up of seizure outcome after surgery for temporal lobe epilepsy and hippocampal sclerosis. J Neurol Neurosurg Psychiatry 84:800-805, 2013. https://doi.org/10.1136/jnnp-2012-304038
25. Hennessy MJ, Elwes RD, Binnie CD, Polkey CE: Failed surgery for epilepsy. A study of persistence and recurrence of seizures following temporal resection. Brain 123 Pt 12:2445-2466, 2000. https://doi.org/10.1093/brain/123.12.2445
26. Janszky J, Janszky I, Schulz R, Hoppe M, Behne F, Pannek HW, Ebner A: Temporal lobe epilepsy with hippocampal sclerosis: Predictors for long-term surgical outcome. Brain 128:395-404, 2005. https://doi.org/10.1093/brain/awh358
27. Jeha LE, Najm IM, Bingaman WE, Khandwala F, Widdess-Walsh P, Morris HH, Dinner DS, Nair D, Foldvary-Schaeffer N, Prayson RA, Comair Y, O'Brien R, Bulacio J, Gupta A, Luders HO: Predictors of outcome after temporal lobectomy for the treatment of intractable epilepsy. Neurology 66:1938-1940, 2006. https://doi.org/10.1212/01.wnl.0000219810.71010.9b
28. Jobst BC, Cascino GD: Resective epilepsy surgery for drug-resistant focal epilepsy: A review. JAMA 313:285-293, 2015. https://doi.org/10.1001/jama.2014.17426
29. Jokeit H, Ebner A, Arnold S, Schuller M, Antke C, Huang Y, Steinmetz H, Seitz RJ, Witte OW: Bilateral reductions of hippocampal volume, glucose metabolism, and wada hemispheric memory performance are related to the duration of mesial temporal lobe epilepsy. J Neurol 246:926-933, 1999. https://doi.org/10.1007/s004150050484
30. Lee AT, Burke JF, Chunduru P, Molinaro AM, Knowlton R, Chang EF: A historical cohort of temporal lobe surgery for medically refractory epilepsy: A systematic review and meta-analysis to guide future nonrandomized controlled trial studies. J Neurosurg 133:71-78, 2020. https://doi.org/10.3171/2019.4.JNS183235
31. Lerner JT, Salamon N, Hauptman JS, Velasco TR, Hemb M, Wu JY, Sankar R, Donald Shields W, Engel J, Jr., Fried I, Cepeda C, Andre VM, Levine MS, Miyata H, Yong WH, Vinters HV, Mathern GW: Assessment and surgical outcomes for mild type I and severe type II cortical dysplasia: A critical review and the UCLA experience. Epilepsia 50:1310-1335, 2009. https://doi.org/10.1111/j.1528-1167.2008.01998.x
32. Mathon B, Bedos Ulvin L, Adam C, Baulac M, Dupont S, Navarro V, Cornu P, Clemenceau S: Surgical treatment for mesial temporal lobe epilepsy associated with hippocampal sclerosis. Rev Neurol (Paris) 171:315-325, 2015. https://doi.org/10.1016/j.neurol.2015.01.561
33. McIntosh AM, Kalnins RM, Mitchell LA, Fabinyi GC, Briellmann RS, Berkovic SF: Temporal lobectomy: Long-term seizure outcome, late recurrence and risks for seizure recurrence. Brain 127:2018-2030, 2004. https://doi.org/10.1093/brain/awh221

34. McIntosh AM, Wilson SJ, Berkovic SF: Seizure outcome after temporal lobectomy: Current research practice and findings. Epilepsia 42:1288-1307, 2001. https://doi.org/10.1046/j.1528-1157.2001.02001.x
35. Meyer AC, Dua T, Ma J, Saxena S, Birbeck G: Global disparities in the epilepsy treatment gap: A systematic review. Bull World Health Organ 88:260-266, 2010. https://doi.org/10.2471/BLT.09.064147
36. Na M, Ge H, Shi C, Shen H, Wang Y, Pu S, Liu L, Wang H, Xie C, Zhu M, Wang J, Shi C, Lin Z: Long-term seizure outcome for international consensus classification of hippocampal sclerosis: A survival analysis. Seizure 25:141-146, 2015. https://doi.org/10.1016/j.seizure.2014.10.006
37. Nayel MH, Awad IA, Luders H: Extent of mesiobasal resection determines outcome after temporal lobectomy for intractable complex partial seizures. Neurosurgery 29:55-60; discussion 60-51, 1991. https://doi.org/10.1097/00006123-199107000-00009
38. Noachtar S, Borggraefe I: Epilepsy surgery: A critical review. Epilepsy Behav 15:66-72, 2009. https://doi.org/10.1016/j.yebeh.2009.02.028
39. Ryvlin P, Cross JH, Rheims S: Epilepsy surgery in children and adults. Lancet Neurol 13:1114-1126, 2014. https://doi.org/10.1016/S1474-4422(14)70156-5
40. Schuele SU, Luders HO: Intractable epilepsy: Management and therapeutic alternatives. Lancet Neurol 7:514-524, 2008. https://doi.org/10.1016/S1474-4422(08)70108-X
41. Siegel AM, Cascino GD, Meyer FB, McClelland RL, So EL, Marsh WR, Scheithauer BW, Sharbrough FW: Resective reoperation for failed epilepsy surgery: Seizure outcome in 64 patients. Neurology 63:2298-2302, 2004. https://doi.org/10.1212/01.wnl.0000147476.86575.a7
42. Spencer DD, Spencer SS, Mattson RH, Williamson PD, Novelly RA: Access to the posterior medial temporal lobe structures in the surgical treatment of temporal lobe epilepsy. Neurosurgery 15:667-671, 1984. https://doi.org/10.1227/00006123-198411000-00005
43. Spencer S, Huh L: Outcomes of epilepsy surgery in adults and children. Lancet Neurol 7:525-537, 2008. https://doi.org/10.1016/S1474-4422(08)70109-1
44. Tanriverdi T, Dudley RW, Hasan A, Al Jishi A, Al Hinai Q, Poulin N, Colnat-Coulbois S, Olivier A: Memory outcome after temporal lobe epilepsy surgery: Corticoamygdalohippocampectomy versus selective amygdalohippocampectomy. J Neurosurg 113:1164-1175, 2010. https://doi.org/10.3171/2009.10.JNS09677
45. Tellez-Zenteno JF, Dhar R, Wiebe S: Long-term seizure outcomes following epilepsy surgery: A systematic review and meta-analysis. Brain 128:1188-1198, 2005. https://doi.org/10.1093/brain/awh449
46. Thom M, Liagkouras I, Elliot KJ, Martinian L, Harkness W, McEvoy A, Caboclo LO, Sisodiya SM: Reliability of patterns of hippocampal sclerosis as predictors of postsurgical outcome. Epilepsia 51:1801-1808, 2010. https://doi.org/10.1111/j.1528-1167.2010.02681.x
47. Tian N, Boring M, Kobau R, Zack MM, Croft JB: Active epilepsy and seizure control in adults - United States, 2013 and 2015. MMWR Morb Mortal Wkly Rep 67:437-442, 2018. https://doi.org/10.15585/mmwr.mm6715a1
48. Tonini C, Beghi E, Berg AT, Bogliun G, Giordano L, Newton RW, Tetto A, Vitelli E, Vitezic D, Wiebe S: Predictors of epilepsy surgery outcome: A meta-analysis. Epilepsy Res 62:75-87, 2004. https://doi.org/10.1016/j.eplepsyres.2004.08.006
49. Tugcu B, Gungor A, Akpinar A, Kinay D, Kuscu DY, Gul G, Kayrak N, Keskinkilic C, Akdemir H, Emel E: Outcome of surgical treatment of hippocampal sclerosis from relatively new epilepsy surgery center. J Neurosurg Sci 60:159-168, 2016.
50. Walker MC: Hippocampal sclerosis: Causes and prevention. Seminars in Neurology, vol 35. Thieme Medical Publishers, 2015:193-200
51. Wieser HG, Ortega M, Friedman A, Yonekawa Y: Long-term seizure outcomes following amygdalohippocampectomy. J Neurosurg 98:751-763, 2003. https://doi.org/10.3171/jns.2003.98.4.0751
52. Yoon HH, Kwon H, Mattson R, Spencer D, Spencer S: Long-term seizure outcome in patients initially seizure-free after resective epilepsy surgery. Neurology 61:445-450, 2003. https://doi.org/10.1212/01.wnl.0000081226.51886.5b
53. Zhang J, Liu W, Chen H, Xia H, Zhou Z, Mei S, Liu Q, Li Y: Identification of common predictors of surgical outcomes for epilepsy surgery. Neuropsychiatr Dis Treat 9:1673-1682, 2013. https://doi.org/10.2147/NDT.S53802

Turk Neurosurg 36(3):450-456, 2026
DOI: 10.5137/1019-5149.JTN.49617-25.5

Original Investigation
Pediatrics

Received: 27.08.2025
Accepted: 06.01.2026
Published Online: 22.05.2026

Brain Metastases in Pediatric Extracranial Solid Tumors: A 20-Year Experience in Challenging a Rare Diagnosis

Dilek GUL[1], Burcu TUFAN TAS[2], Adnan DAGCINAR[3], Zerrin OZGEN[4], Beste M. ATASOY[4]

[1]MH-Marmara University Hospital, Radiation Oncology Clinic, Istanbul, Türkiye
[2]MH-Marmara University Hospital, Pediatric Hematology Oncology Clinic, Istanbul, Türkiye
[3]Marmara University School of Medicine, Department of Neurosurgery, Istanbul, Türkiye
[4]Marmara University School of Medicine, Department of Radiation Oncology, Istanbul, Türkiye

Corresponding author: Beste ATASOY ✉ bmatasoy@yahoo.com

ABSTRACT

AIM: To investigate the clinical features, treatments, and outcomes of pediatric patients with brain metastasis from extracranial solid tumors, which has been known as a rare condition.

MATERIAL and METHODS: Over a 20-year period, 520 children treated for extracranial solid tumors in our radiotherapy clinic were reviewed, and 12 cases (2.2%) of brain metastases were identified. The primary tumors included neuroblastoma (n=5), osteosarcoma (n=3), Ewing sarcoma (n=2), rhabdoid tumor of the kidney (n=1), and Wilms tumor (n=1). Retrospective analysis was performed to evaluate tumor and treatment features. Overall survival was measured from the initial diagnosis. Overall survival after brain metastasis, local control, and brain metastasis progression-free survival were calculated from the time of brain metastasis diagnosis to death.

RESULTS: Median follow-up was 31 months (range, 13–72 months). Brain metastasis developed at a median of 13 months after primary diagnosis (range, 3–69 months). Most brain metastases were supratentorial and solitary, with nine of 12 patients (75%) having solitary lesions and eight of 12 (67%) having supratentorial lesions. Surgical excision was performed in 9 patients (75%). Radiotherapy was administered locally (20–30 Gy, n=7) or to the craniospinal axis (21.6 or 23.4 Gy, n=2). Ten patients died during follow-up, 70% of whom did not experience cranial progression. Local control rate for irradiated lesions was 81.5% (median duration: 22 months). The brain metastasis-free survival was 71.4% (95% confidence interval [CI]: 2.59%–55.41%) with a median of 10 (range, 1–41) months. The 2-year survival rate was 58.3% (95% CI: 6.15%–71.84%). The 2-year overall survival rate after brain metastasis was 16.7% (95% CI: 7.13%–21.53%).

CONCLUSION: Brain metastasis remains rare in pediatric solid tumors. Most patients died from extracranial disease progression rather than cranial relapse. Radiotherapy can effectively relieve symptoms and may delay the progression of brain metastasis. Guidelines may help optimize the treatment of patients with brain metastasis.

KEYWORDS: Brain metastasis, Imaging, Pediatric tumors, Radiotherapy

ABBREVIATIONS: BMPFS: Brain metastasis progression-free survival, **BM:** Brain metastasis, **CNS:** Central nervous system, **MRI:** Magnetic resonance imaging, **RT:** Radiotherapy, **CT:** Chemotherapy, **GTR:** Gross total resection, **STR:** Subtotal resection, **CSI:** Craniospinal irradiation, **CSF:** Cerebrospinal fluid

Dilek GUL : 0000-0003-0382-8842
Burcu TUFAN TAS : 0000-0003-4614-124X
Adnan DAGCINAR : 0000-0001-9532-7820
Zerrin OZGEN : 0000-0002-0307-6890
Beste M. ATASOY : 0000-0003-1320-9105

INTRODUCTION

Brain metastasis (BM) is the most common tumor of the central nervous system (CNS) in adults, accounting for approximately 30% of all intracranial neoplasms. It most commonly arises from primary cancers of the lungs, breast, gastrointestinal tract, kidneys, and melanoma (1,12). In contrast, in the pediatric population, most CNS tumors are primary, and metastatic lesions are rarely identified (10,12,22). Consequently, evidence-based treatment options and prognostic data remain limited (12-14). The reported frequency of BM in pediatric patients ranges from 1.5% to 4.9% in the literature, while autopsy studies report an incidence of 6%–13% (12-14,24). The most common cancers metastasizing to the brain in pediatric patients are soft tissue and osteogenic sarcomas, neuroplastic tumors, and nephroblastoma (15,16,18-21,24,25).

The protective function of the blood-brain barrier may explain why BM is uncommon in children. The blood-brain barrier is a physical barrier that prevents hematogenous spread of tumor cells to the brain. Therefore, it is thought to reduce the risk of BM in pediatric patients, even in the presence of systemic disease (2,26,27). The brain microenvironment is relatively resistant to metastatic growth due to its unique metabolic constraints and limited lymphocyte infiltration, which hinder the survival and colonization of circulating tumor cells. Furthermore, the absence of specific molecular signals or pre-conditioning factors that promote BM in adults might be less significant in pediatric cancers (9).

Since BM is uncommon in pediatric patients, routine cranial imaging is rarely performed, and BM is usually detected only after CNS imaging prompted by symptoms. BM is typically diagnosed between the ages of 11 and 13 years. It generally occurs 8 to 16 months after the primary tumor is diagnosed (19,23). Common symptoms of BM include signs of increased intracranial pressure, motor weakness or sensory deficits, seizures, changes in mental status, headache, nausea and vomiting, nystagmus, ptosis, and visual field defects, all of which indicate focal neurological deficits (16, 25).

Because of the rarity of the condition and variability in clinical protocols, this study examines the frequency and treatment outcomes of CNS metastases in pediatric patients with extracranial solid tumors treated at our radiotherapy clinic over the past 20 years.

MATERIAL and METHODS

Study Design

This retrospective study was approved by the Marmara University Ethics Committee for Non-Interventional Studies (date: October 2024, approval number: 09.2024.1003) and conformed to the ethical principles of the Declaration of Helsinki (2024). A total of 530 patients underwent radiotherapy (RT) for extracranial pediatric tumors between 2000 and 2020. Ten patients were lost to follow-up, and the analyses were based on 520 patients who continued follow-up at our center. In our analysis, 12 (2.2%) patients with BM were included. The characteristics of the study population are summarized in Table I.

Table I: Clinical and Demographic Characteristics of Pediatric Patients with Brain Metastases from Extracranial Solid Tumors (n=12)

Characteristic	Value
Age (Median-ROI) (years)	5.5 (1-18)
Gender (Girl: Boy) (n)	5:7
Brain metastasis in all related tumors*, (%)	
Neuroblastoma	21.7
Osteosarcoma	18.7
Ewing sarcoma	3.6
Wilms' tumor	3.1
Kidney rhabdoid tumor	25.0
Diagnosis in the study cohort (n=12), n (%)	
Neuroblastoma	5 (41.7)
Osteosarcoma	3 (25.0)
Ewing sarcoma	2 (16.7)
Wilms tumor	1 (8.3)
Kidney rhabdoid tumor	1 (8.3)
Complaints, n (%)	
Nausea-vomiting	5 (41.6)
Seizure	4 (33.0)
Ataxia	3 (25.0)
Hemiparesis	2 (16.6)
Abducens palsy	2 (16.6)
Tumor location, n (%)	
Supratentorial	8 (66.7)
Infratentorial	3 (25.0)
Infra- and supratentorial	1 (8.3)
Extracranial metastatic tumor site, n (%)	
None	5 (41.6)
Multiple	3 (25.0)
Lung	1 (8.3)
Bone	1 (8.3)
Radiotherapy details (n=9), n (%)	
30 Gy/10 fractions to the tumor bed	4 (44.4)
21.6 Gy/12 or 23.4 Gy/13 fractions to CSI**	2 (22.2)
20 Gy in 5 fractions to the tumor bed	2 (22.2)
25 Gy/5 fractions to the tumor bed	1 (11.1)

**Total number of patients who were referred to the radiotherapy department due to the risk groups, clinical situations, or protocols; **CSI: Craniospinal irradiation*

Patients who were referred to the radiotherapy clinic either presented with BMs at diagnosis or developed them after treatment for the primary tumor. All BMs were diagnosed using magnetic resonance imaging (MRI) during staging or following the onset of any neurological symptom indicating an intracranial event. In asymptomatic patients, MRI was performed during primary disease progression following systemic treatment.

Statistical Analysis

Overall survival (OS) was calculated from the date of pathological diagnosis to the date of death or last follow-up. BM progression-free survival (BMPFS) was defined as the time from the detection of BM to CNS progression, including the progression of the irradiated lesion or the appearance of a new lesion. Local control was defined as the time from the start of RT to the clinical and radiological progression of the irradiated lesions. Kaplan–Meier analysis was used to assess survival outcomes.

RESULTS

Nine of 12 patients (75%) had solitary lesions, and eight of 12 (67%) were supratentorial. Six of nine patients with solitary lesions (67%) had supratentorial metastases. The remaining three solitary lesions were infratentorial. Among patients with multiple lesions (n=3), two had supratentorial lesions, and one had an infratentorial lesion.

One-third of patients (n=4) were asymptomatic at the time of BM diagnosis. Brain progression was detected in these patients during extracranial disease progression in Wilms tumor (n=1), osteosarcoma (n=1), neuroblastoma (n=1), and Ewing's sarcoma (n=1). One of these patients was diagnosed with extrarenal (intradural extramedullary) Wilms tumor, and an MRI was performed to assess systemic disease spread, given the unusual localization. The patient diagnosed with osteosarcoma did not receive systemic treatment because the parents declined therapy. The patient diagnosed with neuroblastoma was 18 months old, and an MRI was performed following an unusual and unexpected multiple systemic disease progression. The patient with Ewing's sarcoma received multiple chemotherapy (CT) and RT according to the protocols, and an MRI was performed before the last CT treatment.

The frequent initial symptoms were nausea and vomiting; other symptoms included ataxia and abducens palsy. All patients received antiseizure medications following BM diagnosis, per our neurosurgery protocol, until death. Surgical excision was performed in 75% (n=9) of patients. Ten patients died during follow-up, and 70% had no evidence of cranial progression at death.

At the time of BM diagnosis, most patients (66%) also had extracranial metastasis. Regarding BM treatment, seven patients (58%) received a combined regimen including surgery, RT, and CT. Parents of one patient declined all treatments, and the patient died 3 months after the BM diagnosis. Two patients did not undergo RT for BM. Both were <2 years old at the time of diagnosis, with one having a gross total resection (GTR) and the other a subtotal resection (STR). RT was not considered due to the patients' young age or the possibility of postoperative septic shock.

Patients undergoing surgery had the following profiles: GTR in 7, STR in 1, and biopsy in 1. The purpose of surgery in these patients was to provide both symptomatic relief and oncological treatment, including cytoreduction. RT was primarily delivered to one of two patients for whom surgery was not feasible due to tumor location. One of them indicated CT due to lung metastases but died of respiratory distress before starting treatment. The other patient completed both RT and CT.

Nine patients received RT, either locally (20 to 30 Gy, n = 7) or through the craniospinal route (21.6 to 23.4 Gy, n = 2). Craniospinal irradiation (CSI) was administered due to positive cerebrospinal fluid (CSF) cytology, despite the absence of spinal MRI findings. Both patients had previously undergone GTR for cranial BM. In one patient, a second metastatic brain lesion was detected 18 months after completing initial GTR and RT. During follow-up, MRI-confirmed spinal seeding was identified, and the patient later received CSI. However, 6 months after finishing CSI, this patient died from disease progression.

The median follow-up time from the initial diagnosis was 31 months (range, 13–72). The 2-year survival rate was 58.3% (95% confidence interval [CI]: 6.15%–71.84%) (Figure 1). BM developed a median of 13 months (range, 3–69) during treatment and follow-up. The local control rate for irradiated metastatic brain lesions was 75.8%, with a median duration of 22 months (Figure 2). BMPFS was 71.4% (95% CI: 2.59%–55.41%) at a median of 10 (range, 1–41) months (Figure 3).

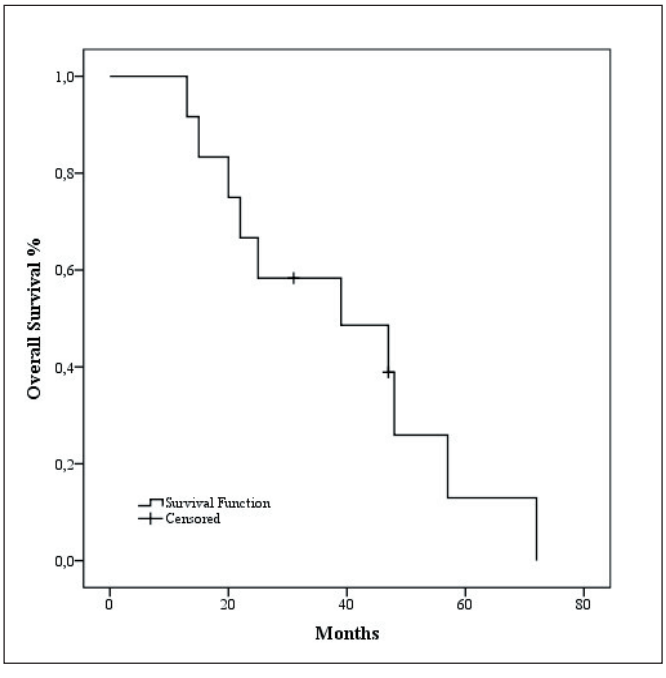

Figure 1: The Kaplan–Meier curve shows the overall survival of pediatric patients with brain metastases from extracranial solid tumors. Censored cases are indicated by tick marks on the survival curve. Months indicate time from primary diagnosis to death or last follow-up.

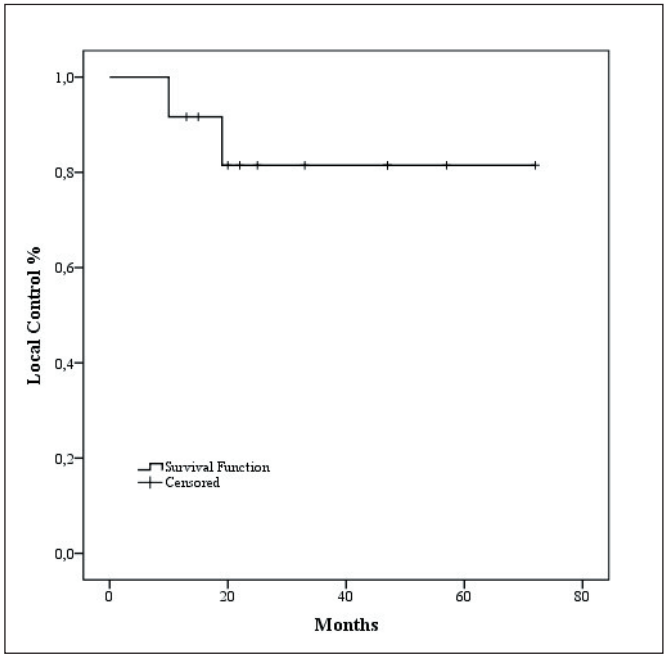

Figure 2: The Kaplan–Meier curve demonstrates local control rates of irradiated brain metastases in pediatric patients with extracranial solid tumors. Tick marks indicate censored observations. Months represent the duration from the start of radiotherapy to clinical or radiological progression of the irradiated lesions.

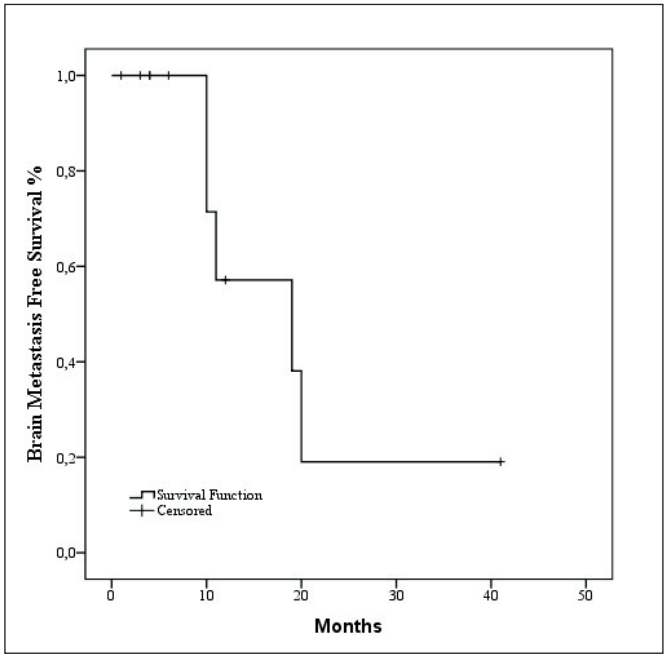

Figure 3: The Kaplan–Meier curve illustrates brain metastasis-free survival in pediatric patients with extracranial solid tumors. Tick marks denote censored events. Months represent the interval from the diagnosis of brain metastasis to the progression of irradiated lesions or the appearance of a newly diagnosed lesion.

The 2-year OS rate after BM was 16.7% (95% CI: 7.13%–21.53%) (Figure 4).

In the neuroblastoma group (n=5), the 2-year OS was 40% (95% CI: 14.26%–35.73%) and the BMPFS was 30% (95% CI: 6.52%–31.47%), with a median follow-up of 25 months (range, 15–47). All five neuroblastoma patients had high-risk disease and were referred to RT.

DISCUSSION

The median time from the diagnosis of the primary tumor to the detection of BM in pediatric solid tumors has been reported to range from 13 to 22 months (2,6-8,12,15). Consistent with previous reports, the median interval in our series was 13 months, with a range of 3 to 69 months. The median follow-up time was 31 (range, 13–72) months from the first diagnosis of the disease.

Neuroblastoma is the most common primary solid tumor that leads to BM in pediatric patients (5,6,8,15). At initial diagnosis, more than 50% of neuroblastoma cases present with widespread disease (5,6,8,15,19). However, BMs account for only 5% of all neuroblastoma cases (8,15,18). In neuroblastoma, CNS metastasis usually arises from adjacent skull metastases, which may lead to parenchymal BM (18). Lung metastases are also rare at diagnosis (6). DuBois et al. reported that 100 out of 2,708 patients with neuroblastoma (3.7%) had lung metastasis. Nearly all patients with lung metastases also have other metastatic sites, and 9% of these patients have BM (6).

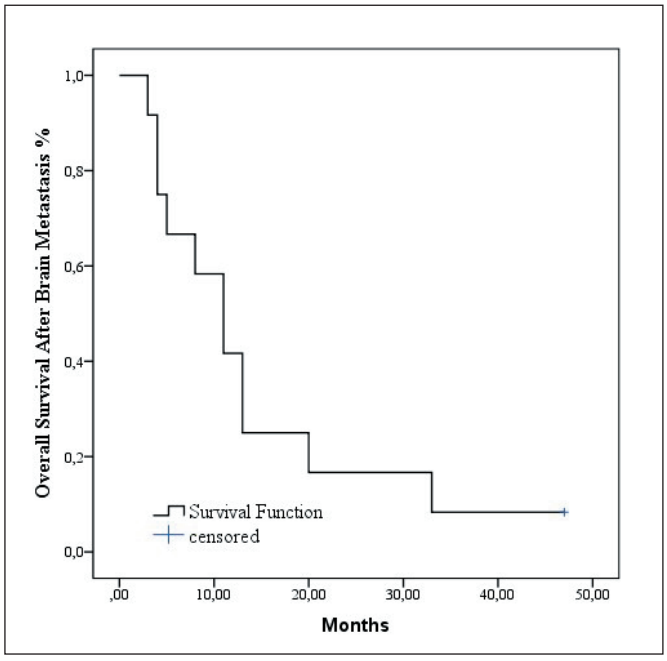

Figure 4: The Kaplan-Meirer curve demonstrates the overall survival in patients with extracranial solid tumor following brain metastasis. Tick marks indicate censored observations. Months represent the duration from brain metastasis to death or last follow-up.

In our study, five patients with neuroblastoma were included; all had high-risk diseases and were referred to RT according to their risk classification. One patient presented with a single supratentorial metastatic focus and no other extracranial metastases. Another patient had multiple metastases, including spinal involvement. Two of the neuroblastoma cases were alive at the time of analysis. Both patients initially presented with multi-organ metastases. On meta-iodobenzylguanidine scans, neither patient showed any uptake, and all MRI evaluations appeared normal. In our cohort, approximately 20% of neuroblastoma cases who were referred to RT developed BM during their treatment and follow-up. However, this rate likely reflects a selection bias, as these patients had high-risk or advanced disease and were referred for RT. Therefore, it may not be representative of the general neuroblastoma population. Moreover, routine cranial imaging may be considered for selected high-risk neuroblastoma patients, particularly those with advanced disease or unusual presentations. Nonetheless, it should be interpreted in the context of selection bias and the rarity of BM in the broader pediatric population. However, more careful cranial imaging evaluation may be warranted in patients with age, myc proto-oncogene, bHLH transcription factor positivity, and a high systemic disease burden (12,28).

Pulmonary metastases are the most common in osteosarcoma, whereas the brain is a rare site of distant metastasis (3,16). Nonetheless, the presence of lung metastases is the most significant factor associated with BMs in children (21). BMs likely originate from hematogenous tumor emboli derived from lung metastases (12). In our study, three patients with osteosarcoma developed BMs, and one of them had lung metastasis at the time of diagnosis. Six of 12 patients had lung metastases when they were diagnosed with BMs.

In our study, the typical presenting symptoms were nausea, vomiting, and seizures. The primary neurological symptoms in children included headaches, lethargy, and seizures (2,7, 11,12). For pediatric patients with non-hematological malignancies and BMs, approximately 10%–15% experience seizures as part of their clinical course. Seizure risk in metastatic cases may be more strongly associated with factors such as multiple lesions, involvement of highly epileptogenic brain regions, cortical involvement, hemorrhagic events, or treatment-related factors. The incidence of seizures was 33% in our cohort, which is higher than that in published reports for pediatric brain tumors and BMs. All metastatic lesions were located in or near the motor cortex. Speech disturbances, hemiparesis, diplopia, and facial palsy due to cranial nerve involvement were also observed, consistent with our cases. Two patients received CSI in our study. Leptomeningeal dissemination has been reported in the literature, in which case CSI may be recommended (4). However, in our cohort, patients received CSI specifically for positive CSF cytology.

Symptomatic treatment of BM involves corticosteroids to reduce peritumoral edema and anticonvulsants to control seizures (7,8,10,11,13). A curative approach includes surgery and/or RT, along with CT. However, the role of chemotherapy in treating BMs remains uncertain. For patients with a single metastasis and no systemic disease, surgery followed by RT and/or CT may be the preferred option. In such cases, combining RT with surgery might be recommended. For patients with multiple BMs, surgery may not be beneficial unless there is a life-threatening symptomatic lesion.

Most affected children ultimately die from their disease, even when brain lesions are successfully managed (12). Many of these children also develop metastases at other sites, which further negatively impact their overall prognosis. Although determining the cause of death in patients with multifocal tumors is challenging, our study found that neurological deterioration was the sole or a contributing cause of death in four of 10 patients who died. In seven patients, death was caused by progression of the primary disease, with no evidence of cranial progression at the time of death, accounting for 70% of cases.

Case series and systematic reviews published through 2024 indicate that cranial metastasis remains rare in pediatric populations, with MRI used selectively (11,16). Meanwhile, clinical management protocols have been actively refined for neuroblastoma, sarcoma, and germ cell tumors. Therefore, routine screening brain MRI is not standard for all patients, but may be considered in high-risk neuroblastoma, alveolar rhabdomyosarcoma, and selected clinical scenarios (neurologic symptoms or highly advanced/metastatic disease).

Our study has several limitations. The retrospective nature of the study, along with differences in RT doses and fields, and variability in patient diagnoses, constituted the foremost limitations. Despite these limitations, RT may improve freedom from neurological progression and increase BMPFS. Our patient cohort was small and included five different tumor types with diverse biological behavior, limiting the interpretation of pooled survival analyses. Therefore, survival and BMPFS rates should be interpreted with caution because of the small cohort size and heterogeneity. No subgroup analyses by diagnosis could be performed to enable robust comparisons or clinical recommendations. The wide confidence intervals for survival outcomes reflected a small sample size and limited statistical power. Therefore, these results should be considered exploratory rather than conclusive, and larger studies are needed for validation.

The limited number of cohorts also restricted the standardization of RT for BM. No stereotactic radiosurgery was planned, none received whole-brain RT, and almost all underwent limited-field (tumor bed) RT. Currently, radiosurgery is not routinely recommended for pediatric patients (17). Furthermore, routine MRI should be included in protocols only for patients with high-risk disease. The frequency of BM in the high-risk group referred for RT might reflect a selection bias and therefore could overestimate the overall incidence. Finally, since this study relied on retrospective data analysis, the outcomes assessed were primarily clinical rather than quality-of-life related.

CONCLUSION

In summary, BM remains a rare event in pediatric extracranial solid tumors. Mortality is predominantly driven by the progres-

sion of systemic disease rather than cranial relapse, and BMs themselves are not the primary cause of death in most cases. The role of CT in treating BMs remains uncertain. Surgery may be considered for patients with a single and/or symptomatic metastatic lesion. RT can effectively relieve symptoms and may delay BM progression. Tailored localized RT may also be recommended to address both the immediate and late radiation-related toxicities. Including the spinal region in imaging and sampling CSF cytology may be recommended before RT, as spinal dissemination can be detected in some patients. Further multicenter studies are needed to better elucidate clinical outcomes and refine imaging recommendations.

Declarations

Funding: This research did not receive any specific grant from funding agencies in the public, not-for-profit, or commercial sectors.

Availability of data and materials: The data that supports the findings of this study are available from the corresponding author upon reasonable request.

Disclosure: All authors declare they have no conflicts of interest.

AUTHORSHIP CONTRIBUTION

Study conception and design: DG, BMA
Data collection: DG, BTT, AD, ZO
Analysis and interpretation of results: DG, BTT, AD, ZO, BMA
Draft manuscript preparation: DG, BMA
Critical revision of the article: DG, BTT, AD, ZO, BMA
Other (study supervision, fundings, materials, etc...): n/a
All authors (DG, BTT, AD, ZO, BMA) reviewed the results and approved the final version of the manuscript.

REFERENCES

1. Arnold SM, Patchell RA: Diagnosis and management of brain metastases. Hematol Oncol Clin North Am 15:1085-1107, vii, 2001. https://doi.org/10.1016/s0889-8588(05)70269-0
2. Bouffet E, Doumi N, Thiesse P, Mottolese C, Jouvet A, Lacroze M, Carrie C, Frappaz D, Brunat-Mentigny M: Brain metastases in children with solid tumors. Cancer 15:79:403-410, 1997. https://doi.org/10.1002/(sici)1097-0142(19970115)79:2<403::aid-cncr25>3.0.co;2-3
3. Briccoli A, Rocca M, Salone M, Guzzardella GA, Balladelli A, Bacci G: High grade osteosarcoma of the extremities metastatic to the lung: long-term results in 323 patients treated combining surgery and chemotherapy, 1985-2005. Surg Oncol 19:193-199, 2010. https://doi.org/10.1016/j.suronc.2009.05.002
4. Cocito C, Martin B, Giantini-Larsen AM, Valcarce-Aspegren M, Souweidane MM, Szalontay L, Dahmane N, Greenfield JP: Leptomeningeal dissemination in pediatric brain tumors. Neoplasia 39:100898, 2023. https://doi.org/10.1016/j.neo.2023.100898
5. Cohn SL, Pearson AD, London WB, Monclair T, Ambros PF, Brodeur GM, Faldum A, Hero B, Iehara T, Machin D, Mosseri V, Simon T, Garaventa A, Castel V, Matthay KK; INRG Task Force: INRG Task Force the International Neuroblastoma Risk Group (INRG) classification system: an INRG Task Force report. J Clin Oncol 10:27:289-297, 2009. https://doi.org/10.1200/JCO.2008.16.6785
6. Dubois SG, London WB, Zhang Y, Matthay KK, Monclair T, Ambros PF, Cohn SL, Pearson A, Diller L: Lung metastases in neuroblastoma at initial diagnosis: A report from the International Neuroblastoma Risk Group (INRG) project. Pediatr Blood Cancer 51:589-592, 2008. https://doi.org/10.1002/pbc.21684
7. Goldman S, Echevarría ME, Fangusaro J: Pediatric brain metastasis from extraneural malignancies: a review. Cancer Treat Res 136:143-168, 2017. https://doi.org/10.1007/978-0-387-69222-7_8
8. Gultekin M, Esen C, Varan A, Akyuz C, Bilginer B, Yildiz F, Gurkaynak M: Pediatric Neuroblastoma with Brain Metastasis: The Prognostic Role of Surgery. Turk Neurosurg 32:204-210, 2022. https://doi.org/10.5137/1019-5149.JTN.33742-21.2
9. Gwak HS: Molecular biology of brain metastases. Brain Tumor Res Treat 11:8-15, 2023. https://doi.org/10.14791/btrt.2022.0045
10. Hudson MM, Neglia JP, Woods WG, Sandlund JT, Pui CH, Kun LE, Robison LL, Green DM: Lessons from the past: opportunities to improve childhood cancer survivor care through outcomes investigations of historical therapeutic approaches for pediatric hematological malignancies. Pediatr Blood Cancer 58:334-343, 2012. https://doi.org/10.1002/pbc.23385
11. Kara L, Unal E, Per H, Kumandas S, Canpolat M, Elmali F, Ozcan A, Yilmaz E, Karakukcu M, Ozdemir MA, Patiroglu T, Gumus H: Neurological complications of children with cancers: Experience from a single center in Türkiye. J Clin Pract Res 46:154-160, 2024. https://doi.org/10.14744/cpr.2024.59622
12. Kebudi R, Ayan I, Görgün O, Ağaoğlu FY, Vural S, Darendeliler E: Brain metastasis in pediatric extracranial solid tumors: survey and literature review. J Neurooncol 71:43-48, 2005. https://doi.org/10.1007/s11060-004-4840-y
13. Klos KJ, O'Neill BP: Brain metastases. Neurologist 10:31-46, 2004. https://doi.org/10.1097/01.nrl.0000106922.83090.71
14. Lamba N, Groves A, Torre M, Yeo KK, Iorgulescu JB: The epidemiology of primary and metastatic brain tumors in infancy through childhood. J Neurooncol 156:419-429, 2022. https://doi.org/10.1007/s11060-021-03927-z
15. Maris JM, Hogarty MD, Bagatell R, Cohn SL: Neuroblastoma. Lancet 23:369:2106-2120, 2007. https://doi.org/10.1016/S0140-6736(07)60983-0
16. Murphy ES, Sahgal A, Regis J, Levivier M, Fariselli L, Gorgulho A, Ma L, Pollock B, Yomo S, Sheehan J, Paddick I, Suh JH, Saxena A, Ahmed MA, Kotecha R: Pediatric cranial stereotactic radiosurgery: Meta-analysis and international stereotactic radiosurgery society practice guidelines. Neuro Oncol 27:517-532, 2025. https://doi.org/10.1093/neuonc/noae204
17. Murphy J, Sundby RT, Resch EE, Rahnama R, Lemberg KM, Maalouf A, Suru A, Fixler J, Ladle BH, Rhee DS, Levin AS, Pallavajjala A, Gocke C, Ladra MM, Groves ML, Acharya S, Gross JM, Llosa NJ, Pratilas CA: Brain Metastasis in pediatric patients with osteosarcoma. Curr Oncol 31:7014-7022, 2024. https://doi.org/10.3390/curroncol 31110516
18. Odone-Filho V, Cristofani LM, Maluf PT, Almeida MTA, Halley N, Vince CSC, de Azambuja AMP, Brumatti M, Lubraico P, da Camara Lopes LHA, Leite KRM, Silva JLF, Plese JPP, Weltman E: Involvement of the central nervous system in neuroblastomas: A potential direct pathway. Med Hypotheses 136:109479, 2010. https://doi.org/10.1016/j.mehy.2019.109479

19. Osawa S, Kumabe T, Saito R, Sonoda Y, Niizuma H, Watanabe M, Tominaga T. Infratentorial brain metastases of pediatric non-epithelial malignant tumors: three case reports. Brain Tumor Pathol 28:167-174, 2011. https://doi.org/10.1007/s10014-010-0014-0
20. Parasuraman S, Langston J, Rao BN, Poquette CA, Jenkins JJ, Merchant T, Cain A, Pratt CB, Pappo AS: Brain metastases in pediatric sarcomas: a single institution experience. Pediatr Blood Cancer 60:1016-1020, 2013. https://doi.org/10.1097/00043426-199909000-00007
21. Paulino AC, Nguyen TX, Barker JL Jr: Brain metastasis in children with sarcoma, neuroblastoma, and Wilms' tumor. Int J Radiat Oncol Biol Phys 57:177-183, 2003. https://doi.org/10.1016/s0360-3016(03)00502-9
22. Singh R, Stoltzfus KC, Chen H, Louie AV, Lehrer EJ, Horn SR, Palmer JD, Trifiletti DM, Brown PD, Zaorsky NG. Epidemiology of synchronous brain metastases. Neurooncol Adv 2:vdaa041, 2020. https://doi.org/10.1093/noajnl/vdaa041
23. Stefanowicz J, Iżycka-Świeszewska E, Szurowska E, Bień E, Szarszewski A, Liberek A, Stempniewicz M, Kloc W, Adamkiewicz-Drożyńska E: Brain metastases in paediatric patients: characteristics of a patient series and review of the literature. Folia Neuropathol 49:271-281, 2011.
24. Suki D, Khoury Abdulla R, Ding M, Khatua S, Sawaya R: Brain metastases in patients diagnosed with solid primary cancer during childhood: experience from a single referral center. J Neurosurg Pediatr 14:372-385, 2014. https://doi.org/10.3171/2014.7.PEDS13318
25. Wiens AL, Hattab EM: The pathological spectrum of solid CNS metastases in the pediatric population. J Neurosurg Pediatr 14:129-135, 2014. https://doi.org/10.3171/2014.5.PEDS13526
26. Wilhelm I, Molnár J, Fazakas C, Haskó J, Krizbai IA: Role of the blood-brain barrier in the formation of brain metastases. Int J Mol Sci 14:1383-1411, 2013. https://doi.org/10.3390/ijms14011383
27. Zhang RD, Price JE, Fujimaki T, Bucana CD, Fidler IJ: Differential permeability of the blood-brain barrier in experimental brain metastases produced by human neoplasms implanted into nude mice. Am J Pathol 141:1115-1124, 1992.
28. Zhu J, Wang J, Zhen ZJ, Lu SY, Zhang F, Sun FF, Li PF, Huang JT, Cai RQ, Sun XF: Brain metastasis in children with stage 4 neuroblastoma after multidisciplinary treatment. Chin J Cancer 34:531-537, 2015. https://doi.org/10.1186/s40880-015-0038-2

Turk Neurosurg 36(3):457-466, 2026
DOI: 10.5137/1019-5149.JTN.49456-25.2

Original Investigation

Neuroanatomy

Received: 16.07.2025
Accepted: 29.09.2025
Published Online: 22.05.2026

Endoscopic Endonasal Approach to Identify the Medial Corridor of the Cavernous Sinus: A Cadaveric Study with Clinical Correlation

Aykut GOKBEL[1], Ayse UZUNER[2], Eren YILMAZ[1], Atakan EMENGEN[3], Musa CIRAK[4], Burak CABUK[5], Ihsan ANIK[5], Savas CEYLAN[3]

[1]Istinye University, Department of Neurosurgery, Istanbul, Türkiye
[2]Afşin State Hospital, Department of Neurosurgery, Kahramanmaras, Türkiye
[3]Bahcesehir University School of Medicine, Department of Neurosurgery, Istanbul, Türkiye
[4]Bakirkoy Dr. Sadi Konuk Training and Research Hospital, Department of Neurosurgery, Istanbul, Türkiye
[5]Kocaeli University School of Medicine, Department of Neurosurgery, Kocaeli, Türkiye

Corresponding author: Savas CEYLAN ✉ ssceylan@yahoo.com

ABSTRACT

AIM: To define the existence and precise anatomical boundaries of the medial corridor (MC) within the cavernous sinus (CS), using an endoscopic endonasal transsphenoidal approach, and to correlate these anatomical findings with clinical patterns of CS invasion in patients with pituitary adenomas.

MATERIAL and METHODS: An endoscopic endonasal transsphenoidal technique was used to perform anatomical dissections on 10 CSs obtained from 5 adult cadaveric heads. Key neurovascular landmarks were systematically identified, and quantitative measurements of their spatial relationships were recorded. To establish clinical relevance, anatomical observations were correlated with radiological and intraoperative findings from 20 patients with pituitary adenomas demonstrating CS invasion on preoperative imaging.

RESULTS: The MC was consistently identified in all cadaveric specimens, confirming its reproducible anatomical presence. The mean distance between the anterior genu of the internal carotid artery (ICA) and the pituitary gland was 5.0 ± 1.5 mm. Clinical correlations revealed that pituitary adenomas preferentially invade the superior compartment of the CS via the MC prior to lateral and posterior extension. The oculomotor nerve (cranial nerve III) was a reliable anatomical landmark defining the lateral boundary of the MC.

CONCLUSION: Comprehensive anatomical delineation of the MC is critical for refining endoscopic surgical strategies, maximizing the extent of safe tumor resection, and minimizing neurovascular morbidity. The consistently identified interval of approximately 5 mm between the anterior genu of the ICA and the pituitary gland provides a robust and practical intraoperative reference point for safe navigation through the MC of the CS.

KEYWORDS: Cavernous sinus, Pituitary adenoma, Internal carotid artery, Endoscopic surgical procedure

ABBREVIATIONS: 3D: Three-dimensional, **C4:** Cavernous segment, **CN:** Cranial nerve, **CS:** Cavernous sinus, **EETA:** Endoscopic endonasal transsphenoidal approach, **ICA:** Internal carotid artery, **MC:** Medial corridor, **SOF:** Superior orbital fissure

Aykut GOKBEL : 0000-0002-9332-3321
Ayse UZUNER : 0000-0002-6471-7452
Eren YILMAZ : 0000-0002-5911-7268
Atakan EMENGEN : 0000-0002-6853-1540
Musa CIRAK : 0000-0002-0175-9655
Burak CABUK : 0000-0003-1198-3869
Ihsan ANIK : 0000-0003-2567-7969
Savas CEYLAN : 0000-0002-2747-8907

INTRODUCTION

Over the past two decades, the progressive evolution of transsphenoidal surgical techniques has greatly advanced the understanding of skull base anatomy. In particular, the integration of endoscopic visualization into transsphenoidal surgery has enabled unparalleled exposure of the deep and previously concealed anatomical regions surrounding the sella turcica, including the planum sphenoidale, clivus, and neurovascular prominences of the optic nerves and internal carotid arteries (4,15). These advancements have not only expanded the anatomical reach of endonasal approaches but also fundamentally reshaped surgical paradigms for lesions involving the parasellar and cavernous regions.

Among these regions, the cavernous sinus (CS) is one of the most anatomically complex and surgically challenging structures of the skull base. Its dense neurovascular content, intricate venous architecture, and intimate relationship with the internal carotid artery (ICA) necessitate a precise and compartmentalized anatomical understanding to ensure surgical safety and efficacy (8). Classical anatomical descriptions by Harris and Rhoton subdivided the CS into four venous regions, namely, anteroinferior (ventral), posterosuperior (dorsal), medial, and lateral, based on their spatial relationships with the ICA (14). Subsequent refinements by Fernandez-Miranda et al. proposed a compartmental framework consisting of superior, posterior, lateral, and inferior regions, which again considered the cavernous ICA (12). More recently, Ceylan et al. further refined this anatomical concept by identifying four distinct compartments, namely, superior, lateral, anteroinferior, and posterior, underscoring the evolving and dynamic nature of CS anatomy (3).

From a surgical perspective, endoscopic approaches to the CS have converged on the definition of two principal operative corridors, namely, the medial corridor (MC) and lateral corridor (7). The MC of the ICA is formed by the C-shaped cavernous segment (C4) of the artery and is medially constrained by the dorsum sellae, providing a potential pathway for medial-to-lateral access. Conversely, the lateral corridor is bounded posteriorly by the cavernous ICA, inferiorly by the vidian nerve, and anteriorly by the medial pterygoid prominence (5). Consistent with this corridor-based concept, Fernandez-Miranda et al. characterized the CS as comprising two principal wall structures, namely, the medial and lateral walls, with each assuming distinct surgical relevance depending on the chosen approach (11). Notably, the medial wall represents the primary interface encountered during endoscopic endonasal surgery, whereas the lateral wall is more frequently addressed via transcranial routes.

Accumulating anatomical and clinical evidence suggests that pituitary adenomas preferentially invade the CS through involvement of the medial wall. Our previous work has demonstrated that medial wall infiltration or compression constitutes a defining feature of CS invasion. However, medial wall disruption alone does not fully explain the observed patterns of tumor extension. Rather, engagement of the venous trabecular network located posterior to the medial wall appears to serve as a critical permissive factor that facilitates tumor progression into the CS (3,5,6). This observation highlights a complex, multistep mechanism of invasion that extends beyond simple wall penetration.

Against this backdrop, the present study was designed to precisely delineate the presence and anatomical boundaries of the MC using the endoscopic endonasal transsphenoidal approach (EETA) while simultaneously elucidating its role in the pathophysiology of CS invasion by pituitary adenomas. A refined understanding of the MC is essential for strategic surgical planning, reduction of neurovascular morbidity, and maximization of safe tumor resection. By integrating meticulous anatomical dissection with clinical correlation, this study aims to further clarify the anatomical–surgical interface of the CS and to contribute to the ongoing refinement of endoscopic skull base surgery.

MATERIAL and METHODS

This anatomical study examined 10 CSs obtained from five adult cadaveric heads. Specimens were either freshly frozen or prepared using arterial silicone injection to enhance vascular visualization. All dissections were performed at the Bahcesehir University Rhoton Laboratory. The study was conducted in accordance with the principles of the Declaration of Helsinki and was approved by the Local Ethics Committee of the Kocaeli University Faculty of Medicine (approval number: KAEK-233; September 20, 2017).

Both three-dimensional (3D) and two-dimensional digital video data were obtained during the dissections. Two-dimensional imaging was performed using 0° and 30° rigid endoscopes (Karl Storz, Tuttlingen, Germany), whereas stereoscopic visualization was achieved using the XION 3D endoscopic imaging system (XION, Berlin, Germany). The 3D endoscopy setup consisted of a MATRIX P Spectar camera processor (XION), a high-definition 3D camera head, and 3D endoscopes with diameters of 2.7 mm and 4 mm.

All endoscopic dissections were conducted through the right nasal cavity using a standard EETA. Following entry into the right nostril, key intranasal landmarks, including the nasal septum and the inferior, middle, and superior nasal turbinates, were systematically identified. The choana and sphenoethmoidal recess were visualized along the medial turbinate and nasal septum. After bilateral identification of the sphenoid ostia, the sphenoid sinus was entered via drilling, and an anterior sphenoidotomy was performed using a binostril technique.

Subsequently, critical skull base landmarks were exposed, including the sellar floor, planum sphenoidale anteriorly, clivus inferiorly, and prominences of the optic nerve and ICA laterally, along with the opticocarotid recesses. The lateral anatomical limits accessible through the endoscopic approach were carefully delineated. The superior sellar wall was opened using a high-speed drill, followed by bone removal and enlargement with a Kerrison rongeur. After dural opening, the anatomical boundaries of the MC were directly visualized.

A complete EETA was employed to define the surgical limits using natural nasal corridors, without the need for any external incisions on the cadaveric specimens. The bone overlying the

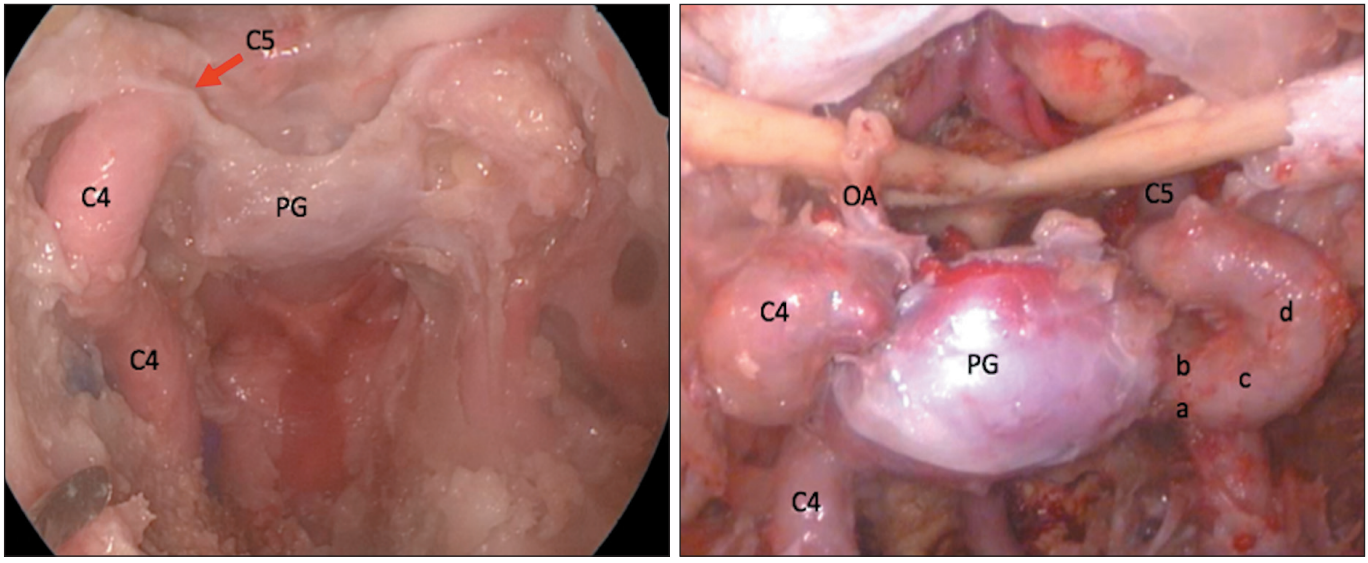

Figure 1: Cavernous (C4) and clinoid (C5) segments of the internal carotid artery; a: short vertical segment, b: posterior genu, c: horizontal segment, d: anterior genu. **PG:** pituitary gland, **OA:** ophthalmic artery.

ICA was subsequently removed using a high-speed drill and Kerrison rongeur, allowing extension of the dissection laterally toward the CS and inferiorly toward the clivus. This technique enabled wide endoscopic exposure of the region extending to the foramen lacerum and proximal carotid ring.

For clinical correlation, the anatomical boundaries of the MC were intraoperatively identified in 20 patients undergoing endoscopic transsphenoidal surgery for pituitary adenomas with lateral and posterior CS extension. In these cases, tumor growth was initially observed within the superior compartment via the MC, followed by secondary extension into the lateral and posterior compartments. These clinical observations provided a practical framework for conceptualizing the 3D architecture and surgical relevance of the MC. The primary surgical objective in all cases was to achieve gross total tumor resection while preserving the integrity of adjacent cranial nerves (CNs) and vascular structures.

RESULTS

In all cadaveric specimens, the C4 segment of the ICA was found to terminate at the proximal dural ring, beginning at the superior margin of the petrolingual ligament encircling the artery. This segment was consistently surrounded by areolar tissue, adipose tissue, the cavernous venous plexus, and postganglionic sympathetic nerve fibers. Anatomically, the cavernous ICA was composed of a vertical segment, posterior bend (medial loop), horizontal segment, and anterior bend (anterior loop). These characteristic anatomical configurations were clearly and consistently identified in all five cadaveric specimens examined in the present study (Figure 1).

The paraclival ICA was observed to continue superiorly into the cavernous portion. The junction between the horizontal segment of the cavernous ICA and the short vertical segment extending from the posterior genu to the proximal dural ring

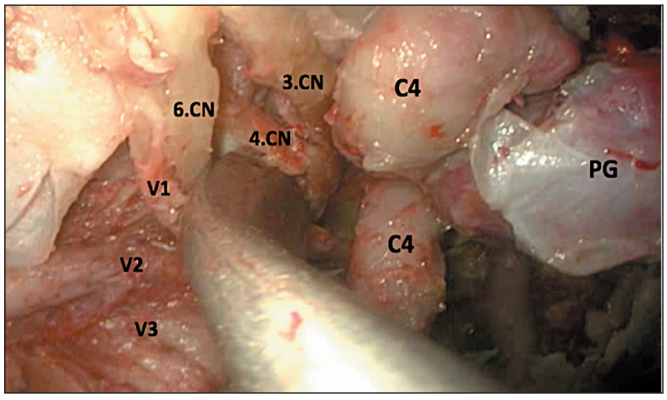

Figure 2: View when the ophthalmic branch of the trigeminal cranial nerve (CN) and the abducens CN are eliminated laterally. **C4:** cavernous segment of the internal carotid artery, **PG:** pituitary gland, **V1:** ophthalmic branch of the trigeminal CN, **V2:** maxillary branch of the trigeminal CN, **V3:** mandibular branch of the trigeminal CN.

was designated as the C4 segment. Careful stripping of the sellar dura and the dural layer overlying the ICA allowed exposure of the neurovascular structures within the CS, including the oculomotor and abducens CNs as well as the pituitary gland (Figure 2).

The neurovascular elements that were systematically examined included the oculomotor (CN III), abducens (CN VI), ophthalmic (V1), and maxillary (V2) divisions of the trigeminal nerve, and the C4 segment of the ICA. In addition, the proximal dural ring, ophthalmic artery, and optic nerve were identified. Following removal of the bone overlying the ICA, the bony lateral sellar compartment was excised to enable tracing of the CNs within the CS. The oculomotor nerve was observed coursing within the lateral wall of the CS at the level of the hor-

Table I: The measurement of the distance between the anterior genu and the pituitary gland to enter the medial corridor in the study on 5 cadavers and 10 cavernous sinuses (CS)

The measurement between the anterior genu and the pituitary gland (mm)	First cadaver	Second cadaver	Third cadaver	Fourth cadaver	Fifth cadaver	Mean±SD
Right CS	6.4	6.2	5.6	4.1	2.9	5.0±1.5
Left CS	5.9	5.3	6.8	3.2	3.4	4.9±1.6

CS: *cavernous sinus.*

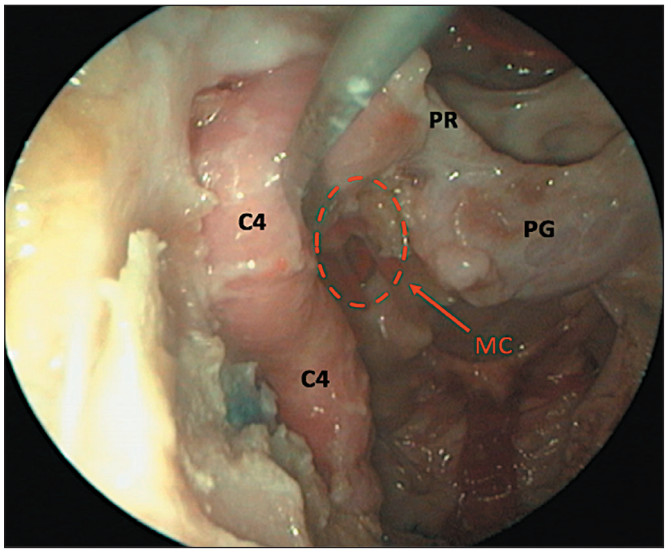

Figure 3: Examination of the medial corridor following mobilization of the cavernous segment of the internal carotid artery. **C4:** cavernous segment of the internal carotid artery, **PG:** pituitary gland, **PR:** proximal ring.

izontal ICA segment, bending around the C4 segment before entering the superior orbital fissure (SOF). The intradural segment of the oculomotor nerve was preserved unless pathological extension involved the roof or lateral wall of the CS.

The most vulnerable portion of the oculomotor nerve was consistently identified adjacent to the anterior genu of the ICA, a region that remains difficult to access through a medial-to-lateral endoscopic approach. The abducens nerve followed a trajectory corresponding to the mid-portion of the vertical C4 segment after exiting Dorello's canal, coursing near the ICA en route to the SOF. The ophthalmic division of the trigeminal nerve traveled parallel to the abducens nerve before entering the SOF. Upon lateral displacement of the abducens nerve and ophthalmic division, the trochlear nerve was identified running parallel to the oculomotor nerve. A clear visualization of the anatomical relationship between the CS and the optic nerve was obtained by opening the dura overlying the optic nerve, planum sphenoidale, and optic protuberance, and tracing it anteriorly to the optic canal (Figure 2).

The MC, as previously described by Fernandez-Miranda et al. (11), and utilized by our group to access the superior compartment of the CS, was distinctly identifiable in all specimens. The anatomical boundaries of the MC were defined superiorly by the proximal dural ring, medially by the pituitary gland, and laterally by the ICA (Figure 3).

During pituitary adenoma surgery, the oculomotor nerve, previously identified and dissected in cadaveric specimens, became visible upon entry into the MC and served as a critical lateral surgical boundary (Figure 4). To further characterize the MC, the horizontal distance between the anterior genu of the ICA and the lateral margin of the pituitary gland was measured, defining a practical entry point into the corridor (Figure 5). The mean distance was approximately 5 mm, and this may have clinical relevance for guiding safe surgical access. For comparative analysis, measurements were categorized into the following two groups: greater than 5 mm and less than 5 mm (Table I).

In the clinical series, pre- and postoperative magnetic resonance imaging of pituitary adenomas confined to the superior compartment clearly demonstrated MC involvement, supporting its role as a preferential pathway for tumor invasion, in close association with the carotid siphon (Figure 6). Intraoperatively, tumor tissue within the MC was removed using a combination of suction and curettage. As dissection progressed toward the lateral aspects of the anterior and posterior ICA segments, suction pressure was deliberately reduced to ensure safe tumor removal. Once the MC was fully exposed and tumor evacuation was completed, the oculomotor nerve was visualized laterally (Figure 7), indicating the lateral limit of the corridor. At this stage, the surgical procedure was terminated to avoid CN injury.

Across the clinical cohort of 20 patients, the patterns of CS compartment invasion, resection extent, patient age, tumor secretory status, and biochemical remission outcomes were systematically analyzed. These findings are summarized in Table II.

DISCUSSION

The CS represents one of the most anatomically intricate regions of the skull base, harboring neurovascular structures of critical functional significance. Consequently, it is a surgically formidable area. A precise understanding of the spatial relationships among the neural and vascular components within the CS is indispensable for effective surgical planning and risk mitigation. Nevertheless, any attempt to classify or compartmentalize such a complex anatomical structure inherently carries the risk of subjective interpretation and artificial boundary definition.

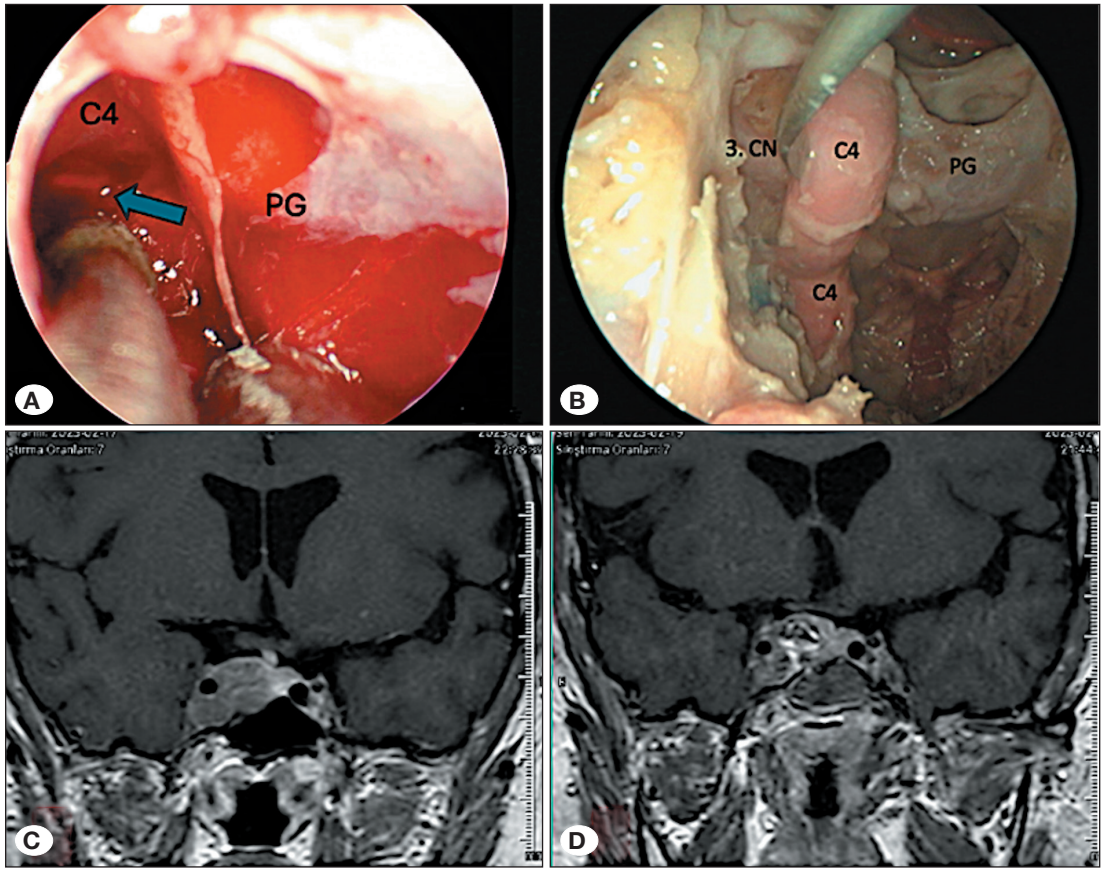

Figure 4: A) Clinical case image demonstrating the oculomotor cranial nerve (CN) indicated by an arrow, the internal carotid artery at the cavernous segment (C4), and the pituitary gland (PG). **B)** Cadaveric dissection showing the detailed anatomy of the relevant structures. **C)** Preoperative magnetic resonance imaging (MRI) revealing tumor extension into both the superior and lateral compartments of the cavernous sinus. **D)** Postoperative MRI demonstrating the absence of residual tumor within the superior and lateral compartments, corroborating intraoperative assessments and confirming the completeness of the resection.

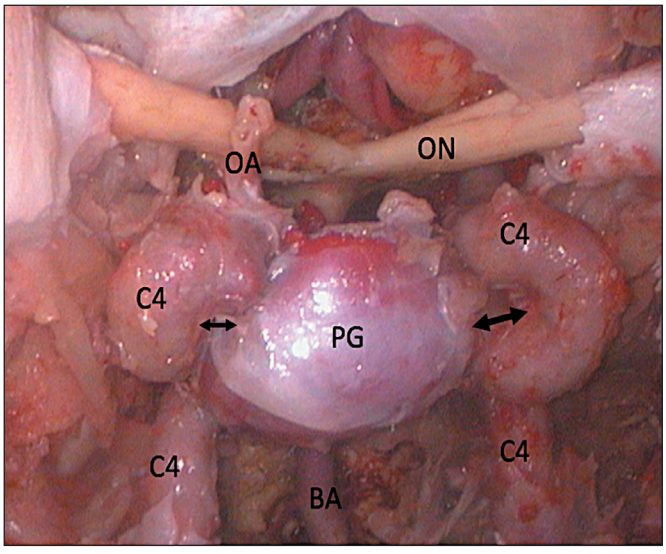

Figure 5: Horizontal measurement between the pituitary gland (PG) and the anterior genu of the cavernous segment (C4) of the internal carotid artery. **BA:** basilar artery, **OA:** ophthalmic artery, **ON:** optic nerve.

Traditionally, transcranial approaches targeting the lateral and superior walls of the CS have been favored for lesion removal. These include the subtemporal approach via the lateral wall, the pterional approach through the superior wall, the transpetrosal–transtentorial approach via the posterior wall, and the contralateral pterional–transsylvian approach through the medial wall (1). However, the effectiveness of transcranial approaches is frequently compromised by the need for brain retraction and the dense concentration of CNs, particularly the oculomotor, trochlear, and abducens nerves, traversing the lateral wall of the CS. Thus, modified endoscopic endonasal approaches through the inferior and medial walls have increasingly been recognized as safer and more anatomically favorable alternatives for CS access.

In the present study, we clearly demonstrated the consistent presence and definable anatomical boundaries of the MC using an EETA. Our findings are consistent with those of Kitano et al. (16), who described a vertical dural incision extending from the posterior to the anterior aspect of the cavernous ICA through the MC, allowing tumor resection up to the superior wall of the CS. In contrast, our technique employed a transverse dural incision with window-shaped dural excision, facil-

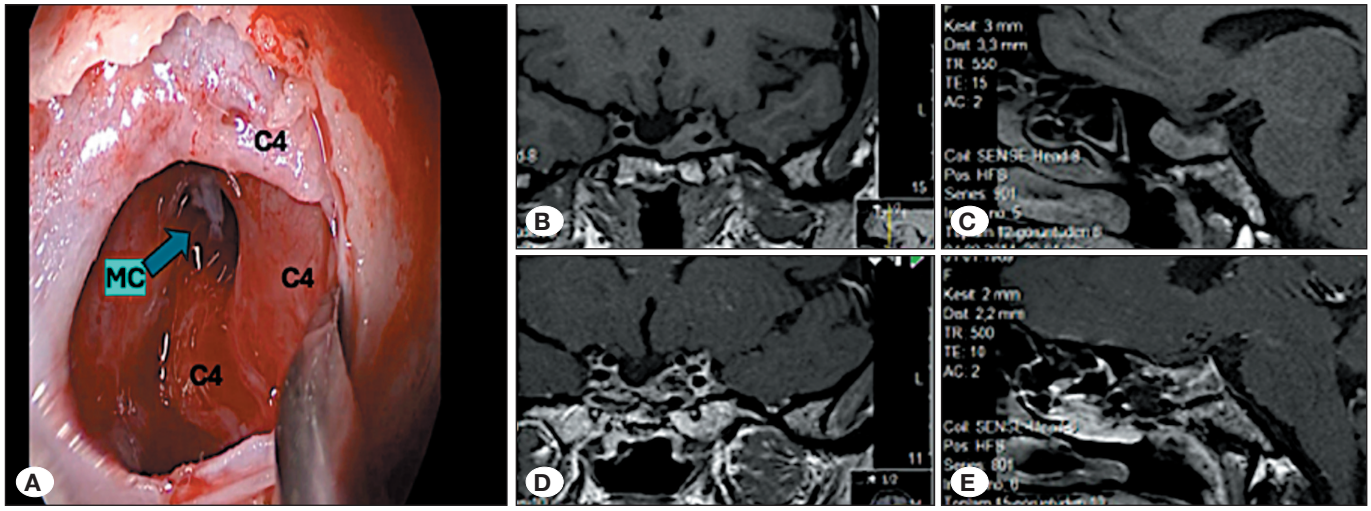

Figure 6: Perioperative **(A)** demonstration of the medial corridor (MC) in one of the cases from our clinical series, along with pre- **(B,C)** and postoperative **(D,E)** magnetic resonance imaging of the same case. **C4:** cavernous segment of the internal carotid artery.

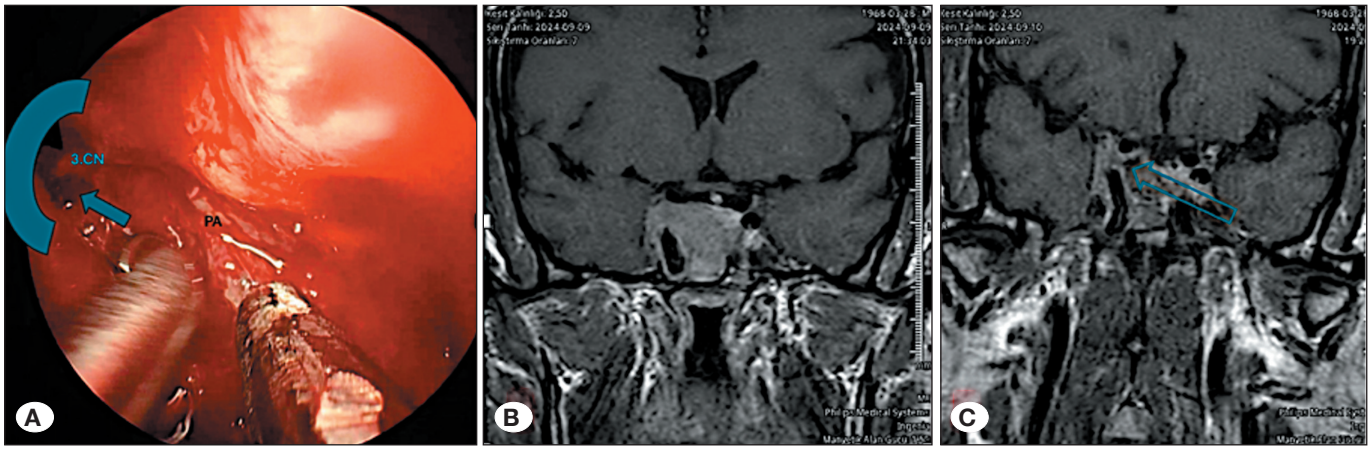

Figure 7: A) The thick C-shaped structure represents the internal carotid artery siphon (C4). The arrow points to the medial corridor (MC), whose lateral boundary is the third cranial nerve (3rd CN). **B)** Preoperative magnetic resonance imaging (MRI) demonstrating tumor extension into the medial corridor. **C)** Postoperative MRI confirming gross total resection of the tumor. **PA:** pituitary adenoma.

itating direct visualization of the spatial relationship between normal pituitary tissue and the posterior genu, horizontal segment, and anterior genu of the ICA. When advancing through the intersegmental space between these ICA components via the MC, the oculomotor nerve was consistently encountered, defining the lateral boundary of the corridor. Accordingly, we propose that intraoperative visualization of the oculomotor nerve during tumor excision within the MC reliably indicates that the lateral extent of safe resection has been reached.

In typical clinical settings, the oculomotor nerve is often visualized indirectly as a reflexive structure during CS surgery. However, in the clinical cases included in our study, invasive tumors occupied the CS and infiltrated its lateral wall, enabling direct and unambiguous visualization of the third CN. This finding underscores the practical surgical relevance of the MC in cases of advanced CS involvement.

Theodosopoulos et al. emphasized that the distance between the ICA and the pituitary gland plays a pivotal role in facilitating access to the lateral CS, and they introduced the concept of a “wide-area” MC (19). Our findings corroborate this observation, particularly in cases where the pituitary gland remains uninvolved and tumor extension is confined to the CS. In the present cadaveric series, a threshold distance of approximately 5 mm between the anterior genu of the ICA and the lateral margin of the pituitary gland was found to be a clinically meaningful parameter. When this distance was ≥5 mm, entry into the MC was consistently more feasible, and controlled ICA manipulation could be performed with greater safety.

It is well recognized that many nonfunctioning pituitary adenomas extending toward the CS are neither biologically aggressive nor truly invasive (18), a phenomenon often attributed to tumor growth through structurally weak regions of the CS

Table II: Distribution of cavernous sinus compartment invasion, extent of resection, age, hormonal activity (secretory vs. non-secretory), and remission status of 20 patients included in the series

Gender	Age (years)	Hormone secretion	Cavernous Sinus Invasion – Compartment	Complication	Resection	Remission
M	28	GH	Superior-Posterior	None	NT	No
M	34	GH	Superior	None	GT	Yes
F	23	NS	Posterior	None	GT	–
F	33	GH	Superior-Posterior	None	ST	No
M	37	PRL	Superior	None	GT	Yes
F	50	GH	Superior	None	GT	Yes
F	29	NS	Superior-Posterior	CSF Leak	GT	–
M	27	GH	Superior	None	GT	Yes
M	37	GH	Superior-Posterior	None	NT	No
M	27	GH	Superior	None	GT	Yes
M	57	GH PRL	Superior, Anteroinferior, Posterior	Epistaxis	ST	No
F	40	GH	Superior	None	GT	Yes
F	28	GH	Superior	None	GT	Yes
M	40	NS	Superior-Posterior	None	NT	–
M	46	NS	Superior-Posterior	None	GT	–
M	37	GH	Superior	None	GT	Yes
M	33	NS	Superior-Posterior	None	GT	–
F	44	NS	Superior	None	GT	–
F	36	GH	Superior	None	NT	No
M	29	GH	Superior	None	GT	Yes

GH: *growth hormone,* ***PRL:*** *prolactin,* ***NS:*** *non-secreting,* ***CSF:*** *cerebrospinal fluid,* ***GT:*** *gross total,* ***NT:*** *near total,* ***ST:*** *subtotal,* ***M:*** *male,* ***F:*** *female.*

wall. Clinical series have demonstrated that when pituitary adenomas invade the CS, progression most commonly occurs via the MC (5,13). At present, no neuroimaging modality allows definitive visualization of the medial wall of the CS. Anatomical studies have variably described this structure as single-layered, double-layered, or thin and loosely organized with focal histological defects (7,9,10). Consequently, while some authors have emphasized tumor histology as the primary determinant of CS invasion, others have highlighted the inherent structural vulnerability of the medial wall as the key facilitating factor (9).

Pituitary adenomas may originate within either the medial or lateral corridors of the cavernous ICA. Lesions extending laterally within the CS frequently invade the anteroinferior ICA region or the MC. Songtao et al. (17) demonstrated that the lamina propria lines the inner surface of the pituitary gland, while the pituitary capsule envelops its outer surface, with the inferolateral capsule being relatively thick and the medial wall being structurally weaker. Following invasion of the lamina propria and pituitary capsule, adenomas may exploit these weak points of the medial wall and extend along the characteristic C-shaped course of the ICA, thereby creating a surgically exploitable endoscopic corridor medial to the cavernous ICA (2). The present series also illustrates a notable anatomical variation in which the horizontal ICA segment coursed unusually close to the midline (Figure 8), further emphasizing the importance of individualized anatomical assessment.

Multiple surgical corridors between neurovascular structures have been described to facilitate endoscopic access to the CS. Corridors lateral to the ICA are generally more directly accessed via ipsilateral expanded endonasal or far-lateral transethmoidal or transsphenoidal approaches. In contrast, the MC of the ICA was more effectively explored through a contralateral endoscopic route, consistent with prior anatomical and clinical studies. In a representative case, advancement through the MC enabled access to the lateral compartment via meticulous dissection along the lateral aspect of the ICA (Figure 9).

From a surgical standpoint, the MC represents the only endoscopic route capable of addressing lesions extending from the sella into the lateral CS while displacing the CNs and ICA laterally, thereby providing access to the lateral sellar compartment (16).

Despite these findings, several limitations inherent to cadaveric studies must be acknowledged. Differences in tumor consistency, prior treatment effects, displacement of neurovascular structures, and anatomical variability of the ICA within the CS may limit direct clinical extrapolation. Most notably, the absence of tumor tissue within the CS in cadaveric speci-

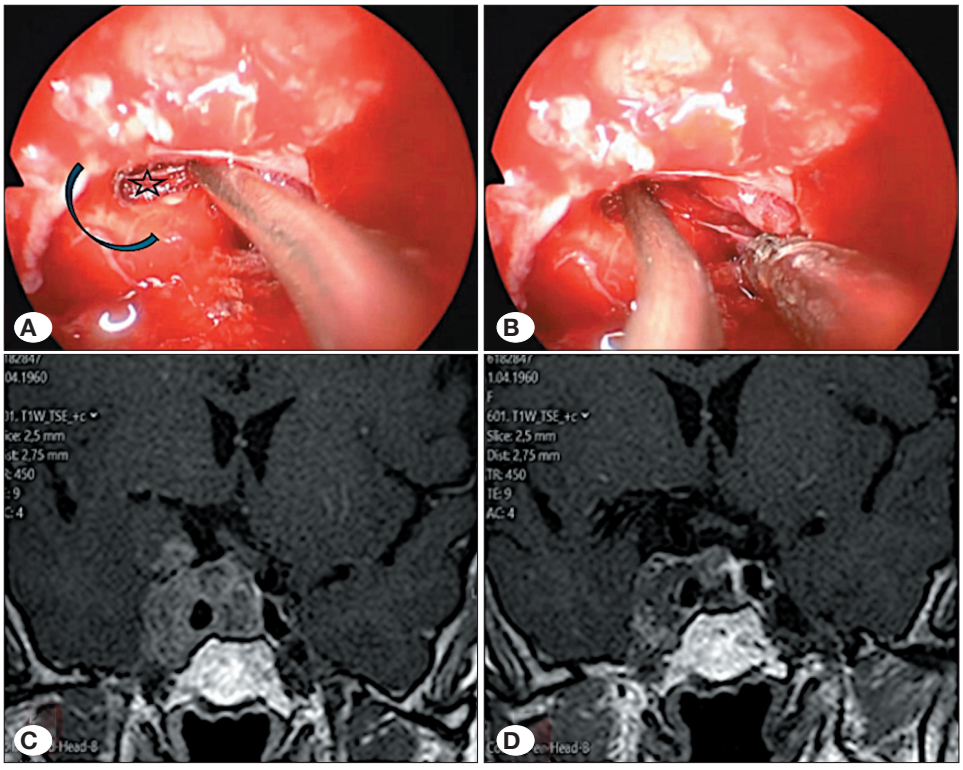

Figure 8: A) This case presents a variation in the anatomy of the internal carotid artery. The tumor is excised by directly accessing the superior and lateral compartments through the medial corridor (MC). Atherosclerotic changes within the horizontal segment extending toward the midline are clearly observed. The medial corridor is delineated by dense fibrotic bands, marked with a star. **B)** The tumor tissue is accessed via the MC using an aspirator, and surgical excision is performed. **C,D)** Pre- and postoperative magnetic resonance imaging demonstrating the tumor status before and after resection.

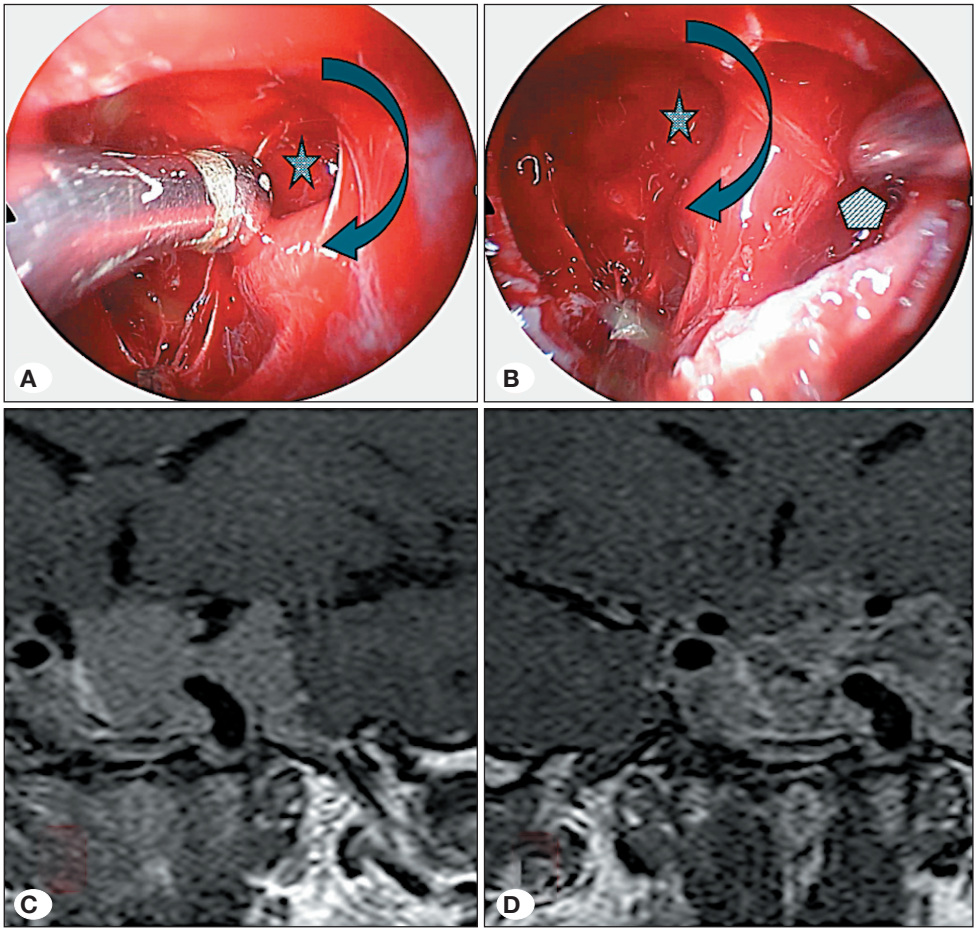

Figure 9: Tumor extension and surgical approaches. In the present case, the tumor extends into the superior and lateral compartments. **A)** The anterior and horizontal segments of the cavernous segment of the internal carotid artery are exposed. Entry is achieved via the medial corridor (marked with a star), allowing access to the tumor located in the superior compartment using an aspirator. **B)** Surgical dissection proceeds laterally to the cavernous segment of the internal carotid artery, and the tumor tissue within the lateral compartment (marked with a pentagon) is accessed and excised. **C,D)** Pre- and postoperative magnetic resonance imaging findings.

mens precludes the assessment of tumor-induced distortion, compression, and fibrotic adhesions that affect critical neurovascular elements. Consequently, the applicability of anatomical observations may vary depending on the extent of tumor invasion and the degree of neurovascular displacement encountered in clinical practice.

CONCLUSION

We have provided a precise anatomical definition and reproducible delineation of the MC using the EETA. The anatomical and clinical findings of this study support the concept that the MC represents a fundamental and preferential pathway for the extension of pituitary adenomas and other intrasellar lesions into the superior, lateral, and posterior compartments of the CS. As such, the MC should be regarded not merely as a surgical access route but as a critical anatomical interface that governs both tumor invasion dynamics and the limits of safe endoscopic resection.

We further demonstrated that the approximately 5-mm interval between the anterior genu of the ICA and the lateral margin of the pituitary gland constitutes a pivotal anatomical determinant at the entry point of the MC. This spatial parameter appears to directly influence surgical accessibility to the MC and the adjacent CS compartments, thereby defining a practical threshold for safe and controlled endoscopic advancement. By integrating high-resolution anatomical measurements with intraoperative and radiological clinical correlations, the findings of our study underscore that a nuanced, quantitative understanding of MC anatomy is indispensable for refining surgical decision-making, maximizing the extent of safe tumor removal, and minimizing the risk of neurovascular morbidity. Collectively, the findings of this study position the MC as a central anatomical and surgical concept in contemporary endoscopic CS surgery.

ACKNOWLEDGEMENTS

The authors express their gratitude to the Bahcesehir University Rhoton Anatomy Laboratory for supplying the cadaveric specimens used in this study.

We also wish to acknowledge the medical staff who contributed to the surgical procedures and data collection for the clinical cases.

Declarations

Funding: This research did not receive any specific grant from funding agencies in the public, commercial, or not-for-profit sectors.

Availability of data and materials: The datasets generated and/or analyzed during the current study are available from the corresponding author by reasonable request.

Disclosure: The authors declare no competing interests.

AUTHORSHIP CONTRIBUTION

Study conception and design: BC, SC
Data collection: AG, AU, EY, AE, MC
Analysis and interpretation of results: AG, BC, IA
Draft manuscript preparation: AG, AU
Critical revision of the article: SC
Other (study supervision, fundings, materials, etc...): SC, AG
All authors (AG, AU, EY, AE, MC, BC, IA, SC) reviewed the results and approved the final version of the manuscript.

REFERENCES

1. Cappabianca P, Alfieri A, de Divitiis E: Endoscopic endonasal transsphenoidal approach to the sella: Towards functional endoscopic pituitary surgery (FEPS). Minim Invasive Neurosurg 41:66-73, 1998. https://doi.org/10.1055/s-2008-1052019
2. Cavallo LM, Cappabianca P, Galzio R, Laconetta G, de Divitiis E, Tschabitscher M: Endoscopic Transnasal Approach To The Cavernous Sinus Versus Transcranial Route: Anatomic Study. Neurosurgery 56:279-389, 2005. https://doi.org/10.1227/01.NEU.0000156548.30011.D4
3. Ceylan S, Anik I, Cabuk B, Caklili M, Anik Y: Extension Pathways of Pituitary Adenomas with Cavernous Sinus Involvement and Its Surgical Approaches. World Neurosurgery 127:986-995, 2019. https://doi.org/10.1016/j.wneu.2019.04.013
4. Ceylan S, Anik I, Koc K, Cabuk B: Extended endoscopic transsphenoidal approach infrachiasmatic corridor. Neurosurg Rev 38:137-147, 2015. https://doi.org/10.1007/s10143-014-0576-0
5. Ceylan S, Koc K, Anık I: Endoscopic endonasal transsphenoidal approach for pituitary adenomas invading the cavernous sinüs. J Neurosurg 112:99-107, 2010. https://doi.org/10.3171/2009.4.JNS09182
6. Ceylan S, Sen HE, Ozsoy B, Ceylan EC, Ergen A, Selek A, Anik Y, Balci S, Cabuk B, Anik I: Endoscopic approach for giant pituitary adenoma: clinical outcomes of 205 patients and comparison of two proposed classification systems for preoperative prediction of the extent of resection. J Neurosurg 136:786-800, 2022. https://doi.org/10.3171/2021.3.JNS204116
7. Ciric I. On the origin and nature of the pituitary gland capsule. J Neurosurg 46:596-600, 1977. https://doi.org/10.3171/jns.1977.46.5.0596
8. de Divitiis E, Cappabianca P, Cavallo LM: Endoscopic transsphenoidal approach: Adaptability of the procedure to different sellar lesions. Neurosurgery 51:699-707, 2002. https://doi.org/10.1097/00006123-200209000-00016
9. Dolenc VV: Anatomy and surgery of the cavernous sinus. Springer, Berlin, 1989. https://doi.org/10.1007/978-3-7091-6942-1
10. Dolenc VV: Relation of the cavernous sinus to the sella. In: Dolenc VV (eds), Anatomy and surgery of the cavernous sinus. Vienna: Springer-Verlag, 1989:118-130, 1989. https://doi.org/10.1007/978-3-7091-6942-1

11. Fernandez-Miranda JC, Gardner P, Snyderman C: Endoscopic endonasal trans cavernous posterior clinoidectomy with interdural pituitary transposition. J Neurol Surg B Skull Base 75: A022, 2014. https://doi.org/10.3171/2014.3.JNS131865
12. Fermandez-Miranda JC, Zwagerman NT, Abhinav K, Lieber S, Wang EW, Snyderman CH, Gardner PA: Cavernous sinus compartments from the endoscopic endonasal approach: anatomical considerations and surgical relevance to adenoma surgery. J Neurosurgery 129:430-441, 2018. https://doi.org/10.3171/2017.2.JNS162214
13. Frank G, Pasquini E: Endoscopic endonasal approaches to the cavernous sinus: Surgical approaches. Neurosurgery 50:675, 2002. https://doi.org/10.1097/00006123-200203000-00059
14. Harris FS, Rhoton AL Jr. Anatomy of the cavernous sinus: A microsurgical study. J Neurosurg 45:169-180, 1976. https://doi.org/10.3171/jns.1976.45.2.0169
15. Jho HD, Ha HG: Endoscopic endonasal skull base surgery: Part 2-The cavernous sinus. Minim Invasive Neurosurg 47:9-15, 2004. https://doi.org/10.1055/s-2004-818346
16. Kitano M, Taneda M, Shımono T, Nakao Y: Extended transsphenoidal approach for surgical management of pituitary adenomas invading the cavernous sinus. J Neurosurg 108:26-36, 2008. https://doi.org/10.3171/JNS/2008/108/01/0026
17. Songtao Q, Yuntao L, Jun P, Chuanping H, Xiaofeng S: Membranous layers of the pituitary gland: a histological anatomic study and related clinical issues. Neurosurgery 64:1-10, 2009. https://doi.org/10.1227/01.NEU.0000327688.76833.F7
18. Taniguchi M, Hosoda K, Akutsu N, Takahashi Y, Kohmura E: Endoscopic endonasal transsellar approach for laterally extended pituitary adenomas: Volumetric analysis of cavernous sinus invasion. Pituitary 18:518-524, 2015. https://doi.org/10.1007/s11102-014-0604-7
19. Theodosopoulos PV, Cebula H, Kurbanov A, Cabero AB, Osorio JA, Zimmer LA, Froelich SC: The medial extra-sellar corridor to the cavernous sinus: Anatomic description and clinical correlation. World Neurosurg 96:417-422, 2016. https://doi.org/10.1016/j.wneu.2016.09.046

Turk Neurosurg 36(3):467-470, 2026
DOI: 10.5137/1019-5149.JTN.48672-25.3

Case Report

Received: 10.03.2025
Accepted: 06.06.2025
Published Online: 22.05.2026

Takayasu Arteritis Complicated with Vertebral Artery Dissection Aneurysm Treated Endovascularly: Report of One Case

Han WANG[1]*, Jiao CHENG[1]*, Zuyao SONG[1], Chao LI[1], Jing YE[1], Liping CHENG[2]*

[1]Central Hospital of Shengli Oilfield, Department of Neurosurgery, Dong ying 257000, China
[2]Central Hospital of Shengli Oilfield, Department of Neurology, Dong ying 257000, China

*These authors have contributed equally to this study.

Corresponding author: Liping CHENG ✉ 15762926015@163.com

ABSTRACT

Takayasu arteritis (TA) is a chronic granulomatous large-vessel vasculitis that primarily affects the aorta and its major branches, such as the subclavian, carotid, and renal arteries. Pathologically, it is characterized by transmural infiltration of lymphocytes and macrophages with granulomatous inflammation, leading to intimal fibrosis and thickening, destruction of medial elastic fibers, and subsequent luminal stenosis or occlusion. Aneurysmal dilation may occur in some cases. We here report a case of TA complicated by a vertebral artery dissecting aneurysm. Our patient was a 47-year-old male who had previously undergone surgical interventions at our institution for a common iliac artery aneurysm and splenic artery aneurysm 6 years and 2 years prior to the present admission, respectively. Most recently, the patient was presented with right shoulder pain and was subsequently diagnosed with a right vertebral artery dissecting aneurysm, for which endovascular intervention was performed. This case underscores the critical importance of long-term clinical surveillance in patients with TA, along with the necessity for aggressive treatment of aneurysms that are identified to have a high risk of rupture.

KEYWORDS: Takayasu arteritis, Aneurysm, Arterial dissection, Interventional radiology

INTRODUCTION

Takayasu arteritis (TA) predominantly affects young women aged ≤ 40 years, with a reported prevalence ranging from approximately 1.1 to 40 cases per million population (4,11). The disease is primarily characterized by intimal thickening of the aorta and its major branches, leading to vessel wall thickening and luminal stenosis (9). In a subset of patients, inflammatory destruction of the arterial media, elastic fibers, and smooth muscle fibers may result in the formation of aneurysms (12,13). Rupture of these aneurysms is associated with high rates of morbidity and mortality, significantly compromising patient prognosis (7). Therefore, early diagnosis and prompt therapeutic intervention are critical to improving outcomes in affected individuals.

Here, we present the case of a 47-year-old male patient with concomitant TA and vertebral artery dissecting aneurysm who underwent endovascular interventional therapy, and we review the related literature.

CASE REPORT

This study was conducted according to the latest revision of the Helsinki Declaration regarding medical research involving human subjects. Informed written consent was acquired from

Han WANG : 0009-0003-6166-1267
Jiao CHENG : 0009-0007-5743-6736
Zuyao SONG : 0009-0008-3479-0422
Chao LI : 0000-0002-1718-9028
Jing YE : 0009-0009-1040-0167
Liping CHENG : 0000-0002-1534-0011

the patient before the study. No IRC board approval was needed for this case report because the patient's identity was kept anonymous.

In March 2019, a 47-year-old male patient who presented with abdominal pain underwent abdominal and lower extremity vascular ultrasound as well as computed tomography angiography (CTA) at our hospital. The imaging revealed an aneurysm of the right common iliac artery, aneurysmal dilation of the superior mesenteric artery, a right renal artery aneurysm, and ulceration of the left renal artery. After consultation with the radiology and rheumatology departments, the patient was diagnosed with TA. During hospitalization, the patient underwent an aortobifemoral bypass graft procedure. In December 2022, the patient experienced rupture and hemorrhage of a splenic artery aneurysm and was admitted to our hospital for splenic artery ligation, during which a blood transfusion was administered (Figure 1).

Two years later, the patient was admitted with a 2-day history of pain in the right shoulder radiating to the occipital and right temporal regions, accompanied by nausea, vomiting, limb weakness, and mental lethargy. A cranial CT scan performed at a local hospital revealed a high-density lesion anterior to the brainstem in the posterior cranial fossa, suggestive of an aneurysm. For further management, the patient was transferred to the neurosurgery department of our hospital. CTA of the head and neck identified a dissecting aneurysm of the right vertebral artery (Figure 2).

Cerebral angiography revealed a dissecting aneurysm at the V4 segment of the right vertebral artery, with a size of approximately 7.8 × 7.5 mm. Subsequently, the aneurysm was treated with LVIS stent-assisted embolization. Intraoperative angiography showed dense embolization of the aneurysm, with the stent deployed effectively and the vertebral artery remaining patent. At the 12-month postoperative evaluation, magnetic resonance angiography imaging showed successful aneurysm exclusion with no signs of recurrence in the right vertebral artery dissection segment (Figure 2).

DISCUSSION

The prevalence of aneurysms in patients with TA is relatively low, with aneurysms predominantly localized in the aorta and its major branches, particularly the subclavian artery, carotid artery, renal artery, and abdominal aorta. Epidemiological studies have reported that the incidence of aneurysms in patients with TA ranges from approximately 16.6% to 31.1% (2,8). In the management of TA-associated aneurysms, pharmacological therapy plays a central role in controlling inflammatory activity, mitigating disease progression, and reducing the risk of aneurysm expansion. Therapeutic regimens typically include glucocorticoids, immunosuppressants (e.g., methotrexate and azathioprine), and biologic agents (e.g., infliximab and tocilizumab). Emerging evidence from recent studies suggests that biologic agents demonstrate superior efficacy and a more favorable safety profile compared with glucocorticoids, with lower complication rates and improved clinical outcomes (5,10). Surgical intervention remains a critical component of treatment, especially for patients with significant compressive symptoms or those at high risk of rapid aneurysm expansion or rupture. Traditional open surgery is generally reserved for cases where endovascular approaches are not feasible. In contrast, endovascular intervention has become the preferred modality for patients with anatomically complex aneurysms or those deemed unsuitable for open surgical procedures due to comorbidities or other risk factors (6,14).

In this case, the patient had a history of ruptured splenic artery aneurysm, and the presence of a large vertebral artery dissecting aneurysm posed an imminent risk of rupture, thus necessitating prompt intervention. Vertebrobasilar artery dissecting aneurysms (VBDAs) are relatively rare, accounting for approximately 3.2–5.5% of all intracranial aneurysms (1). Rupture of such aneurysms can lead to acute hydrocephalus due to hematoma obstruction of the fourth ventricle, and in severe cases, brainstem compression by the hematoma may result in respiratory and circulatory compromise (3). Given the challenges associated with the complex anatomical location of VBDAs, including difficult surgical exposure and high perioperative risks, endovascular intervention has emerged as the preferred treatment modality. Endovascular

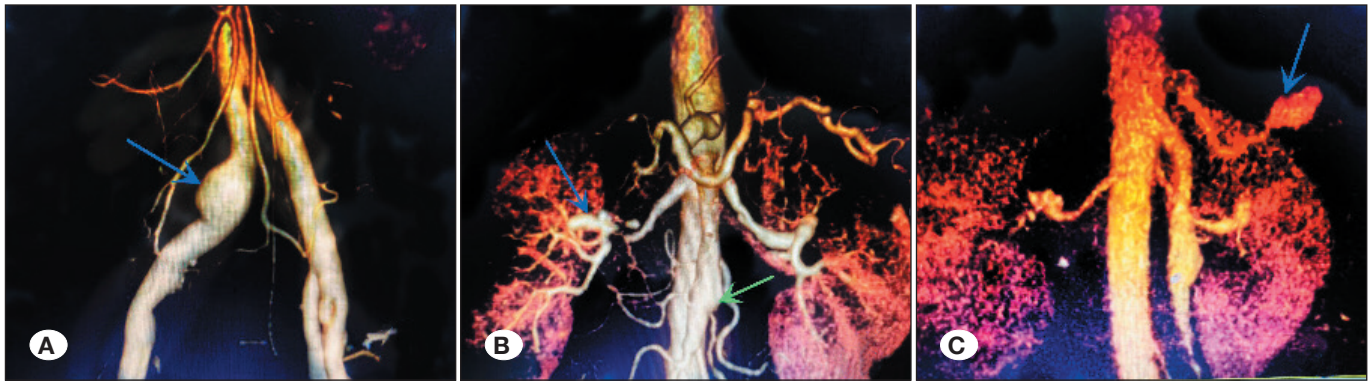

Figure 1: A) Aneurysm of the right common iliac artery (indicated by the blue arrow). **B)** Aneurysmal dilation of the superior mesenteric artery (indicated by the green arrow), and aneurysm of the right renal artery (indicated by the blue arrow). **C)** Aneurysm of the splenic artery (indicated by the blue arrow). These illustrations address the question at hand.

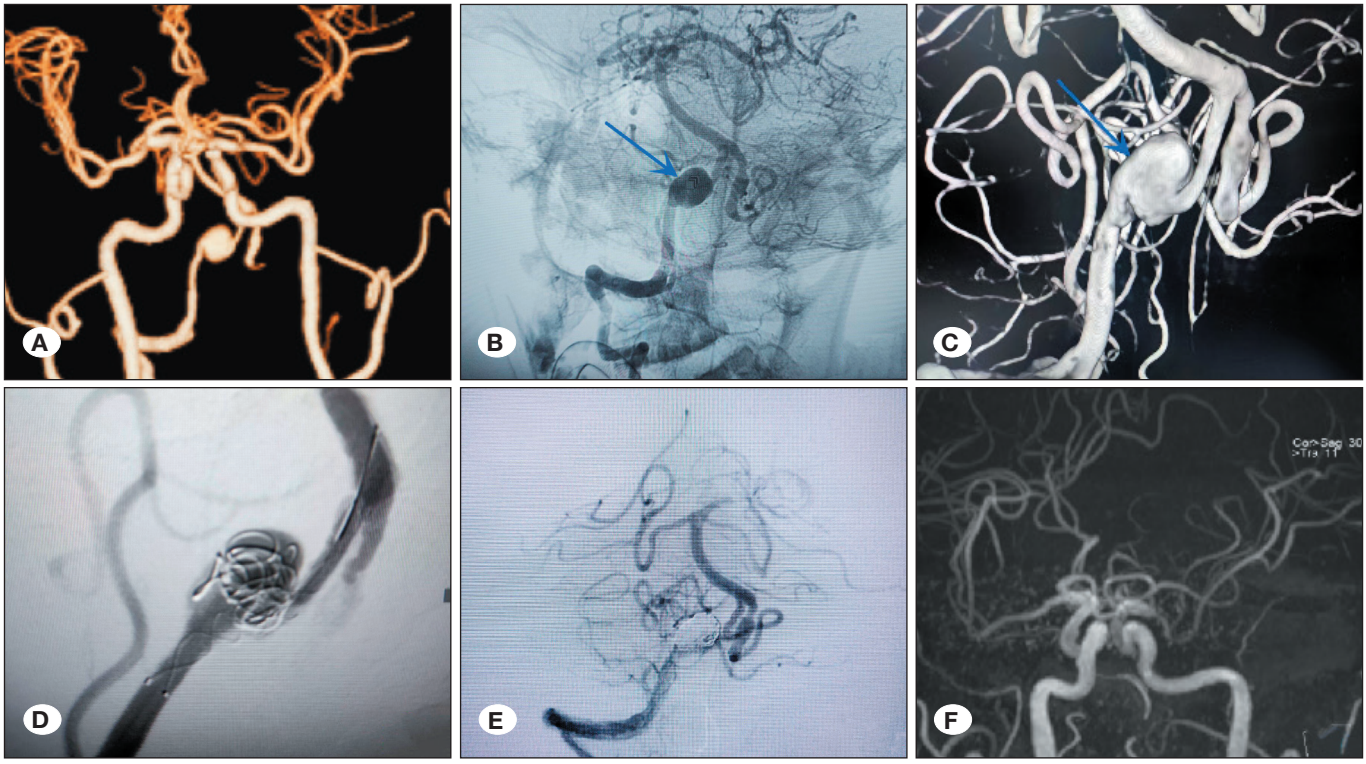

Figure 2: A) Computed tomography angiography (CTA) of the patient showing a dissecting aneurysm of the right vertebral artery. **B, C)** Digital subtraction angiography and three-dimensional reconstruction images showing the dissecting aneurysm of the vertebral artery (indicated by the blue arrow). **D)** Workhorse view of stent-assisted embolization of the aneurysm. **E)** Intraoperative angiogram showing dense embolization of the aneurysm with the parent artery remaining patent, thereby addressing the question at hand. **F)** Postoperative magnetic resonance angiogram obtained at a 1-year follow-up showing no evidence of aneurysm recurrence.

treatment options for VBDAs primarily include stent-assisted coil embolization, flow diverter implantation, and parent artery occlusion. Stent-assisted coil embolization involves placing a stent within the parent artery combined with coil embolization of the aneurysm, which effectively seals the aneurysm sac while maintaining patency of the parent artery (15). Flow diverters, such as the Pipeline embolization device, promote intra-aneurysmal thrombosis and vessel wall reconstruction through their dense mesh design, making them suitable for complex or giant aneurysms. In cases where preservation of the parent artery is not feasible, parent artery occlusion may be performed, provided that adequate collateral circulation is confirmed, to completely disrupt blood flow to the aneurysm.

CONCLUSION

The management of TA complicated by aneurysms necessitates an individualized approach that integrates pharmacological therapy, surgical or endovascular interventions, and long-term follow-up. Early screening and proactive intervention are crucial for aneurysms with irregular morphology or high rupture risk to reduce the likelihood of aneurysm rupture and hemorrhage and improve patient outcomes.

Declarations

Funding: This research did not receive any specific grant from funding agencies in the public, commercial, or not-for-profit sectors.

Availability of data and materials: The datasets generated and/or analyzed during the current study are available from the corresponding author by reasonable request.

Disclosure: The authors declare no competing interests.

Ethical approval: No IRC board approval was needed for this case report because the patient's identity was kept anonymous.

Informed consent: Informed written consent was acquired from the patient before the study.

AUTHORSHIP CONTRIBUTION

Study conception and design: JC, ZS
Data collection: JC
Analysis and interpretation of results: CL, HW
Draft manuscript preparation: JC, HW
Critical revision of the article: LC
Other (study supervision, fundings, materials, etc...): JY
All authors (HW, JC, ZS, CL, JY, LC) reviewed the results and approved the final version of the manuscript.

REFERENCES

1. Beletsky V, Norris JW: Spontaneous dissection of the carotid and vertebral arteries. N Engl J Med 345:467, 2001. https://doi.org/10.1056/NEJM200103223441206
2. Cheng F, Shao Z, Lu QS, Zhao R, Lu FL, Tian B, Peng WJ, Zhao FT, Zhao DB, Cai Q: Aneurysms in Takayasu's arteritis: A retrospective study of Chinese patients. Clin Exp Rheumatol 38 Suppl 124:42-47, 2020
3. Chung J, Cheol Lim Y, Sam Shin Y: Endovascular treatment of intracranial vertebral artery dissection. J Neuroendovasc Ther 15:265-280, 2021. https://doi.org/10.5797/jnet.ra.2020-0150
4. Comarmond C, Biard L, Lambert M, Mekinian A, Ferfar Y, Kahn JE, Benhamou Y, Chiche L, Koskas F, Cluzel P, Hachulla E, Messas E, Resche-Rigon M, Cacoub P, Mirault T, Saadoun D; French Takayasu Network: Long-term outcomes and prognostic factors of complications in takayasu arteritis: A multicenter study of 318 patients. Circulation 136:1114-1122, 2017. https://doi.org/10.1161/CIRCULATIONAHA.116.027094
5. Gon Y, Yoshifuji H, Nakajima T, Murakami K, Nakashima R, Ohmura K, Mimori T, Terao C: Long-term outcomes of refractory Takayasu arteritis patients treated with biologics including ustekinumab. Mod Rheumatol 31:678-683, 2021. https://doi.org/10.1080/14397595.2020.1800560
6. Hinojosa CA, Anaya-Ayala JE, Torres-Machorro A, Lizola R, Laparra-Escareno H: Middle aortic syndrome in Takayasu's arteritis: Report of two surgical cases. Ann Vasc Surg 34:270.e13-7, 2016. https://doi.org/10.1016/j.avsg.2015.12.015
7. Kanda M, Shinoda S, Masuzawa T: Ruptured vertebral artery-posterior inferior cerebellar artery aneurysm associated with pulseless disease-case report. Neurol Med Chir 44:363-367, 2004. https://doi.org/10.2176/nmc.44.363
8. Lefebvre F, Ross C, Soowamber M, Pagnoux C; Canadian Network for Research on Vasculitis (CanVasc). Aneurysmal disease in patients with takayasu arteritis. J Rheumatol 51:277-284, 2024. https://doi.org/10.3899/jrheum.2023-0629
9. Mirouse A, Deltour S, Leclercq D, Squara PA, Pouchelon C, Comarmond C, Kahn JE, Benhamou Y, Mirault T, Mekinian A, Lambert M, Chiche L, Koskas F, Cluzel P, Redheuil A, Cacoub P, Biard L, Saadoun D; French Takayasu Network. Cerebrovascular ischemic events in patients with takayasu arteritis. Stroke 53:1550-1557, 2022. https://doi.org/10.1161/STROKEAHA.121.034445
10. Nakaoka Y, Isobe M, Takei S, Tanaka Y, Ishii T, Yokota S, Nomura A, Yoshida S, Nishimoto N: Efficacy and safety of tocilizumab in patients with refractory Takayasu arteritis: Results from a randomised, double-blind, placebo-controlled, phase 3 trial in Japan (the TAKT study). Ann Rheum Dis 77:348-354, 2018. https://doi.org/10.1136/annrheumdis-2017-211878
11. Rutter M, Bowley J, Lanyon PC, Grainge MJ, Pearce FA: A systematic review and meta-analysis of the incidence rate of Takayasu arteritis. Rheumatology 60:4982-4990, 2021. https://doi.org/10.1093/rheumatology/keab406
12. Saadoun D, Vautier M, Cacoub P: Medium-and large-vessel vasculitis. Circulation 143:267-282, 2021. https://doi.org/10.1161/CIRCULATIONAHA.120.046657
13. Su RJ, Zhang JM, Chen T, Huang YH: Vertebral and carotid artery aneurysms and polyarthritis in a patient with Takayasu arteritis: A case report. Radiol Case Rep 17:832-842, 2022. https://doi.org/10.1016/j.radcr.2021.11.041
14. Vijayvergiya R, Jindal AK, Pilania RK, Suri D, Gupta A, Sharma A, Sinha SK, Singhal M, Bahl A, Singh S: Complex interventions of abdominal aorta and its branches in children with Takayasu arteritis: Clinical experience from a tertiary care center in north-west India. Int J Rheum Dis 22:140-151, 2019. https://doi.org/10.1111/1756-185X.13420
15. Wu Q, Meng Y, Chen A, Xu S, Wang C, Ji Z, Qi J, Yuan K, Shao J, Shi H, Wu P: LVIS-within-enterprise double-stent technique with coil embolization in the treatment of patients with acutely ruptured intracranial vertebrobasilar artery-dissecting aneurysms. Front Neurol 14:1069380, 2023. https://doi.org/10.3389/fneur.2023.1069380

Turk Neurosurg 36(3):471-475, 2026
DOI: 10.5137/1019-5149.JTN.47954-24.0

Case Report

Received: 03.11.2024
Accepted: 11.12.2024
Published Online: 22.05.2026

Ruptured Vertebral Artery Aneurysm in a Patient with Loeys-Dietz Syndrome Type 4: A Sentinel Case Report

Elizabeth E. WICKS, Luke SILVEIRA, Elnur DELAHMETOVIC, John MUSE, Brandon LIEBELT, Bruce TRANMER

The University of Vermont Medical Center, Neurosurgery Department, Burlington, VT, USA

Corresponding author: Elizabeth E. WICKS ✉ elizabeth.wicks@uvmhealth.org

ABSTRACT

Loey-Dietz Syndrome (LDS) is a rare, autosomal dominant connective tissue disorder with an estimated prevalence of less than 1 in 100,000. LDS results from one of several genetic mutations altering the transforming growth factor β (TGF- β) signaling pathway. LDS portends a higher risk of vascular pathology including dissections and aneurysms throughout the arterial system. Though not commonly described, this higher incidence of vascular pathology extends to the cerebrovascular system with several case reports of cerebral aneurysms in patients afflicted with LDS.

Herein, we describe the case of a 39-year-old female with a family history of cerebral and aortic aneurysms who presented with acute onset headache, neck pain, and lower extremity paresis prompting a CT head and subsequent magnetic resonance angiogram remarkable for a subarachnoid hemorrhage secondary to rupture of a large fusiform V4 segment vertebral artery aneurysm. Formal angiogram confirmed this diagnosis, and endovascular treatment was pursued with coil embolization of the aneurysm and parent vertebral artery distal occlusion. Subsequent genetic testing confirmed the patient to be positive for the mutation indicative of type 4 LDS.

Though rare, LDS should be considered as a possible diagnosis in patients presenting with aneurysmal subarachnoid hemorrhage when a family history of systemic vascular pathology is elicited. Confirmatory diagnosis of LDS appropriately spurs additional vascular imaging and family screening to proactively minimize the morbidity of this rare disease.

KEYWORDS: Loeys-Dietz Syndrome, Intracranial aneurysm, Endovascular neurosurgery

ABBREVIATIONS: LDS: Loeys-Dietz Syndrome, **TGF-β:** Transforming growth factor β, **ED:** Ehlers-Danlos Syndrome, **MEN2A:** Multiple endocrine neoplasia type 2A, **TGFβR1:** TGF-β receptor 1, **TGFβR2:** TGF-β receptor 2, **SMAD3:** Mothers against decapentaplegic homolog 3, **TGFβ2:** Transforming growth factor β2 ligand gene, **TGFβ3:**TGF-Beta 3 ligand gene, **FBN1:** Fibrillin 1 gene, **COL3A1:** Collagen Type III Alpha 1 Chain, **COL1A1:** Collagen Type I Alpha 1 Chain

INTRODUCTION

Loeys-Dietz Syndrome (LDS) is a rare autosomal dominant connective tissue disorder with a prevalence of less than 1 in 100,000 (11). LDS affects cardiovascular, craniofacial, cutaneous, ocular, and skeletal tissues. Individuals affected harbor a mutation in one of four genes involved in transforming growth factor β (TGF- β) signaling (11). Though typically associated with high risk of aortic dissections, affected individuals are also at risk of abnormal vasculature including aneurysms and dissections throughout the body's arterial network, including the cerebrovascular arterial tree. While similar to other connective tissue disorders associated with intracranial aneurysms such as Marfan Syndrome and

Elizabeth E. WICKS : 0000-0003-4400-9499
Luke SILVEIRA : 0000-0001-8919-4670
Elnur DELAHMETOVIC : 0009-0009-3718-568X
John MUSE : 0000-0002-2747-6178
Brandon LIEBELT : 0000-0001-8707-9329
Bruce TRANMER : 0009-0008-0053-0083

Ehlers-Danlos Syndrome (EDS) type IV, a robust association has not yet been established between cerebrovascular arterial pathology and LDS. However, there are several case reports of intracranial aneurysms being treated in individuals with LDS (3,5,8). We describe the case of a 39-year-old female with previously undiagnosed LDS who presented with an intradural ruptured right vertebral artery aneurysm successfully treated with endovascular occlusion of the parent vessel.

CASE REPORT

A 39-year-old female with pertinent past medical history of multiple endocrine neoplasia type 2A (MEN2A) syndrome and medically controlled hypothyroidism status post thyroidectomy presented to the emergency department with severe headache, neck pain, photophobia, and paresis. Of note, the patient also had a significant family history of both aortic and cerebral aneurysms. On arrival to the emergency room, she had bilateral lower extremity weakness, but was otherwise neurologically intact. CT head revealed a subarachnoid hemorrhage ventral to the brainstem as well as some additional blood products posteriorly layering in the left lateral ventricle (Figure 1). Subsequent MR cervical spine demonstrated additional hemorrhage extending ventrally through the thecal sac to the thoracic spine. MRI/MRA head and neck revealed a 9 mm x 5mm aneurysm in the right V4 segment of the vertebral artery (Figure 2).

Following identification of the aneurysm, the patient underwent a formal digital subtraction angiogram which confirmed a fusiform, eccentric right vertebral artery dilatation measuring 8 x 7.5 x 9 mm just distal to the right posterior inferior cerebellar artery origin (Figure 3). A guide wire and microcatheter were successfully navigated into the right vertebral artery aneurysm. A series of coils were subsequently deployed into the aneurysm and parent vertebral artery with resultant sacrifice of the right vertebral artery distal to the aneurysm. Upon completion of coiling, complete flow obstruction to the right vertebral artery distal to the aneurysm was obtained (Figure 4A, B). A left vertebral artery injection revealed no retrograde flow into the aneurysm (Figure 4C, D).

Given the patient's significant family history of aortic and cerebral aneurysms as well as a subsequently elicited suspicion for a paternal history of connective tissue disease, Loeys-Dietz Syndrome was proposed as a possible underlying diagnosis and genetic counseling was obtained. While awaiting formal genetic testing results, a screening MR angiogram of the chest, abdomen, and pelvis was performed to assess the patient's systemic vasculature. The aortic arch, thoracic aorta, and abdominal aorta were all without evidence of aneurysm or dissection. However, the patient did have evidence of an 11cm splenic artery aneurysm and was appropriately scheduled with vascular surgery follow up. The patient was ultimately found to have a paternal lineage, pathogenic mutation in the TGFb2 gene. This gene mutation is passed down in the autosomal dominant fashion and diagnostic of Loeys-Dietz Syndrome type 4. (10)

DISCUSSION

LDS is a relatively new clinical entity with a highly aggressive vascular course. Originally described in 2005, LDS and its typical phenotypic manifestations are the result of variable expressivity mutations in multiple genes which alter TGF- β signaling resulting in altered cardiovascular, craniofacial, neurocognitive and skeletal development. (9) Individuals are predisposed to systemic arterial aneurysms and pregnancy-related complications including uterine rupture and death, as well as allergic/inflammatory diseases and increased incidence of gastrointestinal inflammation. Patients afflicted with LDS classically express the triad of hypertelorism, bifid uvu-

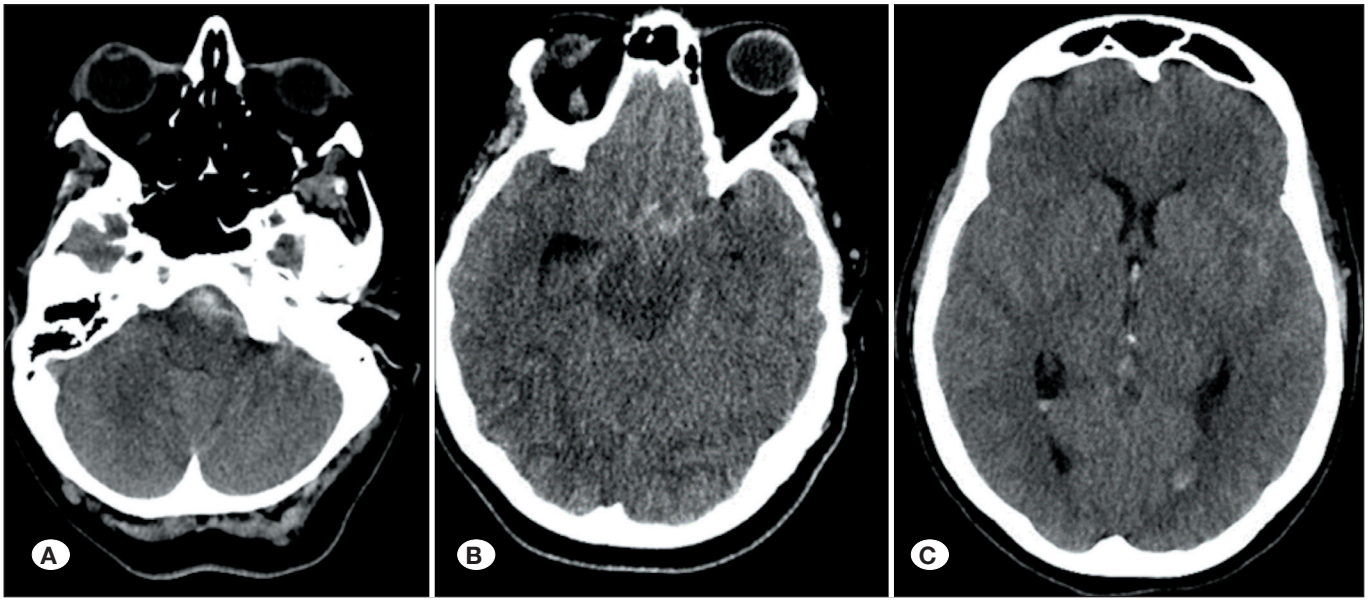

Figure 1: CT head without contrast. Series of axial views portraying subarachnoid hemorrhage ventral to the brainstem **(A,B)** along with layering of blood products within the posterior left lateral ventricle **(C)**.

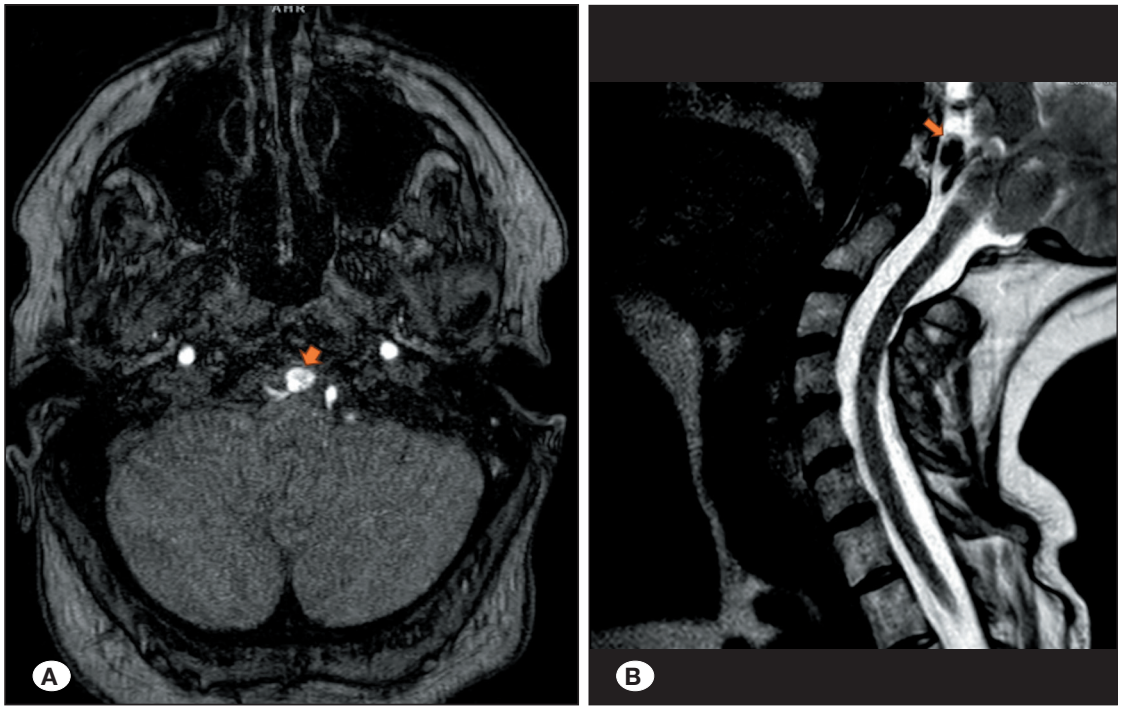

Figure 2: Magnetic Resonance Imaging (MRI) head and neck. **A)** MR Angiogram axial view reveals a 9 x 5 mm aneurysm in the right V4 segment of the vertebral artery (orange arrow). **B)** T2-Weighted MRI cervical spine sagittal view redemonstrating said aneurysm (orange arrow).

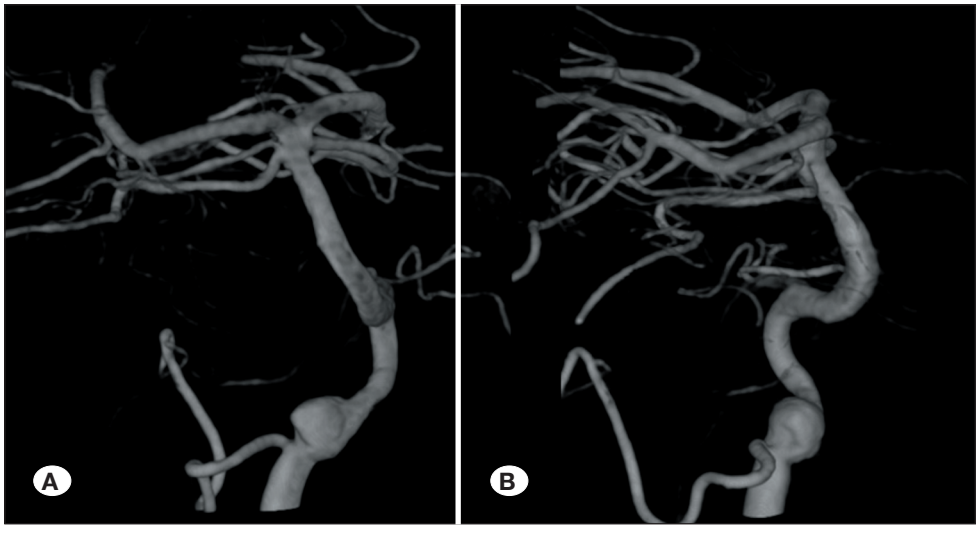

Figure 3: Digital Subtraction Angiogram with 3-dimensional reconstruction. **A)** Rotated antero-posterior and **B)** lateral views demonstrate a fusiform, eccentric right vertebral artery dilatation measuring 8 x 7.5 x 9 mm just distal to the right posterior inferior cerebellar artery origin.

la and or/cleft palate, and generalized arterial pathology. (13) At the time of its initial description, affected individuals were found to have heterozygous mutations in the genes encoding either the type I or type II TGF-b receptor, with the specific phenotypic manifestation being associated with the specific gene affected, resulting in two subtypes; LDS type 1 (mutation in TGF-b receptor 1 (TGFbR1)) and LDS type 2 (mutation in TGF-b receptor 2 (TGFbR2)). This classification system was subsequently expanded to include two additional subtypes, LDS type 3 and LDS type 4, which are associated with gene mutations in the mothers against decapentaplegic homolog 3 (SMAD3) gene and the transforming growth factor b2 ligand gene (TGFb2), respectively. (15) There has also been literature suggesting a fifth variant, LDS 5, which is associated with mutations in the TGF-Beta 3 ligand gene (TGFb3). (7) Regardless of the particular subtype, phenotypic manifestations are variable and range from mild to severe LDS independent of genotypic makeup. Patients most often present with thoracic aortic aneurysms and dissections, but as seen in our case, these are not always present. Surveillance for intracranial aneurysms

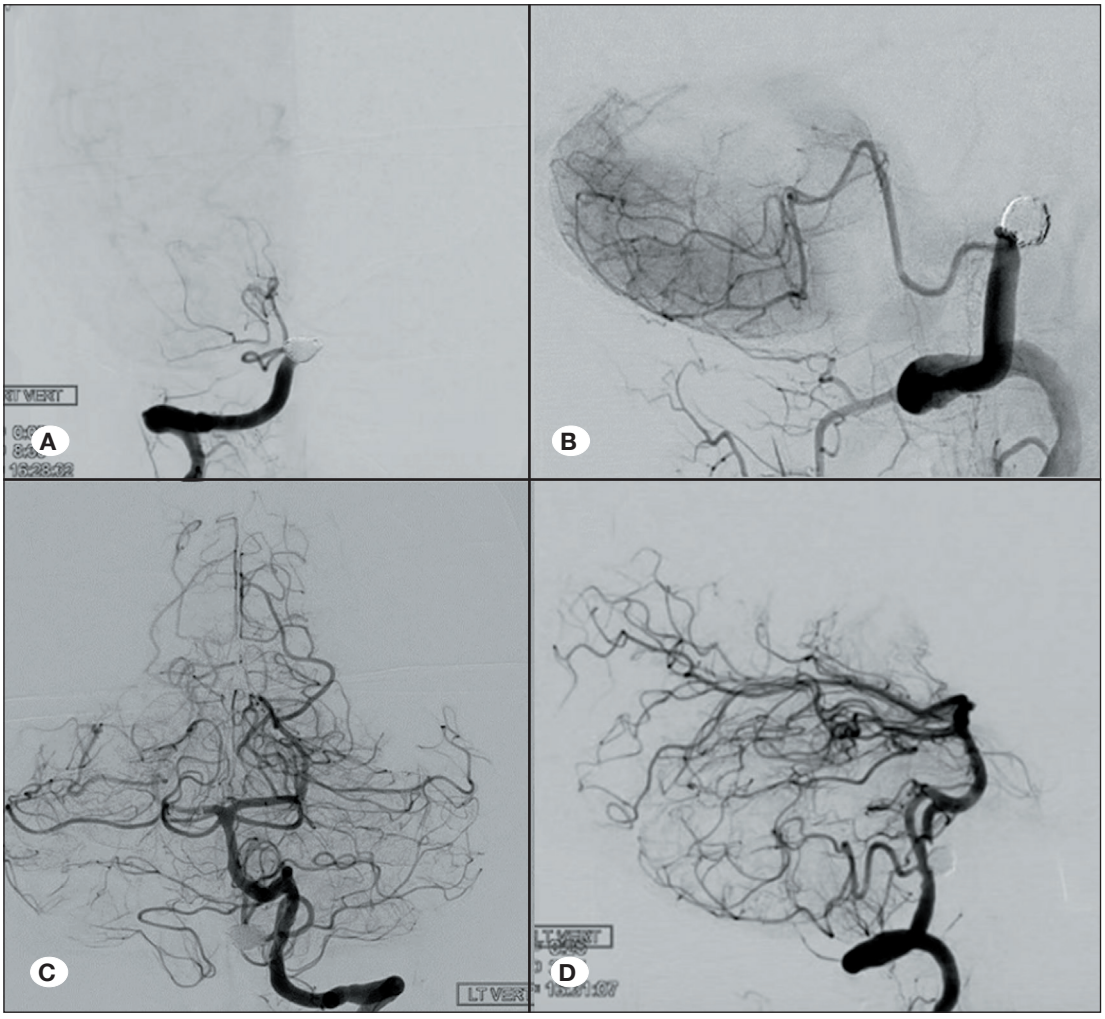

Figure 4: Post-embolization angiogram. **A)** Antero-posterior (AP) and **B)** lateral views of the right vertebral artery after coil embolization showing complete occlusion of the aneurysm along with the parent vessel distal to the aneurysm. **C)** AP and **D)** lateral left vertebral artery injections showing satisfactory perfusion of the posterior circulation via the left vertebral artery with no evidence of retrograde flow into the aneurysm.

should be implemented for all patients with LDS regardless of their genotypic type or phenotypic manifestations.

The first reported case of an intracranial aneurysm in an LDS patient was that of a 20-year-old female with a right carotid ophthalmic aneurysm and fusiform paraclinoid carotid aneurysm treated with an open aneurysm treatment approach. (14) In recent multicenter analyses, the prevalence rate of intracranial aneurysms in LDS patients has been found to be 23-30%. (13) Other studies have shown a significant presence of Chiari malformation type I with those LDS patients who were found to have intracranial aneurysms. (6)

Treatment of intracranial aneurysms in patients with LDS has been accomplished through both open and endovascular methods. Cases have reported successful treatment of aneurysms in LDS patients via open craniotomy and clipping. (5) There have also been reports of successful aneurysm embolization via stent assisted coiling in this patient population. (8) Furthermore, there have been reports of utilizing the pipeline embolization device for flow diversion and curative parent vessel reconstruction in LDS patients without evidence of injury or vessel dissection. (3) This report details the novel case of an adult patient with LDS4 successfully treated for a ruptured vertebral artery aneurysm. Intracranial aneurysm treatment in a patient with LDS 4 has not yet been described.

LDS has a close connection with other connective tissue disorders, having at one point thought to have been a variant of Marfan Syndrome and often being misdiagnosed as such. Each child of an individual with LDS has a 50% chance of developing the pathogenic variant of the disorder. Marfan Syndrome is also inherited in an autosomal dominant fashion and involves skeletal, cardiovascular, and ocular systems, but is caused by a mutation in the fibrillin 1 gene (FBN1) coding for extracellular matrix protein fibrillin-1. (4) Interestingly, the mutation in fibrillin-1 leads to enhanced TGFb signaling, prominently contributing to the pathology of Marfan Syndrome, whereas cytoplasmic kinase mutations in the TGF-b receptors

or ligands are the underlying cause of LDS. (2) Marfan Syndrome is not associated with brain aneurysms, further supporting the role of TGF-b in brain aneurysm formation and the role mutations in signaling pathways can have on clinical presentation.

CONCLUSION

Vascular Ehlers-Danlos Syndrome can also clinically resemble LDS, but is characterized by pathogenic variance in the COL3A1 or COL1A1 genes, which play a role in collagen formation. (1) The TGF-b pathway is an important mediator of immunological maturity, cancer, inflammation and fibrosis, in addition to skeletal, vascular and hematopoietic homeostasis. (12) Further exploration of this pathway and its regulators could lead to novel therapeutic options for connective tissue disorders such as LDS and better understanding of the mechanisms underlying aneurysm formation.

Declarations

Funding: This paper did not receive any specific grant from funding agencies in the public, commercial, or not-for-profit sectors.

Availability of data and materials: The datasets generated and/or analyzed during the current study are available from the corresponding author by reasonable request.

Disclosure: The authors declare no competing interests.

Informed consent: Written informed consents were obtained from the individuals (and/or legal representatives) for the publication of the cases.

AUTHORSHIP CONTRIBUTION

Study conception and design: EEW, LS, JM, BL
Data collection: EEW, LS, ED, JM
Analysis and interpretation of results: EEW, LS, BL, BT
Draft manuscript preparation: EEW, LS
Critical revision of the article: EEW, LS, ED, JM, BL, BT
Other (study supervision, fundings, materials, etc...): BL, BT
All authors (EEW, LS, ED, JM, BL, BT) reviewed the results and approved the final version of the manuscript.

REFERENCES

1. Byers PH: Vascular ehlers-danlos syndrome. In: Adam MP, Feldman J, Mirzaa GM, eds. GeneReviews®. Seattle (WA): University of Washington, Seattle; September 2, 1999
2. Chaudhry SS, Cain SA, Morgan A, Dallas SL, Shuttleworth CA, Kielty CM: Fibrillin-1 regulates the bioavailability of TGFbeta1. J Cell Biol 176:355-367, 2007. https://doi.org/10.1083/jcb.200608167
3. Colby GP, Lin LM, Zeiler SR, Coon AL: Curative reconstruction of a cerebral aneurysm by flow diversion with the Pipeline embolisation device in a patient with Loeys-Dietz syndrome. BMJ Case Rep 2014:bcr2014204412, 2014. https://doi.org/10.1136/bcr-2014-204412
4. Dietz H: FBN1-related marfan syndrome. In: Adam MP, Feldman J, Mirzaa GM, et al., eds. GeneReviews®. Seattle (WA): University of Washington, Seattle; April 18, 2001.
5. Hughes BD, Powers CJ, Zomorodi AR: Clipping of a cerebral aneurysm in a patient with Loeys-Dietz syndrome: Case report. Neurosurgery 69:E746-E55, 2011. https://doi.org/10.1227/NEU.0b013e31821964a3
6. Huguenard AL, Johnson GW, Desai RR, Osbun JW, Dacey RG, Braverman AC: Relationship between phenotypic features in Loeys-Dietz syndrome and the presence of intracranial aneurysms. J Neurosurg 138:1385-1392, 2022. https://doi.org/10.3171/2022.9.JNS221373
7. Hussein D, Olsson C, Lagerstedt-Robinson K, Moreira T: Novel mutation of the TGF-β 3 protein (Loeys-Dietz Type 5) associated with aortic and carotid dissections: Case report. Neurol Genet 7:e625, 2021. https://doi.org/10.1212/NXG.0000000000000625
8. Levitt MR, Morton RP, Mai JC, Ghodke B, Hallam DK: Endovascular treatment of intracranial aneurysms in Loeys-Dietz syndrome. J Neurointerv Surg 4:e37, 2012. https://doi.org/10.1136/neurintsurg-2011-010138
9. Loeys BL, Chen J, Neptune ER, Judge DP, Podowski M, Holm T, Meyers J, Leitch CC, Katsanis N, Sharifi N, Xu FL, Myers LA, Spevak PJ, Cameron DE, De Backer J, Hellemans J, Yan Chen, Elaine C Davis, Catherine L Webb, Wolfram Kress, Paul Coucke, Daniel B Rifkin, Anne M De Paepe, Harry C Dietz: A syndrome of altered cardiovascular, craniofacial, neurocognitive and skeletal development caused by mutations in TGFBR1 or TGFBR2. Nat Genet 37:275-281, 2005. https://doi.org/10.1038/ng1511
10. Loeys BL, Dietz HC: Loeys-dietz syndrome. In: Adam MP, Feldman J, Mirzaa GM, et al., eds. GeneReviews®. Seattle (WA): University of Washington, Seattle; February 28, 2008.
11. Loeys BL, Schwarze U, Holm T, Callewaert BL, Thomas GH, Pannu H, De Backer JF, Oswald GL, Symoens S, Manouvrier S, Roberts AE, Faravelli F, Greco MA, Pyeritz RE, Milewicz DM, Coucke PJ, Cameron DE, Braverman AC, Byers PH, De Paepe AM, Dietz HC: Aneurysm syndromes caused by mutations in the TGF-beta receptor. N Engl J Med 355:788-798, 2006. https://doi.org/10.1056/NEJMoa055695
12. Massagué J: TGFβ signalling in context. Nat Rev Mol Cell Biol 13:616-630, 2012. https://doi.org/10.1038/nrm3434
13. Perez-Vega C, Domingo RA, Tripathi S, Ramos-Fresnedo A, Martínez Santos JL, Rahme RJ, Freeman WD, Sandhu SS, Miller DA, Bendok BR, Brinjikji W, Quinones-Hinojosa A, Meyer FB, Tawk RG, Fox WC: Intracranial aneurysms in loeys-dietz syndrome: A multicenter propensity-matched analysis. Neurosurgery 91:541-546, 2022. https://doi.org/10.1227/neu.0000000000002070
14. Rahme RJ, Adel JG, Bendok BR, Bebawy JF, Gupta DK, Batjer HH: Association of intracranial aneurysm and Loeys-Dietz syndrome: Case illustration, management, and literature review. Neurosurgery 69:E488-E493, 2011. https://doi.org/10.1227/NEU.0b013e318218cf55
15. van de Laar IM, Oldenburg RA, Pals G, Roos-Hesselink JW, de Graaf BM, Verhagen JMA, Hoedemaekers YM, Willemsen R, Severijnen LA, Venselaar H, Vriend G, Pattynama PM, Collée M, Majoor-Krakauer D, Poldermans D, Frohn-Mulder IME, Micha D, Timmermans J, Hilhorst-Hofstee Y, Bierma-Zeinstra SM, Willems PJ, Kros JM, Oei EHG, Oostra BA, Wessels MW, Bertoli-Avella AM: Mutations in SMAD3 cause a syndromic form of aortic aneurysms and dissections with early-onset osteoarthritis. Nat Genet 43:121-126, 2011. https://doi.org/10.1038/ng.744

Turk Neurosurg 36(3):476-482, 2026
DOI: 10.5137/1019-5149.JTN.48836-25.2

Case Report

Received: 08.04.2025
Accepted: 14.07.2025
Published Online: 22.05.2026

Pre-Therapeutic Vascular Anatomical Evaluation in Penetrating Cerebrovascular Injuries: Insights from Two Cases

Jinwei LEI, Gongbin WEI

Chongqing University Central Hospital, Chongqing Emergency Medical Center, Department of Traumatology, Chongqing 400000, China

This study has been presented at the 27th Annual Congress of Chinese Society of Emergency Medicine, between November 29 and December 1, 2024 at Shenyang, Liaoning Province, China.

Corresponding author: Gongbin WEI ✉ weigb2000@163.com

ABSTRACT

Penetrating cerebrovascular injuries (PCVIs) are often life-threatening, with trauma to the carotid or vertebral arteries potentially causing severe neurological deficits. This study aimed to retrospectively examine two cases of severe penetrating cerebrovascular injury with unstable hemodynamics that resulted in markedly different neurological outcomes. The first patient was struck by a high-speed metal rod, sustained injuries to the right common carotid and right vertebral arteries and was admitted to our hospital 10 h after the trauma. The second patient, who was stabbed, sustained an injury to the right vertebral artery and was admitted to our hospital 1 h after the trauma. Both patients had injuries in zone II of the right lateral neck. The first patient underwent ligation of the right vertebral artery and anastomosis of the right common carotid artery using an interposition graft from the autologous great saphenous vein, resulting in an asymptomatic infarction of the ipsilateral frontal lobe. The second patient only underwent ligation of the right vertebral artery, which ultimately led to an occipital lobe infarction and subsequent visual field deficits. These contrasting outcomes underscore the critical influence of cerebrovascular anatomical variations. Penetrating cerebrovascular injuries may pose significant risks of neurological impairment, particularly in the presence of important vascular anatomical variants. Revascularization should be considered as a primary treatment option for patients with cerebral vessel malformations.

KEYWORDS: Cerebrovascular trauma, Carotid artery injuries, Traumatic vertebral artery dissection, Neurologic deficits, Anatomic variation

ABBREVIATIONS: BP: Blood pressure, **CCA:** Common carotid artery, **CT:** Computed tomography; **CTA:** CT angiography, **DSA:** Digital subtraction angiography, **PCVI:** Penetrating cerebrovascular injury, **PComA:** Posterior communicating artery, **PRBC:** Packed red blood cells, **VA:** Vertebral artery

INTRODUCTION

Penetrating cerebrovascular injury (PCVI) is an uncommon, but fatal condition (4,23). The common carotid artery (CCA), a major conduit of blood to the head and neck, and the vertebral artery (VA), which is responsible for supplying the posterior part of the brain, are crucial components of the cervical vascular system. Injuries to these arteries, whether blunt or penetrating, carry high morbidity and mortality rates (16,25).

For penetrating neck injuries, clinicians typically opt for selective surgical interventions following a thorough examination, particularly to assess digestive and respiratory functions (21,25). Surgical exploration becomes mandatory in patients with hemodynamic instability, whereas a selective treatment strategy is employed for stable patients, reducing unnecessary surgeries by approximately 59% (21). Studies have primarily reported general treatment outcomes, indicating that these approaches are safe (17).

Jinwei LEI : 0000-0001-7886-0535 Gongbin WEI : 0000-0002-7565-571x

However, few investigations have examined the relationship between neurological dysfunction, the severity of penetrating cerebrovascular injuries, and cerebrovascular anatomy. This study aimed to analyze the treatment outcomes in two PCVI cases, with a particular focus on neurological deficit complications.

CASE REPORT

Case 1

A 57-year-old female was struck on the right lateral neck (zone II) by a high-speed, 10 cm metal rod (Figure 1A and 1B). Upon admission to a local hospital, computed tomography (CT) angiography (CTA) indicated suspected perforations of the CCA and VA (Figure 1C). An initial exploratory surgery failed to control the bleeding. The patient was intubated, sedated, maintained on the vasopressor norepinephrine, and transferred to our emergency room approximately 10 h post-injury. Exploratory surgery was immediately performed again in the operating room.

Intraoperatively, both the right CCA and VA were found to be lacerated with near-complete transection (both Biffl grade V) (Figure 2A, Table I) (2,6). The VA was ligated first. The CCA was debrided and temporarily shunted using a modified T-tube, followed by definitive reconstruction with an autologous great saphenous vein graft harvested from the contralateral thigh (Figure 2B-D). CCA repair was completed in approximately 30 min, after which the patient's hemodynamics stabilized. The total intraoperative blood loss was 1,500 mL, requiring transfusion of 6 units of packed red blood cells (PRBCs) and 950 mL of autologous whole blood.

Postoperatively, non-contrast cranial CT revealed a small ipsilateral frontal lobe infarction (Figure 3A), although the patient remained neurologically intact. Routine Doppler ultrasonography revealed thrombosis at the CCA anastomotic site. A subsequent CTA revealed vascular occlusions measuring 5 cm in the right CCA and 3.5 cm in the right VA (Figure 3B and 3C). Although stent graft placement via digital subtraction angiography (DSA) was attempted, contralateral CCA stenosis precluded this intervention. The patient received dual antiplatelet therapy (aspirin 100 mg/day and clopidogrel 75 mg/day) for 3 months along with a therapeutic dose of enoxaparin (4,000 AXaIU/day).

The patient developed a midsternal wound infection that resolved following debridement and negative pressure wound therapy. In addition, the patient experienced hoarseness, and ipsilateral vocal cord paralysis was detected via laryngoscopy. The patient ultimately achieved complete recovery and was discharged without any residual complications.

Table I: Biffl Classification for Traumatic Cerebrovascular Injury (2)

Biffl grade	Description
I	Luminal irregularity or dissection with < 25% luminal narrowing
II	Dissection or intramural hematoma with ≥ 25% luminal narrowing, intraluminal thrombus, or raised intimal flap
III	Pseudoaneurysm
IV	Occlusion
V	Transection with free extravasation

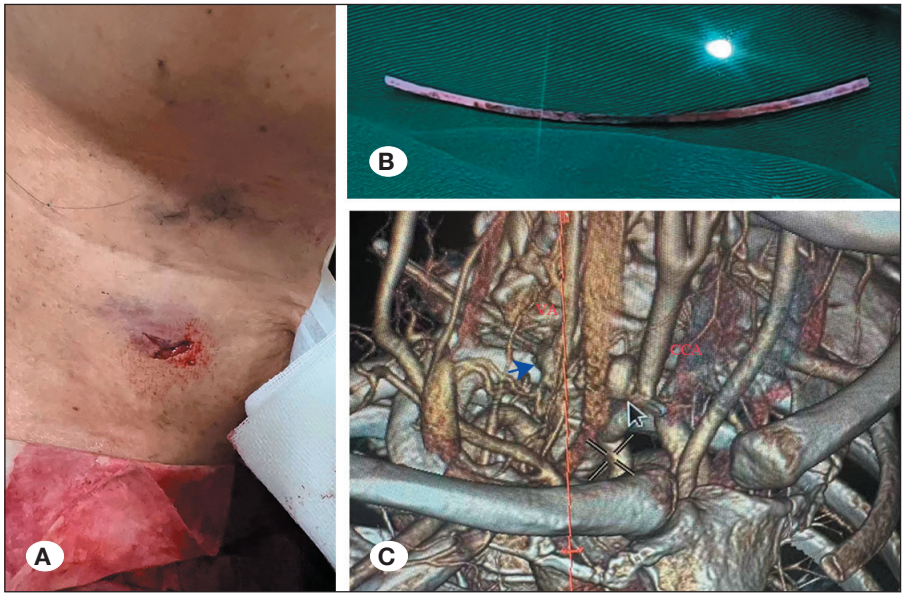

Figure 1: Preoperative images of case 1. **A)** The location of penetrating injury in the neck. **B)** Metal rod penetrating the neck. **C)** Preoperative CTA showing injured segments of the right CCA and VA. The blue arrow indicates the injured segment of the right VA and the black arrow indicates the injured segment of the right CCA. **Abbreviations: CCA:** common carotid artery; **CTA:** computed tomography angiography; **VA:** vertebral artery.

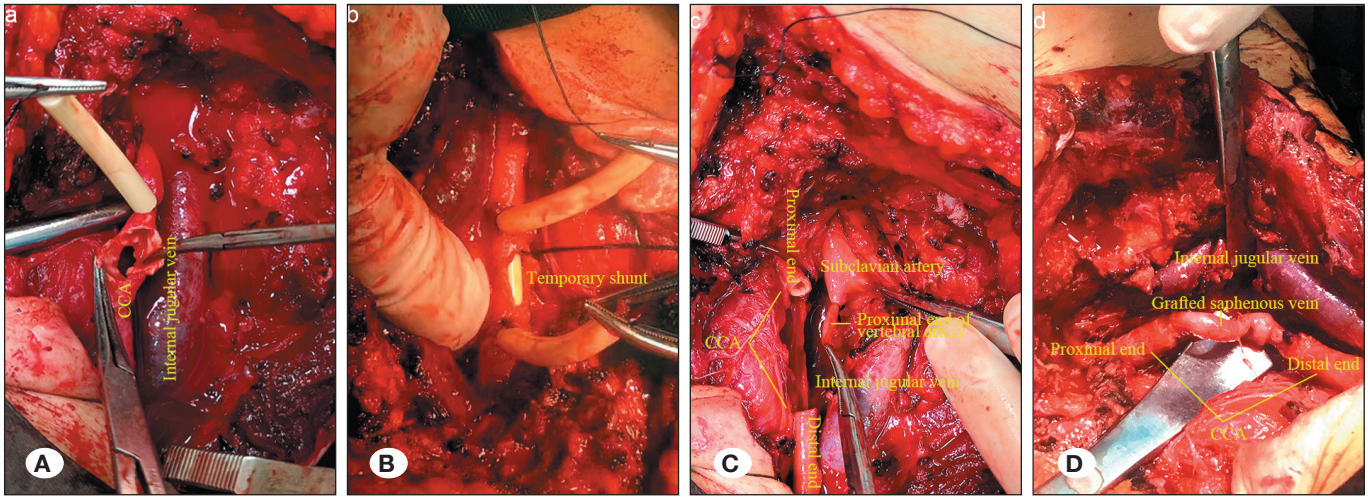

Figure 2: Intraoperative images of case 1. **A)** The laceration site in the right CCA. **B)** Temporary shunting procedure prior to anastomosis. **C)** Trimming the injured right CCA segment. **D)** Anastomosis was performed using a self-great saphenous vein graft from the contralateral thigh. Abbreviations: CCA, common carotid artery.

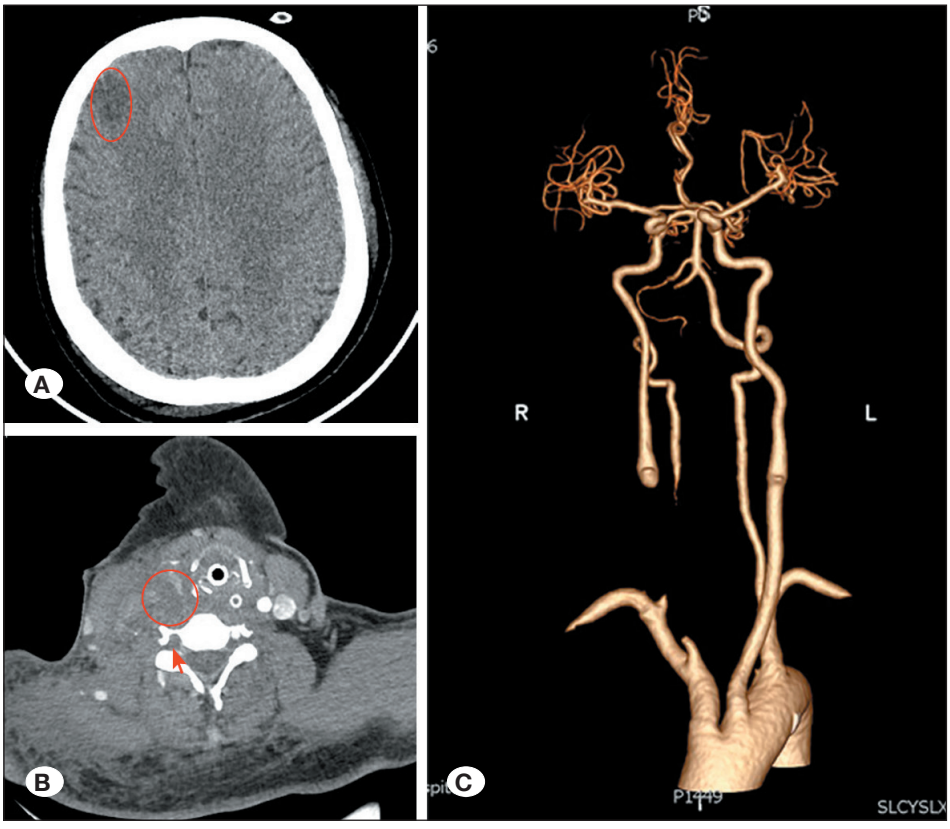

Figure 3: Postoperative images of case 1. **A)** Non-contrast cranial CT showing a small ischemic infarction in the ipsilateral frontal cerebral lobe. **B)** Postoperative occlusion of the injured CCA and VA segments. The red circle indicates the occluded right CCA segment. Red arrow indicates an occluded segment of the right VA. **C)** CTA showing the relative occluded lengths of the right CCA and VA. **CCA:** Common carotid artery; **CT:** Computed tomography; **CTA:** computed tomography angiography; **VA:** vertebral artery.

Case 2

A 31-year-old male presented to our trauma center approximately 1 h after sustaining multiple stab wounds involving the right lateral neck (zone II), head, right anterior chest, and left elbow. On admission, the patient was conscious but hemodynamically unstable with tachycardia (heart rate, 120 beats per minute), tachypnea (respiratory rate, 24 breaths per minute), and hypotension (blood pressure (BP) 70/50 mmHg). Active hemorrhage from the right neck wound was noted, accompanied by hematemesis. Initial hemorrhage control was achieved using a Foley catheter with balloon tamponade (Figure 4A). Resuscitation included transfusion of 2 units of PRBCs and vasopressor support through a central venous catheter, resulting in hemodynamic improvement (systolic BP > 90 mmHg). Emergency CTA demonstrated luminal narrow-

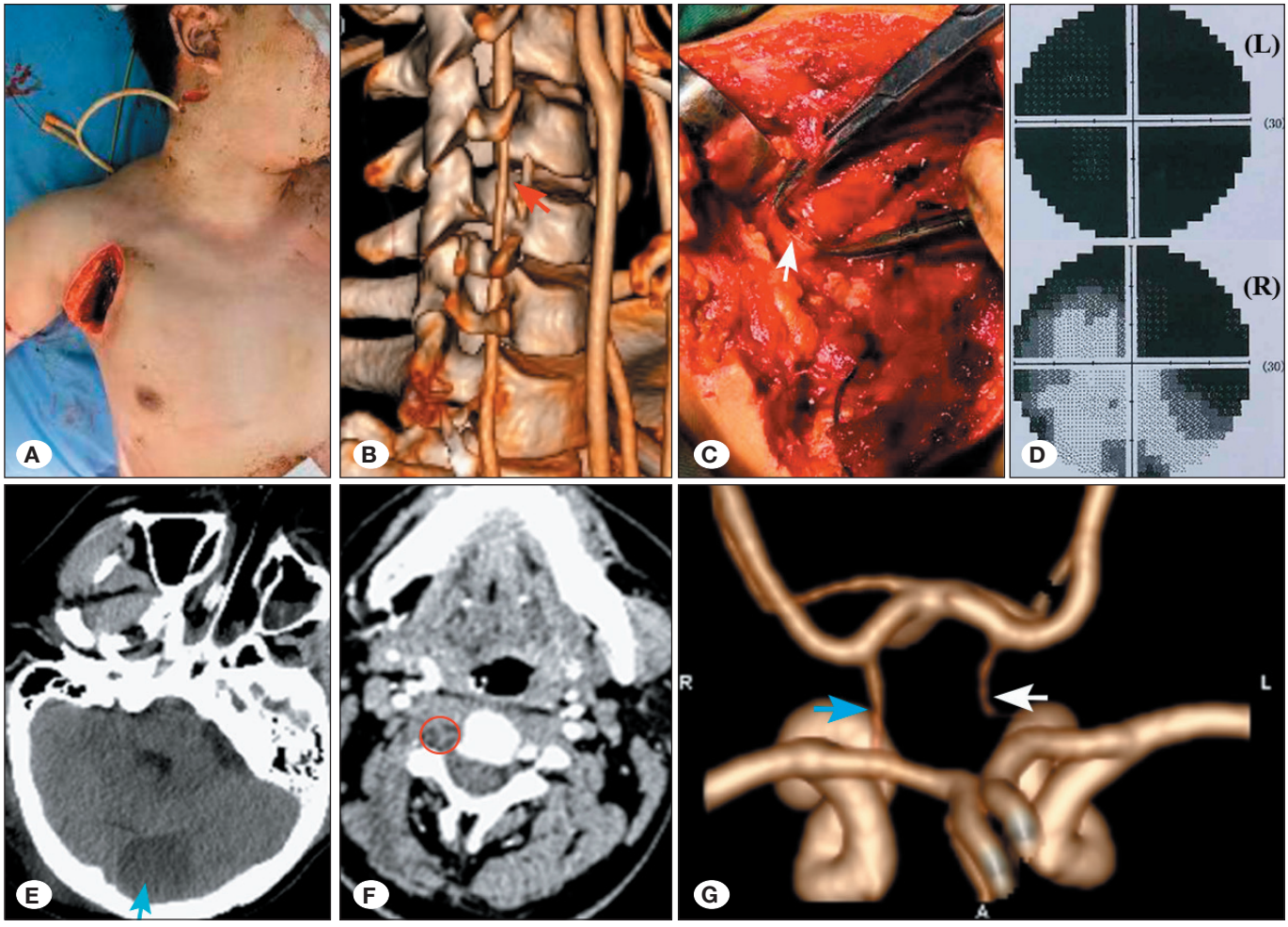

Figure 4: Pre-, intra-, and postoperative images of case 2. **A)** Foley catheter with a balloon tamponade was used to control the hemorrhage. **B)** Preoperative CTA showing injured segments of the right VA (red arrow). **C)** Laceration of proximal esophagus (white arrow). **D)** Grayscale visual field analysis showing complete left eye blindness and right homonymous hemianopsia (upper panel: left eye; lower panel: right eye). **E)** Postoperative non-contrast cranial CT imaging showing an ischemic infarction in the left occipital lobe (blue arrow). **F)** Postoperative occlusion of the injured VA segment (red circles). **G)** CTA showing occlusion of the left PComA (white arrow) and hypoplasia of the right PComA (blue arrow). **CT:** Computed tomography; **CTA:** Computed tomography angiography, **VA:** Vertebral artery; **PComA:** Posterior communicating artery.

ing of the right vertebral artery at the C5 transverse foramen segment, consistent with a vascular injury (Figure 4B). Subsequently, the patient was transported to the operating room for exploratory surgery.

Surgical exploration confirmed complete transection (Biffl grade V) of the right VA and the accompanying vein, along with laceration of the proximal esophagus (Figure 4C). The vertebral vessels were surgically ligated and primary esophageal repair was performed by placing a closed suction drain adjacent to the repair site. The procedure resulted in an estimated blood loss of 500 mL, requiring transfusion of 6 units of PRBCs and 350 mL of fresh frozen plasma. The patient received enoxaparin monotherapy (4,000 AXaIU/day) for thromboembolic prophylaxis.

The patient developed almost complete left eye blindness and right homonymous hemianopia postoperatively, with visual field defects confirmed by standardized ophthalmic perimetry (Figure 4D). Non-contrast cranial CT revealed an acute infarction in the left occipital lobe. Subsequent CTA revealed occlusion of the right VA and left posterior communicating artery (PComA) along with hypoplasia of the right PComA (Figures 4E-G). The patient was discharged with persistent visual field deficit.

DISCUSSION

PCVI accounts for approximately 25% of penetrating neck injuries, with the carotid artery involved in 80% of cases and the vertebral artery in 43% (13). These injuries carry high risks of hypovolemic shock, ischemic cerebral infarction, and mortality. Reported mortality rates range from 2.6% to 26%, whereas ischemic infarction ranges from 9% to 30% (5,18). Persistent neurological deficits have been reported in up to

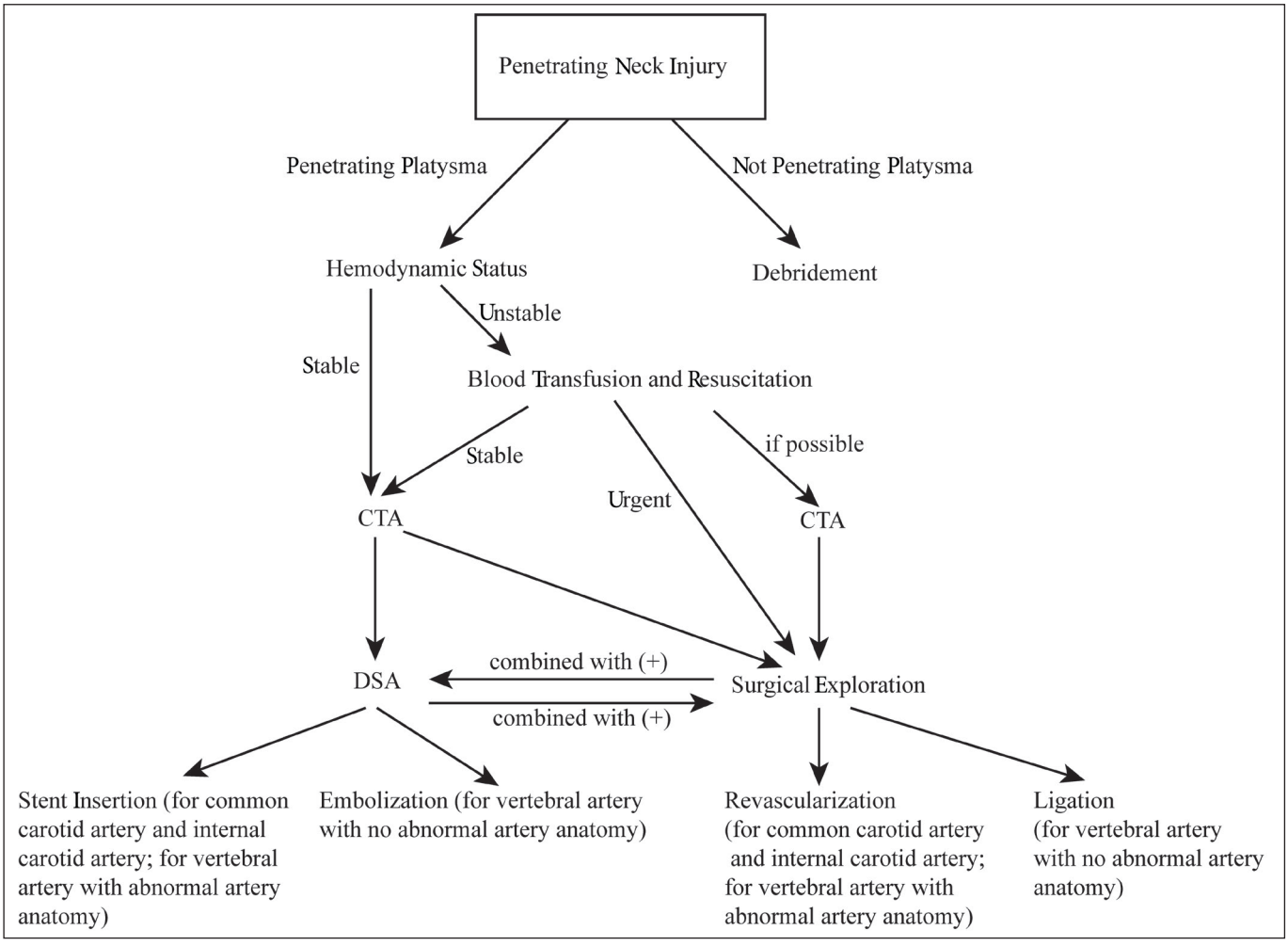

Figure 5: Treatment algorithm of penetrating neck injury involving cerebrovascular injuries. **CTA:** computed tomography angiography, **DSA:** digital subtraction angiography.

80% of cases (26). Both cases in this study involved severe Biffl grade V cerebrovascular injuries. Previous studies have consistently demonstrated that higher Biffl grades are strongly correlated with an increased incidence of in-hospital stroke (22,26).

The CCA and internal carotid artery serve as the principal conduits for the anterior cerebral circulation. As such, injuries to these arteries are particularly threatening to cerebral perfusion. Current management protocols recommend DSA for hemodynamically stable patients with zone I (between the cricoid cartilage and clavicle) or zone III (above the mandible) injuries, where the anatomical complexity favors endovascular approaches (18). In contrast, hemodynamically unstable patients require immediate surgical exploration regardless of the injury location. Both cases presented here involved zone II injuries (between the mandible and the cricoid cartilage) that necessitated open surgical intervention.

Revascularization of the CCA or internal carotid artery remains the preferred treatment for eligible patients, except in cases of preoperative neurological deficits, in which arterial ligation may be required (7,18). Current evidence suggests that CCA ligation should be considered only in comatose patients with prograde flow during surgical exploration, as documented in a previous study (12). The available revascularization options include primary repair and interposition grafting when anatomically feasible. Temporary intravascular shunt placement, while serving as a damage-control technique, has been associated with an increased risk of stroke and mortality (5).

The unique hemodynamic characteristics of the circle of Willis predispose patients to cerebral infarction when ipsilateral arterial supply is diminished or absent (19). In the first case, the patient was sedated upon arrival at the emergency department, which prevented immediate neurological assessments. Despite a 10-h delay from injury to treatment, successful interposition grafting was achieved using the contralateral great saphenous vein. Postoperative imaging revealed thrombosis at the anastomotic site with subsequent development of a small, asymptomatic right frontal lobe infarction. The likely pathophysiological mechanisms include: (a) cerebral hypoperfusion secondary to hemorrhagic shock and (b) thromboembolic events originating from the injured right CCA. The preserved blood flow through the contralateral CCA and VA (Figure 3C) likely limited the extent of the cerebral infarction.

Literature typically recommends ligation or embolization for unilateral VA injuries (10,18,21). VA ligation is generally considered to carry minimal risk of cerebral complications, particularly unilateral injuries (10). Notably, bilateral VA injuries require prompt intervention through endovascular techniques or cervical immobilization to maintain adequate posterior circulation perfusion and prevent catastrophic neurological outcomes (9). Hypotension has been found to increase the risk of stroke by 1.32-fold compared to patients without hypotension, particularly in those with internal watershed infarctions (3,22). In case 2, the patient developed a left occipital lobe infarction and bilateral visual field defects after the injury. Left occipital lobe infarction may partially contribute to the bilateral visual field defects. However, near-blindness of the left eye cannot be explained only by left occipital lobe infarction and requires further investigation. The infarction area is always ipsilateral to the injured vertebral artery; however, this was not the case here (1). The infarction likely resulted from multiple contributing mechanisms: (a) cerebral hypoperfusion secondary to hypotensive shock, leading to a critical reduction in effective cerebral blood flow; (b) ligation of the right VA, which significantly diminished posterior circulation; (c) occlusion of the left PComA combined with hypoplasia of the right PComA, further limiting collateral perfusion to the posterior cerebral circulation and exacerbating ischemia in the left occipital lobe; and (d) thromboembolism originating from the site of injury to the right VA. A previous study also revealed that small (<1 mm in diameter) or absent ipsilateral PComAs contribute to the occurrence of ischemic infarction (19). This finding underscores the need for a cautious approach to VA injury management, particularly in cases of hypovolemic shock and vascular anatomical variants.

Preoperative CTA plays a critical role in detecting circles of Willis abnormalities, including stenoses or congenital malformations, which may worsen cerebral ischemia during hypotensive shock or reduced arterial flow. Research has highlighted several aspects of the risks associated with VA injuries. Anatomical predispositions to injury, such as artery placement relative to cervical structures, increase susceptibility to trauma-induced vertebrobasilar insufficiency (15). Even when ligation appears successful, pseudoaneurysms and thromboembolisms have been reported, necessitating long-term monitoring (14). Preoperative CTA is particularly valuable for evaluating potential collateral pathways, including deep cervical arterial networks, which may significantly influence post-ligation ischemic outcomes (20). Studies have also confirmed that unilateral vertebral artery ligation can be performed safely only when preoperative evaluations demonstrate adequate compensatory flow from the contralateral artery (8). Thus, the second patient's severe neurological deficits following VA ligation directly correlated with the preexisting circle of Willis abnormalities. Occlusion of the left PComA in case 2 further contributed to decreased blood flow in the posterior cerebral circulation, particularly on the left side. In contrast, the first patient avoided major complications despite combined carotid and vertebral injuries, probably because of the preserved normal vascular anatomy.

The revascularization of VA injuries typically involves the use of endovascular stents (17). A significant limitation was the lack of suitable-caliber stents (11). Embolization is a viable salvage option when distal stent deployment is not feasible. The complex anatomical course of the VA through the transverse foramina and cervical plexus makes open surgical repair particularly demanding. However, innovative techniques show promise. V3 segment-deep cervical artery anastomosis may effectively restore posterior circulation perfusion (24), whereas bypass grafting from the ipsilateral external carotid artery to the VA at the C1 level has demonstrated clinical efficacy (8).

The two cases in this series collectively demonstrate that revascularization should constitute the primary treatment strategy for both CCA and VA injuries. Methods such as open surgical ligation or embolization may be acceptable under specific circumstances as mentioned above. Based on these findings, we proposed a promising treatment algorithm (Figure 5). A critical component of this approach is comprehensive preoperative vascular imaging (initially with CTA, and DSA if necessary) of the carotid arterial and vertebral arterial systems to identify potentially compromising anatomical variants before ligation of the great vessels. Therefore, DSA may be an option for the diagnosis, treatment, and follow-up of patients with stable disease. Careful consideration should be given to avoid ligation or embolization to minimize the risk of symptomatic cerebral infarction in certain cases. Additionally, the anatomical zone of neck injury should be considered when selecting the appropriate treatment strategy.

CONCLUSION

Anatomic variation is a critical determinant of outcomes in penetrating cerebrovascular injury. Revascularization is essential to prevent cerebral infarction and permanent neurologic impairment when treating patients with significant cerebrovascular variants.

Declarations

Funding: This work was supported by a grant from Chongqing University Central Hospital (Grant No. SYRCCY20230315).

Availability of data and materials: The datasets generated and/or analyzed during the current study are available from the corresponding author by reasonable request.

Disclosure: The authors declare no competing interests.

Informed consent: We obtained written informed consent from patients for the publication of this case report.

AUTHORSHIP CONTRIBUTION

Study conception and design: JL, GW
Data collection: JL
Analysis and interpretation of results: JL, GW
Draft manuscript preparation: JL
Critical revision of the article: JL, GW
Other (study supervision, fundings, materials, etc...): JL, GW
All authors (JL, GW) reviewed the results and approved the final version of the manuscript.

REFERENCES

1. AlBayar A, Sullivan PZ, Blue R, Leonard J, Kung DK, Ozturk AK, Chen HI, Schuster JM: Risk of vertebral artery injury and stroke following blunt and penetrating cervical spine trauma: A retrospective review of 729 patients. World Neurosurg 130:e672-e679, 2019. https://doi.org/10.1016/j.wneu.2019.06.187
2. Biffl WL, Moore EE, Offner PJ, Brega KE, Franciose RJ, Burch JM: Blunt carotid arterial injuries: Implications of a new grading scale. J Trauma 47:845-853, 1999. https://doi.org/10.1097/00005373-199911000-00004
3. Bladin CF, Chambers BR: Clinical features, pathogenesis, and computed tomographic characteristics of internal watershed infarction. Stroke 24:1925-1932, 1993. https://doi.org/10.1161/01.STR.24.12.1925
4. Boggs HK, Kiang SC, Tran Z, Mukherjee K, Tomihama RT: Analysis of extracranial cerebrovascular injuries: Clinical predictors of management and outcomes. Ann Vasc Surg 100:53-59, 2024. https://doi.org/10.1016/j.avsg.2023.10.022
5. DiBartolomeo AD, Williams B, Weaver FA, Matsushima K, Martin M, Schellenberg M, Inaba K, Magee GA: Risk factors for stroke in penetrating cerebrovascular injuries. J Vasc Surg 80:1064-1070, 2024. https://doi.org/10.1016/j.jvs.2024.05.061
6. Foreman PM, Griessenauer CJ, Kicielinski KP, Schmalz PGR, Rocque BG, Fusco MR, Sullivan JC, Deveikis JP, Harrigan MR: Reliability assessment of the Biffl Scale for blunt traumatic cerebrovascular injury as detected on computer tomography angiography. J Neurosurg 127:32-35, 2017. https://doi.org/10.3171/2016.7.JNS16849
7. Halpern AL, Burton CR, Steward LT: Ligation of common carotid artery after penetrating neck trauma. J Trauma Acute Care Surg 87:505-507, 2019. https://doi.org/10.1097/TA.0000000000002289
8. Hoshino Y, Kurokawa T, Nakamura K, Seichi A, Mamada T, Saita K, Miyoshi K: A report on the safety of unilateral vertebral artery ligation during cervical spine surgery. Spine (Phila Pa 1976) 21:1454-1457, 1996. https://doi.org/10.1097/00007632-199606150-00011
9. Irawany V, Nasution VAF, Amalia N: Bilateral vertebral artery injury leads to brain death following traumatic brain injury: A case report. J Med Case Rep 18:106, 2024. https://doi.org/10.1186/s13256-024-04432-3
10. Koh DH, Choi HC, Shin HS, Baek HJ, Koh EH, Park MJ, Choi DS: Endovascular treatment of traumatic vascular injuries in the head and neck region. Medicina (Kaunas) 60:269, 2024. https://doi.org/10.3390/medicina60020269
11. Leiderman DBD, Zerati AE, Wolosker N, Hoffmann Melo HA, da Silva ES, De Luccia N: Endovascular treatment of penetrating injury to the vertebral artery by a stab wound: Case report and literature review. Ann Vasc Surg 45:267.e261-267.e265, 2017. https://doi.org/10.1016/j.avsg.2017.06.145
12. Liekweg WG, Greenfield LJ: Management of penetrating carotid arterial injury. Ann Surg 188:587-592, 1978. https://doi.org/10.1097/00000658-197811000-00001
13. Lodhia J, Chugulu S, Wampembe E, Chilonga K, Msuya D: Traumatic left common carotid artery thrombosis with ischemic brain injury: A case report. Int J Surg Case Rep 111:108891, 2023. https://doi.org/10.1016/j.ijscr.2023.108891
14. Meier DE, Brink BE, Fry WJ: Vertebral artery trauma: Acute recognition and treatment. Arch Surg 116:236-239, 1981. https://doi.org/10.1001/archsurg.1981.01380140082021
15. Moskopp ML, Sannwald LW, Burbelko M, Moskopp D: Operative V2 decompression for traumatic vertebrobasilar insufficiency: Illustrative case. J Neurosurg Case Lessons 5:CASE2358, 2023. https://doi.org/10.3171/CASE2358
16. Nagatomo K, Tsutsumi Y, Tsuchiya A, Togo M, Ishigami K, Soma Y, Sato M, Yasuda S: Right proximal common carotid artery injury. J Trauma Acute Care Surg 91:e18-e20, 2021. https://doi.org/10.1097/TA.0000000000003223
17. Piper K, Rabil M, Ciesla D, Agazzi S, Ren Z, Mokin M, Guerrero WR: Penetrating vertebral artery injuries: A literature review and proposed treatment algorithm. World Neurosurg 148:e518-e526, 2021. https://doi.org/10.1016/j.wneu.2021.01.021
18. Roon AJ, Christensen N: Evaluation and treatment of penetrating cervical injuries. J Trauma 19:391-397, 1979. https://doi.org/10.1097/00005373-197906000-00001
19. Schomer DF, Marks MP, Steinberg GK, Johnstone IM, Boothroyd DB, Ross MR, Pelc NJ, Enzmann DR: The anatomy of the posterior communicating artery as a risk factor for ischemic cerebral infarction. N Engl J Med 330:1565-1570, 1994. https://doi.org/10.1056/NEJM199406023302204
20. Son JI, An TY, Ko MJ, Park SW, Lee YS: Occlusion of both vertebral arteries with development of collateral circulation from the deep cervical artery after cervical spine trauma. Korean J Neurotrauma 18:374-379, 2022. https://doi.org/10.13004/kjnt.2022.18.e57
21. Teixeira F, Metidieri Menegozzo CA, do Couto Netto SD, Poggeti RS, de Sales Collet E Silva F, Birolini D, de Oliveira Bernini C, Utiyama EM: Safety in selective surgical exploration in penetrating neck trauma. World J Emerg Surg 11:32, 2016. https://doi.org/10.1186/s13017-016-0091-4
22. Tran A, Fernando SM, Rochwerg B, Hawes H, Hameed MS, Dawe P, Garraway N, Evans DC, Kim D, Biffl WL, Inaba K, Engels PT, Vogt K, Kubelik D, Petrosoniak A, Joos E: Prognostic factors associated with risk of stroke following blunt cerebrovascular injury: A systematic review and meta-analysis. Injury 55:111319, 2024. https://doi.org/10.1016/j.injury.2024.111319
23. Tunthanathip T, Phuenpathom N, Saehaeng S, Oearsakul T, Sakarunchai I, Kaewborisutsakul A: Traumatic cerebrovascular injury: Prevalence and risk factors. Am J Emergency Med 38:182-186, 2020. https://doi.org/10.1016/j.ajem.2019.01.055
24. Vetter M, Iwanaga J, Choi PJ, Yilmaz E, Oskouian RJ, Tubbs RS: A novel microsurgical procedure for revascularization of the vertebral artery. World Neurosurg 122:e302-e306, 2019. https://doi.org/10.1016/j.wneu.2018.10.026
25. Wang D, Zhao Y, Cha B, Fang P, Liu Y: Penetrating neck trauma with common carotid artery injury caused by a percussive drill: A case report. Medicine (Baltimore) 98:e15750, 2019. https://doi.org/10.1097/MD.0000000000015750
26. Wathen C, Santangelo G, Muhammad N, Ellens N, Catanzaro S, Singh A, Dagli MM, Petrov D, Ozturk AK, Bender M, Stone JJ, Schuster J: Management and outcomes of cerebrovascular injuries after gunshot wounds to the cervical spine. Clin Neurol Neurosurg 243:108376, 2024. https://doi.org/10.1016/j.clineuro.2024.108376

Turk Neurosurg 36(3):483-488, 2026
DOI: 10.5137/1019-5149.JTN.49346-25.2

Case Report

Received: 30.06.2025
Accepted: 07.08.2025
Published Online: 22.05.2026

Accessory Nerve Meningioma of the Foramen Magnum: A Rare Neurosurgical Entity

Mohammed ALADDAM[1], Mehmet Ali KAHRAMAN[1], Simge SEZGIN[1], Gulsen ISHAKOGLU[1], Burak BAYRAKTAR[1], Tuce SOYLEMEZ AKKURT[2], Mehmet Sabri GURBUZ[1]

[1]Istanbul Medeniyet University, Prof. Dr. Suleyman Yalcin City Hospital, Department of Neurosurgery, Istanbul, Türkiye
[2]Istanbul Medeniyet University, Prof. Dr. Suleyman Yalcin City Hospital, Department of Pathology, Istanbul, Türkiye

Corresponding author: Mehmet Sabri GURBUZ ✉ mehmetsabrigurbuz@gmail.com

To watch the surgical videoclip, please visit https://www.turkishneurosurgery.org.tr/uploads/video/JTN-surgical.mp4

ABSTRACT

Meningiomas, which are the most common primary intracranial tumors, frequently arise from the dura of the convexities, parasagittal regions, and skull base. The accessory nerve (cranial nerve XI) at the level of the foramen magnum is an exceptionally uncommon site of origin. To date, only a few cases have been clearly documented in the literature. We report the case of a 66-year-old woman who presented with dizziness, headaches, and left-sided shoulder weakness. The lesion was initially presumed to be a regular foramen magnum meningioma. Intraoperatively, the spinal accessory nerve was centrally engulfed by the tumor, with gross invasion of the nerve sheath and no identifiable dissection plane. The final histopathology confirmed the diagnosis of a World Health Organization Grade I meningioma. Accessory nerve meningiomas are exceedingly rare and can closely mimic the more common dural-based foramen magnum tumors.

KEYWORDS: Accessory nerve, Meningioma, Foramen magnum, Cranial nerve, Microsurgical resection

ABBREVIATIONS: MRI: Magnetic resonance imaging, **SSTR2A:** Strong Somatostatin Receptor 2A, **CN:** Cranial nerve

INTRODUCTION

Meningiomas are the most common primary intracranial tumors, accounting for approximately half of all benign central nervous system neoplasms. They arise from the arachnoid cap cells of the meninges and can theoretically occur at any location within the central nervous system (11). While most meningiomas involve the cerebral convexities, parasagittal region, or skull base, some may originate in association with the cranial nerves (CNs) (4). Although optic nerve sheath meningiomas are well-documented and represent approximately 1% of all intracranial meningiomas (2), meningiomas may also originate from other CNs. Reported cases include those involving the trigeminal nerve (CN V) (3) and the oculomotor nerve (CN III) (1), among others, each presenting with distinct clinical features. In contrast, meningiomas arising from or intimately associated with the lower CNs—particularly the accessory nerve (CN XI)—are exceedingly rare.

Extra-axial solid tumors at the level of the foramen magnum are typically diagnosed as meningiomas. Schwannomas are less common but may be considered when there is a single CN deficit and no clear dural tail on imaging. However,

Mohammed ALADDAM : 0009-0004-2289-2975
Mehmet Ali KAHRAMAN : 0009-0005-3719-654X
Simge SEZGIN : 0009-0003-5398-1404
Gulsen ISHAKOGLU : 0000-0003-4830-6394
Burak BAYRAKTAR : 0009-0006-4317-5961
Tuce SOYLEMEZ AKKURT : 0000-0003-3030-7030
Mehmet Sabri GURBUZ : 0000-0002-3764-389X

accessory nerve meningiomas are extremely rare and can easily be overlooked by both radiologists and neurosurgeons. Surgical resection remains the mainstay of treatment for large lesions, but its complex relationship with the accessory nerve poses considerable challenges.

The present report aimed to describe a rare case of a foramen magnum meningioma originating from the accessory nerve, highlighting the diagnostic challenges associated with non-dural-based foramen magnum CNs meningiomas, discussing the surgical approach and nerve preservation strategy, and sharing the histopathological properties and radiological findings of this rare clinical entity.

CASE REPORT

A 66-year-old woman without any relevant medical history was referred to our neurosurgery outpatient clinic due to a 6-month history of dizziness, occipital headaches, and left-sided shoulder pain. Neurological examination revealed mild weakness of the left shoulder upon elevation (Medical Research Council Grade 3/5) and a positive Romberg sign. No other CN deficits or other myelopathic signs were noted.

Brain magnetic resonance imaging (MRI) demonstrated a homogeneously enhancing lesion at the foramen magnum (Figure 1). The lesion was radiologically consistent with a foramen magnum meningioma, although no clear dural tail was noted on imaging. Computed tomography scans showed no hyperostosis or bony involvement.

The patient was offered surgical resection and provided informed consent. She was placed in a lateral position and underwent a left-sided far-lateral craniotomy. Intraoperatively, the tumor was found to encase the accessory nerve (Figure 2). A specimen was sent for frozen section analysis, which revealed that the tumor was most consistent with a meningioma. Notably, no dural attachment of the lesion was observed.

Upon careful microsurgical dissection, the tumor was found to invade the nerve sheath of the accessory nerve, and a clear surgical plane could not be identified. Dissection was performed by identifying the intact nerve's proximal and distal ends and carefully navigating through the lesion with the goal of preserving the nerve's anatomical and functional integrity (Figure 2).

Histopathological examination confirmed the diagnosis of a meningioma, with immunohistochemical negativity for S100 and SOX10, thus ruling out the diagnosis of a schwannoma, and strong somatostatin receptor 2A positivity confirming the diagnosis of a meningioma arising from the accessory nerve (Figure 3).

The patient tolerated the procedure well and exhibited no new neurological deficits postoperatively. Follow-up MRI showed complete resection of the lesion, with the 6-month follow-up MRI scan demonstrating no residual or recurrent tumor (Figure 4).

DISCUSSION

Although the foramen magnum is a recognized site for meningioma development, most of these tumors originate from the dura in the lower posterior fossa and foramen magnum. Yasargil et al. have reported that foramen magnum meningiomas originate from the dural entry point of the vertebral artery on the intradural side (12). However, although rare, foramen magnum meningiomas may arise directly from the accessory nerve. The preoperative diagnosis of such lesions can be challenging; yet clinicians should maintain a high index of suspicion for accessory nerve meningiomas when encountering homogeneously enhancing masses that lack a dural tail and lie in close anatomical proximity to the course of the accessory nerve.

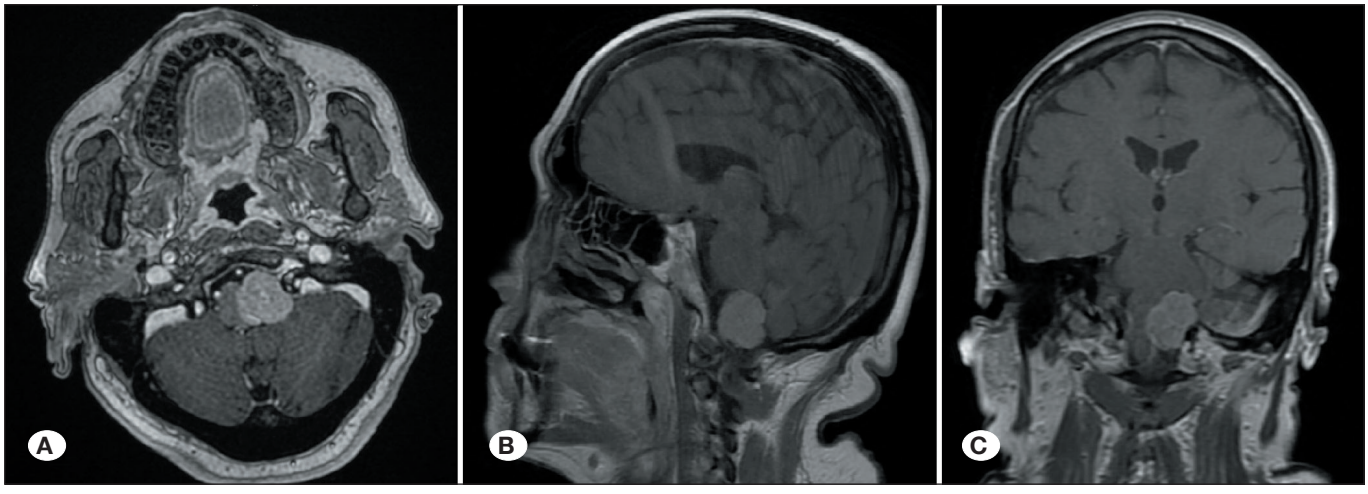

Figure 1: Preoperative contrast enhanced T1W magnetic resonance imaging scans revealed a well-circumscribed, diffusely enhancing left-sided lesion at the level of the foramen magnum (**A:** axial, **B:** sagittal, **C:** coronal sections). The imaging characteristics were suggestive of a meningioma; however, the absence of a clear dural attachment raised the differential diagnosis of other pathologies, including a schwannoma or, less commonly, a meningioma not originating from the dura.

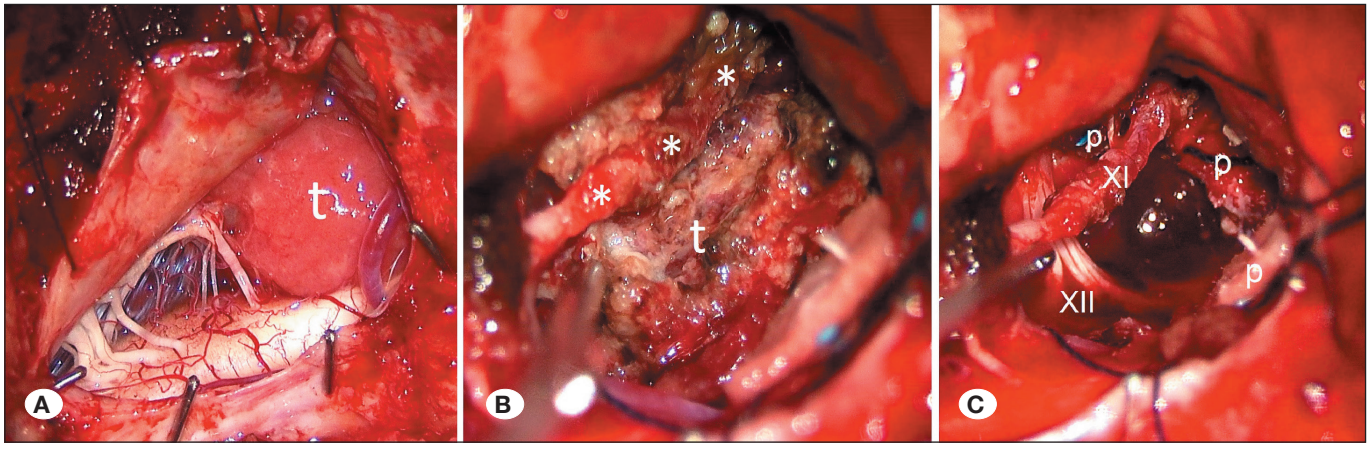

Figure 2: Intraoperative views of accessory nerve meningioma resection via a far-lateral approach. **A)** Intraoperative photograph following surgical exposure via a left-sided far-lateral approach. A well-circumscribed tumor (t) is visualized at the level of the foramen magnum. **B)** Intraoperative view demonstrating the tumor dissection process. The accessory nerve (*) is seen after being dissected from the tumor (t), revealing gross invasion of the nerve sheath and absence of a clear dissection plane. Microsurgical dissection was performed between the proximal and distal nerve segments under high magnification to preserve the nerve's integrity. **C)** Intraoperative view showing the accessory nerve (XI) after complete circumferential dissection and separation of the tumor. The label (p) marks the cottonoid patties within the operative field.

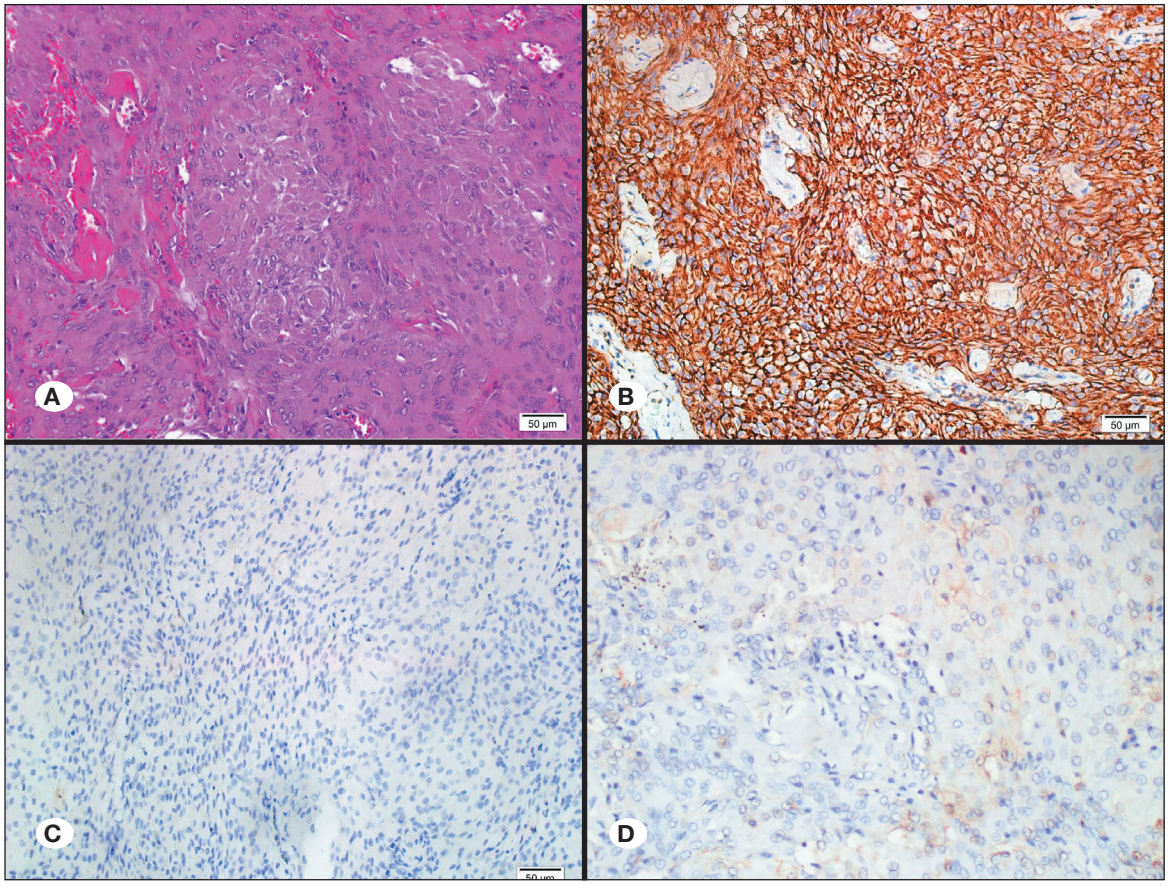

Figure 3: Histopathological and immunohistochemical features of the tumor confirming the diagnosis of meningioma. **A)** Histopathological appearance of the tumor. The lesion comprised cells with abundant eosinophilic cytoplasm, oval nuclei, and a syncytial growth pattern (hematoxylin & eosin staining; magnification ×400). **B)** Tumor cells demonstrate diffuse immunoreactivity for somatostatin receptor 2A (SSTR2A), consistent with a diagnosis of a meningioma (×200). **C)** SOX10 expression was not observed in the tumor cells, supporting the exclusion of a schwannoma or other neural crest-derived neoplasms (×200). **D)** Diffuse strong S100 staining was not observed in the tumor cells (×200).

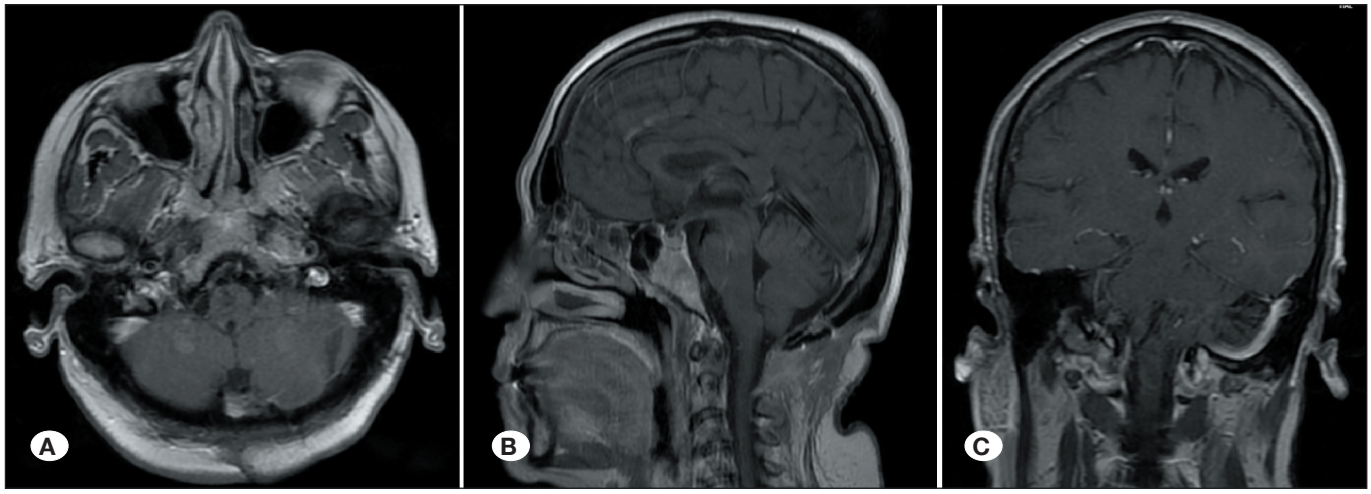

Figure 4: A six-month postoperative magnetic resonance imaging scans demonstrating gross total resection of the lesion, with no evidence of residual or recurrent tumor (**A:** axial, **B:** sagittal, **C:** coronal sections).

Apart from optic nerve sheath meningiomas—which are uniquely encased by true meningeal layers—accessory nerve meningiomas are exceedingly rare and, by definition, lack a dural attachment. The origin of these tumors may involve ectopic arachnoid cap cells along the perineural arachnoid extensions or displaced meningeal elements in the CN sheath.

Unlike most foramen magnum meningiomas, which displace or encase nearby nerves, direct infiltration of the nerve sheath considerably complicates surgical resection. In such cases, the absence of a dissection plane between the tumor and nerve makes microsurgical dissection a difficult and tedious process. A practical approach, as in our case, involves identifying the nerve's proximal and distal ends, followed by intratumoral dissection to preserve the nerve's continuity. In our experience, intraoperative neurophysiological monitoring was valuable in guiding the resection process and avoiding irreversible damage. Ultimately, in these rare cases, a meticulous microsurgical technique remains critical for accessory nerve preservation.

The present case report emphasizes the importance of understanding the normal anatomy, particularly in certain locations such as the foramen magnum region where critical neurovascular structures are densely clustered and lie in close proximity to each other. The accessory nerve is purely a motor nerve that innervates the sternocleidomastoid and trapezius muscles. In foramen magnum lesions, the absence of a dural tail, in addition to their homogeneous enhancement, anatomical proximity to the course of the spinal accessory nerve, and the presence of accessory nerve paresis can help raise suspicion for an accessory nerve meningioma. However, it is still difficult to include accessory nerve meningioma in the differential diagnosis because only a few cases have been reported in the literature. When surgically treating these lesions, comprehensive knowledge of the anatomy and microsurgical principles as well as careful neuromonitoring are of utmost importance to preserve the nerve. When the neurosurgeon is familiar with the anatomical course of the CNs, particularly the accessory nerve, as in the present case, it is possible to identify that the nerve ends within the tumor and originates from the site of engulfment. Neuromonitoring, including nerve stimulation, can easily confirm the nerve and facilitate the surgical course. Another unusual aspect for the neurosurgeon is that this meningioma is not attached to the dura at any point. In the present case, the lesion seemed to be floating, freely movable, and to be easily pulled out; however, this situation can be very deceiving, as forcing the lesion out may lead to the avulsion or transection of the accessory nerve.

To the best of our knowledge, only six cases of accessory nerve meningiomas have been reported in the literature (Table I). Among these, only three cases were foramen magnum meningiomas (5,7,9), whereas the remaining cases were upper cervical lesions. Kobyakov et al. have described a cystic tumor with a solid component arising from the nerve sheath, whereas Mohri et al. reported a solid lesion eccentrically adherent to the accessory nerve with a favorable dissection plane (5,7). Contrarily, our case involved the spinal accessory nerve being centrally engulfed by the tumor, with clear evidence of gross nerve sheath invasion and no identifiable dissection plane (Figure 2). This reinforces the uniqueness of our case, both anatomically and surgically, contributing to the limited literature on this rare entity.

Accessory nerve meningiomas are exceedingly rare and can radiologically mimic common dural-based foramen magnum meningiomas. The present case highlights the importance of including the accessory nerve meningiomas in the differential diagnosis of foramen magnum lesions, particularly when a dural tail cannot be identified on the MRI scan. Intraoperatively, the absence of a favorable dissection plane and gross nerve sheath invasion—as seen in our case—can pose considerable surgical challenges. Nevertheless, functional preservation may still be achievable through meticulous microsurgical dissection performed under high magnification and illumination, guided by anatomical knowledge and intraoperative neurophysiological monitoring. The present case contributes to the limited

Table I: Reported Cases of Foramen Magnum Meningiomas in the Literature with Key Clinical and Surgical Characteristics

Case	Author(s)	Year	Age/ Sex	Presentation	Preoperative Examination	Location and side	Histology	Surgical Approach	Outcome
1	Thomé et al. (9)	2003	61/F	Ataxia, left hemiparesis, myelopathy	Minimal left-sided motor impairment (grade 4–5/5), positive Babinski's reflex, positive Romberg test, slightly decreased proprioception, incoordination and dysmetria on the left side	Bilateral, foramen magnum	S-100 positive, EMA positive, vimentin positive	Midline suboccipital + C1 laminectomy	No recurrence at the 3-year follow-up (presentation was likely secondary to neurodegenerative disease)
2	Tatagiba et al. (8)	2005	35/M	Right shoulder pain and accessory nerve paralysis	Complete accessory nerve palsy on the right side	Right jugular foramen	Meningothelial, invasion of the epineural space,	cervical-transmastoid paracondylar approach to the jugular foramen.	Postoperative hoarseness and dysphagia later improved.
3	Liechty et al. (6)	2007	9/M	Closely followed up for multiple meningiomas/ schwannomas	Right eye blindness, nystagmus on the left side	Right spinal accessory nerve at the C1 level	Psammomatous, neurofibromatosis II	C1 laminectomy	No recurrence at 3 years
4	Mohri et al (7)	2019	69/F	Dizziness and bilateral shoulder pain	Spinal accessory nerve palsy (difficult in raising the shoulder, deficit of 3/5) on the left side	Left spinal accessory nerve at the foramen magnum	Meningothelial meningioma, positive for EMA	Midline suboccipital with C1 laminectomy	Improvement in shoulder strength
5	Ueno et al. (10)	2022	57/F	Headache	No deficit	Right spinal accessory nerve at C1–C2	Atypical meningioma, positive staining for epithelial membrane antigen and progesterone receptors	C1 laminectomy with restricted posterior foramen magnum osteotomy	Neurologically intact postoperatively
6	Kobyakov et al. (5)	2024	53/M	Occipital headache	No focal deficit	Left spinal accessory nerve at the foramen magnum	Angiomatous meningioma, progesterone receptor (PR)-positive, positive epithelial membrane antigen EMA	midline suboccipital approach	Uneventful recovery
7	**Present Case**	2025	66/F	Dizziness, headache	Mild weakness of left shoulder elevation (3/5), positive Romberg sign	Left spinal accessory nerve at the foramen magnum	Meningothelial meningioma, SOX-negative, S-100 negative, gross invasion of the accessory nerve sheath	Left-sided far-lateral approach	Left trapezius/SCM weakness 3/5, later improved

literature on accessory nerve meningiomas and underscores the need for a high preoperative index of suspicion and surgical adaptability in managing atypical skull base tumors.

CONCLUSION

Accessory nerve meningiomas are exceedingly rare and can radiologically mimic regular foramen magnum meningiomas. Although there is no clear cleavage plan between the nerve and tumor, functional preservation may still be achievable through meticulous microsurgical dissection, guided by anatomical knowledge and neurophysiological monitoring.

Declarations

Funding: This research did not receive any specific grant from funding agencies in the public, commercial, or not-for-profit sectors.

Availability of data and materials: The datasets generated and/or analyzed during the current study are available from the corresponding author by reasonable request.

Disclosure: The authors declare no competing interests.

Informed consent: The patient's written informed consent was acquired.

AUTHORSHIP CONTRIBUTION

Study conception and design: MSG, MA, MAK

Data collection: MAK, SS, Gİ

Analysis and interpretation of results: MSG, MA, TSA

Draft manuscript preparation: MA, MAK

Critical revision of the article: MSG

Other (study supervision, fundings, materials, etc...): BB, MSG

All authors (MA, MAK, SS, GI, BB, TSA, MSG) reviewed the results and approved the final version of the manuscript.

REFERENCES

1. Doi K, Otani N, Hagita D, Horiuchi M, Takeuchi S, Toyooka T, Wada K, Hayashi M, Mori K: A case of meningioma originating from the oculomotor nerve. World Neurosurg 143:197-201, 2020. https://doi.org/10.1016/j.wneu.2020.07.089
2. Dutton JJ: Optic nerve sheath meningiomas. Surv Ophthalmol 37:167-183, 1992. https://doi.org/10.1016/0039-6257(92)90135-g
3. Fujimoto Y, Kato A, Taniguchi M, Maruno M, Yoshimine T: Meningioma arising from the trigeminal nerve: A case report and literature review. J Neurooncol 68:185-187, 2004. https://doi.org/10.1023/b:neon.0000027774.19801.af
4. Huntoon K, Toland AMS, Dahiya S: Meningioma: A review of clinicopathological and molecular aspects. Front Oncol 10:579599, 2020. https://doi.org/10.3389/fonc.2020.579599
5. Kobyakov NG, Bezbabicheva TS, Shishkina LV, Arustamyan SR, Pitskhelauri DI: Meningioma obolochek dobavochnogo nerva. Klinicheskii sluchai i obzor literatury [Accessory nerve meningioma. A case report and literature review. Zh Vopr Neirokhir Im N N Burdenko 88:90-95, 2024. https://doi.org/10.17116/neiro20248803190
6. Liechty P, Tubbs RS, Loukas M, Blount JP, Wellons JC, Acakpo-Satchivi L, Oakes WJ, Grabb PA: Spinal accessory nerve meningioma in a paediatric patient: A case report. Folia Neuropathol 45:23-25, 2007.
7. Mohri M, Yamano J, Saito K, Nakada M: Spinal accessory nerve meningioma at the foramen magnum with medullar compression: A case report and literature review. World Neurosurg 128:158-161, 2019. https://doi.org/10.1016/j.wneu.2019.05.013
8. Tatagiba M, Koerbel A, Bornemann A, Freudenstein D: Meningioma of the accessory nerve extending from the jugular foramen into the parapharyngeal space. Acta Neurochir 147:909-910, 2005.https://doi.org/10.1007/s00701-005-0520-8
9. Thomé C, Grobholz R, Boschert J, Schmiedek P: Bilateral meningiomatous lesions of the spinal accessory nerves. Acta Neurochir 145:309-313; discussion 313, 2003. https://doi.org/10.1007/s00701-002-1059-6
10. Ueno H, Tsutsumi S, Hashizume A, Sugiyama N, Ishii H: Atypical meningioma originating from the spinal accessory nerve. Surg Neurol Int 13:598, 2022. https://doi.org/10.25259/SNI_1085_2022
11. Wiemels J, Wrensch M, Claus EB: Epidemiology and etiology of meningioma. J Neurooncol 99:307-314, 2010. https://doi.org/10.1007/s11060-010-0386-3
12. Yasargil MG, Mortara RW, Curcic M: Meningiomas of the basal posterior cranial fossa. In: Krayenbuhl H, (ed). Advances and Technical Standards in Neurosurgery. Vol. 7. Wien: Springer-Verlag 1980:1–115. https://doi.org/10.1007/978-3-7091-7051-9.

Turk Neurosurg 36(3):489-490, 2026
DOI: 10.5137/1019-5149.JTN.49720-25.2

Obituary

Received: 20.08.2025
Accepted: 05.12.2025
Published Online: 22.05.2026

In Memory of Dr. Zeki Oral

Ilhan ELMACI

Professor of Neurosurgery, Acıbadem Kent Hospital, İzmir, Türkiye

Corresponding author: Ilhan ELMACI ✉ ilhanelmaci@yahoo.com

ABSTRACT

Dr. Zeki Oral was born in Anamur in 1940. He completed his primary and secondary education in Anamur and his high school education in Bursa. In 1966, he graduated from Istanbul Faculty of Medicine and, in the same year, began his neurosurgery residency at Hacettepe Faculty of Medicine. Following his residency, he completed his military service at Kasımpaşa Naval Hospital, where he subsequently continued to work as a specialist physician. He then began his first post-residency instructor position at Taksim Training Hospital. With the enactment of the full-time practice law, he resigned from public service. After working for a period as a private practitioner, he accepted an invitation to serve as Chief of Neurosurgery Deparment at Bakırköy Mental and Neurological Diseases Hospital. After twenty years in this role, he decided to retire in 2012. He passed away on March 4, 2025.

KEYWORDS: Dr Zeki Oral, Turkish neurosurgeon, In memory of

Dr. Zeki Oral was born in Anamur in 1940. He completed his primary and secondary education in Anamur and attended high school in Bursa. He graduated from the Istanbul Faculty of Medicine in 1966, and in that same year, he began his neurosurgery residency at Hacettepe University Faculty of Medicine. Upon completing his residency, he fulfilled his military service at Kasımpaşa Naval Hospital, where he continued to serve as a specialist physician. His first academic appointment after residency was at Taksim Training Hospital. With the enactment of the full-time law, he was required to resign from public service. After several years working as a private practitioner, he accepted an invitation to become Clinical Chief at Bakırköy Mental and Neurological Diseases Hospital, a position he held for twenty years until his retirement in 2012. Dr. Oral passed away on March 4, 2025.

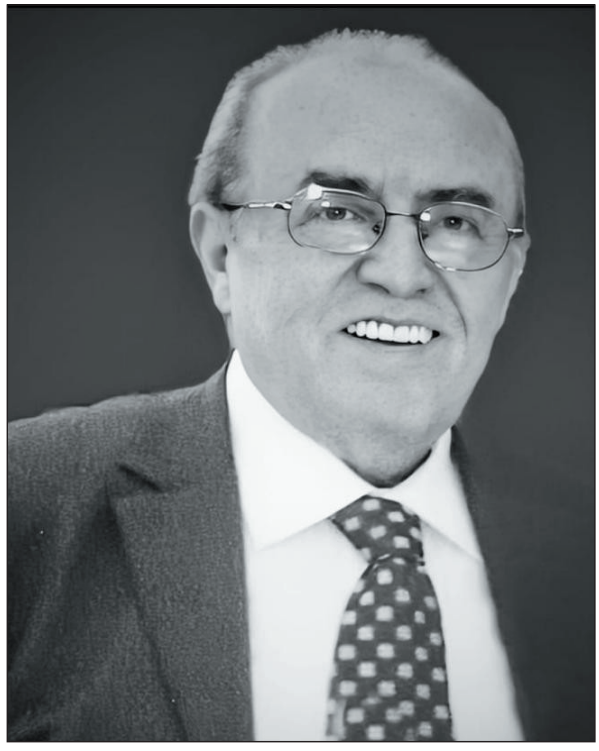

As a distinguished neurosurgeon and dedicated educator, Dr. Oral was a quintessential master of his field, embodying exceptional knowledge, experience, clarity, and patience. He exemplified the principle that professional success in neurosurgery arises from a rigorous clinical process—beginning with the initial patient encounter and neurological examination, proceeding through the selection of appropriate radiological studies, and culminating in thoughtful treatment planning. These principles, together with surgical proficiency, form the foundation of neurosurgical training worldwide, and Dr. Oral's teaching reflected them fully as he guided his students to lis-

Ilhan ELMACI : 0000-0001-9433-0307

ten attentively, ask the right questions, and manage each step of patient care with professionalism.

We experienced this firsthand in the outpatient clinic with Dr. Oral. We presented patients' medical histories along with the findings of their physical and neurological examinations, reviewed the radiological studies together, and formulated treatment plans under his guidance. This process was profoundly instructive, teaching each of his students the importance of professional demeanor, attentive listening to patients and their families, and effective clinical management through asking the right questions.

I recall the engaging and educational morning rounds during which in-patients were reviewed and updates were presented by the senior resident. Decisions regarding follow-up and treatment planning were made collectively. As a fair and impartial professional Dr. Oral maintained an equitable and impartial approach toward all trainees. At the end, each resident performed all surgical procedures required by their level of seniority in a timely manner, completed their thesis by the residency exam date, therefore passing their exam successfully, and obtaining their specialty certification.

Dr. Zeki Oral's character was shaped by strong principles, integrity, and a clear worldview. He spoke directly and expressed his thoughts without ambiguity. He valued clarity and had little tolerance for unnecessary complexity. His humanistic and democratic perspective guided his conduct in both clinical and personal interactions. He did not approve of secrecy or closed-door dealings. In difficult or contentious situations he would first listen to both sides, understand the issue in detail, before expressing a considered opinion. Especially during our daily morning clinic meetings, he would raise a topic or tell a relevant anecdote to point to the solution to the problem. The intended message was always delivered effectively.

He was a good man, a skilled neurosurgeon, an instructive clinical chief, and a mentor. Although he appeared strict due to his adherence to principles, he was open to progress and new practices.

We trained during a period when microsurgery was rapidly expanding in scope and influence. Dr. Oral welcomed our eagerness to learn with genuine enthusiasm and unwavering support. He set clear expectations within the limits of the available resources and ensured that our development progressed appropriately. Before attempting any technique we had not yet mastered, he emphasized the necessity of completing the requisite "learning curve" or performing the procedure under the guidance of an experienced mentor.

Neurosurgery residency training is not solely about performing operations or developing technical skills; it is fundamentally about shaping a professional. The discipline comprises both art and craft. The first involves the human and aesthetic approach, while the second encompasses skill. It is through the harmony of these two that professional depth can be achieved. What follows then depends on the energy, ambition, and choices of the specialist after training.

I have many colleagues who were trained under his guidance. Each of them worked and continues to work as neurosurgeons who are recognized for their knowledge, experience, dedication, and diligence.

Among Dr.Oral's, the main awards were:

- Service Award, Turkish Neurosurgical Society, 2004
- Service Award, Society of Nervous System Surgery, 2015
- Certificate of Appreciation, 50th year as a specialist in neurosurgery, Turkish Neurosurgical Society, 2021

Dr. Oral also served as founding editor of the "Düşünen Adam Dergisi - The Journal of Psychiatry and Neurological Sciences. His leadership and vision have made significant contributions to the academic field beyond his roles in surgery and teaching.

He emphasized the importance of learning new things and pursuing activities outside of one's career. After retiring in 2012, he returned to his hometown of Anamur in Mersin and devoted himself to agriculture, particularly to growing bananas, one of the region's most important crops. He gained sufficient knowledge in this field and obtained a certificate. The happiness he felt from working the land and ultimately obtaining a tangible product brought him great joy. *(Reference: Mehmet Seçer, "Ustalardan Hayata Dair: Zeki Oral," Spinal Peripheral Nerve Surgery Bulletin Journal, April 2019, Issue: 83)*

He saw his profession not only as a job that brought him happiness, but also as a field that defined meaningful human relationships. He was charming at social gatherings and meetings, and his circle was always crowded. He was a respected person in terms of his personal and professional relationships, whose opinions were held in high regard, sought after, and missed.

We remember and commemorate our esteemed Dr. Zeki Oral with respect, gratitude, and longing.

Dr. İlhan Elmacı

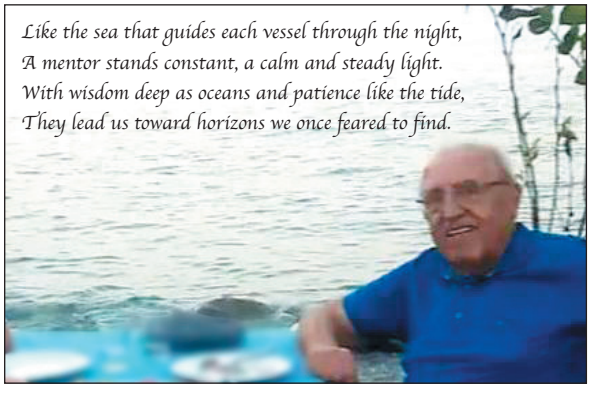

Editorial Response

Dr. Zeki Oral will be remembered as a prominent neurosurgeon, a committed teacher, and a person of morality and a mentor whose influence extended to generations of trainees. His dedication to clinical excellence, ethical practice and thoughtful mentorship exemplify the enduring values of neurosurgery. The academic community remembers him with deep respect and gratitude.

Editorial Board of Turkish Neurosurgery

Turkish Neurosurgery
Official Journal of the Turkish Neurosurgical Society

Volume 36 • Number 3 • May 2026